ISSN 2301-1092 • ISSN (en línea) 2301-1106

MEMORIA

INVESTIGACIONES EN INGENIERÍA

Nº 29

FACULTAD DE INGENIERÍA

UM
UNIVERSIDAD DE MONTEVIDEO

MEMORIA

Investigaciones en Ingeniería

ISSN 2301-1092 • ISSN (en línea) 2301-1106

Núm. 29 (2025)

Sumario

Págs.

Editorial – Ingeniería, sostenibilidad y resiliencia.

Presentamos con satisfacción el Número 29 de la Revista Memoria Investigaciones en Ingeniería, publicación gestionada por la Universidad de Montevideo (Uruguay), que una vez más se reafirma como un espacio de encuentro para trabajos que abordan, desde la ingeniería, desafíos técnicos, económicos, ambientales y sociales de gran relevancia. Este nuevo número se distingue por su diversidad geográfica y temática, con contribuciones provenientes de América Latina y Asia, y por un hilo conductor muy definido: el compromiso con la sostenibilidad, la resiliencia y la innovación tecnológica al servicio de la sociedad.

El volumen se abre con un estudio sobre las repercusiones económicas y técnicas del cierre de bancos de materiales en el cerro de San Juan, en las ciudades de Tepic y Xalisco, en 2022. Este trabajo pone en evidencia cómo las decisiones relativas al aprovechamiento de recursos naturales impactan, de manera simultánea, en la actividad productiva, la infraestructura y el entorno, aportando elementos clave para la planificación territorial y la gestión responsable de materiales.

En la misma línea de preocupación por la gestión del riesgo, se presenta un análisis de modelos hidrodinámicos aplicado al caso de la inundación en Río Grande do Sul, Brasil, acompañado de una propuesta de cambio cultural basada en la predicción y la anticipación. La combinación de modelado técnico con una reflexión sobre la cultura del riesgo ofrece una visión integral de cómo las herramientas de la ingeniería pueden y deben contribuir a sociedades más preparadas y resilientes frente a eventos extremos.

Varios artículos de este número abordan la transición energética y la movilidad sostenible desde distintos contextos. Por una parte, se incluye un estudio de viabilidad para la electrificación de vehículos en Pakistán, donde se analizan condicionantes técnicos y económicos que pueden extrapolarse a otros países en desarrollo. Por otra parte, se presenta un análisis de las barreras para la masificación del uso de vehículos eléctricos privados en el transporte urbano de pasajeros en Lima, Perú, donde convergen factores regulatorios, de infraestructura, económicos y de aceptación social.

La búsqueda de eficiencia y optimización técnica se refleja en diversos estudios experimentales y numéricos. Uno de ellos explora, mediante simulación CFD, el efecto de la geometría de la válvula Tesla sobre el comportamiento del flujo inestable y la caída de presión, contribuyendo al diseño más eficiente de dispositivos sin partes móviles. En un ámbito más cercano al usuario doméstico, otro trabajo analiza el rendimiento de refrigeradores que emplean el refrigerante R134a con distintos lubricantes, ofreciendo una comparación detallada que puede guiar mejoras en la eficiencia energética y en la vida útil de los equipos.

La economía circular y el aprovechamiento de materiales reciclados ocupa un lugar destacado en el número, a través de un estudio dedicado a las propiedades de tracción e impacto de polímeros reciclados como polipropileno, cloruro de polivinilo, poliamida y polietileno. Los resultados dialogan directamente con la necesidad global de reducir residuos y mejorar la calidad y trazabilidad de los materiales reutilizados en aplicaciones industriales.

La ingeniería aplicada a la agricultura y a la seguridad laboral también se hace presente. En el ámbito agroalimentario, se propone una solución de agricultura vertical inteligente y sostenible basada en IoT para abordar desafíos agrícolas en Pakistán, combinando sensorización, automatización y uso eficiente de recursos. Esta contribución se ve complementada por una revisión de aplicaciones recientes de tecnologías digitales en la agricultura, que ofrece un panorama actualizado sobre cómo la digitalización está transformando la producción, el monitoreo y la toma de decisiones en el sector. En el campo de la seguridad y salud en el trabajo, otro artículo realiza una evaluación de riesgos laborales y presenta medidas de mitigación en la sección de encolado y lapeado de una planta de fabricación de medidores de gas, recordando que la ingeniería industrial tiene un componente profundamente humano vinculado a la protección de las personas trabajadoras.

Cierra este número un estudio computacional sobre el impacto directo de un rayo de 200 kA en tanques externos de techo flotante. Este trabajo, situado en la intersección entre la ingeniería eléctrica, la seguridad industrial y la gestión de infraestructuras críticas, pone de relieve la importancia de los modelos avanzados para prevenir fallos catastróficos y diseñar sistemas de protección más robustos.

https://doi.org/10.36561/ING.29.1
ISSN 2301-1092 • ISSN (en línea) 2301-1106

Desde el Comité Editorial de la Revista Memoria Investigaciones en Ingeniería expresamos nuestro agradecimiento a quienes contribuyeron con sus trabajos y al cuerpo de revisión, cuyo esfuerzo y rigor garantizan la calidad científica de cada artículo.

Agradezco una vez más al Mag. Ing. Fernando Hernández y a la Lic. Valentina Morandi su profesional trabajo para que este número sea realidad.

Invitamos a nuestra comunidad de lectores (académicos, profesionales y estudiantes) a explorar este número 29, convencidos de que encontrarán en sus páginas no solo resultados de investigación de alto nivel, sino también inspiración para seguir poniendo la ingeniería al servicio del desarrollo sostenible y del bienestar de nuestras sociedades.

Dr. Ing. Rafael Sotelo
Editor en Jefe
Facultad de Ingeniería
Universidad de Montevideo

https://doi.org/10.36561/ING.29.1
ISSN 2301-1092 • ISSN (en línea) 2301-1106

Análisis de las repercusiones económicas y técnicas del cierre de bancos de materiales del cerro de San Juan, en las ciudades de Tepic y Xalisco, en el año 2022

Analysis of the economic and technical repercussions of the closure of material banks on San Juan Hill, in the cities of Tepic and Xalisco, in 2022

Análise das repercussões econômicas e técnicas do fechamento dos bancos de materiais no Cerro San Juan, nas cidades de Tepic e Xalisco, em 2022

Carlos Alberto Hoyos Castellanos[1], William Herbe Herrera León[2],
Fernando Treviño Montemayor[3], Fernando Aguirre Camacho [4]

Recibido: 20/11/2024 Aceptado: 02/03/2025

Resumen. - El 9 de mayo de 2022, el Gobernador de Nayarit, Dr. Miguel Ángel Navarro Quintero, tomó la decisión de cerrar el acceso a los bancos de materiales pétreos que tenían más de 30 años de explotación del cerro de San Juan, en los municipios de Tepic y Xalisco, Nayarit. Posterior a ello, hubo repercusiones que aún no han terminado de ser evaluadas, entre las que podemos incluir las siguientes: Incremento del precio de los materiales de construcción; Inmediata falta de disponibilidad de gravas y arenas en la región, lo que ha sido resuelto con bancos foráneos; Encarecimiento del mercado de la construcción; Suspensión de obras en proceso, que posteriormente fueron terminadas (la mayor parte de ellas), con los naturales incrementos de precios; Dificultad para conseguir los materiales para construcción; Vandalización de los bancos de materiales que fueron clausurados; Pérdida de mano de obra y de fuentes de empleo, del personal de los bancos de materiales y de las obras que en su momento estaban en proceso; Sustitución de materiales para la fabricación de piezas de mampostería; Incertidumbre del cumplimiento de las normas de construcción por las gravas y arenas de los bancos emergentes, y de la uniformidad de sus características; Repentino menoscabo de la experiencia que plantas concreteras, constructores, obreros de la construcción y cuadrillas de colado habían acumulado con los agregados conocidos de los bancos ahora clausurados. A la fecha, no se han hecho públicas las políticas que se hayan implantado o acciones tomadas para el proceso de restauración de las afectaciones en las zonas donde había los bancos de materiales, pero los efectos de los cierres aún continúan.

Palabras clave: Bancos de materiales, Gravas y arenas, Materiales para concreto, Normatividad de materiales de construcción

[1] Doctor En Dirección de Proyectos. Instituto Tecnológico de Tepic en Tecnológico Nacional de México, hoyoscarlos@ittepic.edu.mx, ORCID iD: https://orcid.org/0000-0001-5965-1375

[2] Doctor En Ciencias de los ámbitos antrópicos. Instituto Tecnológico de Tepic en Tecnológico Nacional de México, wherrera@ittepic.edu.mx, ORCID iD: https://orcid.org/0009-0008-4643-6260

[3] Maestro en Estructuras. Instituto Tecnológico de Tepic en Tecnológico Nacional de México, ftrevino@ittepic.edu.mx, ORCID iD: https://orcid.org/0000-0003-3924-7660

[4] Maestro en Ingeniería en Terminal en Construcción. Instituto Tecnológico de Tepic en Tecnológico Nacional de México, faguirre@ittepic.edu.mx, ORCID iD: https://orcid.org/0009-0000-9277-1002

Este es un artículo de acceso abierto distribuido bajo los términos de una licencia de uso y distribución CC BY-NC 4.0. Para ver una copia de esta licencia visite http://creativecommons.org/licenses/by-nc/4.0/

Summary. - *On May 9, 2022, the Governor of Nayarit, Dr. Miguel Ángel Navarro Quintero, made the decision to close access to the banks of stone materials that had been exploited for more than 30 years on the San Juan Hill, in the municipalities of Tepic and Xalisco, Nayarit (Gobierno del Estado de Nayarit, 2022). After that, there were repercussions that have not yet been evaluated, among which we can include the following: Increase in the price of construction materials; Immediate lack of availability of gravel and sand in the region, which has been resolved with foreign banks; Rising prices of the construction market; Suspension of works in progress, which were subsequently completed (most of them), with the natural price increases; Difficulty in obtaining construction materials; Vandalization of material banks that were closed; Loss of labor and sources of employment, of the personnel of the material banks and of the works that were in process at the time; Substitution of materials for the manufacture of masonry pieces; Uncertainty of compliance with construction standards by the gravels and sands of the emerging banks, and of the uniformity of their characteristics; Sudden deterioration of the experience that concrete plants, builders, construction workers and casting crews had accumulated with the known aggregates of the now closed banks. To date, the policies that have been implemented or actions taken for the restoration process of the damage in the areas where there was material banks have not been made public, but the effects of the closures still continue.*

Keywords: *Materials bank, Gravel and sand, Concrete materials, construction materials regulations.*

Resumo. ***-*** *No dia 9 de maio de 2022, o Governador de Nayarit, Dr. Miguel Ángel Navarro Quintero, tomou a decisão de fechar o acesso aos bancos de materiais pétreos explorados há mais de 30 anos no Cerro San Juan, nos municípios de Tepic. e Xalisco, Nayarit (Governo do Estado de Nayarit, 2022). Depois disso, houve repercussões que ainda não foram avaliadas, entre as quais podemos incluir as seguintes:Aumento do preço dos materiais de construção; Falta imediata de disponibilidade de cascalho e areia na região, que foi resolvida com bancos estrangeiros; Aumento dos preços do mercado de construção; Suspensão de obras em andamento, que foram posteriormente concluídas (a maioria delas), com os aumentos naturais de preços; Dificuldade na obtenção de materiais de construção; Vandalização de bancos de materiais que estavam fechados; Perda de mão de obra e de fontes de emprego, do pessoal dos bancos de materiais e das obras que estavam em andamento na época; Substituição de materiais para fabricação de peças de alvenaria; Incerteza do cumprimento das normas de construção por parte dos cascalhos e areias dos bancos emergentes, e da uniformidade das suas características; Deterioração repentina da experiência que fábricas de concreto, construtores, trabalhadores da construção civil e equipes de fundição acumularam com os agregados conhecidos dos bancos agora fechados. Até à data, as políticas que foram implementadas ou as ações tomadas para o processo de restauração dos danos nas áreas onde existiam bancos de materiais não foram tornadas públicas, mas os efeitos dos encerramentos continuam.*

Palavras-chave: *Bancos de materiais, cascalho e areia, materiais de concreto, regulamentos de materiais de construção.*

1. Objetivo. - En este artículo se hace un análisis de las consecuencias de las decisiones que tomó el Gobierno del Estado de Nayarit con respecto al cierre de los bancos de materiales pétreos en el cerro de San Juan de los municipios de Tepic y Xalisco, en mayo del 2022. Entender las afectaciones a la economía y a la industria de la construcción en general, y los beneficios que se esperan obtener con la decisión tomada por el gobierno estatal.

Figura I. Imagen de la explotación del cerro de San Juan, en Tepic y Xalisco, Nayarit. Fuente [1]

2. Resultados y Discusión. - Las ciudades de Tepic y Xalisco, y varias de las localidades que se desarrollan alrededor de estas cabeceras municipales, tradicionalmente obtenían sus materiales pétreos de la explotación de los bancos de materiales ubicados en el cerro de San Juan.

De acuerdo con una investigación realizada al respecto por este cuerpo académico, los bancos registrados en el 2019 en la Dirección de Evaluación Ambiental de la Secretaría de Desarrollo Rural del Estado de Nayarit se presentan en la siguiente relación.

NOMBRE del banco de extracción	MUNICIPIO	PROMOVENTE
EL LIMÓN	TEPIC	ERNESTO CRUZ ZAMBRANO REPRESENTANTE LEGAL DE TERRACERIAS, PAVIMENTOS Y CAMINOS S.A. DE C.V.
ARENERA LA HUEVONA	XALISCO	C. RODOLFO LÓPEZ LOZA
EL PORTEZUELO	XALISCO	C. FERNANDO GONZÁLEZ ORTEGA REPRESENTANTE LEGAL DE CONSTRUCCIONES Y TERRACERIAS DEL VALLE DE MATATIPAC, S.A. DE C.V.
BANCO DE MATERIAL PÉTREO CASTILLO	XALISCO	RUBÉN CASTILLO CASTILLO
BANCO DE MATERIAL PÉTREO PARCELA 57	XALISCO	LETICIA GARCIA ORTEGA
BANCO DE MATERIAL PÉTREO SANTA RITA	XALISCO	C. ANTONIO SIFUENTES NAVARRO/PÉTREOS Y AGREGADOS DEL NAYAR, S.A. DE C.V./ CONSULTOR AMBIENTAL ING. MARCELINO GÓMEZ
EXTRACCION DE MATERIALES PETREOS: BANCO EL LIMON II	EL LIMON / TEPIC	ING. ERNESTO CRUZ ZAMBRANO / TEPYC, S.A. DE C,V,
CLADIMACO EJIDO EL MOLINO II	XALISCO	FRANCISCO AZCONA PARRA
BANCO DE MATERIAL PETREO "CERRO EL VOLCAN"	TEPIC	HECTOR MANUEL FLETES ROBLES/SECRETARIO DE LA CTM SECCION 130/ CONSULTOR AMBIENTAL ING. ROBERTO MEZA B.
BANCO DE EXTRACCION DE MATERIAL PETREO EL ZACUAL	TEPIC	EMILIO CERVANTES/COMISARIADO EJIDAL DEL EJIDO DE MORA
NIVELACION DE PREDIO RUSTICO CON APROVECHAMIENTO DE MATERIALES PETREOS	TEPIC	GRACIELA ORTEGA SARRIA/ CONSULTOR AMBIENTAL ING. ERIKA MARCELA DELGADO
EXTRACCION DE MATERIALES PETREOS EL HORMIGON	TEPIC	EJIDO CAMICHIN DE JAUJA/ CONSULTOR AMBIENTAL LUIS ENRIQUE ORAMAS
BANCO DE EXTRACCION DE MATERIALES PETREOS EL ZORRO	TEPIC	MARCO ANTONIO SILVA CARVAJAL
EXTRACCION DE MATERIALES PETREOS EN MINAS NUEVAS BANCO EL RINCON	TEPIC	ING. ERNESTO CRUZ ZAMBRANO/TERRACERIAS, PAVIMENTOS Y CAMINOS SA DE CV
BANCO DE EXTRACCIÓN DE MATERIAL PÉTREO "LA CASTAÑEDA"	TEPIC	C. HERIBERTO CASTAÑEDA ARCINEDA/ CONSULTOR AMBIENTAL ING. RAÚL CÓRDOVA RUELAS
BANCO DE MATERIAL "LA BENDICIÓN"	XALISCO	C. JOSÉ ROSARIO VERA VALDIVIA/ JHONY O. VERA VALDIVIA. josvaldovera@gmail.com
BANCO DE EXTRACCIÓN DE MATERIAL PÉTREO "NUEVA GALICIA"	TEPIC	C. ÁLVARO MONTES CARRILLO/ CONSULTOR ING. RAÚL CÓRDOVA RUELAS
BANCO DE MATERIAL PÉTREO "BETHEL"	TEPIC	C. LUIS GONZALO GARCÍA LEPE/ CONSULTOR AMBIENTAL ING. ROBERTO MEZA BALTAZAR
BANCO DE MATERIAL "LAS ÁGUILAS"	XALISCO	ARTURO ARELLANO GUILLEN// CONSULTOR ING. RAÚL CÓRDOVA RUELAS
BANCO DE MATERIAL "LA REPISA"	TEPIC	ING. ERNESTRO CRUZ ZAMBRANO
BANCO DE MATERIAL "EL EJIDO"	XALISCO	MARCO ANTONIO SILVA CARVAJAL E IVÁN PETROVICH LÓPEZ MUÑOZ
BANCO DE MATERIAL EL GÜERO SÁNCHEZ	TEPIC	JUAN FRANCISCO SÁNCHEZ PÉREZ
ACONDICIONAMIENTO DE PARCELA PARA USO AGRÍCOLA "LA MEZCALERA"	XALISCO	RENÉ ADRÍAN GARCÍA CASTILLO/CONSULTOR AMBIENTAL ING. ROBERTO MEZA BALTAZAR
BANCO DE MATERIAL CARREÓN	TEPIC	JOSÉ CARREÓN HERNÁNDEZ/CONSULTOR AMBIENTAL ING. ROBERTO MEZA BALTAZAR
BANCO DE MATERIAL PETREO LO DE LAMEDO	TEPIC	ALMA ARACELI HÉRNANDEZ SÁNCHEZ/CONSULTOR AMBIENTAL ING. ROBERTO MEZA BALTAZAR
BANCO DE MATERIAL PETREO LOS CAMICHINES	XALISCO	CINTHIA JOCELIN ARELLANO RIVERA/CONSULTOR AMBIENTAL ING. ROBERTO MEZA BALTAZAR

Figura II. Municipio y promovente por banco de extracción.

La mayoría estaban en el cerro de San Juan y producían la cantidad suficiente y necesaria para desarrollar las construcciones de ambas ciudades.
El precio del viaje de arena y grava, a inicios del año 2022, fluctuaba entre los 800 y 1000 pesos, dependiendo del proveedor principalmente, y del uso que se le iba a dar al material, ya fuera para obra gruesa (concretos y morteros básicamente) o para acabados.
Algunos de esos bancos de materiales destinaban su producción para la venta al público en general y otros más servían a empresas particulares para la fabricación y venta de concretos hidráulicos y asfálticos, block y otros productos procesados.
Otros bancos pertenecían a empresas que estaban asociadas o en consorcios con constructoras de edificaciones o vías terrestres, entre otras especialidades.
Estas explotaciones de materiales se abrieron desde hace más de 30 años. Aunque no hay alguna documentación pública que lo demuestre, debido al contacto con el medio de la construcción podemos hacer esa afirmación.

En mayo del 2022, sorprendió el anuncio realizado por el Gobierno del Estado de Nayarit, directamente por el Gobernador Dr. Miguel Ángel Navarro Quintero, en el sentido de que se suspendían de manera inmediata las concesiones existentes para la explotación de los bancos de materiales que extraían gravas, arenas y jales (nombre con el que se conoce a la arena pumítica o pumicita en la región) del denominado cerro de San Juan [1], y sólo se les permitiría a las compañías concesionarias retirar el material que ya tuvieran procesado, aunque este último anuncio fue realizado días después debido a la demanda de materiales para la construcción.
Las razones que se argumentaron fueron que no se podía permitir que unos cuantos particulares estuvieran acabando con el ecosistema que representaba el cerro de San Juan, y que dicha depredación ya no sería permitida.

Esta medida fue aplaudida por algunos y rechazada por otros. Las repercusiones fueron inmediatas, entre ellas las siguientes:

- Suspensión inmediata de obras de construcción en desarrollo realizadas por particulares, debido a la falta de disponibilidad de los materiales básicos para las edificaciones, y por el encarecimiento de estos. El viaje de arena o grava se incrementó en cuestión de horas de los 800 pesos originales hasta los 7,000 pesos.
- La obra pública se encareció por el incremento de los costos, generando una gran cantidad de solicitudes de revisión de proyectos y reclamaciones.
- Se paralizó el mercado de la construcción debido a que proyectos que estaban en planes de iniciar en mayo o junio de 2022, tuvieron que ser reprogramados por el incremento del costo de la construcción.
- Se tuvieron que buscar fuentes alternas de materiales para la construcción, incrementando los costos de los agregados debido al costo del flete para llevarlos a las ciudades de Tepic y Xalisco. Esto incrementó también la explotación de otros bancos de materiales.
- Debido a la suspensión súbita de obras privadas y municipales, muchos trabajadores de la construcción se quedaron sin empleo por al menos unas semanas, mientras se niveló el problema de los precios. También el personal de las minas vio afectado sus ingresos, ya que las compañías no podían seguir pagando los sueldos si ya no había negocios que atender.
- Se tuvo que emplear la fuerza pública para vigilar que los bancos de materiales clausurados fueran realmente cerrados. En la realidad, la explotación siguió durante varios días, pero la realizaban por la noche y sacaban los materiales de manera más disimulada.

A mediano plazo, se han cambiado algunos procesos de fabricación de blocks y ladrillos, sustituyendo la arena con otros materiales. Por ejemplo, para sustituir la arena de los blocks hechos con jal, una parte del mismo jal es molido más fino para usarlo en sustitución de la arena, o algunas piezas de block las empezaron a fabricar con tezontle triturado. Desgraciadamente, no hay una autoridad que vigile que las piezas fabricadas para los muros de mampostería ya sean blocks o ladrillo rojo recocido, cumplan con lo que indican las normas y reglamentos en cuanto a sus características como capacidad de carga, absorción de humedad, entre otras, por lo que no hay forma de asegurar que dichos elementos podrán funcionar para realizar construcciones seguras para carga vertical o sismo.

No se puede afirmar con seguridad en una edificación cuánto porcentaje es de arena y grava, sin embargo, sí podemos asegurar que son elementos de la mayor relevancia porque están presentes en prácticamente todas las etapas de la construcción, desde la cimentación, los muros, las estructuras y los acabados. Siendo así, el incremento del costo de estos insumos tiene un impacto mayúsculo en el costo de la construcción en general.

Posteriormente, el Gobierno del Estado de Nayarit anunció que se "asignará por concurso las concesiones en los nuevos bancos de materiales, regulados para su explotación con el cumplimiento estricto de mandatos legales en la materia" [2]. Afirmó que solo podrán participar interesados con capacidad técnica.

Hasta esta fecha, no se han hecho los procesos para renovar las concesiones de las minas en el cerro de San Juan, por lo que aún traen materiales pétreos de otras regiones para su uso en la construcción. Actualmente el precio promedio del viaje de arena o grava de 7 metros cúbicos ronda en los $4,000 en promedio, llegando en algunos casos a los $7,000, lo que ha incidido que el Estado de Nayarit sea uno de los lugares más caros para construir en México.

Región	Estados	Precio en pesos promedio por m2	Variación % anual
Centro-Sur	Ciudad de México, Estado de México, Hidalgo y Morelos	$29,201	-1.40%
Sureste	Quintana Roo, Yucatán, Campeche y Tabasco	$20,999	0.10%
Oeste	Colima, Jalisco, Michoacán y Nayarit	$19,004	9.40%
Noreste	Coahuila, Nuevo León y Tamaulipas	$18,884	9.20%
Noroeste	Baja California, Baja California Sur, Chihuahua, Durango, Sinaloa y Sonora	$18,106	4.20%
Centro-Norte	Aguascalientes, Guanajuato, Querétaro, San Luis Potosí y Aguascalientes	$15,982	4.10%
Oriente	Puebla, Veracruz y Tlaxcala	$14,408	10.70%
Suroeste	Chiapas, Guerrero y Oaxaca	$14,334	4.40%

Figura III. Precio y variación anual por región y estado.

Este dato fue obtenido de un estudio realizado por Grupo Tinsa, el cual fue publicado por el Economista [3], de donde se obtuvo el anterior cuadro comparativo del precio de construcción por metro cuadrado.

2.1. Aspectos técnicos de los materiales actuales. - En 2019 desarrollamos un proyecto de investigación que determinó las características de gravas y arenas disponibles en las ciudades de Tepic, Nayarit. Dicho proyecto fue apoyado por el programa de fortalecimiento de cuerpos académicos del Prodep en 2019. Los resultados de los análisis de los materiales recopilados en ese primer proceso fueron publicados en el año 2021 [4]. A continuación, se muestran algunos de los resultados que se generaron en dicho proceso de investigación, correspondientes al banco de materiales Cladimaco, ubicado en el Cerro de San Juan.

En dichas gráficas se puede apreciar que los materiales analizados no cumplían con absoluto rigor a lo que indica la normatividad vigente, sin embargo, los resultados estaban bastante cercanos y sólo requerirían algunos ajustes para cumplir las normas aplicables [5].

Las normas que se aplicaron en la revisión de los materiales se listan a continuación:

- NMX-C- 073-ONNCCE-2004, Industria de la construcción, Agregados, Masa Volumétrica, Método de Prueba
- NMX-C-164-ONNCCE-2014, Industria de la construcción, Agregados, Determinación de la densidad relativa y absorción de agua del agregado grueso
- NMX-C-165-ONNCCE-2014, Industria de la Construcción, Agregados, Determinación de la densidad relativa y absorción de agua del agregado fino, método de ensayo
- NMX-C-170-1997-ONNCCE, Industria de la construcción, agregados, reducción de las muestras de agregados obtenidas en el campo al tamaño requerido para las pruebas
- NMX-C-083-ONNCCE-2014, Industria de la construcción, concreto, determinación de la resistencia a la compresión de especímenes, método de ensayo
- NMX-C-111-ONNCCE-2014. Industria de la construcción, Agregados para concreto hidráulico, especificaciones y métodos de ensayo
- NMX-C-109-ONNCCE-2013, Industria de la construcción, Concreto Hidráulico, Cabeceo de especímenes

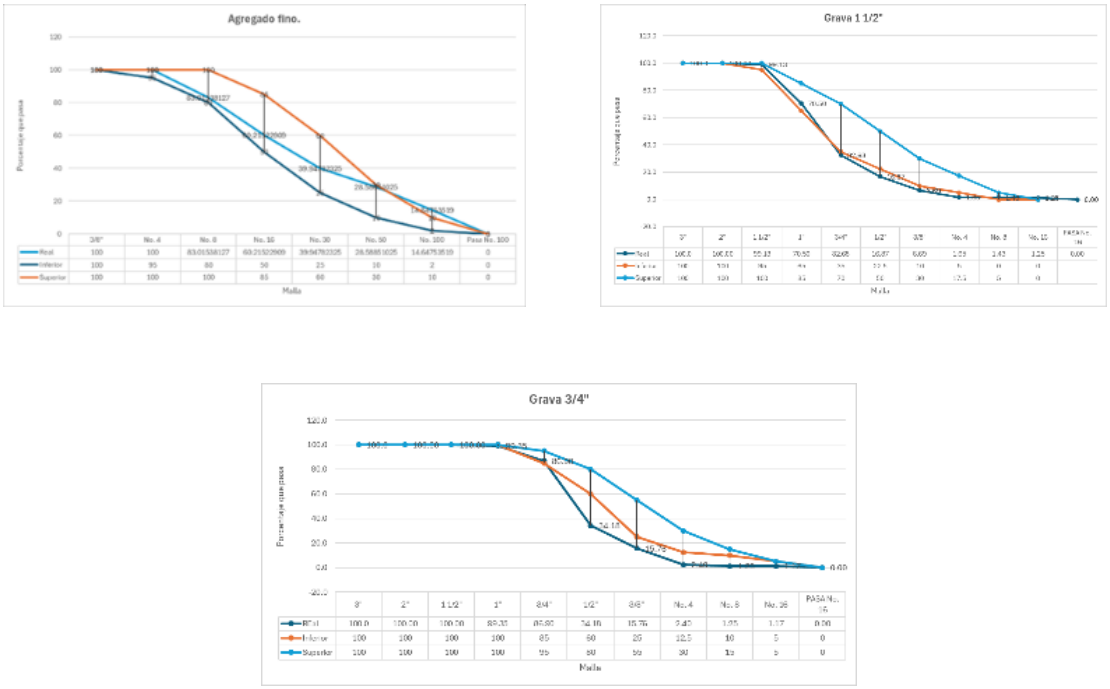

Figura IV. Gráficas de los resultados de los análisis de materiales del banco de materiales Cladimaco, 2019. Fuente: elaboración propia

Con respecto a su utilización en la elaboración del concreto, los resultados que se obtuvieron llevaron a concluir que se producían concretos que cumplían la normatividad y que sería necesario hacer los diseños de mezcla apropiados para asegurar que el concreto utilizado en las obras sea el que se especifique para cada caso específico.
Esta situación siempre ha sido difícil de cumplir, especialmente en obras de tamaño mediano o menores, como es el caso de las casas habitación promedio, donde definitivamente no hay la seguridad de que los concretos que se utilicen durante su construcción tenga la resistencia a la compresión adecuada. Tal vez en obras de mayor envergadura, donde se utiliza concreto premezclado, el diseño se hace por las empresas que lo suministran y sus procesos de diseño de mezcla, fabricación y de control de calidad son cumplidos con mayor rigor ya que es parte de su servicio y su responsabilidad.

El detalle principal es que no hay una entidad que se encargue de vigilar que la producción de los materiales de construcción cumpla las normas vigentes, y el reglamento de construcción no indica que se deban cumplir dichas normas y mucho menos establece los medios para verificar ese cumplimiento.

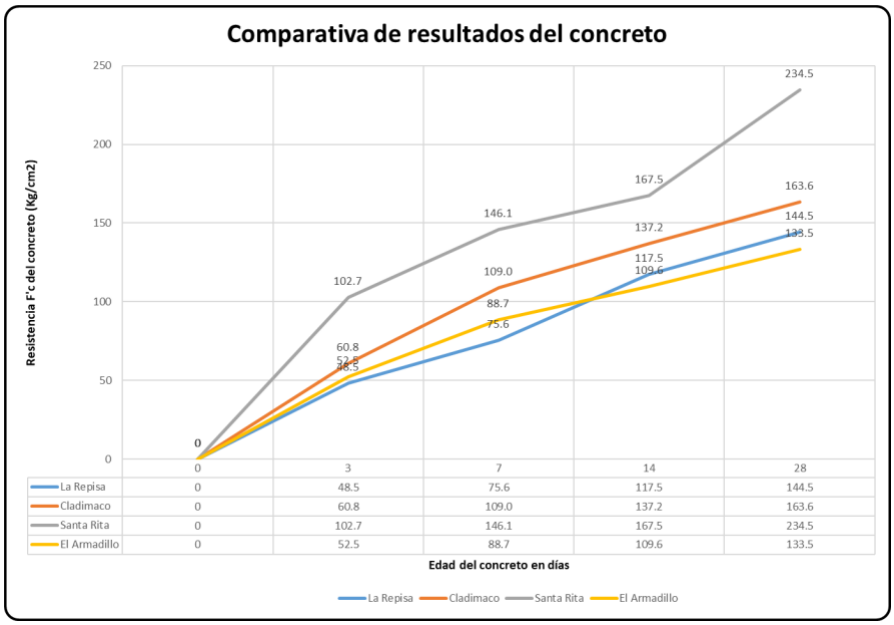

Figura V. Resultados de las pruebas de concreto realizado con los materiales en el año 2019. Fuente: elaboración propia

Con respecto a los materiales que se están usando a partir de la clausura de la explotación del cerro de San Juan en las ciudades de Tepic y Xalisco, se obtuvieron arenas y gravas de proveedores que los suministran al público en general. Este proceso se llevó a cabo como parte del desarrollo de una investigación por alumnos de la carrera de Ingeniería Civil del Instituto Tecnológico de Tepic, durante el semestre enero junio 2024. Cabe especificar que, si bien los materiales fueron obtenidos directamente de los proveedores, los ensayos de laboratorio fueron desarrollados por 2 equipos diferentes de alumnos para validar los resultados.
Los análisis granulométricos de los materiales arrojaron los resultados que se muestran a continuación.

Proveedor Cladimaco. -

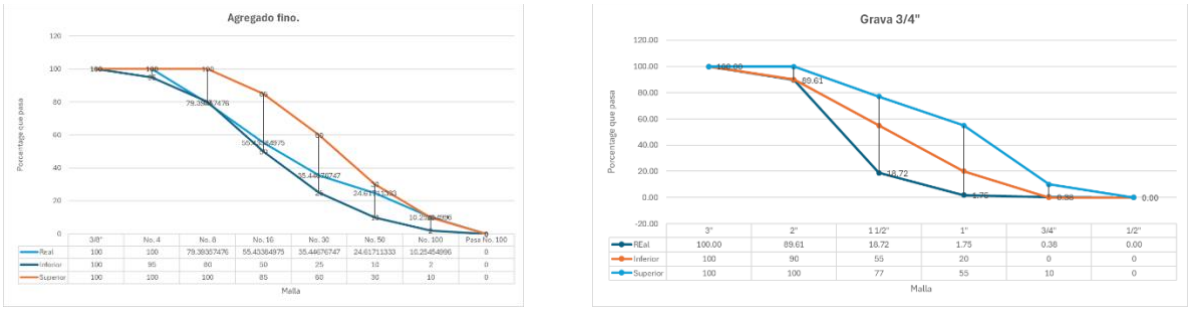

Figura VI. Resultados de las pruebas a los materiales del proveedor Cladimaco. Fuente: elaboración propia

En ambas gráficas se observa que la arena sí cumple y la grava definitivamente no cumple con la granulometría que indica la normatividad vigente. Estos materiales son producto de las explotaciones que se hicieron antes del cierre definitivo de los bancos del cerro de San Juan, y que al estar ya procesados el gobierno permite su venta para su aprovechamiento.

Proveedor Tepic. –

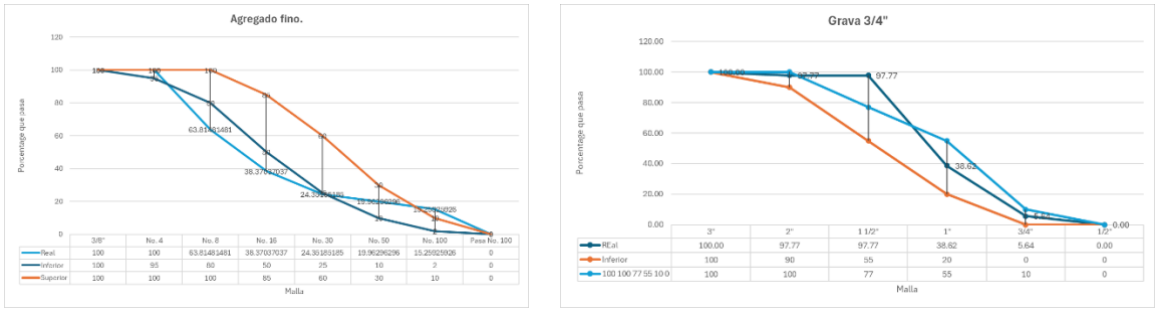

Figura VII. Resultados de las pruebas a los materiales del proveedor Tepic. Fuente: elaboración propia

La tendencia de ambos materiales se acerca a la distribución de granulometría que marca la norma, aunque en ambos casos se pueden hacer mejoras para lograr mejores resultados.

Proveedor Arza. -

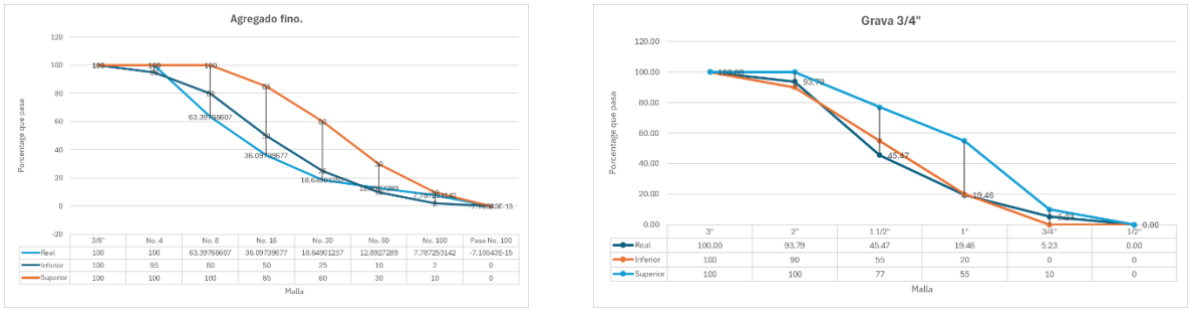

Figura VIII. Resultados de las pruebas a los materiales del proveedor Arza. Fuente: elaboración propia

Ambos materiales tienen una granulometría que está fuera de los márgenes que indica la norma actual. Sería necesaria una revisión de los procesos de producción del banco (trituración, cribado, homogenización) para realizar los ajustes que permitan asegurar un mejor material.

Proveedor Gonzag. -

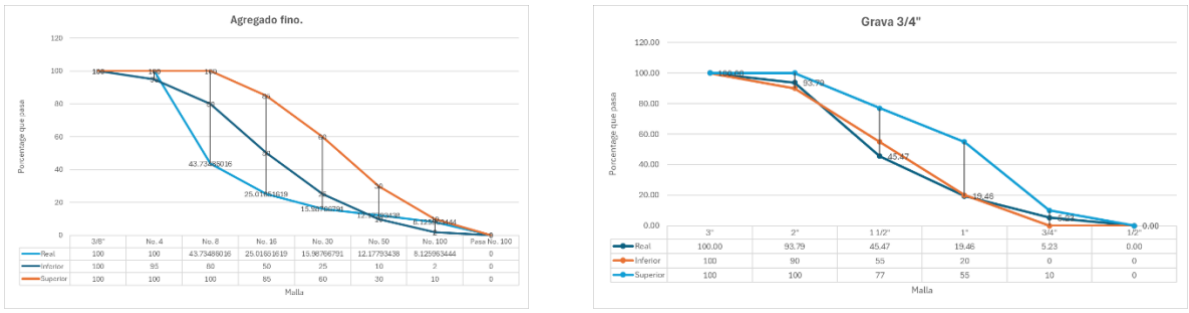

Figura IX. Resultados de las pruebas a los materiales del proveedor Gonzag. Fuente: elaboración propia

La arena que entrega este proveedor está muy fuera de rango con respecto a los límites que marca la norma, por lo que se deduce que tiene pocos finos y requiere que su proceso de fabricación sea mejorado. Con respecto a la grava de ¾”,

los resultados son bastante aceptables, aunque presenta también una pequeña cantidad de material fino. Esta grava es la que tiene un mejor perfil de granulometría de todas las que fueron analizadas.

2.2. Resultados de pruebas a concretos. - Para poder comparar los concretos que se producen con los materiales que ofrecen los distintos proveedores, se realizó un diseño de mezcla para un concreto f'c=250 kg/cm2, que se aplicó para todos los materiales de los proveedores. Este diseño consistió en la siguiente proporción de materiales:

Cemento PCP-30: 1.9345 Kgs
Arena: 2.8143 Kgs
Grava: 3.4079 Kgs
Agua: 1.088 Lts

Se realizaron las mezclas de los concretos con estas proporciones y se generaron los cilindros de concreto para realizar las pruebas a compresión correspondientes, previo proceso de curado. Los resultados que se obtuvieron se muestran en la siguiente gráfica.

En general los resultados obtenidos de los concretos son aceptables, sólo los materiales del proveedor Gonzag muestran un resultado menor que podría requerir mayor vigilancia cuando sean utilizados, aunque podemos establecer que sí son funcionales para la fabricación de concreto estructural, y con el uso del procedimiento generalmente aceptado del se pueden realizar ajustes que permitan mezclas de resistencia apropiada y baja variabilidad.

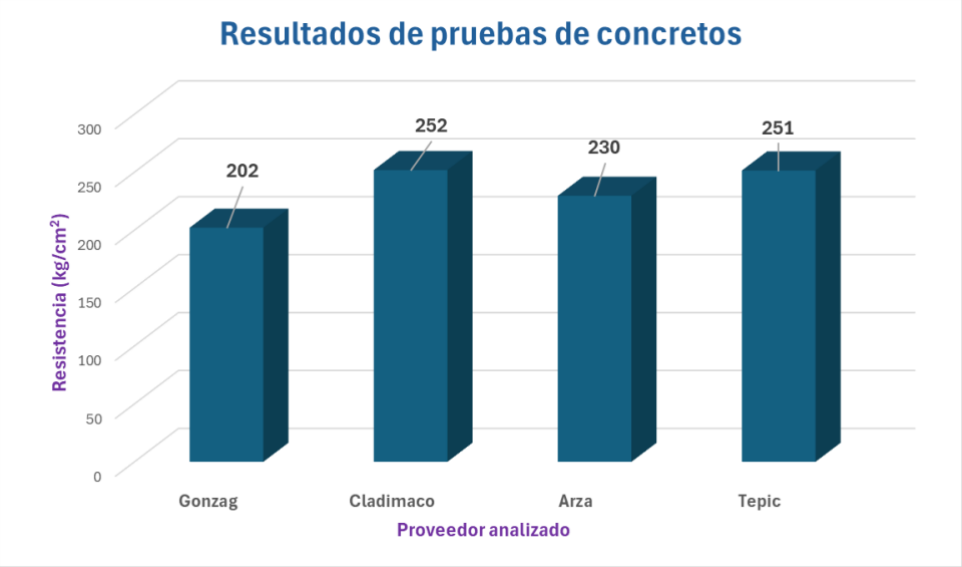

Figura X. Resultados de las pruebas a los concretos fabricados con los materiales de los diferentes proveedores. Fuente: elaboración propia.

3. Conclusiones. - De acuerdo con lo que ha sucedido en el mercado de la construcción en Nayarit desde el año 2022 a la fecha, periodo en el cual se vieron afectados los precios de la construcción en general en el estado por el cierre de los bancos de materiales del cerro de San Juan, podemos establecer las siguientes afirmaciones:

- El costo de los materiales pétreos afecta directamente al mercado de la construcción e indirectamente a muchos otros actores económicos que coexisten, ya que se ven afectados los trabajadores que ya no tendrán el mismo poder adquisitivo, y al ser principalmente personas de bajos recursos, el impacto social es notable.
- Los precios de las casas en el mercado se incrementaron hasta en un 50% de manera inmediata, ya que la falta de capacidad de construir nuevas edificaciones hizo que las que estaban disponibles subieran su precio de venta.
- Las decisiones políticas que se toman sin hacer los estudios previos que permitan implementar medidas que atenúen los efectos de la aplicación de estos actos, generan repercusiones que posteriormente no se pueden

solucionar de forma simple. Actualmente el precio de los materiales pétreos en Tepic y Xalisco es 5 veces mayor al que había antes de tomar la decisión mencionada en esta ponencia.

- Es necesario implementar medios técnicos que aseguren que los materiales de construcción que se usan actualmente cumplan las normas y reglamentos correspondientes, para mitigar los efectos que puedan ser generados por acciones externas a la construcción misma.
- Se requiere la revisión y actualización de los reglamentos de construcción de los municipios del Estado de Nayarit, para que se logre un mejor control de los materiales que se utilizan en los diferentes proyectos de construcción, así como de articular los procesos necesarios para que se cumplan las indicaciones de las normas y reglamentos de construcción aplicables en cada caso específico.
- Esta es un área de oportunidad para el Instituto Tecnológico de Tepic, para poder articular acciones que, en conjunto con las cámaras relacionadas con la industria de la construcción (CMIC, CNEC, Canacem, Canadevi), los colegios de ingenieros y arquitectos, además de los gobiernos estatal y municipales, logren incidir en la sociedad del Estado de Nayarit, asegurando materiales de mejor calidad, así como construcciones funcionales y seguras.

References

[1] Gobierno del Estado de Nayarit. (2022, Mayo) Gobierno de Nayarit. [Online]. https://www.nayarit.gob.mx/detiene-miguel-angel-navarro-quintero-ecocidio-de-tres-decadas-en-el-cerro-san-juan/

[2] Luis Martín Sánchez, "Nayarit: Gobierno licitará extracción de materiales pétreos del cerro San Juan," *La Jornada*, pp. 1-3, May 2022.

[3] Nallely Hernández, "¿Buscas casa? Haz números: precio del metro cuadrado ronda los 19,000 pesos," *El Economista*, Junio 2022.

[4] Carlos Alberto Hoyos Castellanos, Fernando Treviño Montemayor, Alberto González Peña, J. Jesús Vázquez Magaña, and Gabriel Estrada Padilla, "Análisis de gravas y arenas de bancos de materiales para la construcción de las ciudades de Xalisco y Tepic, Nayarit, México," *Revista de la Alta Tecnología y Sociedad*, vol. 13, no. 1, pp. 52-61, 2021.

[5] Organismo Nacional de Normalización y Certificación de la Construcción y la Edificación, S.C., NMX-C-111-ONNCCE-2014, 2014.

Nota contribución de los autores:

1. Concepción y diseño del estudio
2. Adquisición de datos
3. Análisis de datos
4. Discusión de los resultados
5. Redacción del manuscrito
6. Aprobación de la versión final del manuscrito

CAHC ha contribuido en: 1, 2, 3, 4, 5 y 6.
WHHL ha contribuido en: 1, 2, 3, 4, 5 y 6.
FTM ha contribuido en: 1, 2, 3, 4, 5 y 6.
FAC ha contribuido en: 1, 2, 3, 4, 5 y 6.

Nota de aceptación: Este artículo fue aprobado por los editores de la revista Dr. Rafael Sotelo y Mag. Ing. Fernando A. Hernández Gobertti.

Un análisis de modelos hidrodinámicos y una propuesta de cambio cultural basada en predicciones: el caso de la inundación del Río Grande do Sul, Brasil

An Analysis of Hydrodynamic Models and a Proposal of Cultural Change based on predictions: The case of the Rio Grande do Sul Flood, Brazil

Uma análise de modelos hidrodinâmicos e proposta de mudança cultural baseada em previsões: o caso da enchente do Rio Grande do Sul, Brasil.

Cristiano Trindade[1]

Recibido: 15/01/2025 Aceptado: 25/04/2025

Resumen. - El mayor episodio de crisis climática extrema en Brasil, las inundaciones y anegamientos en el estado de Rio Grande do Sul-RGS en mayo de 2024, han puesto en evidencia la urgente necesidad de repensar la infraestructura urbana y las prioridades de investigación en contextos de falta de acceso al conocimiento y planificación territorial desorganizada. Este estudio tiene como objetivo principal analizar la relación entre la gestión de inundaciones y la implementación de medidas estructurales y no estructurales. A través de una revisión bibliográfica sistemática, se identifican soluciones basadas en modelos hidrodinámicos con potencial de aplicación para prevenir y mitigar inundaciones en entornos urbanos. Asimismo, se realiza una evaluación crítica de las estrategias empleadas durante la gran inundación en Rio Grande do Sul, proponiendo alternativas más efectivas y sostenibles. El RGS también enfrenta problemas culturales con un efecto cascada – intentos graves de separatismo del resto de Brasil y constantes actos de machismo y racismo, con diversas muertes, debido al pensamiento de superioridad – que impactan en la gestión de crisis. A partir de este enfoque, se plantea la siguiente pregunta de investigación: ¿Qué papel desempeña la cultura en la gestión del conocimiento sobre inundaciones y drenaje, especialmente en relación con el uso de modelos hidrodinámicos? Esta cuestión da lugar a la propuesta de un modelo integrado de Inteligencia Cultural, Gestión del Conocimiento y Participación Social, orientado a optimizar el diseño y la implementación de planes de control de inundaciones. Inicialmente, tras un análisis comparativo con los modelos CRESTv2.1, HEC-RAS, MIKE 21, cGAN-Flood, se consideró la aplicación del modelo de pronóstico Hydropol2D; sin embargo, se identificaron limitaciones importantes, como la omisión de los efectos de la actividad agrícola sobre la dinámica hidrológica. En consecuencia, se sugiere reemplazar Hydropol2D por el modelo SWAT+ (Soil and Water Assessment Tool), en combinación con el módulo de agua subterránea (GWFlow), el cual permite una simulación más precisa de los procesos hidrológicos superficiales y subterráneos. Esta herramienta integrada no solo ofrece mayor capacidad para evaluar el impacto de usos del suelo y prácticas agrícolas, sino que también mejora la precisión en la modelación de escenarios de drenaje urbano.

Palabras clave: Cambio cultural, gestión del conocimiento, modelos hidrodinámicos, inteligencia organizacional, SWAT+ GWFlow, planificación urbana.

[1] Doctor en Estrategia y Gestión de Proyectos, Skema Business School, Lille (Francia), cristianotrindade@protonmail.com, ORCID iD: https://orcid.org/0000-0002-8025-7871

Memoria Investigaciones en Ingeniería, núm. 29 (2025). pp. 15-38
https://doi.org/10.36561/ING.29.3
ISSN 2301-1092 • ISSN (en línea) 2301-1106 – Universidad de Montevideo, Uruguay
Este es un artículo de acceso abierto distribuido bajo los términos de una licencia de uso y distribución CC BY-NC 4.0. Para ver una copia de esta licencia visite http://creativecommons.org/licenses/by-nc/4.0/

Summary. - *The largest episode of extreme climate crisis in Brazil, the floods and inundations in the state of Rio Grande do Sul-RGS in May 2024, have highlighted the urgent need to rethink urban infrastructure and research priorities in contexts of lack of access to knowledge and disorganized territorial planning. The main objective of this study is to analyze the relationship between flood management and the implementation of structural and non-structural measures. Through a systematic literature review, solutions based on hydrodynamic models with potential application to prevent and mitigate floods in urban environments are identified. Likewise, a critical evaluation of the strategies employed during the major flood in Rio Grande do Sul is carried out, proposing more effective and sustainable alternatives. The RGS also faces cultural problems with a cascading effect—serious attempts at separatism from the rest of Brazil and constant acts of machismo and racism, with several deaths, due to the belief of superiority—that impact crisis management. Based on this approach, the following research question is posed: What role does culture play in knowledge management about floods and drainage, especially in relation to the use of hydrodynamic models? This question gives rise to the proposal of an integrated Cultural Intelligence, Knowledge Management, and Social Participation model, aimed at optimizing the design and implementation of flood control plans. Initially, a comparative analysis of the CRESTv2.1, HEC-RAS, MIKE 21, and cGAN-Flood models was considered, and the application of the Hydropol2D forecasting model was considered. However, important limitations were identified, such as the omission of the effects of agricultural activity on hydrological dynamics. Consequently, it is suggested to replace Hydropol2D with the SWAT+ (Soil and Water Assessment Tool) model, in combination with the groundwater module (GWFlow), which allows a more precise simulation of surface and subsurface hydrological processes. This integrated tool not only offers greater capacity to assess the impact of land uses and agricultural practices, but also improves the accuracy in modeling urban drainage scenarios. Keywords: cultural change, knowledge management, hydrodynamic models, organizational intelligence, SWAT+ GWFlow, urban planning.*

Keywords: *Cultural change, knowledge management, hydrodynamic models, organizational intelligence, SWAT+ GWFlow, urban planning.*

Resumo. - *O maior episódio de crise climática extrema no Brasil, as enchentes e inundações no estado do Rio Grande do Sul (RGS) em maio de 2024, evidenciaram a necessidade urgente de repensar a infraestrutura urbana e as prioridades de pesquisa em contextos de falta de acesso ao conhecimento e planejamento territorial desorganizado. O principal objetivo deste estudo é analisar a relação entre o manejo de enchentes e a implementação de medidas estruturais e não estruturais. Por meio de uma revisão sistemática da literatura, identificam-se soluções baseadas em modelos hidrodinâmicos com potencial aplicação na prevenção e mitigação de enchentes em ambientes urbanos. Da mesma forma, realiza-se uma avaliação crítica das estratégias empregadas durante a grande enchente no Rio Grande do Sul, propondo alternativas mais eficazes e sustentáveis. O RGS também enfrenta problemas culturais com efeito cascata – sérias tentativas de separatismo em relação ao restante do Brasil e constantes atos de machismo e racismo, com diversas mortes, devido à crença na superioridade – que impactam o manejo de crises. Com base nessa abordagem, formula-se a seguinte questão de pesquisa: Qual o papel da cultura na gestão do conhecimento sobre enchentes e drenagem, especialmente em relação ao uso de modelos hidrodinâmicos? Esta questão leva à proposta de um modelo integrado de Inteligência Cultural, Gestão do Conhecimento e Participação Social, com o objetivo de otimizar o planejamento e a implementação de planos de controle de enchentes. Inicialmente, foi realizada uma análise comparativa dos modelos CRESTv2.1, HEC-RAS, MIKE 21 e cGAN-Flood, considerando-se também a aplicação do modelo de previsão Hydropol2D. Contudo, foram identificadas limitações importantes, como a omissão dos efeitos da atividade agrícola sobre a dinâmica hidrológica. Consequentemente, sugere-se a substituição do Hydropol2D pelo modelo SWAT+ (Soil and Water Assessment Tool), em combinação com o módulo de águas subterrâneas (GWFlow), que permite uma simulação mais precisa dos processos hidrológicos superficiais e subterrâneos. Essa ferramenta integrada não só oferece maior capacidade de avaliação do impacto do uso do solo e das práticas agrícolas, como também aprimora a precisão na modelagem de cenários de drenagem urbana. Palavras-chave: mudança cultural, gestão do conhecimento, modelos hidrodinâmicos, inteligência organizacional, SWAT+ GWFlow, planejamento urbano.*

Palavras-chave: *Mudança cultural, gestão do conhecimento, modelos hidrodinâmicos, inteligência organizacional, SWAT+ GWFlow, planejamento urbano.*

1. Introducción. - Brasil, con su geografía diversa y extensos sistemas fluviales, es altamente propenso a riesgos hidrometeorológicos, incluyendo inundaciones (Marengo et al., 2021, 2020). A lo largo de los años, el país ha experimentado numerosas inundaciones catastróficas que han desempeñado un papel significativo en la configuración de sus marcos de gestión de desastres (Debortoli et al., 2017; Tompkins et al., 2008).

Webber et al. (2024) encontraron que el estado de Rio Grande do Sul (RGS) en Brasil experimentó la mayor crisis climática de su historia en abril y mayo de 2024. Los niveles de lluvia fueron extremadamente altos y las estrategias institucionales y de la sociedad civil fueron insuficientes para prevenir escenarios altamente destructivos, una catástrofe que causó grandes daños a la sociedad (Ferreira, 2024).

El impacto más grave y directo fue en la vida de las personas afectadas por inundaciones urbanas y rurales en ciertas áreas del estado (Figura I).

A finales de mayo de 2024, el número de muertes registradas se acercaba a doscientas personas, había muchas desaparecidas y más de 600.000 personas desplazadas de sus hogares (Sun et al., 2024).

Figura I. Inundación de Porto Alegre, en el Lago Guaíba --- fotografía de Douglas Rohers.

Rio Grande do Sul, como el resto de Brasil, sufre mucho la falta de conocimiento para gestionar sus inmensos recursos naturales y debido a eso la gente más pobre sufre muchas inundaciones. A diferencia de otros países latinos como Uruguay, Argentina, Chile y Portugal, a los brasileños realmente no les gusta leer. De todos los países de América del Sur, que ya es bastante deficitaria en el área de conocimiento pues sus culturas están más centradas en la comunicación verbal debido a la facilidad del idioma, Brasil es el país que menos lee según la Asociación Internacional de Lectura (Conselho Brasil Sul) - datos del 2000, y por eso está constantemente bajo el agua. En los últimos 20 años, 4.255 personas murieron como consecuencia de desastres ambientales en Brasil y otros 8 millones se quedaron sin hogar, según un estudio de la Secretaría Nacional de Defensa y Protección Civil. El índice representa una pérdida económica de R$ 24 mil millones y 212 muertes al año, en promedio.

El número de accidentes que involucran aviones también es bastante alto (129 accidentes desde 1915).

Según la Asociación Internacional de Lectura Conselho Brasil Sul -datos de 2000-, mientras los brasileños leen en promedio 1 libro al año, chilenos, uruguayos y argentinos leen 4 libros en el mismo período. En comparación con los países más desarrollados, los lectores brasileños son aún más escasos: en los países desarrollados se leen alrededor de 20 libros al año por cada habitante.

La Cámara Brasileña del Libro (CBL, 2024), en la sexta edición de su estudio “Retratos de la Lectura en Brasil”, reveló que en los últimos cuatro años se ha producido una disminución de 6,7 millones de lectores, lo que implica que el 53% de la población no había leído ni una parte de un libro en los tres meses previos al estudio.

La falta de acceso al conocimiento y del deseo de adquirirlo, sumada a la abundancia de distracciones, además de la influencia de las playas (donde los latinos tienden a abrir bares y restaurantes en lugar de negocios), y la constante acumulación de información, dificulta la comprensión de los hechos. Por ello, la OCDE constató que Brasil es el país con mayor índice de creencia en noticias falsas entre 21 países (OCDE, 2024).

Según el IBGE (2020), en Brasil hay alrededor de 30 millones de personas analfabetas funcionales. Es muy extraño que Brasil, siendo la décima economía más grande del mundo, tenga 62,5 millones de personas (29,4% de la población brasileña) viviendo en la pobreza y, entre ellos, 17,9 millones (8,4% de la población) son extremadamente pobres (Banco Mundial, 2021).

Varios autores denuncian la indiferencia del gobierno hacia los más pobres y aquellos sin acceso al conocimiento en Brasil (Macedo, 2024; Silva e Silva, 2010; Menezes, 2019; Pitombeira e Oliveira, 2025; Souza, 2018; Libâneo, 2016). En Brasil, alrededor de 33 millones de personas viven sin acceso a agua potable y 100 millones de personas no tienen sistema de alcantarillado, según datos divulgados por el Instituto Trata Brasil.

En el caso que nos ocupa, en cuanto a la falla del sistema de protección de Porto Alegre, Capital do RGS, si se hubiera realizado la operación y mantenimiento, los efectos de la inundación se habrían minimizado.

De hecho, un documento firmado por más de 40 ingenieros y técnicos de saneamiento afirma que el sistema de protección contra inundaciones de Porto Alegre falló porque no recibió el mantenimiento necesario[2].

El sistema cuenta con varias bombas y compuertas y la falla de solo una de ellas podría provocar el colapso del sistema. En particular, en el evento de mayo de 2024, de acuerdo con el Departamento Municipal de Agua e Esgoto- DMAE, una de las compuertas falló y el sistema eléctrico de la sala de máquinas no estaba diseñado para funcionar inundado. En este caso, para evitar el riesgo de descarga eléctrica, se apagó todo el sistema de bombeo, provocando un efecto cascada.

En entrevista, la Máster en Planificación Urbana y Regional, ingeniera Nanci Giugno explicó que “la ciudad cuenta con dos sistemas: compuertas y drenaje. Ambos no funcionaron”[3] .

Además de los procesos de operación y mantenimiento del sistema, un modelo de pronóstico de inundaciones es de gran valor para la gestión de inundaciones. Es posible, con un horizonte de previsión de 1-2 días, predecir con cierta precisión el impacto de las inundaciones en las ciudades.

Según Nonnemacher y Fan (2023), por cada real gastado en sistemas de prevención de inundaciones, se pueden ahorrar alrededor de R$ 40,00 reduciendo los posibles daños por inundaciones en Rio Grande do Sul. Para una correcta prevención, un sistema que cuente con nuevas estaciones pluviométricas, un equipo con acceso a conocimiento relevante en Hidrología, Agricultura e Geografía y generación de resultados efectivos.

A nivel de pronóstico, es necesario no sólo pronosticar las precipitaciones, sino también el nivel del agua, la profundidad de las calles, manzanas y todo el sistema de infraestructura de las ciudades. En las ciudades que no cuentan con sistemas de protección contra inundaciones (es decir, diques), la previsión y la alerta, especialmente a la hora de viajar, son esenciales para reducir los impactos de las inundaciones. Para ello se necesitan datos precisos de estaciones de seguimiento y modelos adecuados y rápidos para predecir los efectos de la inundación. La acción conjunta de unas adecuadas previsiones y un correcto seguimiento de las estructuras de protección es la estrategia ideal para la gestión de inundaciones.

[2]https://g1.globo.com/jornal-nacional/noticia/2024/05/23/engenheiros-afirmam-que-porto-alegre-nao-fez-a-manutencao-adequada-do-sistema-de-protecao-contra-inundacoes.ghtml

[3]https://sul21.com.br/noticias/geral/2024/05/eu-nao-teria-aberto-as-comportas-diz-ex-diretor-do-dep-e-do-dmae

Según una nota técnica titulada “Criterios hidrológicos para la adaptación al cambio climático: Lluvias e inundaciones extremas en la Región Sur de Brasil” publicada recientemente por Paiva et al. (2024) los proyectos de infraestructura o planificación a gran escala, para los cuales se suelen adoptar tiempos de retorno de 50 años o más, deben poder superar la mayor inundación de la historia, independientemente del tiempo de retorno estimado para esta inundación. Por definición, un tiempo de retorno (TR) es un intervalo de tiempo en años en el que una inundación ocurre en promedio al menos una vez.

La planificación urbana de las ciudades generalmente establece riesgos tolerables asociados a estos sistemas, de manera que los sistemas de microdrenaje (es decir, galerías pluviales, drenajes pluviales) se diseñan para tiempos de retorno del orden de 10 a 25 años, mientras que las obras de macrodrenaje, es decir, las asociadas Los ríos y canales con mayor magnitud suelen estar diseñados para tiempos de retorno del orden de 50 a 100 años. Con el cambio climático se debe revisar el concepto de riesgo tolerable para los proyectos de drenaje debido a la no estacionariedad de las precipitaciones. Es decir, es necesario un gran Proyecto de Macrodrenaje Urbano para hacer frente a incidentes de inundaciones.

Conceptualmente, es claro que es necesario disminuir el caudal de los cuatro ríos que fluyen sobre el lago Guaíba y luego sobre las seis estaciones de bombeo de agua cruda - EBAB (cinco en Guaíba y una en Jacuí), y también sobre las seis represas (tres en Bento Goncalves). Para ello es necesario elaborar estudios detallados sobre el comportamiento hidrológico-hidráulico de las cuencas de cada uno de los ríos que sirvan de base para un enfoque integrado de la planificación de las cuencas hidrológicas, en particular de las aguas superficiales y subterráneas.

Rathore et al. (2025) enfatizan la necesidad crítica de una gestión integrada de cuencas hidrográficas y sistemas mejorados de pronóstico de inundaciones para mitigar los riesgos de inundaciones futuras.

Hay dieciocho represas en Rio Grande do Sul, y en mayo de 2024 seis se encuentran en situación de emergencia, con riesgo inminente de falla, una de las cuales ya se ha roto parcialmente. Debido a la gran pendiente de la cuenca del río Taquari-Antas, un gran volumen de escorrentía llega rápidamente al complejo de presas, especialmente cuando las lluvias se distribuyen con mayor intensidad en la cabecera de la cuenca, como ocurrió con este evento en mayo de 2024. Según una técnica publicada recientemente por el Instituto de Investigaciones Hidráulicas (IPH) , algunas estaciones pluviómetros registraron acumulaciones de lluvia superiores a los 1000 mm en dos semanas. En varias temporadas, el volumen de precipitación en este corto período de tiempo fue superior al 40% del volumen esperado para todo el año. Algunos procesos de descarga de inundaciones pueden gestionarse en pequeños embalses a lo largo del río. Estos embalses no sólo atenúan los volúmenes de escorrentía, sino que también reducen la alta concentración de contaminantes transportados por la escorrentía y, por tanto, sus impactos en las operaciones de las plantas potabilizadoras. Sin embargo, en el caso de una gran inundación como la ocurrida en mayo de 2024, la solución de medidas estructurales como el uso de embalses es prácticamente inviable dado el gran volumen que sería necesario almacenar para tener mínimos efectos de mitigación. Las medidas no estructurales pueden ser el camino más coherente para el futuro y, en el caso particular de las medidas estructurales, se deben realizar estudios detallados para evitar posibles daños e impactos ambientales.

En consecuencia, Rathore et al. (2025) destacan que la intensidad creciente de eventos climáticos extremos, en gran parte impulsado por el cambio climático antropogénico, ha resultado en cambios en los patrones de precipitación. El cambio en el patrón contribuye a un aumento en la frecuencia y la gravedad de los eventos de inundación (Meng et al., 2025; Mitchell et al., 2006; Wasko et al., 29 2021).

Uno de los principales causantes de los gases de efecto invernadero son los fertilizantes químicos, y esta investigación sugiere el uso de polvo de roca como sustituto, particularmente en el cultivo Gaucho (RGS) donde los agricultores tienen mayor tendencia a utilizar fertilizantes rusos.

Este trabajo se divide en cuatro capítulos. La primera sección proporciona un análisis comparativo de modelos hidrodinámicos. La sección analiza la cultura brasileña, con foco en la cultura gaucha (RGS). La sección 3 aborda la importancia de los planes de emergencia estándar para la gestión de riesgos y la participación social basados en las prácticas de GC e IO. La sección 4 finalmente presenta los modelos Cultura – Conocimiento – Inteligencia (CCI) con base en lo expuesto en las secciones anteriores.

2. Un análisis comparativo de modelos hidrodinámicos. - Rathore et al. (2025) identifican las zonas afectadas por las inundaciones de mayo de 2024 en Porto Alegre, Brasil, utilizando técnicas avanzadas de teledetección y geoespaciales. Estos conjuntos de datos combinan observaciones de teledetección y datos geoespaciales auxiliares, cada uno de los cuales aporta información crucial para la delimitación precisa de la extensión de las inundaciones y la evaluación del impacto, mediante la integración de imágenes multiespectrales de Sentinel-1 SAR, Sentinel-2 y PlanetScope, y contornos derivados del DEM de Copernicus.

Chen et al. (2023) explican que el ciclo hidrológico es complejo y que los modelos hidrológicos precisos pueden ayudarnos a comprender mejor el ciclo hidrológico y a tomar decisiones informadas sobre la gestión del agua.

Según Rennó y Suares (2022), un modelo hidrológico se puede definir como una representación matemática del flujo de agua y sus componentes sobre una determinada área de la superficie y/o subsuelo de la Tierra. En este sentido, los modelos hidrodinámicos, que resuelven las ecuaciones fundamentales del flujo, pueden ser utilizados para predecir el comportamiento de las inundaciones.

Existe una estrecha interrelación entre la modelización hidrológica, biológica y ecológica, ya que el transporte de materiales a través del agua está influenciado por actividades biológicas, que pueden aumentar o reducir la concentración de estos materiales. Además, el régimen de flujo del agua tiene un impacto en diversos hábitats.

Los modelos hidrodinámicos se construyen para analizar los procesos que ocurren cuando los fluidos fluyen, no limitándose a flujos "laminares", sino también a flujos "turbulentos", como los que se producen durante grandes inundaciones.

Los modelos hidrodinámicos ambientales son herramientas fundamentales para la gestión y planificación de intervenciones en cuerpos de agua naturales, ya que permiten analizar tres fenómenos clave (ROSSMAN, 2001):

- Circulación Hidrodinámica: Evalúa los cambios en las cantidades de movimiento (masa × velocidad), que generan variaciones en los niveles y corrientes del agua.
- Calidad del Agua: Examina el transporte de sustancias que afectan la composición del agua y su calidad.
- Procesos Sedimentológicos: Analiza los ciclos de erosión, transporte y deposición de sedimentos que afectan la morfología o morfodinámica.

El propósito de estos modelos es simular los movimientos, transportes, caudales y flujos de agua y sus componentes (gases, salinidad, nutrientes, calor, sedimentos, entre otros).

Stokes Oceanografía (2023) divide el proceso de modelización en 10 pasos: 1) Elaboración de un modelo conceptual del fenómeno; 2) Recolección de datos de entrada; 3) Definición de los límites del dominio numérico; 4) Digitalización del litoral o, en el caso de cuencas fluviales, utilización de modelos de elevación del terreno; 5) Construcción de una malla numérica para discretizar el espacio en intervalos finitos; 6) Generación de la batimetría de ríos, canales y embalses; 7) Definición de los escenarios de simulación y condiciones de contorno; 8) Configuración y montaje de rondas de simulación; 9) Análisis de los resultados; y 10) Repetición del proceso hasta que los resultados simulados se aproximen a los observados, para finalmente presentar los resultados.

En Brasil, el Portal HidroWeb es la fuente de datos más utilizada en estudios hidrológico-hidrodinámicos. Esta herramienta proporciona acceso a la información recopilada por la Red Hidrometeorológica Nacional (RHN), gestionada por la Agencia Nacional del Agua (ANA), como series históricas de caudales observados, batimetría, entre otros. Sin embargo, las observaciones de flujo no son los únicos datos necesarios para los modelos hidrológicos e hidrodinámicos. Es imprescindible contar con modelos más completos que incluyan el comportamiento de las cuencas fluviales, el contenido de humedad del suelo, las propiedades topográficas, el uso del suelo y los datos sobre la distribución temporal y espacial de las precipitaciones, lo cual complica aún más el proceso de modelización. En países como Estados Unidos, se dispone gratuitamente de mapas y series completas de alta resolución a nivel nacional, lo que facilita la construcción de modelos de predicción de inundaciones.

Rathore et al. (2025), por ejemplo, utilizaron datos diarios de precipitación satelital de la colección GPM-IMERG Nivel 3 de Ejecución Tardía (https://gpm.nasa.gov/data/directory/) disponible con una resolución espacial de 10 km (Huffman et al., 2019) para examinar los eventos de precipitación extrema que provocaron inundaciones en Brasil (RGS) a principios de mayo de 2024.

Es importante señalar que no siempre estarán disponibles las series de datos de caudales para un río y período específicos. Los ríos pequeños, por ejemplo, no están incluidos en la red de monitoreo de la Agencia Nacional de Aguas - ANA. Sin embargo, es posible obtener estos datos indirectamente, mediante cálculos de proporcionalidad de áreas de cuencas cercanas o a través de curvas de lluvia y escorrentía. Estas "regionalizaciones" pueden servir para estimar caudales en ríos de menor tamaño, aunque en eventos extremos, estos métodos no son aplicables.

Getirana et al. (2012) señalan que las superficies de aguas abiertas dependen en gran medida de la geometría y topografía de los ríos. La geometría influye en la posibilidad de desbordamiento del río, mientras que la topografía determina el área inundada en función del volumen de agua desbordado. No obstante, ambos factores presentan limitaciones debido a los problemas con los datos de entrada requeridos. Los errores en los Modelos Digitales de Elevación (MDE) continúan siendo una de las principales fuentes de incertidumbre al modelar las interacciones entre ríos y llanuras aluviales. En particular, los MDE basados en satélites no son adecuados para proporcionar perfiles precisos de elevación de llanuras aluviales. El enfoque de "quema de llanuras aluviales", que toma en cuenta mapas detallados de ríos y llanuras, ha demostrado ser eficaz para ajustar gradualmente las elevaciones de los píxeles en zonas inundadas (Getirana et al., 2012).

Gomes Júnior et al. (2023) explican que los modelos hidrológicos, hidrodinámicos y de transporte de contaminantes son esenciales para la toma de decisiones en la mitigación de inundaciones y la mejora de la calidad del agua (Fan y Collischonn, 2014). Existen diversos modelos en la literatura que permiten cuantificar procesos hidrodinámicos a distintas escalas temporales y espaciales.

A nivel de eventos de respuesta rápida y cuencas urbanas, el modelo 2D de autómatas celulares ponderados (WCA2D) (Guidolin et al., 2016) utiliza un enfoque basado en autómatas celulares para distribuir la escorrentía y estimar mapas de inundación en la superficie del agua. Este modelo ha demostrado ser útil para realizar simulaciones de inundaciones a gran escala debido a su alto rendimiento computacional y bajo requerimiento de memoria, con un compromiso mínimo en precisión, lo que facilita realizar una gran cantidad de simulaciones para análisis de riesgos. Este modelo 2D de inundaciones terrestres se integra con el modelo 1D CADDIES para redes de alcantarillado, desarrollado por Austin et al. (2014), lo que proporciona un modelo simplificado de drenaje urbano para el modelado de inundaciones urbanas. Sin embargo, en grandes inundaciones, el efecto del micro drenaje se reduce significativamente frente a los grandes volúmenes de precipitación y escorrentía generados.

Un enfoque reciente de juegos serios es el desarrollado por Gomes Jr. (2024), que creó un juego para simular el colapso de una presa y permitir a los usuarios comprender la magnitud de la fuerza del agua que llegaría a una ciudad, su altura y velocidad. Este juego se aplicó a 21 represas, incluyendo Brumadinho y la represa 14 de Julho. Además, Gomes Junior et al. (2023) destacan el modelo HydroPol2D, que contribuye al campo de los modelos hidrológicos e hidrodinámicos al permitir el modelado 2D de inundaciones y calidad del agua, simulando la transferencia de impulso

de las llanuras de inundación, el cálculo de la infiltración y evapotranspiración distribuida espacialmente, así como el transporte y destino de contaminantes. Estos enfoques proporcionan un análisis más integrado del comportamiento hidrológico de las cuencas fluviales, contribuyendo a una mejor comprensión de los procesos que influyen en la escorrentía de los ríos.

HydroPol2D also advances hydroinformatics by creating a fully explicit numerical model coupled with an adaptive time-stepping method to guarantee numerical stability for the water quantity and quality models of HydroPol2D. Moreover, HydroPol2D also allows the use of Graphics Processing Unit (GPU) calculations and have open source versions in Matlab and Python (Gomes Junior et al., 2023).

El software HEC-RAS, desarrollado por el Cuerpo de Ingenieros del Ejército de los Estados Unidos, permite simular flujos bidimensionales a partir de la resolución numérica de ecuaciones de aguas someras. Este modelo incorpora varios factores, como la inercia, el gradiente de presión, los efectos gravitacionales, la fricción, la turbulencia y los efectos de Coriolis, que describen cómo las corrientes de agua y aire se comportan en diferentes hemisferios. Sin embargo, uno de los principales desafíos de HEC-RAS es su alto coste computacional, especialmente cuando se intenta simular inundaciones a alta resolución. Los detalles de las formulaciones y los esquemas numéricos utilizados en la versión 6.1.0 del modelo se describen en Brunner (2016).

Para la creación de un mapa topográfico compuesto, se fusionaron múltiples bases de datos. En la región del río Amazonas y en áreas de aguas abiertas de la llanura aluvial, se utilizó la topografía estimada por Fassoni-Andrade et al. (2020a), con una resolución espacial de 30 metros (disponible en data.mendeley.com/datasets/vn599y9szb/1). Este mapeo fue realizado digitalizando cartas náuticas de los ríos y aplicando el método Flood2Topo (Fassoni-Andrade et al., 2020) a partir de datos ópticos satelitales (Gomes Júnior et al., 2023).

Lago et al. (2024) evaluaron el desempeño del modelo HEC-RAS comparándolo con un modelo propuesto que empleaba el cGAN-Flood para predecir inundaciones en siete cuencas urbanas de las ciudades de San Antonio y São Paulo. Los resultados mostraron que el uso de MAP junto con cGAN-Flood mejoró la precisión en los mapas de inundaciones, identificando las áreas inundadas y estimando las profundidades del agua. Sin embargo, el modelo subestimó en algunos casos el volumen total de inundación (vt). Además, el cGAN-Flood no es capaz de predecir velocidades de flujo, un parámetro clave para la generación de mapas de riesgo. Otra limitación es que el modelo cGAN-Flood solo fue entrenado para predecir la expansión de inundaciones, lo que restringe su uso en situaciones con variabilidad en los datos de entrada o cuando se requieren pronósticos de inundaciones más detallados.

Pese a estas limitaciones, cGAN-Flood demostró ser 50 y 250 veces más rápido que los modelos WCA2D y HEC-RAS, respectivamente. Sin embargo, para mejorar su aplicabilidad, se necesitan más investigaciones. El uso de herramientas de inteligencia artificial, que a menudo carecen de un aprendizaje profundo sobre el comportamiento hidrológico de las cuencas fluviales, debe hacerse con cautela, dado el déficit de datos observacionales de calidad. La implementación a gran escala de estas técnicas requiere un escenario con amplios datos de monitoreo de inundaciones, donde se puedan entrenar modelos de aprendizaje automático basados en observaciones confiables del comportamiento de las cuencas.

En un estudio realizado por Fassoni-Andrade et al. (2023), se explicó cómo el modelo HEC-RAS utiliza una malla computacional no estructurada, cuya orientación y tamaño de las celdas varían según la topografía. Esto permite incluir saltos topográficos para definir la orientación de las celdas computacionales. Los investigadores también aplicaron pausas para digitalizar manualmente los contornos topográficos de las riberas de los ríos. En las zonas de llanura aluvial, las isolíneas correspondientes a umbrales de frecuencia de inundación del 90% y 60% fueron obtenidas a partir del mapa de frecuencia de inundaciones desarrollado por Fassoni-Andrade et al. (2020).

Los errores en la cartografía topográfica, las condiciones de los límites aguas abajo y la falta de representación de procesos hidrológicos en la llanura aluvial, como la infiltración local, la precipitación, la evaporación y el flujo de aguas

subterráneas, son fuentes de incertidumbre al modelar la extensión de las inundaciones. Esto es especialmente relevante durante períodos de escasez de agua (Fassoni-Andrade et al., 2023).

Por otro lado, Long et al. (2023) mejoraron las simulaciones de flujo mediante la combinación de modelos hidrológicos e hidrodinámicos. Construyeron un modelo hidrológico utilizando la herramienta de evaluación de la cuenca del lago Dongting (SWAT), que simula el flujo actual en áreas con pocos datos, y lo combinaron con el sistema hidrodinámico MIKE21, un modelo que incluye condiciones de contorno adicionales y ajusta las escalas características de los datos de entrada. Este enfoque de modelización es útil cuando se enfrenta la falta de datos en áreas específicas.

Un proceso comúnmente utilizado en la modelización es la regionalización (Arsenault et al., 2019) [2], que consiste en transferir información hidrológica desde áreas con datos de medición a aquellas que carecen de ellos (Bao et al., 2012; Yang et al., 2020) [3] [31]. Jillo et al. (2017) [19] aplicaron un modelo de lluvia-escorrentía en áreas de observación con escasos datos, utilizando este método de regionalización para estimar la producción de agua en zonas cercanas. Sin embargo, los resultados no fueron validados.

En la región del río Amazonas y en las zonas de llanura aluvial, se utilizó la topografía estimada por Fassoni-Andrade et al. (2020) con una resolución de 30 metros, disponible en el portal de Mendeley. Este mapeo fue creado mediante la digitalización de cartas náuticas de ríos y la aplicación del método Flood2Topo. En cuanto a los modelos combinados, los investigadores chinos, liderados por Yuannan Long, también emplearon el modelo SWAT para el análisis hidrológico en áreas de bajos datos, combinándolo con el sistema hidrodinámico MIKE21 para mejorar las simulaciones del flujo.

De Angelis y Gomes Júnior (2024) encontraron que el modelo HydroPol2D podría ser una solución de bajo costo para predecir el comportamiento hidrológico-hidráulico de las cuencas fluviales. Este modelo estima mapas de inundaciones con profundidades de agua en calles, barrios, canales y toda la cuenca hidrográfica. Investigaciones recientes utilizando HydroPol2D también se han centrado en generar mapas de riesgo cada 15 minutos, lo que permite una toma de decisiones más efectiva. Sin embargo, la calidad de los resultados podría mejorar si se contara con más datos. En el estado de Rio Grande do Sul, actualmente existen 1.700 estaciones pluviométricas y fluviométricas, pero solo el 25% de ellas transmiten datos en tiempo real, lo que limita el funcionamiento de los modelos hidrodinámicos, a menos que se utilicen datos proporcionados por la población a través de videos y fotografías (De Angelis y Gomes Júnior, 2024).

Otro modelo hidrodinámico conocido es CRESTv2.1. La versión más mejorada y ampliamente utilizada, CRESTv2.1, presentó múltiples avances, incluyendo (a) la implementación de parámetros distribuidos, (b) la sustitución de tres capas de suelo por una sola para reducir los requisitos de parámetros, (c) la inclusión de la relación de área impermeable, (d) la inclusión de un parámetro multiplicador de lluvia para mitigar el sesgo de forzamiento de la precipitación, y (e) la autocalibración, entre otros (Shen et al., 2017; Xue et al., 2013, 2016). El modelo CREST ha demostrado ser eficiente y eficaz en el monitoreo de inundaciones; sin embargo, presenta una serie de limitaciones que deben abordarse para seguir mejorando y simular adecuadamente ambos extremos hidrológicos. Por ejemplo, el modelo CREST pareció presentar ramas de caída mucho más pronunciadas en el hidrograma en comparación con los datos de observación (Chen et al., 2020); la estructura monocapa del suelo podría causar errores en las estimaciones de humedad del suelo, y la falta de simulación del almacenamiento y el enrutamiento de aguas subterráneas podría subestimar la cantidad de agua en simulaciones hidrológicas a largo plazo (Kan et al., 2017). Además, al considerar la gestión del agua para lograr la sostenibilidad, especialmente en regiones con precipitaciones fluctuantes en el tiempo, la modelización de las aguas subterráneas ya no es un componente insignificante (Asrie y Sebhat, 2016; Massuel et al., 2017).

Finalmente, Le Li et al. (2021) proporcionan nuevas perspectivas sobre las interacciones complejas y no lineales entre los procesos hidrológicos y los cambios ambientales. El modelo SWAT, desarrollado por el Departamento de Agricultura de los EE. UU. (USDA), sigue siendo una de las herramientas más utilizadas para simular la dinámica de sedimentos y nutrientes en cuencas de macroescala, mesoescala y microescala (Arnold et al., 1998).

El modelo SWAT ha demostrado ser una herramienta valiosa para identificar los principales procesos hidrológicos que influyen en las cargas de nitrato en las zonas de estudio, especialmente durante las estaciones secas. Entre los datos clave requeridos para su implementación se incluyen el modelo de elevación digital (DEM), mapas de uso del suelo, mapas de tipos de suelo, datos meteorológicos diarios, registros de calidad del agua y prácticas agrícolas de manejo. En este estudio, se utilizó un DEM de 30 metros de resolución (Asmat V2), obtenido del sitio web del USGS (http://www.usgs.gov), para la delimitación de la cuenca (Le Li et al., 2021). No obstante, Castellanos-Osorio (2025) y Sánchez-Gómez (2024 y 2025) encuentran que la representación de las aguas subterráneas en el modelo base SWAT+ se ha señalado como una limitación importante. Según Yimer et al. (2023), los sistemas de drenaje agrícola son fundamentales para evacuar el exceso de agua subterránea y mantener niveles adecuados de oxígeno para el crecimiento de los cultivos. No obstante, estos sistemas también generan impactos ambientales e hidrológicos relevantes, como la disminución de lo volumen de agua subterránea y el incremento del transporte de contaminantes hacia aguas abajo.

Para evaluar estos efectos, los investigadores han recurrido a herramientas de modelado hidrológico más avanzadas, como el modelo SWAT+ acoplado al módulo de flujo subterráneo GWFlow. Este enfoque permite analizar cómo el drenaje agrícola puede agotar los niveles freáticos, alterando los procesos hidrológicos naturales. La construcción de modelos con y sin sistemas de drenaje agrícola facilita la evaluación de sus efectos sobre la geohidrología.

En el futuro, la investigación debería enfocarse en medir los flujos de drenaje y calibrar modelos geohidrológicos para mejorar la comprensión de las dinámicas entre agua subterránea y drenaje agrícola. Estas acciones ayudarían a reducir la incertidumbre en la predicción de los flujos de agua durante la estación seca y en otros componentes del balance hídrico. La cuantificación precisa del agua drenada es esencial para evaluar sus impactos ambientales.

Yimer et al. (2023) descubrieron que el drenaje agrícola es una práctica común para mejorar la productividad de los cultivos, ya que mejora la humedad del suelo y mantiene la zona radicular adecuadamente aireada. El drenaje de agua agrícola puede reducir significativamente los niveles de agua subterránea y afectar la hidrología de la cuenca. Por lo tanto, la construcción de modelos con y sin estas características puede indicar un impacto adverso en el proceso geohidrológico. Por lo tanto, el modelo independiente Soil Water Assessment Tool (SWAT+) se desarrolló inicialmente para simular el caudal en la salida de la cuenca de Kleine Nete. Posteriormente, se integró en el modelo SWAT+ un módulo de agua subterránea de base física y distribución espacial (gwflow) y se calibró para la descarga del caudal en la salida de la cuenca (Yimer et al., 2023).

En los estudios de caso analizados, el modelo SWAT+ acoplado con GWFlow mostró un mejor desempeño en comparación con la versión independiente de SWAT+ (Arnold, 1998). Además, Bailey et al. (2023) desarrollaron una versión avanzada del módulo GWFlow, físicamente fundamentada e integrada espacialmente con SWAT+, capaz de simular tanto el flujo superficial como el subterráneo a escala de cuenca, incorporando de forma explícita el drenaje agrícola en su estructura.

Sánchez-Gómez et al. 2025 encontraron que, entre los modelos hidrológicos a escala de cuenca, la herramienta de evaluación de suelos y agua (SWAT) es uno de los más utilizados (Arnold et al. 2012; Fu et al. 2019; Gassman et al. 2014). SWAT siempre fue capaz de simular algunas acciones de gestión (es decir, liberación de embalses, transferencias de agua, riego), si bien de una manera simplista y limitada (Neitsch et al. 2009). Por lo tanto, generalmente se combinaba con otro software (p. ej., Ashraf et al. 2017; Ayele et al. 2022; Dash et al. 2022; Phung et al. 2022; Zhang et al. 2023).

Una versión completamente reestructurada del modelo, SWAT+, se lanzó hace algunos años e incorpora nuevas capacidades (Bieger et al. 2017). La flexibilidad del modelo para simular acciones de gestión se ha mejorado notablemente en SWAT+. La simulación de embalses fue la tarea más desafiante de este trabajo debido a los múltiples factores involucrados (calibración del modelo, implementación de transferencias de agua, embalses aguas arriba, confiabilidad de los datos observados), además de las tablas de decisión. Las tablas de decisión de liberación construidas permitieron considerar diferentes escenarios y resultaron en una simulación precisa para muchos de los embalses simulados. La introducción de tablas de decisión de liberación en SWAT+ ha aumentado la flexibilidad para simular

estos elementos relevantes de la gestión hídrica. La simulación de embalses con SWAT se ha abordado en varios trabajos (p. ej., Liu et al., 2019; Marak et al., 2020; Zhang et al., 2012), pero las limitaciones de versiones anteriores de SWAT llevaron a cambios en el código (p. ej., Jordan et al., 2022; Kim et al., 2021; Wang et al., 2023) o a la incorporación de los modelos a otro software (Anand et al., 2018).

SWAT+ también fue utilizado para simular la operación de embalses por Wu et al. (2020), quienes presentaron las rutinas de embalses SWAT+ y desarrollaron e implementaron numerosas tablas de decisión de liberación para los EE. UU., incluyendo un procedimiento de calibración para las tablas de decisión (Sánchez-Gómez et al., 2025). Sánchez-Gómez (2024) encontró que los modelos hidrológicos se utilizan ampliamente para respaldar la gestión de los recursos hídricos, incluyendo la evaluación de los impactos de los escenarios (Hakala et al., 2019; Molina-Navarro et al., 2018). La representación del proceso del modelo, sus limitaciones, los supuestos realizados por el modelador y otros factores como los procedimientos de calibración contribuyen a la incertidumbre en las predicciones del modelo (Goderniaux et al., 2015; Hakala et al., 2019; Karlsson et al., 2016; Mendoza et al., 2015; Smerdon, 2017).

Para reducir la incertidumbre de la simulación, se deben analizar múltiples variables de salida, garantizando que la cuenca modelada y sus características se reproduzcan de la forma más realista posible (es decir, el balance hídrico, los componentes del caudal y otras variables hidrológicas clave) (Arnold et al., 2015). Un procedimiento recomendado para garantizar que los modelos funcionen correctamente para una variable específica (p. ej., el caudal) por las razones correctas (p. ej., contribuciones realistas de la escorrentía superficial y el caudal subterráneo) es la calibración suave (SC).en el que los parámetros del modelo se restringen con base en información blanda antes de realizar una calibración dura (HC) (Chawanda et al., 2020; Sanchez-Gomez et al., 2025).

Castellanos-Osorio (2025) va en la misma dirección y encontró que el acoplamiento de SWAT+ con el nuevo módulo GWFLOW mejora la interacción agua superficial-subterránea. • Un enfoque de calibración basado en FDC ayuda a reproducir con precisión el caudal base del modelo. Los enfoques de calibración de los modelos (1) SWAT+ y (2) SWAT + GWFLOW se centraron en ajustar los caudales bajos, lo que permitió una mayor precisión en los caudales diarios para estimar los caudales ambientales. Además, uno de los principales desafíos fue la necesidad de datos piezométricos para definir mejor las condiciones de contorno iniciales e información geohidrológica completa sobre el área de estudio, que podría variar significativamente. Una simulación precisa de la hidrología depende de estos datos El modelo acoplado SWAT + GWFLOW exhibió una precisión superior en todo el hidrograma, capturando condiciones de caudal alto, medio y bajo con mayor precisión que el modelo independiente. La inclusión de la dinámica del agua subterránea mediante el módulo GWFLOW mejoró significativamente la simulación del caudal base, lo que resultó en una representación realista del balance hídrico de la cuenca. Por lo tanto, el modelo SWAT + GWFLOW es una herramienta eficaz no solo para la estimación del caudal ambiental, sino también para la planificación hidrológica y la toma de decisiones en cuencas donde los procesos hídricos subterráneos son críticos (Castellanos-Osorio, 2025).

Yimer et al. (2023) encontraran que el modelo SWAT+gwflow representa el caudal de un pozo en gran parte de la cuenca del Escalda. Además, el conjunto de datos cuadriculados arrojó resultados satisfactorios al forzar el modelo (geo)hidrológico, lo que sugiere su utilidad para dichos estudios regionales. Finalmente, el hecho de que el uso del conjunto de datos global (disponible para cualquier ubicación) para el desarrollo del modelo diera como resultado una simulación precisa del caudal y la carga hidráulica indica la oportunidad de aplicar este modelo acoplado en regiones con escasez de datos (que carecen de información sobre estudios geológicos y propiedades de los acuíferos).

El modelo acoplado SWAT+GWFLOW debe articularse en la práctica con la Gestión del Conocimiento Agrícola e Hidráulico, tanto en términos de compartir como de crear y aplicar este conocimiento, como la comprensión del drenaje agrícola en toda su estructura (procesos hidrológicos superficiales y subterráneos). Todas estas formas de abordar el conocimiento están fuertemente impactadas por la cultura, como se verá a lo largo del trabajo. Por eso, si la cultura es muy cerrada o tiene dificultades en estos tres procesos, es importante desarrollar la inteligencia cultural, que trata de la capacidad de conocer, adaptar y comparar-retener lo bueno en términos de valores, supuestos, tradiciones y creencias de otras culturas. Las medidas estructurales (como las obras hidráulicas) y las estrategias no estructurales (como los programas educativos y de transferencia de conocimientos) dependen de la voluntad del sector público y privado, tanto

en términos de aprendizaje como de inversión. Puede que no haya tal interés porque gastar en esas medidas puede tener una ganancia menor que utilizar los recursos para una campaña electoral basada en obras que lleguen a los formadores de opinión de la sociedad y no a la población ribereña, que es pobre y no tiene acceso al conocimiento.

Muchos residentes viven muy cerca del agua, a veces incluso en contra de las normas, por lo que es necesario entender cómo se puede gestionar mejor la urbanización y la impermeabilización del suelo. Además, falta una buena comunicación por parte de las autoridades públicas para instruir a la población sobre cómo reducir los riesgos y cómo comportarse en determinadas situaciones. La importancia de una cultura de prevención y predicción es fundamental, pero esto requiere capacitación de todas las personas involucradas y campañas gubernamentales para cambiar la cultura nacional. Silveira y Dewes (1993) explican que uno de los primeros intentos de realizar una gestión integrada de los recursos hídricos en Rio Grande do Sul surgió en 1971 a través de la iniciativa del CEEIBG - Comité Ejecutivo de Estudios Integrados de la Cuenca del Guaíba. El CEEIBG tuvo como objetivo mejorar la calidad ambiental de la cuenca del río Guaíba, buscando compatibilizar las actividades desarrolladas por entidades federales, regionales, estatales y municipales con el uso integrado de los recursos hídricos y la preservación de la calidad del agua. Más recientemente, la Ley nº 10.350 del 30 de diciembre de 1994 instituyó el Sistema Estatal de Recursos Hídricos, reglamentando el artículo 171 de la Constitución del Estado de Rio Grande do Sul, modificada por la Ley nº 11.560 del 22 de diciembre de 2000 y por la Ley nº 11.685 del 8 de noviembre de 2001. Aún más recientemente, se creó el Plan Estatal de Recursos Hídricos (PERH), un instrumento de gestión previsto en las Leyes Estatal y Federal de Aguas (Ley Estatal nº 10.350/1994 y Ley Federal nº 9.433/1997) que tiene como objetivo orientar la implementación de la política de recursos hídricos y la gestión del agua, definiendo los objetivos, principios y directrices a nivel estatal. Sin embargo, como se puede observar, el informe de sequía más reciente disponible en el Portal SEMA es de 20211. Este informe solo incluye Análisis y Pronóstico Meteorológico con algunos hidrogramas de los principales ríos de Rio Grande do Sul. La Secretaría de Estado de Medio Ambiente e Infraestructura (Sema) fue creada en 1999 y es el órgano central del Sistema Estatal de Protección Ambiental (Sisepra), responsable de gestionar la política ambiental en Rio Grande do Sul.

3. El preocupante movimiento separatista en Rio Grande do Sul y el impacto de la mayor inundación del Estado. - El Movimiento por la Independencia de la Pampa (MIP) fue creado en 1990 por Irton Marx, y defiende la separación del estado de Rio Grande do Sul del resto de Brasil y ya ha conseguido más de un millón de firmas en ese sentido1. El grupo más conocido es el Movimiento Gaucho Tradicionalista (MTG). El tradicionalismo gaucho es considerado por sus miembros como el movimiento cultural popular más grande del mundo en la actualidad. Oliven (2006), basado en información del folclorista y tradicionalista Lessa (1985), refiere la participación directa de dos millones de personas en el MTG – y en su sitio web menciona la existencia de 1.400 entidades tradicionalistas afiliadas. Según los tradicionalistas, el culto a las tradiciones gauchas ocurre en Nueva York, Lisboa, París y Japón, como consecuencia de la "diáspora" de gauchos de Rio Grande do Sul por Brasil y el mundo (Kaiser, 1999). El sociólogo Luvizotto (2009) investigó la etnicidad y el separatismo en la cultura gaucha, analizando cómo interactúan en el contexto del movimiento que pretende emancipar a Rio Grande do Sul del resto de Brasil. Para el gaucho, el "brasileño" es el otro, el extraño, la persona distante que no forma parte de ese espacio y de esas relaciones. Hablamos de ese otro sin miedo, se permite criticar, acusar y nombrar: "El 'brasileño' es lento, travieso, perezoso" (Luvizotto, 2009). Esto se debe a que RGS está arraigada en tradiciones muy fuertes que considera generan mayor honestidad que el resto del país, cuyas características de personalidad fueron identificadas por Lourenção et al. (2019) como: sensual, astuta, alegre, creativa, hospitalaria, amigable y cordial. La amabilidad, para ocultar la falta de conocimiento, fue identificada por Buarque de Holanda (1936) en el libro Raíces de Brasil, lo cual fue ratificado por Gylberto Freire (2010 y 2015) y Caio Junior (1945). En Brasil, algunos críticos han comprendido el impacto de la cultura en el comportamiento. Freitas (1997), aunque reconoce el carácter diverso y heterogéneo de la cultura brasileña, concluyó que los rasgos nacionales para un análisis organizacional serían: jerarquía, personalismo, astucia, sensualidad y espíritu aventurero. El perfil del brasileño típico, delineado por Buarque de Holanda (1975) como una oposición simétrica al ascético protestante norteamericano, tiene las siguientes características: individualismo personalista, búsqueda de placeres inmediatos, desprecio por la comunidad y los ideales a largo plazo.

Si bien esto ha cambiado un poco en las últimas dos décadas, históricamente Brasil no estaba integrado ni cultural ni económicamente con las demás naciones de la región. Muchos brasileños ni siquiera se identificarían como

latinoamericanos. Durante más de un siglo, Brasil compitió por la supremacía sobre Sudamérica. Sin embargo, desde la Copa del Mundo (2014) y los Juegos Olímpicos (2016) en adelante, Brasil y Perú se han convertido en socios económicos y sociales a través de un alto nivel de corrupción a través de la empresa brasileña más grande: el escándalo de Odebrecht en Brasil es uno de los casos de corrupción corporativa más grandes de la historia. The Mechanism es una serie de televisión brasileña de drama político creada por José Padilha y Elena Soarez (2018), inspirada libremente en hechos reales, sobre Un escándalo estalla en Brasil durante una investigación de presunta corrupción gubernamental a través de empresas petroleras y de construcción. José Padilha teve que fugir do pais porque también revelou como o governoro arma as favelas para evitar a coesao social contra ele. Neves Costa, Ferreira & Pontes de Campos (2024) explican que una operación "lavado de autos" conducida por Juiz Sergio Moro, mayor operación contra una corrupción en Brasil que comenzó a principios de 2014 y se extinta en 2021, solo podría compararse con las "manos limpias" de Italia, ate porque as duas culturas tem muitas similaridades (Bertonha, 2010). Una vasta e intrincada red de corrupción quedó gradualmente al descubierto para sacudir la frágil democracia hasta sus cimientos (Neves Costa, Ferreira & Pontes de Campos, 2024).

En 2021, el Supremo Tribunal Federal consideró que el entonces juez Sérgio Moro actuó de forma parcial al juzgar al expresidente Lula, lo que resultó en la anulación de las pruebas producidas bajo su liderazgo en la Lava Jato y el cese de la Operación.

4. El modelo Cultura–Conhecimento–Inteligencia (CCI) y la Gestión del Conocimiento en el Contexto de Desastres. - Roland (2000) aportó explicaciones prácticas sobre la formación de las culturas y la relación entre el Estado, el conocimiento y la inteligencia. Diversos estudios han vinculado factores históricos y ecológicos con la evolución de culturas colectivistas o individualistas. Fincher et al. (2008) y Murray y Schaller (2010) encontraron que los países con una alta prevalencia de patógenos antes del siglo XX tendieron a desarrollar culturas más colectivistas. La lógica subyacente es que, en contextos de alta carga patógena, las normas colectivistas—caracterizadas por el control del comportamiento individual y una actitud más cerrada hacia los forasteros—ofrecen ventajas adaptativas al limitar la propagación de enfermedades.Otras explicaciones sobre el origen del colectivismo e individualismo incluyen factores agrícolas y ecológicos. Por ejemplo, Talhelm et al. (2014) argumentan que las sociedades basadas en el cultivo del arroz, que requiere mayor coordinación y trabajo colectivo, desarrollan una orientación más colectivista, en contraste con las culturas del trigo. Asimismo, Buggle (2015), retomando ideas de Wittfogel (1957), sugiere que la necesidad histórica de sistemas de riego extensivos favoreció la aparición de estructuras sociales más centralizadas y colectivistas. En cambio, Knudsen (2017) halló que una fuerte dependencia histórica de la pesca está más asociada con culturas individualistas, dado que esta actividad promueve la autonomía.

Roland (2000) también propuso que la geografía influyó en si las sociedades se desarrollaban bajo sistemas estatistas o de mercado. Aquellos países que hoy requieren una gobernanza estatal más fuerte tienden a poseer culturas más colectivistas, mientras que donde florecieron sistemas de mercado emergieron culturas más individualistas. En América del Sur, por ejemplo, los marcos legales tienden a centrarse en disputas entre individuos, como los conflictos por propiedad, lo cual refleja una orientación cultural individualista. Desde un enfoque antropológico, Edward Tylor fue el primero en definir la cultura en su obra Primitive Culture (1871), considerándola un fenómeno natural que puede estudiarse científicamente. Tylor sostenía que la cultura sigue patrones y causas regulares, lo que permite formular leyes sobre su evolución. Kroeber, por su parte, entendía la cultura como un proceso acumulativo resultado de las experiencias históricas de generaciones previas. Este proceso, según él, moldea o limita la creatividad individual. Tanto Kroeber como Félix Keesing coincidieron en que no existe una relación genética con la cultura: cualquier persona puede adoptar la cultura del lugar donde crece, independientemente de su origen biológico. Kroeber incluso sostenía que la cultura es lo que realmente distingue al ser humano de los animales, ya que le permite trascender sus limitaciones biológicas.

De estas ideas se desprenden cinco principios clave:

1. La cultura, junto con la herencia genética, determina el comportamiento humano y sus logros.
2. El ser humano actúa conforme a normas culturales; sus instintos han sido modulados por un prolongado proceso evolutivo.
3. A través de la adquisición cultural, el aprendizaje supera la influencia de comportamientos genéticamente determinados.
4. Como se reconoce desde la Ilustración, es el aprendizaje —ya sea por socialización o endoculturación— lo que determina el comportamiento humano y sus capacidades.
5. La cultura es un proceso acumulativo que puede tanto estimular como restringir la creatividad individual.

En términos de desarrollo económico, diversos académicos coinciden en que los gobiernos deben colocar a la ciencia en el centro de sus estrategias de crecimiento y recuperación económica. La ciencia genera conocimiento, y este, a su vez, impulsa la innovación, mejora la calidad de vida, fortalece la democracia, impulsa el crecimiento económico y aporta soluciones a problemas complejos. Sin embargo, Rothberg y Erickson (2004) advierten que el conocimiento, por sí solo, es estático y sólo adquiere valor cuando se aplica.

En 1989, Richard Ackoff propuso una taxonomía ampliamente aceptada en el campo de la gestión del conocimiento (Knowledge Management, KM), que distingue entre datos, información, conocimiento e inteligencia. Según Davenport y Prusak (1998), los datos son registros objetivos y discretos de eventos; en organizaciones, suelen ser transacciones estructuradas. La información, en cambio, se entiende como un mensaje —en forma de documento, comunicación visual o auditiva— que tiene un emisor y un receptor.

El conocimiento va más allá: es una combinación dinámica de experiencias, valores, información contextual y conocimientos técnicos que permite interpretar y aplicar nueva información. Este conocimiento se forma en la mente de los individuos y es inherentemente complejo, estructurado e intuitivo, por lo que no siempre puede ser articulado de forma clara o lógica (Davenport et al., 1998).

La transformación del conocimiento en inteligencia implica un proceso humano de interpretación, análisis, integración, predicción y acción. La información se contextualiza según los valores y criterios de quien toma decisiones, quien luego aplica este conocimiento en situaciones concretas para generar inteligencia. Rothberg y Erickson (2004) subrayan que el conocimiento se construye socialmente mediante colaboración, pero carece de valor si no se aplica. En resumen, el conocimiento constituye la base de la inteligencia, mientras que la inteligencia representa el conocimiento en acción para resolver problemas.

Choo (2002) define la inteligencia como un ciclo continuo de actividades que incluye la percepción del entorno, la construcción de conocimiento y la generación de sentido a partir de la interpretación, todo ello apoyado en la memoria de experiencias pasadas.

A partir de estos fundamentos teóricos, se construye el modelo Cultura-Conocimiento-Inteligencia (CCI), ilustrado en la Figura 1.

Las premisas fundamentales del modelo CCI son:
(i) La cultura se compone de creencias, valores, supuestos y tradiciones de una sociedad (Schein, 1985).
(ii) Para que la educación cumpla su función transformadora, el currículo debe ser reorganizado en torno a los cuatro pilares del aprendizaje: aprender a conocer, aprender a hacer, aprender a vivir juntos y aprender a ser (Nan-Zhao, 2000).
(iii) La inteligencia se sostiene sobre tres pilares fundamentales: predicción, estrategia y acción (Rothberg y Erickson, 2004).

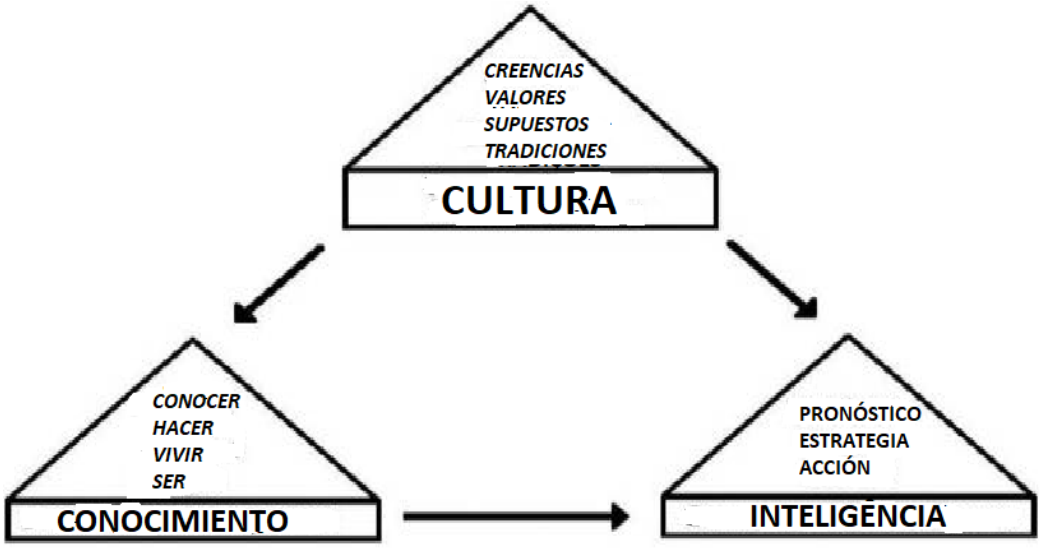

Figura II. El modelo Cultura-Conocimiento-Inteligencia (adaptado de Choo, 1998)

El modelo CCI se fundamenta en tres hipótesis clave (Tabla I).

Hipoteses	Fuentes	Resultados
La cultura tiene un impacto positivo en el conocimiento	El éxito de la implementación de un sistema de gestión del conocimiento depende estrechamente de Análisis crítico de la cultura organizacional existente (de Ré et al., 2017).	SOPORTADO
El cambio cultural tiene un impacto positivo en la inteligencia	La cultura afecta los comportamientos organizacionales y sociales, cómo actuarán las personas en una situación determinada, como el pensamiento y la toma de decisiones (Schein, 1985).	SOPORTADO
El conocimiento (KM) tiene un impacto positivo en la inteligencia	Rothberg y Erickson (2004) aclaran que el conocimiento sin aplicación es inofensivo. En resumen, el conocimiento es la base de la inteligencia, ya que la inteligencia es el conocimiento en acción para resolver problemas.	SOPORTADO

Tabla I. Hipótesis en el modelo CCI

El modelo Cultura-Conocimiento-Inteligencia (CCI) demuestra cómo la cultura influye tanto en la producción de conocimiento como en la capacidad para generar inteligencia práctica. En el caso de las recientes inundaciones en Rio Grande do Sul, se evidenció que una cultura marcada por la inmediatez y la falta de planificación a largo plazo —incluyendo la ausencia de inversiones en obras preventivas que no rinden rédito electoral inmediato— impactó negativamente en la generación y aplicación del conocimiento, en especial el conocimiento tácito. Este tipo de conocimiento, basado en la experiencia práctica, es difícil de codificar y compartir, pues depende de la confianza, el compromiso y la identidad social de las comunidades técnicas.

La falta de mecanismos eficaces para transformar la experiencia acumulada por técnicos y académicos en acciones concretas, tanto antes como después de eventos críticos (como la inundación de salas de máquinas y el sobrepaso de presas), refleja cómo la inteligencia operativa también fue limitada por la cultura institucional predominante.

La aplicación práctica del modelo CCI, en particular en la gran inundación de mayo de 2024, puede hacerse por ejemplo a partir de las dificultades de comunicación detectadas entre la Universidad y el gobierno, entre el gobierno y la sociedad y entre la Universidad y la sociedad. La Relatoría Especial sobre Derechos Económicos, Sociales, Culturales y

Ambientales (REDESCA) de la Comisión Interamericana de Derechos Humanos (CIDH) publica el informe "Impactos de las inundaciones en Rio Grande do Sul: observaciones y recomendaciones para la garantía de los derechos económicos, sociales, culturales y ambientales" . El informe destaca los impactos desproporcionados sobre los grupos en situación de mayor vulnerabilidad, entre ellos las niñas y mujeres, las personas afrodescendientes, los pueblos indígenas y comunidades tradicionales, las personas con discapacidad, las personas mayores, la población LGBTQIA+, los migrantes y refugiados, así como los trabajadores rurales e informales. Además, con base en la información recopilada durante la visita y el análisis de los datos disponibles, el informe identifica fallas estructurales que pueden haber contribuido a la magnitud de los impactos sobre DESCA, incluyendo la degradación ambiental, la expansión de la agroindustria, el debilitamiento de la legislación ambiental, la falta de mantenimiento de los sistemas de contención de inundaciones y el crecimiento urbano con baja resiliencia ambiental.

5. Gestión del Conocimiento y Comunidades de Práctica (CoP). - La Gestión del Conocimiento (GC) busca sistematizar, codificar y redistribuir el conocimiento tácito dentro de las organizaciones para convertirlo en conocimiento explícito (Rothberg y Erickson, 2004). Ante la naturaleza interdisciplinaria de los desafíos que implican las inundaciones, se requiere la creación de espacios públicos de calidad que promuevan la colaboración entre investigadores, tomadores de decisiones y comunidades. La conciencia social sobre el cambio climático y sus consecuencias debe ser fortalecida mediante participación ciudadana activa, lo cual garantiza que las soluciones sean culturalmente apropiadas y aceptadas por la sociedad.

Un elemento clave para esta integración del conocimiento es el uso de herramientas como el Índice de Vulnerabilidad Social de Cutter (Cutter, Boruff & Shirley, 2012), que permite anticipar impactos, evaluar necesidades y diseñar sistemas de alerta temprana más eficaces.

Como herramienta de aplicación práctica de la GC en este estudio, se proponen las Comunidades de Práctica (CoP) o Foros Comunitarios.

Morgado da Silva y Araújo (2019) [23] señalan que los Foros Comunitarios pueden contribuir significativamente a la construcción de ciudadanía, al proporcionar un espacio democrático donde se debaten y transforman los conflictos éticos y sociales. Las CoP se basan en la gestión del conocimiento socialmente distribuido, pero requieren mediación experta para evitar interpretaciones erróneas o sobrecarga informativa.

Oliveira y Villardi (2014), siguiendo a Gherardi (2003), destacan que las emociones, deseos e identidades personales afectan profundamente la forma en que se produce y comparte conocimiento. Las personas no solo buscan conocimiento por utilidad práctica, sino también como una meta en sí misma. No obstante, Moura (2009) señala que las CoP han sido poco estudiadas desde una perspectiva crítica.

Lave y Wenger (1991) y Wenger (2000) reconocen que las CoP no son neutras: pueden ser espacios de aprendizaje y creatividad, pero también de exclusión o rigidez institucional. Participar en ellas implica dialogar, compartir experiencias, construir significados y contribuir a procesos colectivos de reflexión, lo que fomenta el aprendizaje organizacional (Souza-Silva y Davel, 2007).

Una CoP efectiva debe tener tres elementos clave (Wenger, 2006):

1. Dominio: Un área de conocimiento común que da identidad al grupo, con miembros comprometidos que se valoran mutuamente por su experiencia y competencias.
2. Comunidad: Un entorno colaborativo donde se intercambian experiencias, se resuelven problemas y se construyen relaciones de aprendizaje.
3. Práctica: La base compartida de experiencias, herramientas, historias y métodos que sustentan la acción colectiva.

La participación progresiva, también conocida como Participación Periférica Legítima (Gherardi et al., 1998), permite a los nuevos miembros aprender mediante la interacción informal y adquirir legitimidad dentro del grupo.

6. Propuesta: Crear una CoP sobre Prevención de Inundaciones. - Se propone establecer una Comunidad de Práctica orientada a compartir mejores prácticas y lecciones aprendidas para la mitigación de inundaciones, con especialistas asignados por área temática. Estos expertos facilitarían el debate, analizarían propuestas y canalizarían recomendaciones concretas hacia la toma de decisiones. Uno de los efectos esperados de esta dinámica es la transformación cultural institucional.

Según De Angelis (2023), hay tres desafíos fundamentales para lograrlo:

1. Fomentar una cultura de intercambio de conocimientos dentro y fuera del sector público.
2. Utilizar herramientas digitales inteligentes que conviertan información en conocimiento contextualizado y sabiduría aplicada.
3. Reforzar la participación activa de ciudadanos, funcionarios y empresas en la producción de nuevo conocimiento, apoyados por sistemas expertos que analicen y faciliten el proceso colaborativo.

7. Planes de Emergencia y Tecnología Aplicada. - El cambio cultural propuesto a través de la gestión del conocimiento y el desarrollo de inteligencia organizacional es clave para diseñar planes de emergencia más eficaces. Según De Angelis (2024), estos deben combinar medidas estructurales (como obras hidráulicas) con estrategias no estructurales (como programas educativos y de transferencia de conocimiento).

Herramientas tecnológicas como el software HAZUS de FEMA (EE.UU.) permiten estimar daños potenciales por fallas de presas y realizar análisis costo-beneficio, facilitando así la planificación de infraestructura y rezonificación en áreas vulnerables (De Angelis y Gomes Júnior, 2024).

Araújo (2024) [1] advierte que, tras desastres, el 40% de las empresas no reabren, y otro 25% cierra en el plazo de un año, según datos de FEMA. Esto subraya la urgencia de acciones como el dragado de la cuenca del río Taquari, una necesidad debatida por más de cuatro décadas.

8. Innovación Tecnológica y Energía Sostenible. - En cuanto a sostenibilidad, Wendland et al. (2023) destacan el papel de materiales sintéticos avanzados para mejorar la eficiencia en la producción, almacenamiento y uso de energía. Tecnologías como celdas solares, baterías avanzadas y catalizadores eficientes pueden reducir la dependencia de combustibles fósiles y mitigar el cambio climático.

Respecto al transporte, especialmente el público —una fuente significativa de emisiones de CO_2—, el hidrógeno verde representa una alternativa prometedora. Aunque su costo de producción aún supera al del hidrógeno derivado de fuentes fósiles, se espera que esta brecha disminuya pronto. El hidrógeno renovable se obtiene por electrólisis utilizando electricidad de fuentes sostenibles (solar, eólica, hidroeléctrica, geotérmica, mareomotriz), o bien mediante biogás o conversión bioquímica de biomasa, siempre que se cumplan criterios de sostenibilidad.

9. El Modelo Biodinámico – Hidrodinámico. - La agricultura biodinámica, que utiliza polvo de roca para reducir la fuerte necesidad de fertilizantes químicos, tiene el potencial de mejorar los indicadores climáticos y hídricos.

Como hemos visto, los fertilizantes químicos, además de contaminar el agua, aumentan el secuestro de carbono en el suelo, lo que ayuda a aumentar las temperaturas y por tanto las precipitaciones.

Los modelos hidrodinámicos se utilizan en casos de inundaciones e inundaciones para predecir la densidad del agua cerca del aliviadero y crear un plan de descarga de inundaciones ideal.

Como encontró Angelis (2014), un plan de emergencia depende de la variabilidad de las propiedades hidráulicas e hidrológicas, ya que los indicadores hidráulicos se ven impactados por el uso de la tierra y luego por el cambio climático.

Este trabajo sugiere las siguientes Comunidades de Práctica para compartir conocimientos y experiencias para mejorar el proceso de toma de decisiones:

1- Agricultura y Cambio Climático
2- Modelos hidrodinámicos y datos necesarios
3- Mejora de la previsión en casos de inundaciones
4- Planes de emergencia y relación con la población
5- Estructuras eléctricas de salas de máquinas.

Con base en esta revisión de la literatura, se construye el modelo de relación entre el modelo de Agricultura Biodinámica y el Modelo Hidrodinámico:

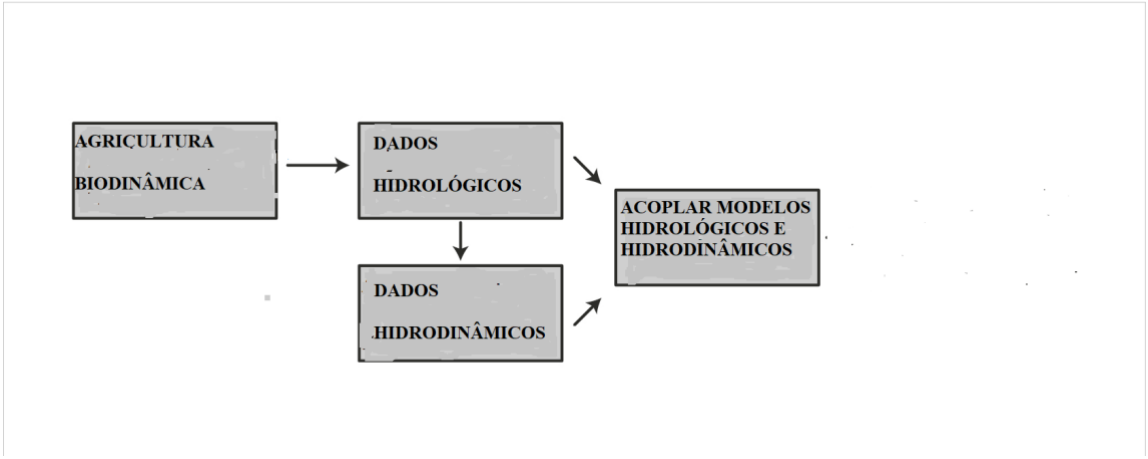

Es importante destacar en este modelo que la mejora en los datos agrícolas mejoró los datos hidrológicos e hidrodinámicos dada la relación con el cambio climático e incluso el respeto al medio ambiente.

10. Resultados e Discusión. - El principal resultado de esta revisión de la literatura fue considerar el modelo Hydropol2d como una solución de bajo costo para la predicción del comportamiento hidrocálico hidrológico de la cuenca de Río Grande do Sul, en particular estimando mapas de inundación que contienen profundidades de agua en las calles, bloques, vecindarios, canales y, en consecuencia, en todo el hilo.

Y no solo eso. Como hemos visto, el modelo Hydropol2D se puede utilizar para evaluar el riesgo de arrastre de las personas, generando mapas de riesgo cada 15 minutos que pueden usarse como una ayuda para la toma de decisiones.

Sin embargo, este trabajo llama la atención sobre la necesidad de datos de la lluvia y las estaciones fluviométricas y sugiere la mejor estructura de estas estaciones, así como a la construcción de nuevas por el poder público.

Es importante tener en cuenta que el tema del cambio cultural es aún más importante que el modelo Hydropol2D en sí. Esto se debe a que el uso de soluciones paliativas se observó tanto en la inundación 2023 y 2024 que hizo que el empeoramiento de la situación que dejó a 151 muertos, más de 100 faltantes y más de 600 desplazados.

Las alertas meteorológicas de que habría fuertes lluvias se emitieron con aproximadamente cinco días de anticipación.

No hubo mantenimiento en las estructuras existentes para proteger contra las inundaciones, incluidos diques, compuertas y bombas, hasta el punto de que el sistema colapsó antes de alcanzar el límite de inundación de 6 m. Como vimos, las bombas, que estaban inundadas, no pudieron bombear agua fuera de la ciudad debido a su imposibilidad de funcionar con exceso de agua.

Obviamente también hubo una falta de trabajo en equipo multidisciplinario para gestionar mejor la urbanización y el sellado del suelo, particularmente en comunidades que viven cerca de zonas de inundación.

Sin un plan de Gestión del Conocimiento e Inteligencia Organizacional, faltó una buena comunicación por parte de las autoridades públicas para instruir a la población sobre cómo reducir riesgos y cómo actuar en situaciones de emergencia.

11. Conclusión. - El artículo presenta dos modelos de investigación que se retroalimentan: el modelo Cultura-Conocimiento-Inteligencia (CCI) y el modelo de gestión de riesgos con participación social. El primer modelo demuestra la importancia de aprender de otras culturas, la inteligencia cultural, como incluyendo que el tema de las inundaciones es un problema global y por ende la necesidad de intercambiar conocimientos y experiencias con otros países, en particular Argentina.

Los efectos del cambio climático, asociado a la ocupación de zonas inundables, hacen que eventos como el de mayo de 2024 puedan ser cada vez más frecuentes. Sin embargo, la capacidad matemática actual de los modelos de previsión permite, con un intervalo razonable del orden de unos pocos días, predecir el impacto de las inundaciones con cierta precisión y servir de base para planes de actuación de emergencia. Para ello, es necesario recopilar datos de elevación, precipitaciones, batimetría y otros que sirvan como información de entrada para los modelos de pronóstico. Estados como Santa Catarina o Pernambuco cuentan con información de este tipo. Estas y otras medidas fueron sugeridas por investigadores del Instituto de Investigaciones Hidráulicas a finales de 2023 tras las inundaciones de noviembre, pero no fueron seguidas por los organismos públicos responsables.

Los investigadores también denuncian la cuestión gubernamental del mantenimiento de las obras (diques de contención y barreras anti-inundaciones). Los sistemas de protección, especialmente en Porto Alegre, requieren una intensa movilización de agentes capacitados para el correcto funcionamiento de compuertas y salas de máquinas. Preservar la memoria de las personas sobre los impactos sin precedentes de la inundación de 2024 no solo debe servir como una advertencia para la población, sino también presentarse en acciones adecuadas y frecuentes para la operación y mantenimiento de los sistemas de protección.

Paiva et al. (2024) recomiendan que los proyectos y la planificación de infraestructuras sean adaptables y flexibles, y que faciliten o no inviabilicen su ampliación (e.g. ancho de puentes, tramos de alcantarillas, altura de coronación de presas y diques), permitiendo así considerar futuras incrementos en los valores de referencia, dado un cierto riesgo asociado a eventos hidrológicos extremos.

La formación de equipos responsables de gestionar los sistemas de protección con frecuencia y no sólo durante las inundaciones debe ser una prioridad. Este trabajo pretende buscar pautas para una solución sin necesariamente encontrar culpables. La población afectada es la que más sufre al tener que desplazarse desde zonas previamente estables, y esto trae consigo la importancia de la inteligencia y sus tres pilares 1. predicción (responsabilidad del modelo hidrodinámico), 2. estrategia y acción (responsabilidad del plan de emergencia con participación social).
Como se analiza en este trabajo, es necesaria una mejor relación entre la Universidad y el gobierno con la participación de la población para que quienes tienen conocimiento y experiencia puedan tener mejores datos hidrológicos, no solo de precipitaciones, sino también de niveles de agua en toda la infraestructura de las ciudades. sistema para alimentar sus modelos de predicción, estrategia y acción. Además, se necesita un plan de emergencia estándar para todo el Estado que pueda replicarse en todo Brasil, considerando la educación de la población, particularmente de las poblaciones ribereñas y ribereñas.

12. Sugerencia para futuros estudios. - Según Gomes Junior et al. (2023), los estudios futuros incorporarán la variabilidad espacial de la precipitación y la evapotranspiración en cuencas hidrográficas a gran escala, especialmente para la modelización en períodos de sequías persistentes con inundaciones sin precedentes. Las investigaciones futuras deberían integrar datos socioeconómicos con análisis geoespaciales para comprender mejor los impactos en cascada de las inundaciones en las poblaciones vulnerables y fundamentar estrategias equitativas de desarrollo de la resiliencia.

Referencias

[1] Araújo. L. Emergência climática traz necessidade de mudança em parâmetros de risco de desastres. Jornal do Comércio. 2024. Disponivel em https://www.jornaldocomercio.com/cadernos/empresas-e-negocios/2024/05/1155968-emergencia-climatica-traz-necessidade-de-mudanca-em-parametros-de-risco-de-desastres.html

[2] Arsenault, R., Breton-Dufour, M., Poulin, A., Dallaire, G., & Romero-Lopez, R. Streamflow prediction in ungauged basins: analysis of regionalization methods in a hydrologically heterogeneous region of Mexico. Hydrological Sciences Journal. 2019. 64(11), 1297–1311.

[3] Bao, Zhenxin, et al. "Comparison of regionalization approaches based on regression and similarity for predictions in ungauged catchments under multiple hydro-climatic conditions." Journal of Hydrology 466 (2012): 37-46.

[4] Brunner, G. W. HEC-RAS river analysis system, 2D modeling users' manual. U.S. Army Corps of Engineer, Institute for Water Resource, Hydrologic Engineering Center. 2016.

[5] Choo, C.W. The Knowing Organisation, Oxford University Press, New York, NY. 1998.

[6] Davenport, T.H. and Prusak, L. Working Knowledge, 2nd ed., Harvard Business School Press, Boston, MA. 2000.

[7] Cutter, S., B. Boruff y L. Shirley. “Social vulnerability to environmental hazards”, Social Science Quarterly, 2003. vol. 84, N° 2

[8] De Angelis, C. T. Um modelo e Plano de Emergência Padronizado para as inundações. Jornal do Comércio. 2024. Dispononível em https://www.jornaldocomercio.com/opiniao/2024/07/1165074-um-modelo-e-plano-de-emergencia-padronizado-para-as-inundacoes.html

[9] De Angelis, C. T. Um plano de educação ambiental baseado na educação infantil, participação social: um estudo de caso na Aldeia Terere em Sidrolândia. Revista Ambientale. Revista da Universidade Estadual de Alagoas/UNEAL. 2023. Disponível em https://periodicosuneal.emnuvens.com.br/ambientale/article/view/535

[10] De Angelis, C. T. Gomes Júnior, M. N. Uma sugestão de modelo hidrodinâmico para prever e gerir inundações . Jornal do Comércio. 2024. Disponível em https://www.jornaldocomercio.com/opiniao/2024/07/1160994-uma-sugestao-de-modelo-hidrodinamico-para-prever-e-gerir-inundacoes.html

[11] Do Lago, Cesar & Brasil, José & Nóbrega, Marcus & Mendiondo, Eduardo & Giacomoni, Marcio.. Improving pluvial flood mapping resolution of large coarse models with deep learning. Hydrological Sciences Journal, 2024. 69(5), 607–621. https://doi.org/10.1080/02626667.2024.2329268

[12] Fassoni-Andrade, A. C. Paiva, R. C. Rudorff, C. M. Barbosa, C.C. Leão, E. M. High-resolution mapping of floodplain topography from space: A case study in the Amazon, Remote Sensing of Environment,Volume 251, 2020.

[13] Fassoni-Andrade, A. C. Durand, F. Azevedo,A. Bertin,X. Santos,L.G. Khan, J. U. Testut, Moreira, D. M. Seasonal to interannual variability of the tide in the Amazon estuary, Continental Shelf Research,Volume 255, 2023.

[14] Getirana, A., Boone, A., Yamazaki, D., Decharme, B., Papa, F., & Mognard, N. The hydrological modeling and analysis platform (HyMAP): Evaluation in the Amazon basin. Journal of Hydrometeorology, 2012. 13, 1641–1665

[15] Gomes Júnior, M. N. Giacomoni, M. H. Richmond, F. A. Mendiondo, E. M. Global optimization-based calibration algorithm for a 2D distributed hydrologic-hydrodynamic and water quality model, Environmental Modelling & Software, Volume 179, 2024.

[16] Gomes Júnior, M. N. Lago, C. A. Rápalo, L. M. Oliveira, P. T. Giacomoni, M. H. Mendiondo, E. M. HydroPol2D — Distributed hydrodynamic and water quality model: Challenges and opportunities in poorly-gauged catchments, Journal of Hydrology, Volume 625, Part A, 2023,

[17] Guidolin, M., Chen, A. S., Ghimire, B., Keedwell, E. C., Djordjevic, S., & Savic, D. A. "A weighted cellular automata 2D inundation model for rapid flood analysis". Environmental Modelling & Software, 2016. 84, 378-394.

[18] Hu, D. Chen, Z. Li, Z. Zhu, Y. An implicit 1D-2D deeply coupled hydrodynamic model for shallow water flows, Journal of Hydrology, Volume 631, 2024,

[19] Jillo, A. Y., Demissie, S. S., Viglione, A., Asfaw, D. H., & Sivapalan, M. Characterization of regional variability of seasonal water balance within Omo-Ghibe River Basin, Ethiopia. Hydrological Sciences Journal, (2017). 62(8), 1200–1215.

[20] Kroeber, A. L. The Concept of Culture in Science. The Journal of General Education. Vol. 3, No. 3 , pp. 182-196 (15 pages). Published By: Penn State University Press. 1949.

[21] Li, G. Zhu, H. Jian, H. Zha, W. JWang, J. Shu, Z. Yao, S. Han, H. A combined hydrodynamic model and deep learning method to predict water level in ungauged rivers, Journal of Hydrology, Volume 625, Part A,2023.

[22] Long, Y. Chen, W. Jiang, C. Huang, Z. Yan, S. Wen, X. Improving streamflow simulation in Dongting Lake Basin by coupling hydrological and hydrodynamic models and considering water yields in data-scarce areas, Journal of Hydrology: Regional Studies, Volume 47, 2023.

[23] Morgado da Silva, M., Araújo, U. APRENDIZAGEM-SERVIÇO E FÓRUNS COMUNITÁRIOS: ARTICULAÇÕES PARA A CONSTRUÇÃO DA CIDADANIA NA EDUCAÇÃO AMBIENTAL. Revista de Educação Ambiental. Vol. 24, n. 1. 2019. Disponível em https://periodicos.furg.br/ambeduc/article/view/8157

[24] Nonnemacher, Lara & Fan, Fernando. Análise da viabilidade econômica da previsão de cheias no Rio Grande do Sul. Revista de Gestão de Água da América Latina. 2023. 20. 8. https://doi.org/10.21168/rega.v20e8.

[25] Paiva, R. Collischonn, W. Miranda, P. Petry, I. Dornelles, F. Goldenfum, J. Fan, F. Ruhoff, A. e Fagundes, H. Critérios hidrológicos para adaptação à mudança climática: Chuvas e cheias extremas na Região Sul do Brasil. Relatório IPH-UFRGS. 2024. Disponivel em https://www.ufrgs.br/iph/wp-content/uploads/2024/05/CriteriosAdaptacaoMudancaClimaticaChuvasCheiasExtremasSul.pdf

[26] Rennó, C.D.; Soares, J. V. Modelos hidrológicos para gestão ambiental. Cursos INPE. 2022. Disponível em: <http://www.dpi.inpe.br/geopro/modelagem/relatorio_modelos_hidrologicos.pdf>.

[27] Rosman, P. C.C. Um Sistema Computacional de Hidrodinâmica Ambiental – Capítulo 1 (pp 1-161) do livro Métodos Numéricos em Recursos Hídricos, Vol. 5. Editora ABRH e Fundação COPPETEC. 2001.

[28] Rothberg, H. N. Erickson, G. S.. "From Knowledge to Intelligence: Creating Competitive Advantage in the Next Economy.". 2004.

[29] Schein, Edgar H. Organizational Culture and Leadership. San Francisco: Jossey-Bass Publishers. 1985.

[30] Stokes Oceanografia. Estudos sobre modelos hidrodinâmicos. 2023. Disponível em http://stokesoceanografia.com.br/2020/08/07/modelos-hidrodinamicos1/

[31] Yang, Linhan, et al. "Effects of the Three Gorges Dam on the downstream streamflow based on a large-scale hydrological and hydrodynamics coupled model." Journal of Hydrology: Regional Studies 40 (2022): 101039.

Nota contribución de los autores:

1. Concepción y diseño del estudio
2. Adquisición de datos
3. Análisis de datos
4. Discusión de los resultados
5. Redacción del manuscrito
6. Aprobación de la versión final del manuscrito

CT ha contribuido en: 1, 2, 3, 4, 5 y 6.

Nota de aceptación: Este artículo fue aprobado por los editores de la revista Dr. Rafael Sotelo y Mag. Ing. Fernando A. Hernández Gobertti.

Feasibility Study for the Electrification of Vehicles in Pakistan

Estudio de viabilidad para la electrificación de vehículos en Pakistán

Estudo de viabilidade para a eletrificação de veículos no Paquistão

Asad A. Naqvi [1(*)], Wassam Uddin [2], S.M. Saadullah [3], M. Zaviyar Abbas Noori [4], M. Omer Farooq [5]

Recibido: 13/03/2025 Aceptado: 10/07/2025

Summary. - Electric vehicles (EVs) have shown to be a viable alternative to fossil fuel vehicles (FFVs) in industrialized countries. The reason for the adoption of EVs in industrialized countries is that they outperform FFVs in terms of fuel usage, resulting in lower fuel imports, minimal environmental footprints, and less maintenance. The introduction of EVs in a developing country is a very demanding and challenging task. In this paper, the technical as well as economic aspects of introduction of EVs in Pakistan has been thoroughly explored. The statistical vehicle sale data for the past years has been considered to estimate the EVs requirement as per the Pakistan EV policy 2019. From the estimation, the electrical energy requirement to meet the policy targets has been calculated. From the calculated energy requirement, the details of charging infrastructure in major cities like Karachi, Islamabad, Lahore, etc. have been determined. It was found that EV charging station must be present for every 3x3 km radius. Further, from the estimated EVs, the cost saved by not using fossil fuels which should be required to run FFVs has been determined. It has been concluded from the economic perspective that EVs can significantly decrease the requirement of fossil fuel and can result in huge amount of cost saving by not using Fossil fuel.

Keywords: Electric Vehicles, Emissions, EV Policy, Oil Import, Pakistan.

[1] Assistant Professor, Department of Mechanical Engineering, NED University of Engineering and Technology (Pakistan), asadakhter@cloud.neduet.edu.pk, ORCID iD: https://orcid.org/0000-0001-6290-3115

[2] Undergrad Student, Department of Mechanical Engineering, NED University of Engineering and Technology (Pakistan), wassamuddin23@gmail.com, ORCID iD: https://orcid.org/0009-0006-9443-7140

[3] Undergrad Student, Department of Mechanical Engineering, NED University of Engineering and Technology (Pakistan), ssaadullah@njcu.edu, ORCID iD: https://orcid.org/0009-0003-1786-6599

[4] Undergrad Student, Department of Mechanical Engineering, NED University of Engineering and Technology (Pakistan), zaviyarabbas2000@gmail.com, ORCID iD: https://orcid.org/0009-0000-3544-2237

[5] Undergrad Student, Department of Mechanical Engineering, NED University of Engineering and Technology (Pakistan), omerf5014@gmail.com, ORCID iD: https://orcid.org/0009-0009-1882-7819

Memoria Investigaciones en Ingeniería, núm. 29 (2025). pp. 39-53
https://doi.org/10.36561/ING.29.4
ISSN 2301-1092 • ISSN (en línea) 2301-1106 – Universidad de Montevideo, Uruguay
Este es un artículo de acceso abierto distribuido bajo los términos de una licencia de uso y distribución CC BY-NC 4.0. Para ver una copia de esta licencia visite http://creativecommons.org/licenses/by-nc/4.0/

Resumen. - *Los vehículos eléctricos (VE) han demostrado ser una alternativa viable a los vehículos de combustibles fósiles (VCF) en los países industrializados. La razón de la adopción de VE en estos países radica en su menor consumo de combustible, lo que se traduce en menores importaciones de combustible, un impacto ambiental mínimo y un menor mantenimiento. La introducción de VE en un país en desarrollo representa un desafío considerable. En este trabajo, se analizan exhaustivamente los aspectos técnicos y económicos de la introducción de VE en Pakistán. Se han considerado los datos estadísticos de ventas de vehículos de los últimos años para estimar la necesidad de VE según la política de VE de Pakistán de 2019. A partir de esta estimación, se calculó la demanda de energía eléctrica para cumplir con los objetivos de la política. Con base en esta demanda energética calculada, se determinaron los detalles de la infraestructura de carga en las principales ciudades como Karachi, Islamabad y Lahore. Se concluyó que debe haber una estación de carga para VE cada 3x3 km. Además, a partir de la cantidad estimada de VE, se calculó el ahorro en costos derivado de la eliminación del uso de combustibles fósiles, necesarios para el funcionamiento de los VCF. Desde una perspectiva económica, se ha llegado a la conclusión de que los vehículos eléctricos pueden reducir significativamente la necesidad de combustibles fósiles y generar un enorme ahorro de costes al no utilizarlos.*

Palabras clave: *Vehículos eléctricos, emisiones, política de vehículos eléctricos, importación de petróleo, Pakistán.*

Resumo. - *Os veículos elétricos (VEs) têm se mostrado uma alternativa viável aos veículos movidos a combustíveis fósseis (VFCs) em países industrializados. A razão para a adoção de VEs nesses países é que eles superam os VFCs em termos de consumo de combustível, resultando em menores importações de combustível, menor impacto ambiental e menos manutenção. A introdução de VEs em um país em desenvolvimento é uma tarefa muito exigente e desafiadora. Neste artigo, os aspectos técnicos e econômicos da introdução de VEs no Paquistão foram explorados detalhadamente. Os dados estatísticos de vendas de veículos dos últimos anos foram considerados para estimar a demanda por VEs, conforme a política de VEs do Paquistão de 2019. A partir dessa estimativa, calculou-se a demanda de energia elétrica para atingir as metas da política. Com base na demanda de energia calculada, foram determinados os detalhes da infraestrutura de recarga em grandes cidades como Karachi, Islamabad, Lahore, etc. Constatou-se que uma estação de recarga para VEs deve estar presente a cada 3x3 km de raio. Além disso, a partir da estimativa de VEs, determinou-se a economia de custos resultante da não utilização de combustíveis fósseis, que seriam necessários para o funcionamento de VFCs. Do ponto de vista econômico, concluiu-se que os veículos elétricos podem diminuir significativamente a necessidade de combustíveis fósseis e resultar em uma enorme economia de custos ao não utilizar esses combustíveis.*

Palavras-chave: *Veículos elétricos, emissões, política para veículos elétricos, importação de petróleo, Paquistão.*

1. Background. - Global warming is damaging our planet at a very rapid rate. The driving force for global warming is carbon emissions. Around 43 billion tons carbon dioxide was produced through human activities in 2019 [1]. Due to these carbon emissions, Pakistan is facing lot of issues like higher air quality index, acid rains, etc. while Pakistan is the fifth most powerless nation in the face of climate change because it cannot control proficient climate change and relies on oil (petrol or diesel) primarily due to its easy availability and lower cost than other resources. Transport sector contributes around 24% in the global carbon emissions [2] due to dependence on fossil fuels which becomes the reason that many developed and undeveloped countries are planning to switch from Fossil Fuel-based Vehicles (FFVs) to EVs to reduce GHG emissions.

Currently, Pakistan's GHG emissions are growing by 6% per year, or 18.5 million tonnes of carbon dioxide (CO2) equivalent, in which the transport sector contributes around 22.69% of total annual GHG emissions [3] as can be seen in Figure 1. As a result, the best alternative solution is Electric Vehicles, which are gaining popularity and interest due to their advantages over conventional vehicles. The Pakistani government is also showing an interest in breaking into the market for electric vehicles in Pakistan. The government of Pakistan devised an "Electric Vehicles Policy" in 2019, which will aid in the adoption of EVs and have an impact on Pakistan's automotive industry growth, as well as help alleviate the country's massive debt burden. According to the government's policy handout, the target for EV adoption until 2030 is 30% of current vehicle sales [4], similar to other countries in the region.

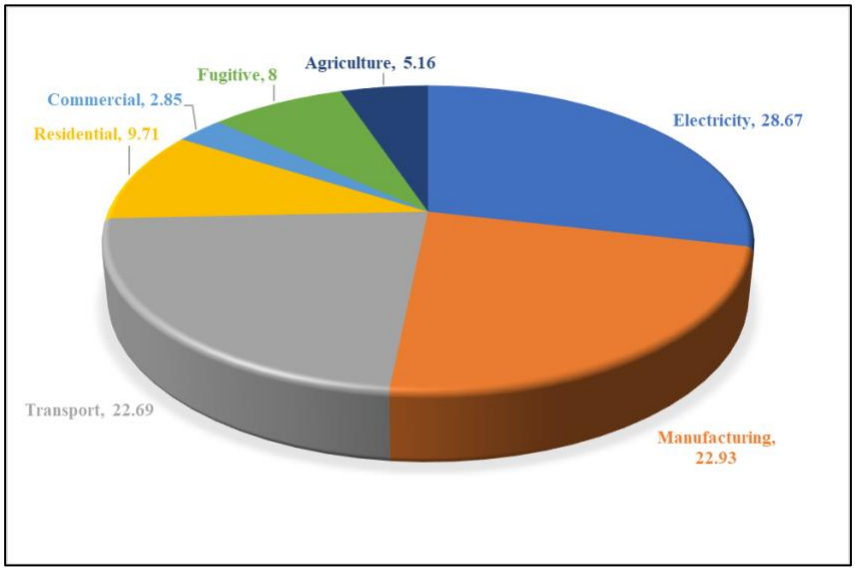

Figure I. Breakdown of GHG emission by sector [3]

1.1 Penetration of EVs in Developed countries. -

China: China is presently the world's largest oil importer. China's external oil dependence reached 70 percent in 2018 [5]. For China's energy security and environmental protection, limiting oil use is critical. The electric vehicle is often regarded as the most effective means of resolving these issues. Because of the development of electric vehicles, China's oil demand is expected to peak in 2029. Increased electric car penetration will boost economic production while also lowering nitrogen oxide emissions in China. Though carbon emissions will rise under the current power structure, the development of electric vehicles has the potential to significantly reduce CO2 emissions if non-fossil energy becomes the dominant energy source in the future in China [6].

European Countries: Europe, behind China, is the world's second-largest market for electric vehicles. The European electric vehicle (EV) market is expected to grow at an unprecedented rate by 2020.

More than 1.36 million new electric passenger cars, including battery-electric (BEV) and plug-in hybrid electric vehicles (PHEV), were sold in the region in 2019, up 143 percent from the previous year. Due to high sales, Europe surpassed China as the world's largest EV market in 2020. This occurred during a time when the automotive sector was through major instability [7].

EV sales in Europe climbed by 20% because of COVID-19, despite a 20% reduction in overall new car sales in Europe. The market share of electric vehicles has climbed to 11%. Several European markets have made significant progress. Greater percentages of new electric vehicle sales: 75% in Norway, 32% in Sweden, and 25% in the Netherlands and Finland has18%, Denmark has16%, Switzerland and Portugal has14%, Germany has13%, while France, Belgium, and the United Kingdom have 11% [8].

1.2 Penetration of Electric Vehicles in Pakistan's neighbouring countries. -

India: Electricity consumption in India has been increasing at a rate of 8–10 percent per year. The Indian government is actively promoting the use of electric vehicles in the Indian market. The National Electric Mobility Mission Plan (NEMMP) 2020 has been launched by the government of India to further evaluate their plans for the penetration of electric vehicles in their country [9]. The future analysis is done to determine the electric vehicle fleet, and then the future energy consumption per year is forecasted for 2030 using several scenarios of 20%, 30%, and 100% electrification of cars, as these targets are to be met by the Indian government. The results of a yearly cost-saving analysis for the researchers of India have discovered various types of automobiles, and they are as follows: There are four different categories of electric vehicles to consider: two-wheelers, three-wheelers, passenger vehicles, and commercial vehicles. It is believed that a two-wheeler travels 20 km per day, a three-wheeler travels 80 km per day, passenger vehicles travel 100 km per day, and commercial vehicles travel 250 km per day. The above part contains energy usage, which is used for further investigation. The charging unit cost of power is considered Rs. 5. The cost of fuel is calculated at Rs. 75 per litre. The cost-saving study is based on automobiles projected in 2030, with 100 percent electric vehicles being taken into account. As there will be around 4 million vehicles on the road in the future, there will be a significant increase in energy demand if they are all-electric [10].

India is a developing country, there is a pressing need to transition to electric vehicles as the gap between crude oil use and production widens. As India is a developing country, it is keener to adopt and penetrate the electrical vehicles in their country to evolve country to an industrialized and developed country. With these imperatives, electric vehicles would surely gain traction in India's future automobile market.

Bangladesh: Bangladesh is a country that is quite similar to our country and it is facing similar difficulties in the adoption of Electric Vehicles. EV adoption and penetration in Bangladesh becomes very challenging due to several barriers. Batteries run almost all the electric vehicles (i.e. bikes, auto-rickshaws, and electric bikes) in Bangladesh. A study showed that more than 0.5 million EVs are running in Bangladesh and these ingest 450 MW of electric power daily from the national grid [11], [12]. As the number of electric vehicles (EVs) grows, so does the demand for EV accessories and charging stations. According to the demand, the charging station, which is an important parameter, appears to be insufficient in Bangladesh. As a result, the electric car owner uses the residential rate to recharge the batteries in their home. In this sense, the power industry of Bangladesh has had a system failure, and a considerable quantity of revenue from this sector has been lost. In Bangladesh, there are no accurate statistics on EVs. As a result, the government is unable to take appropriate action in this matter. In Bangladesh, there are varieties of factors that influence EV adoption. Inadequate EV charging stations (EVCS), battery technology, power supply unavailability, excessive charging costs, pollution, and so on. So the study shows that Bangladesh is also facing the same barriers and difficulties to be feasible in the adoption of EVs [13]

1.3 Need of EVs in Pakistan. - In Pakistan, the transportation sector has experienced double-digit expansion. Almost the entire transportation sector is reliant on oil-based products, and the government spends nearly USD 13 billion annually on oil imports. The bill for oil imports is estimated to exceed USD 30 billion by 2025 if our transportation sector continues to grow at the same double-digit rate [14]. Pakistan's power sector has also suffered difficulties, with power generation failing to meet the country's power demand for the past decade. However, in the coming years, the situation will drastically deteriorate, and Pakistan will face a power-generating shortage. The country has already signed up for a new generation, according to the National Transmission and Dispatch Company (NTDC), bringing its overall power generation capacity to 41,981 MW peak generation [15]. In Pakistan, EVs will be able to take advantage of the power supply glut in the next years. After accounting for all transmission and distribution losses, we estimate that a daily supply of 1000 MW may fully charge about 500,000 EVs [16]. The installation of charging stations in every practical range on highways, motorways, and local roads is a significant consideration for capital expenditure in

charging stations for the expanding use of EVs in Pakistan. To improve governance, intelligent metering should be installed at each EV charging station to better control and monitor the power level while also providing an efficient payment system. To make the most of charging stations, more alternatives with multiple chargers, such as slow and rapid charging connections with variable charging rates, are necessary at each station. Users can make use of the benefits of slow charging ports at lower rates without having to rush; fast charging ports, which use more energy to replenish the battery and take less time to complete, will benefit hurried clients.

1.4 Challenges in the adoption of EVs. - Governments all around the world are encouraging users to switch from fossil-fuel vehicles to electric vehicles, but the technology still faces several serious challenges before becoming widely adopted. With 63 percent of consumers assuming that an EV is out of their budget, the capital cost has always been a big element in the EV purchasing decision [17]. With battery costs, declining and cost parity between EVs and ICE vehicles expected by 2026 [18], attention is turning to the problem of scaling the necessary infrastructure and raw material supply to enable mass adoption of EVs.

Charging stations are harder to find than traditional gas stations and are usually limited by investment costs and difficult infrastructure development. In addition, charging in places where you normally park, such as at home or work, presents unique challenges as this reduces the network of functioning charging stations and discourages consumers from switching to electric vehicles. Increased EV adoption adds to the pressure on the grid, which may necessitate new grid infrastructure investment to match the increased demand. As utilities and power companies try to figure out how to comprehend the quickly developing EV industry, forecasting when and where this electricity is needed is a new problem. Charging EVs at off-peak hours, such as late at night or early in the morning, reduces the danger of grid overload.

Grey energy networks, which rely heavily on fossil fuels, reduce the use of EVs as a means for businesses and consumers to reduce emissions. As a result, it is critical to decarbonize the grid as much as possible to persuade purchasers that switching to an EV is profitable and decreases carbon emissions [19]. EVs consume around six times the number of mineral inputs as ICE vehicles. According to the IEA (International Energy Agency), 70 million EVs on the road by 2040 would be followed by a 30-fold rise in mineral consumption [12]. There is no lack of these subsurface resources; the question is whether they will be harvested responsibly, by social responsibility governance, and in time to fulfill demand. It is expected that there would be a nickel scarcity and difficulties in scaling up lithium production. Because of the supply scarcity, producers may employ lower-quality mineral inputs, reducing battery performance [20].

Steps to allay these challenges: With the move to electric vehicles well underway, propelled by increased environmental concerns, government laws, and financial incentives, the obstacles created by this transformation are only mounting. Fortunately, AIoT-assisted technology (Artificial intelligence of things), when combined with other hardware, industrial, and supply chain solutions, allows us to overcome numerous problems. Battery monitoring, analytics, and recycling help to alleviate supply bottlenecks caused by increased demand for necessary battery materials by prolonging battery lifetime and reusability.

Smart and flexible charging technology utilizes idle power from car batteries to give additional electrical supply to the grid at times of high demand, in other circumstances, just intelligently stops, or decreases charging power. In contrast, it allows users to recharge during off-peak hours for one-third or less of the peak-hour charging price, lowering grid congestion and consumer costs during peak hours [21]. The charging system can better anticipate abrupt peaks in electricity consumption by allowing EV owners to plan to charge based on power limits, price, and priority, as well as sell unused power back to the grid.

On an integrated digital platform, energy management systems choreograph an energy system's generation assets (such as solar or wind power installations) and demand assets (such as EV chargers, heating and cooling systems, and lights). This enables real-time asset health and performance monitoring via the Internet of Things (IoT) connection and AI-driven algorithms, which maximize renewable energy consumption while lowering operating costs and system investments. It also enables the co-optimization of EVs and stationary storage with other grid-connected [19].

Exhaustion of Environment: Due to the effects of climate change, Pakistan has already been designated as the fifth most susceptible country [22]. Burning additional fossil fuels, including oil, will only exacerbate the problem. Pakistan's emissions are predicted to treble by 2020 and triple by 2030 [23], according to the National Economic and Environmental Development Study (NEEDS) study. Other harmful substances like sulphur dioxide (SO2), nitrogen dioxide (NO2), particulate matter (PM), PM10, and PM2.5, will also increase in the atmosphere because of increased fossil fuel combustion. Pakistan generates over 37% of its electricity from renewable sources [24].

When this is combined with the efficiency of EVs, environmental emissions are reduced by 70-80% when compared to FFVs. This indicates that, while electric vehicles have no particulate emissions, they have a 70-80% reduction in environmental emissions across the entire energy value chain [16]. Therefore, we can say that a step toward electric vehicles is the best solution to overcome the exhaustion of the environment in Pakistan.

1.5 Research Gap and Novelty. - From the preceding discussion, one can come with a conclusion that EVs is an attractive way to replace the fossil fuel-based transportation, to avoid the carbon emissions. But it is important to consider the technical requirements of the EVs for its implementation. In this research, the technical aspects of the EVs requirement have been thoroughly investigated. Moreover, the costing of the EVs including cost saved due to implementation of EVs have been discussed to investigate its economic aspects in Pakistan.

2. Methodology. - For the technical investigation, the immense amount of statistical data from different institutions in Pakistan is gathered. This section deals with the gathered data and information that are used in the prediction of vehicles by 2030, the number of electric vehicles, the energy required for these electric vehicles, the charging infrastructure required in motorways and major cities, the amount of oil barrels that can be saved from the penetration of electric vehicles and the cost saved from this EV penetration is discussed.

2.1. Prediction of Car Sales by 2030. - To predict the future number of vehicles that are going to be on the roads of Pakistan by 2030, the data is collected from registered vehicles of different categories from 2006 to 2019 and is presented in Table 1.

Year	2 wheelers	3 wheelers	4 wheelers	Cabs	buses	trucks
2006	137,892	6821	68610	1976	8779	9497
2007	144,081	12853	109053	1034	2999	3127
2008	175,768	11842	108006	2032	7796	8370
2009	1,089,538	33917	68487	16419	3627	5175
2010	1,476,832	64563	155213	1769	3686	8956
2011	1,718,229	56799	212729	19208	12898	15813
2012	1,669,346	57390	186794	1375	4973	6309
2013	1,836,893	85606	156652	190	4056	6377
2014	2,074,979	92929	277587	22254	4887	8271
2015	2,149,560	112289	218346	3081	6324	7626
2016	2,287,405	91673	262874	131	6580	8649
2017	2,278,212	80224	299039	227	7004	6829
2018	2,174,543	75709	207936	62	4741	3304
2019	736,248	20375	69318	52	839	6770

Table I. Vehicle sale over the year [25]

Prediction of EVs by 2030: For the Prediction of EVs in Pakistan by 2030, two different scenarios mentioned in Table 2 are considered that are according to medium-term targets and long-term targets of NEVP 2019 [4].

EV Penetration Targets	Medium-term targets (5 years)	Long-term targets (2030)
4 Wheelers (cars jeeps vans small busses)	100,000 EVs	30% of new sales
2 or 3 Wheelers	500,000 EVs	50% of new sales
Buses	1000 EVs	50% of new sales
Trucks	1000 EVs	30% of new sales

Table II. EV penetration targets [4]

Using the results from the calculations done for the prediction of sales of vehicles, the estimated number of EVs can be calculated for both scenario 1 and scenario 2

Charging Infrastructure: The calculation of the power requirement of EVs in Pakistan by 2030 for both scenarios 1 and 2 are done by the formula given below

$$E = N \times d \times e \qquad \text{Eq. 1}$$

Where,
E = Energy Consumed per day in kWh
N = Number of EVs
d = Average traveling distance in km
e = Energy consumption in kWh per km

Table 3 shows the average distance in km travelled by different categories of vehicles and their average energy consumption in kWh per km [26].

Vehicle Type	Average traveling distance in km	Energy consumption in kWh per km
2 and 3 Wheelers	20	0.0241
4 Wheelers	20	0.215
Buses	36	1.35
Trucks	100	1.242

Table III. Energy requirement by different EV [26]

According to the EV policy, there must be one DC fast charging station in every 3 by 3 km range in all the major cities like Karachi, Islamabad, Lahore, etc. So, 9 meter-sq is divided by the area of the city to get the amount of charging stations in that city [4].

$$\boldsymbol{Y} = \frac{\boldsymbol{A}}{\boldsymbol{9}} \qquad \text{Eq. 2}$$

Where,
Y = Number of charging stations
A = Area of city in meter-sq
Since, for the initial steps the policy aims at building charging infrastructure in the major cities that is why smaller cities are not considered. However, on motorways and highways, the policy suggests building a charging station every 15 km on all important motorways and highways.

Economic Analysis: Pakistan is a net importer of oil and its products. Beyond that, transport is the second largest user of energy after industry and accounts for about 34 percent of total final energy consumption and almost 59 percent of liquid fuel consumption in Pakistan. That is, air, sea, and road transport account for more than half of oil consumption (59 percent) followed by the power sector (32 percent) and industry (8 percent)

On average, the study finds growth of about 12.5 percent in the demand for petrol and about 9.6 percent in the demand for diesel in the road transport of Pakistan [14]. The number of barrels of oil extracted from the Pakistan economic survey is presented in Table 4 [27]

Years	Cost	M.T	Barrels of Oil
2010-11	8,761.50	N/A	N/A
2011-12	12,582.90	N/A	N/A
2012-13	12362.5	N/A	N/A
2013-14	12,221.10	N/A	N/A
2014-15	8,896.60	12,678,825	48,663,450
2015-16	5,584.80	11,241,367	7,053,648.25
2016-17	6,683.10	15,791,893	67,816,976.25
2017-18	8,393.30	19,223,622	19,106,751.5
2018-19	361.7	232,206	346,492
2019-20	6,417.30	13,521,203	9,968,162.75
2020-21	5,471.00	16,862,412	41,196,704

Table IV. Pakistan's Oil Import

Now talking about the benefit that the Introduction of EVs can make to the current situation of oil imports in Pakistan, we know that the transport sector is the biggest consumer of oil in Pakistan and accounts for 34 percent of energy consumption and 59 percent of the liquid fuel consumption
Using the average oil import cost and using the data from Scenario 1 and scenario 2 we can estimate the saved cost using the formula given below

$$\boldsymbol{Cost\ Saved} = (\boldsymbol{Average\ oil\ import\ cost\ X\ 0.34}) - (\boldsymbol{Average\ oil\ import\ cost\ X\ 0.34\ X\ Percentage\ of\ FFVs}) \quad \textit{Eq. (3)}$$

Here the factor (Average oil import cost X 0.34) represents the percentage of oil cost used in the transport sector.

3. Results and Discussions. - To study the trend of vehicle sales with respect to time, statistical software Minitab was utilized to create regression models for diverse vehicle categories. The sales statistics, as indicated in Table 1, underwent linear regression analysis to determine patterns over time. The findings in various vehicle categories are depicted in Figure 1. It is clear from the regression analysis that vehicle sales have been on a rising trend during the years. Various models were examined to find the best fit for each vehicle type. For two-wheelers, the linear regression model proved the most appropriate with an R-square value of 85.69%. This signifies that the model is able to forecast two-wheeler sales with about 85.69% accuracy and has a margin of error of 14%. The high correlation indicates a consistent pattern of growth in two-wheeler sales over time. For four-wheelers, the best-fitting model was found to be the quadratic regression model with an R-square of 68.71%. This relatively lower R-square indicates that the quadratic model does not forecast four-wheeler sales with great accuracy. The precision of this model is less than that of the linear model for two-wheelers, which means that other factors besides time contribute a great deal to four-wheeler sales, which makes the sales fluctuate to a point that it cannot be fully accounted for by a plain time-based model. In the case of three-wheelers, the linear regression model proved to be suitable, as was the case for two-wheelers. Although the model has decent predictive power, there is some error involved, which indicates that other factors affecting the trend must be taken into account in order to make a more precise forecast.

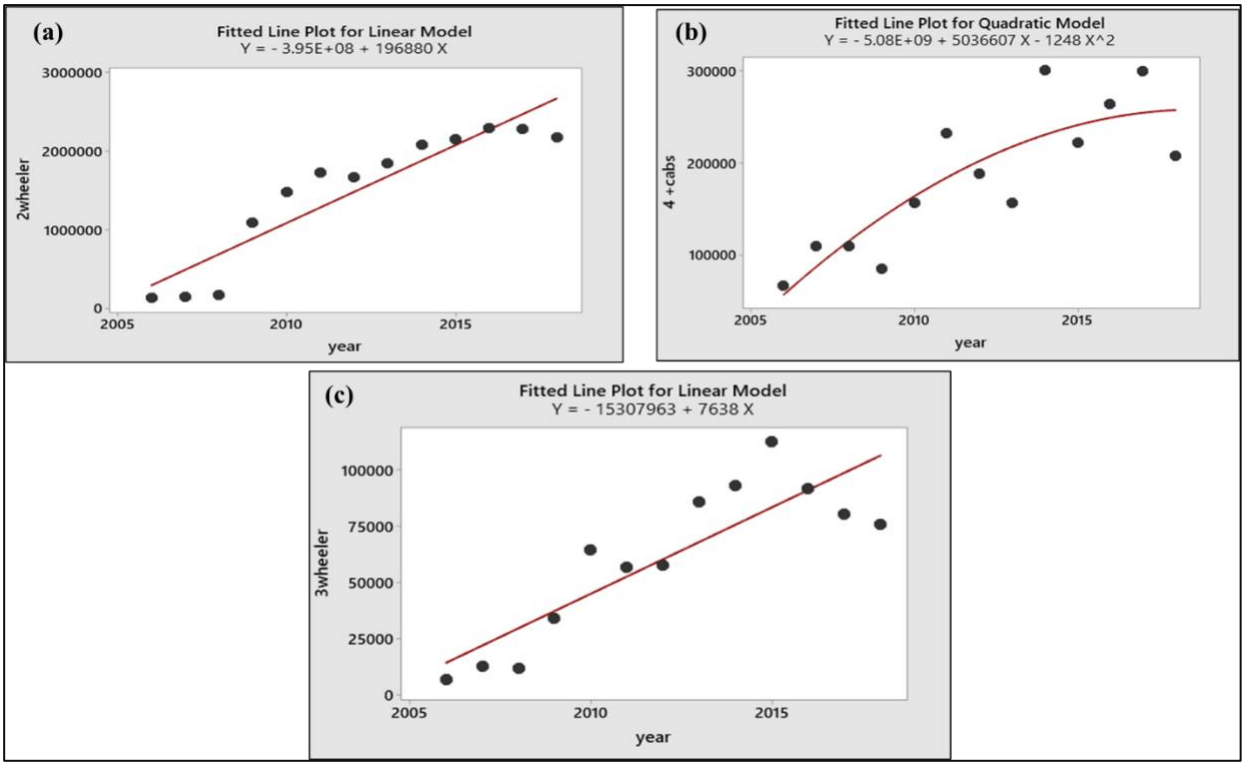

Figure II. Regression model for estimation of Vehicles Sale by 2030 (a) 2 wheelers (b) 4 wheelers (c) 3 wheelers.

2 Wheelers	$S = -3.95 \times 10^8 + 196880(year)$	Eq. 4
3 Wheelers	$S = -15307963 + 7638(year)$	Eq. 5
4 Wheelers	$S = -5.08 \times 10^9 + 5036607(year) - 1248(year)^2$	Eq. 6

Table V. EV prediction model

Considering medium-term targets as Scenario 1 and long-term targets as scenario 2, the number of EVs are estimated for from Equations 4, 5, and 6, which are obtained from the regression model applied on the data gathered for vehicle sales over the past 15 years and the results have been presented in Figure 3. From where, it is clear that for medium targets, around 4.3 million cumulative 2 and 3 wheelers EVs will be required, while to meet the long term targets the required combined 2 and 3 EVs should 11.6 million by 2030. To meet the targets, the 4 wheelers EVs should be around 300,000 for medium targets while for long term targets, these should be around 715,000 by 2030. These numbers show that there would be a good quantity of EVs that will be present in 2030 and to run these EVs the significant amount of electrical energy would be required. The electricity required to run the EVs have been estimated using Equation 1 and the results have been presented in Figure 4. For Scenario 1, around 6.5 GWh electrical energy is required on daily basis to run the EVs out of which 2.1 GWh/day will be required by 2 and 3 wheelers while 4.4 GWh/day will be required by 4 wheelers. For long-term targets, termed as Scenario 2, more electrical energy will be required because of high number of EVs. Around 16.28 GWh/day electrical energy will be required to meet the long-term targets. Out of which, 5.633 GWh/day will be required by 2 and 3 wheelers while the rest of energy will be required by the 4 wheelers.

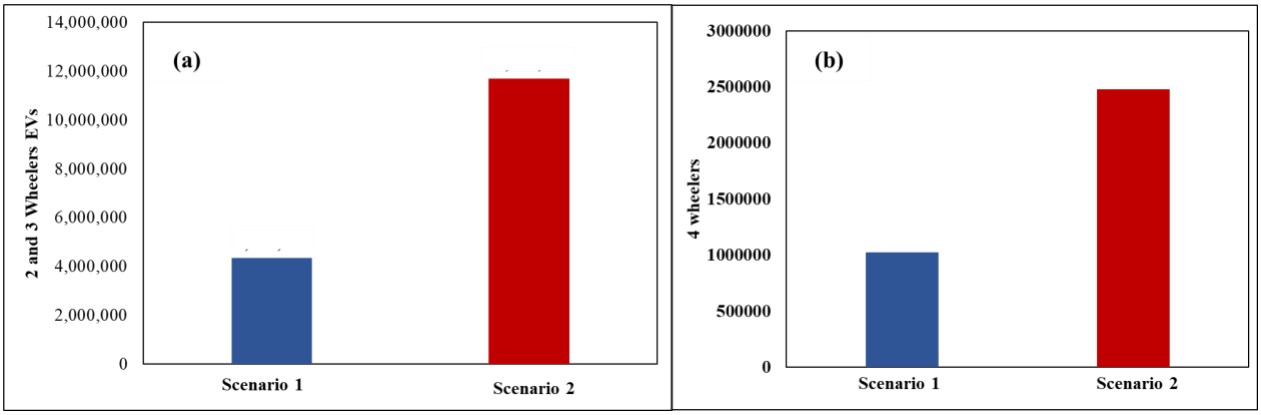

Figure III. EVs prediction (a) 2 and 3 wheelers (b) 4 wheelers.

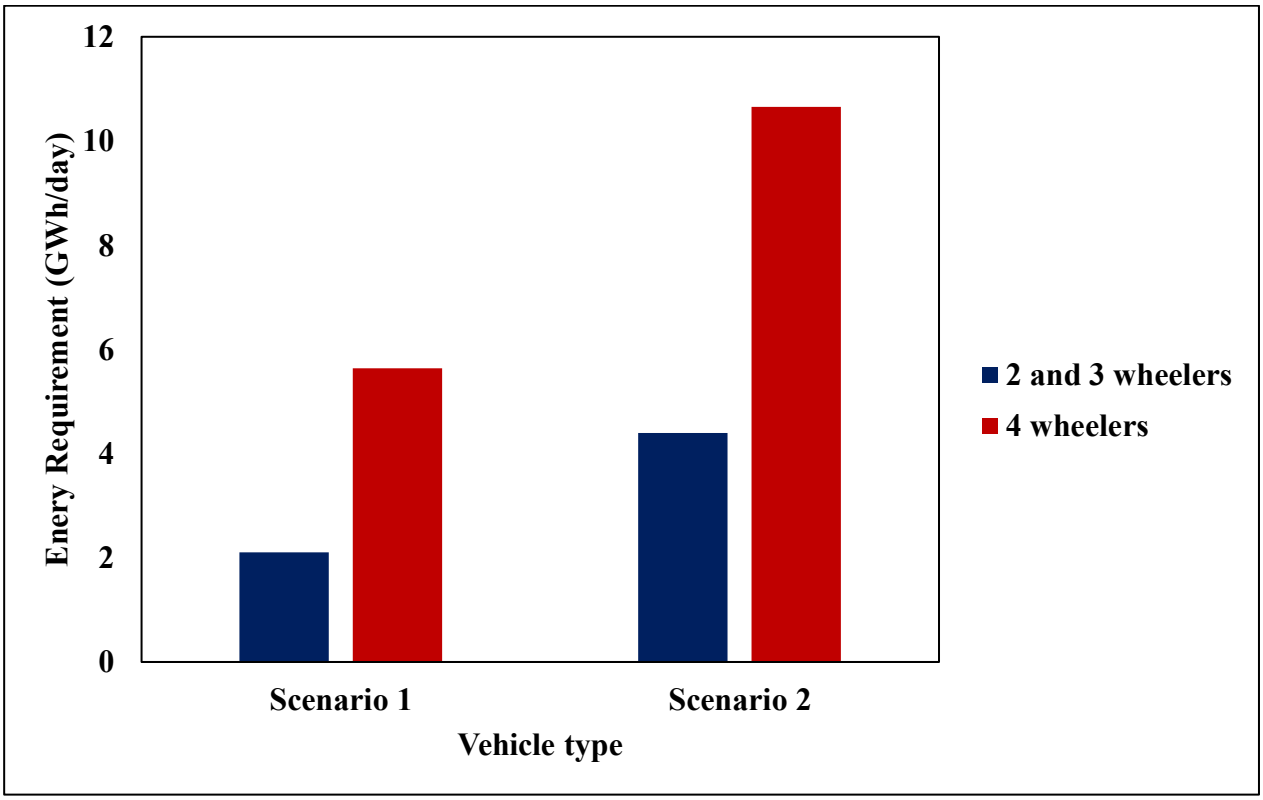

Figure IV. Electrical Energy Requirement by different EVs.

The charging infrastructure requirement for major cities of Pakistan has been estimated by using Equation 2 and the results are presented in Table 6. The charging infrastructure requirement has been estimated by considering the policy requirement which restricts one DC fast charging station in every 3 by 3 km range in all the major cities like Karachi, Islamabad, Lahore, etc. These charging stations must be enough to support the electrical energy requirement by EVs. The area of Karachi is 3780 km. sq. so for 1 DC charging station in every 3 by 3 km, there will be a need for 420 charging stations only in Karachi. Similarly for other major cities like Lahore, Islamabad, Faisalabad, Peshawar, Rawalpindi, Gujranwala, Hyderabad, and Quetta, the number of charging stations would be 197,100, 144, 23, 29, 27, 32, and 19 respectively. Since the policy aims at building charging infrastructure in the major cities that is why smaller cities are not considered, the number of charging stations to be installed in these cities by 2030 sums up to be 991.

City	Number of Stations
Lahore	197
Islamabad	100
Faisalabad	144
Peshawar	23
Rawalpindi	29
Gujranwala	27
Quetta	19
Hyderabad	32
Karachi	420
Total	991

Table VI. Charging Stations required in Major Cities.

The economic assessment of electric vehicles (EVs) begins with quantifying the cost benefits that stem from their use, which can be computed as the difference between EV utilization expenses and FFV utilization costs. In Pakistan, the transport industry uses oil the most, as it makes up 34% of energy consumption and 59% of liquid fuels. Financial savings due to lesser oil consumption were calculated using Scenario 1 and Scenario 2 data, assumptions and average oil import price as shown in Equation 3. The results are presented in Tables 7 and 8. In Scenario 1, the total cost savings is estimated at $812 million, while Scenario 2 estimates the cost savings at $2,149 million. All cost figures are in USD. This showcases the remarkable economic impact that EV integration offers for the transport sector. If adapted, Pakistan would reduce the burden its imported oil has on the economy, curb trade imbalance, and improve energy independence. It also contributes to sustainable development through advancing cleaner transportation options. Both scenarios greatly showcase the savings that would be seen in costs, which demonstrates the positive economic outlook that EV integration brings.

Scenario 1					
YEAR	TOTAL VEHICLES	EVs	FFV	% OF FFV	COST SAVED (Mil. $)
2021	32,777,068	75,903	32,701,165	99.77%	6.279856805
2022	37,608,978	235,053	37,373,925	99.38%	16.94872923
2023	42,633,853	482,984	42,150,869	98.87%	30.72137116
2024	47,849,197	830,284	47,018,913	98.26%	47.05592934
2025	53,252,514	1,282,301	51,970,213	97.59%	65.29985323
2026	58,841,308	1,846,006	56,995,302	96.86%	85.0772001
2027	64,613,083	2,528,277	62,084,806	96.09%	106.1125401
2028	70,565,343	3,335,901	67,229,442	95.27%	128.1988555
2029	76,695,592	4,275,569	72,420,023	94.43%	151.1770904
2030	83,001,334	5,353,881	77,647,453	93.55%	174.9226881
				TOTAL	**811.7941139**

Table VII. Cost saving for Scenario 1.

Scenario 2					
YEAR	TOTAL VEHICALS	EV SCENARIO 2	FFV	% OF FFV	COST SAVED (Mil. $)
2021	32,777,068	199,664	32,577,404	99.39%	16.51935157
2022	37,608,978	618,902	36,990,076	98.35%	44.62652185
2023	42,633,853	1,277,397	41,356,456	97.00%	81.25195391
2024	47,849,197	2,194,608	45,654,589	95.41%	124.3783385
2025	53,252,514	3,389,769	49,862,745	93.63%	172.6205406
2026	58,841,308	4,881,891	53,959,417	91.70%	224.9925793
2027	64,613,083	6,689,758	57,923,325	89.65%	280.7710869

2028	70,565,343	8,831,931	61,733,412	87.48%	339.4115783
2029	76,695,592	11,326,745	65,368,847	85.23%	400.4950923
2030	83,001,334	14,192,313	68,809,021	82.90%	463.693047
				TOTAL	**2148.76009**

Table VIII. Cost saving for Scenario 2.

4. Conclusion. - The predictions and calculations done in this paper indicate that the introduction of EVs in Pakistan's transport sector will be beneficial for lowering carbon emissions by replacing conventional cars. The introduction of EVs will also be encouraging private and government sectors to invest in clean and renewable energy, however, the clean energy generation in Pakistan is already gradually growing as discussed above moreover it will promote the idea of clean and renewable energy among normal individuals. Talking about power, these electric vehicles will need 6.5 GWh/day and 16.28 GWh/day according to Scenario 1 and 2 respectively. Other than the environmental benefits of EVs in Pakistan there is also a huge economic benefit too, Pakistan being a net importer of oil is a huge burden on Pakistan's economy currently Pakistan imported 41,196,704 barrels of oil in the year 2020-21 from which almost 34% will be for the transport sector, this indicates that replacing conventional vehicles with EVs will directly affect Pakistan's economy. According to the calculations done in this paper, the total cost saved over the period of 10 years from scenario 1 is estimated to be 812 million dollars and can reach 2149 million dollars if we consider scenario 2. All this discussion leads to the result that EVs are the best option for Pakistan to deal with Environmental issues and with the burden of oil import in the country. A renewed EV policy by the government of Pakistan is much needed to accelerate EV growth by further decreasing import duties on EVs and related technology to increase public awareness by providing incentives to the buyers, moreover invest in building up infrastructure and charging stations across the motorways and highways of Pakistan.

5. Declaration. - The authors would like to declare that there is no conflict of interest. Authors would also like to declare the use of Artificial Intelligence in improving the overall text of the manuscript.

References

[1] A. A. Naqvi, A. Ahmed, T. Bin Nadeem, L. A. Khan, and I. U. Ahad, "Energy and stress analysis of a hybrid photovoltaic thermal module," *Case Stud. Therm. Eng.*, vol. 47, no. January, p. 103114, 2023, doi: 10.1016/j.csite.2023.103114.

[2] A. A. Naqvi, A. Zahoor, A. A. Shaikh, F. A. Butt, F. Raza, and I. U. Ahad, "Aprotic lithium air batteries with oxygen-selective membranes," *Mater. Renew. Sustain. Energy*, no. 0123456789, 2022, doi: 10.1007/s40243-021-00205-w.

[3] K. A. Mir, P. Purohit, and S. Mehmood, "Sectoral assessment of greenhouse gas emissions in Pakistan," *Environ. Sci. Pollut. Res.*, vol. 24, no. 35, pp. 27345–27355, 2017, doi: 10.1007/s11356-017-0354-y.

[4] G. of P. Ministry of Climate Change, "National Electric Vehicle Policy," 2019.

[5] K. H. Wang and C. W. Su, "Does high crude oil dependence influence Chinese military expenditure decision-making?," *Energy Strateg. Rev.*, vol. 35, p. 100653, 2021, doi: 10.1016/j.esr.2021.100653.

[6] B. Lin and W. Wu, "The impact of electric vehicle penetration: A recursive dynamic CGE analysis of China," *Energy Econ.*, vol. 94, p. 105086, 2021, doi: 10.1016/j.eneco.2020.105086.

[7] E. E. Agency, "New registrations of electric vehicles in Europe." [Online]. Available: https://www.eea.europa.eu/en/analysis/indicators/new-registrations-of-electric-vehicles

[8] S. Wappelhorst, D. Hall, M. Nicholas, and N. Ltsey, "Analyzing Policies To Grow the Electric Vehicle Market in European Cities," *ICCT White Pap.*, no. February, pp. 1–43, 2020, [Online]. Available: https://theicct.org/sites/default/files/publications/EV_city_policies_white_paper_fv_20200224.pdf

[9] G. of I. Department of Heavy Industry, Misnistry of Heavy ndustries a& Public Enterprises, "National Electric Mobility Mission Plan 2020," 2012.

[10] A. Jain, H. R. Jariwala, and U. Mhaskar, "Feasibility Analysis for the Penetration of Electric Vehicles in India in Future," *8th Int. Conf. Comput. Power, Energy, Inf. Commun. ICCPEIC 2019*, pp. 68–72, 2019, doi: 10.1109/ICCPEIC45300.2019.9082380.

[11] S. Z. Rajper and J. Albrecht, "Prospects of electric vehicles in the developing countries: A literature review," *Sustain.*, vol. 12, no. 5, 2020, doi: 10.3390/su12051906.

[12] F. Biro, "The Role of Critical Minerals in Clean Energy Transitions," 2021. doi: 10.1787/f262b91c-en.

[13] M. R. Ahmed and A. K. Karmaker, "Challenges for Electric Vehicle Adoption in Bangladesh," *2nd Int. Conf. Electr. Comput. Commun. Eng. ECCE 2019*, pp. 1–6, 2019, doi: 10.1109/ECACE.2019.8679288.

[14] A. Malik, "Munich Personal RePEc Archive Fuel Demand in Pakistan's TRansport Sector Fuel Demand in Pakistan's Transport Sector," *Munich Pers. RePEc Arch. Fuel*, no. 103455, 2018.

[15] G. of P. Finance Division, "Energy." doi: 10.1515/9783110214130.214.

[16] N. Ullah *et al.*, "Electric vehicles in Pakistan: Policy recommendations volume I cars," *Lums.Edu.Pk*, 2019, [Online]. Available: https://web.lums.edu.pk/~eig/pdf/evPrinting.pdf

[17] S. Li, L. Tong, J. Xing, and Y. Zhou, "The market for electric vehicles: Indirect network effects and policy design," *J. Assoc. Environ. Resour. Econ.*, vol. 4, no. 1, pp. 89–133, 2017, doi: 10.1086/689702.

[18] G. Fenton, "Price parity for electric cars and ICE vehicles by 2026," Top Charger.

[19] Luiz Avelar, "The road to an EV future still has a few potholes. Here's how to fix them," Energy Transition.

[20] Annonimas, "How are supply chains and gray power markets working?" [Online]. Available: https://www.think-renewable.com/knowledge-hub/supply-chain-electricity-markets

[21] Driivz, "Smart EV Charging and Energy Management: the Essential Guide." [Online]. Available: https://driivz.com/blog/ev-smart-charging-benefits/

[22] S. M. Abubakar, "https://www.dawn.com/news/1520402," *Dawn*, p. 2019. [Online]. Available: https://www.dawn.com/news/1520402

[23] D. V. A. A. UMAR, "Carbon emissions in Pakistan likely to rise about 300% by 2030," *Express Tribune*, 2018.

[24] Anno, "Pakistan Energy Situation," Energy Pedia. [Online]. Available: https://energypedia.info/wiki/Pakistan_Energy_Situation

[25] National Transport Research Centre, "Motor Vehicles on Road in Pakistan upto 30th June, 2024."

[26] Numbeo, "Traffic in Pakistan." [Online]. Available: https://www.numbeo.com/traffic/country_result.jsp?country=Pakistan

[27] G. of P. Finance Division, "Pakistan Economic Survey," 2022.

Author contribution:

1. Conception and design of the study
2. Data acquisition
3. Data analysis
4. Discussion of the results
5. Writing of the manuscript
6. Approval of the last version of the manuscript

AAN has contributed to: 1, 2, 3, 4, 5 and 6.

WU has contributed to: 1, 2, 3, 4, 5 and 6.

SMS has contributed to: 1, 2, 3, 4, 5 and 6.

MZAN has contributed to: 1, 2, 3, 4, 5 and 6.

MOF has contributed to: 1, 2, 3, 4, 5 and 6.

Acceptance Note: This article was approved by the journal editors Dr. Rafael Sotelo and Mag. Ing. Fernando A. Hernández Gobertti.

Effect of Tesla valve geometry on unsteady flow behavior and pressure drop - A CFD study

Efecto de la geometría de la válvula Tesla en el comportamiento del flujo inestable y la caída de presión: un estudio de CFD

Efeito da geometria da válvula Tesla no comportamento do fluxo instável e na queda de pressão - Um estudo de CFD

Muhammad Shakaib [1(*)], Muhammad Ehtesham ul Haque [2], Syed Muhammad Fakhir Hasani [3]

Recibido: 08/04/2025 Aceptado: 23/07/2025

Summary. - Computational fluid dynamics (CFD) simulations are carried out to examine the effect of geometric parameters of Tesla valve on flow patterns, pressure drop and flow diodicity. In forward flow, the flow is relatively smooth with less flow resistance. The low velocity regions are present at the entrance to the curved section and at the junction of the curved section and the exit channel, where flow separation takes place. In reverse flow, the flow is quite irregular, and major recirculation zones are observed in the bottom branch, in addition to the top-curved and exit sections. The simulations with small time steps show that the flow is steady when the flow takes place in the forward direction. The flow is mostly transient; however, when the fluid flows in the reverse direction, particularly at higher Reynolds numbers. The effect of geometric parameters such as the angles subtended by the curved section (with the horizontal) shows that optimal values of these angles exist. For a certain range of angles, diodicity is greater than 2. The effect of multi-staging of the Tesla valve is studied, and it is found that the flow unsteadiness and overall diodicity increase with the number of stages.

Keywords: Micro/Nano Fluidics, Tesla Valve, Computational Fluid Dynamics, Pressure drop, Diodicity.

[1] Professor, Department of Mechanical Engineering, NED University of Engineering and Technology (Pakistan), mshakaib@neduet.edu.pk, ORCID iD: https://orcid.org/0000-0003-0699-1987

[2] Assistant Professor, Department of Mechanical Engineering, NED University of Engineering and Technology (Pakistan), mehaque@neduet.edu.pk, ORCID iD: https://orcid.org/0000-0001-8751-348X

[3] Associate Professor, Department of Mechanical Engineering, Imam Mohammad Ibn Saud Islamic University (Saudi Arabia), smhasani@imamu.edu.sa, ORCID iD: https://orcid.org/0000-0002-6202-1996

Memoria Investigaciones en Ingeniería, núm. 29 (2025). pp. 54-73
https://doi.org/10.36561/ING.29.5
ISSN 2301-1092 • ISSN (en línea) 2301-1106 – Universidad de Montevideo, Uruguay
Este es un artículo de acceso abierto distribuido bajo los términos de una licencia de uso y distribución CC BY-NC 4.0. Para ver una copia de esta licencia visite http://creativecommons.org/licenses/by-nc/4.0/

Resumen. - *Simulaciones de dinámica de fluidos computacional (CFD) fueron realizadas para examinar el efecto de los parámetros geométricos de la válvula Tesla en los patrones de flujo, la caída de presión y la diodicidad del flujo. En flujo directo, el flujo es relativamente suave y presenta poca resistencia. Se observan regiones de baja velocidad en la entrada de la sección curva y en la unión de esta con el canal de salida, donde se produce la separación del flujo. En flujo inverso, el flujo es bastante irregular y se observan importantes zonas de recirculación en la rama inferior, además de en las secciones superior curva y de salida. Las simulaciones con pasos de tiempo pequeños muestran que el flujo es estacionario en la dirección directa. Sin embargo, el flujo es mayormente transitorio en la dirección inversa, particularmente a números de Reynolds elevados. El efecto de parámetros geométricos como los ángulos subtendidos por la sección curva (con respecto a la horizontal) muestra que existen valores óptimos para estos ángulos. Para un cierto rango de ángulos, la diodicidad es mayor que 2. Se estudia el efecto de la multietapa de la válvula Tesla y se encuentra que la inestabilidad del flujo y la diodicidad general aumentan con el número de etapas.*

Palabras clave: *Microfluídica/nanofluídica, válvula Tesla, dinámica de fluidos computacional, caída de presión, diodicidad.*

Resumo. ***-*** *Simulações de dinâmica dos fluidos computacional (CFD) foram realizadas para examinar o efeito dos parâmetros geométricos da válvula Tesla nos padrões de fluxo, na queda de pressão e na diodicidade do fluxo. No fluxo direto, o fluxo é relativamente suave, com menor resistência. Regiões de baixa velocidade estão presentes na entrada da seção curva e na junção da seção curva com o canal de saída, onde ocorre a separação do fluxo. No fluxo reverso, o fluxo é bastante irregular e grandes zonas de recirculação são observadas no ramo inferior, além das seções curvas superiores e de saída. As simulações com pequenos passos de tempo mostram que o fluxo é estável quando ocorre na direção direta. O fluxo é predominantemente transiente quando o fluido flui na direção reversa, particularmente em números de Reynolds mais altos. O efeito de parâmetros geométricos, como os ângulos subtendidos pela seção curva (com a horizontal), mostra que existem valores ótimos para esses ângulos. Para uma determinada faixa de ângulos, a diodicidade é maior que 2. O efeito do funcionamento em múltiplos estágios da válvula Tesla é estudado, e constata-se que a instabilidade do fluxo e a diodicidade geral aumentam com o número de estágios.*

Palavras-chave: *Micro/Nanofluidos, Válvula Tesla, Dinâmica dos Fluidos Computacional, Queda de pressão, Diodicidade.*

1. Introduction. - A non-return valve (NRV) is a common device in piping systems that allows the fluid to flow in one direction while restricting its flow in the opposite direction. The 'one-way' operation of the valve in these systems may be necessary for various reasons, such as safe operation of the mechanical equipment, avoiding mixing or contamination of fluid streams or in general to ensure desired system performance. Many of the NRVs utilize a ball/poppet with a seat and spring arrangement. The ball moves in a particular direction due to fluid force, allowing the fluid flow in one direction while blocking it in the opposite direction. Another type of non-return valve is the Tesla valve, which, because of its geometrical design, offers more resistance when fluid flows in the reverse direction compared to its forward movement. It does not require any manual or electronic operation, and unlike other NRV types, it does not have any internal moving element to open or close the flow passage. Invented more than a century ago by Nikola Tesla (1920), its use has reemerged in recent times due to its potential application in microfluidic devices. Tesla valves have been found useful in applications where low flow rates are required or in situations where moving parts can cause a significant reduction in the overall efficiency of the device. The Tesla valve behaves much like a diode in electronics, which allows the current to flow only in one direction and blocks the current flow in the opposite direction. Like a diode, the Tesla valve offers higher flow resistance due to its complex geometry, creating vortex-type flow structures as it flows in one direction and offers much less resistance when its flow direction is reversed. This feature of the Tesla valve is defined in terms of its diodicity, which is the ratio of the pressure drop in the reverse direction to the pressure drop in the forward direction. The pressure drop in forward/reverse direction or diodicity depends on the geometrical characteristics of the Tesla valve, the fluid properties and the flow velocities. The resurfacing of the Tesla valve technology in modern-day micro and nano fluidics has been discussed in detail in a historical review paper by Purwidyantri and Prabowo (2023). A comprehensive literature review shows that several studies exist that investigate the various parameters of the Tesla valve. Nobakht et al. (2013) carried out CFD simulations and studied flow behavior in various sections of the Tesla valve. The work showed that significant energy loss occurs at the Y-junction when the flow is in the reverse direction. Zhao et al. (2024) considered straight-through Tesla valves with blades. It was shown that the pressure loss increased with an increase in blade width, inclination and pitch. The computational work of Zhang et al. (2024) found that the pressure drop in the Tesla valve improved with an increase in valve width. However, the improvement became insignificant when the width was made too large. Khabarova et al. (2017) carried out experiments for fluid diode devices. They showed that the flow becomes unstable and transient when the Reynolds number is greater than 500. A few papers, in addition to fluid flow, study related processes of heat transfer or phase changes in the Tesla valve. For example, Han et al. (2024) examined the two-phase boiling flow in several microchannel geometries. The results showed that vapor backflow was reduced in the Tesla valve channel, which improved the flow boiling performance. Huang et al. (2024) performed flow and thermal analysis that showed the presence of numerous eddies at the entrance of the valve, which greatly influenced the heat transfer rate. A Tesla valve with a symmetric shape was studied by Liu and co-researchers (2022), and they proved that the Hagen number was proportional to the square of the Reynolds number at higher velocities. Jiang et al. (2025) investigated temperature and pressure oscillations to suggest design improvements in a Tesla valve. The study by Du et al. (2023) predicted fluid flow and heat transfer performance in a Tesla valve using an artificial neural network technique. The optimal designs from their work increased the thermal and hydraulic efficiencies by 27% and 78%, respectively. Apart from these papers, several others considered Tesla valve for different applications such as photovoltaic thermal process (Hai et al., 2024; Zhao et al., 2024), hydrogen production unit (Chen et al., 2025) and printed circuit heat exchanger (Chou et al., 2024) All the previously published papers indicate that the design of Tesla valve can significantly affect the flow structure, diodicity and other performance parameters. In this paper, we have studied the effect of geometric parameters of Tesla valve on transient velocity profiles, pressure drop and diodicity. To the authors' knowledge, no study exists that examines the influence of Tesla valve geometry on unsteady flow behavior. Based on the fluid flow analysis, suitable geometries are proposed that can result in higher values of diodicity.

2. Methodology. -

2.1 Tesla valve geometry and computational domain. - To examine flow behavior in a Tesla valve, a computational domain was constructed as shown in Figure I. The valve consists of an inlet, an intermediate section consisting of branched channels for two possible flow paths and an outlet. One branched region is straight, while the other is curved. The curvature of the curved channel is defined with the help of two angles, α and β, which are the angles made by the

end and beginning sections of the curved branch with the horizontal. The height of the channel is 0.3 mm, and the outer radius of the curved section is 0.75 mm.

2.2 Boundary conditions and assumptions. - The effect of geometry on flow patterns and pressure drop is studied by specifying the inlet either to the left edge or to the (inclined) right end. These two cases are termed 'forward' and 'reverse' flow, respectively. Velocity was specified at the inlet, and a pressure outlet boundary condition was used at the outlet. The other surfaces were defined as 'wall', where the no-slip condition was applied. The effect of body force/gravity was neglected. The fluid was assumed to be water, which is a Newtonian and an incompressible fluid. The fluid properties, such as density and viscosity, thus, were constant and equal to 998.2 kg/m3 and 0.001 kg/m.s, respectively.

2.3 Grid generation. - The domain was divided into small volumes of quadrilateral shape using a grid. The grid was refined in the portions where the variation in velocity was expected to be higher, such as near the walls and in the regions where the fluids from two branches mix. The grid size was sufficient to obtain reliable pressure drop and diodicity values. For example, the results of diodicity were compared for valve geometries with α = 45° and 60° at Re = 2000 for various grid sizes, as shown in Figure II. The difference in diodicity was found to be less than 1% when cells were greater than 25000 cells, indicating that the results are independent of the grid. The convergence criterion for normalized residuals of continuity and velocity components was 1 x 10^{-5}.

2.4 Governing equations and discretization. - Since most microfluidic applications involve low velocities, the problem in most cases turns out to be that of laminar two-dimensional flow. The governing equations were the continuity and the momentum equations for 2D unsteady flow that were solved using the Ansys Fluent code.

$$\frac{\partial u}{\partial x}+\frac{\partial v}{\partial y}=0 \qquad (1)$$

$$\frac{\partial u}{\partial t}+u\frac{\partial u}{\partial x}+v\frac{\partial u}{\partial y}=-\frac{1}{\rho}\frac{\partial p}{\partial x}+\nu\left(\frac{\partial^2 u}{\partial x^2}+\frac{\partial^2 u}{\partial y^2}\right) \qquad (2)$$

$$\frac{\partial v}{\partial t}+u\frac{\partial v}{\partial x}+v\frac{\partial v}{\partial y}=-\frac{1}{\rho}\frac{\partial p}{\partial y}+\nu\left(\frac{\partial^2 v}{\partial x^2}+\frac{\partial^2 v}{\partial y^2}\right) \qquad (3)$$

In equations (1-3), u and v are velocity components in x- and y-directions, respectively, p is pressure, ρ is density, and ν is kinematic viscosity. The equations were discretized using the QUICK scheme, and the pressure-velocity coupling was achieved using the SIMPLEC algorithm. Reynolds numbers up to 2000 were considered, and values of α and β were varied from 15°-60° and 30°-75°, respectively. The Reynolds number is defined as:

$$Re=\frac{\rho v d_h}{\mu} \qquad (4)$$

Where d_h is hydraulic diameter, which is equal to twice of channel height h and μ is absolute viscosity.

At higher Reynolds numbers, particularly in the case of 'reverse' flow, the solution did not converge under steady conditions, indicating that the flow was not perfectly laminar. The solution in such a situation was obtained in unsteady mode without addition of any turbulence model. The unsteady/transient simulations were carried out using a second-order implicit scheme with a time step of 0.002 ms.

The performance of the device is compared using diodicity Di, which is defined as:

$$Di=\frac{\Delta p_R}{\Delta p_F} \qquad (5)$$

A higher value of diodicity indicates that the device has better flow directional control and is desirable.

2.5 Validation. - To validate the computational findings of this study, comparisons were made with previously published experimental and numerical results. The diodicity for one of the geometries considered in this paper (α = 45°, β = 75°) was calculated at different Reynolds numbers and compared with the experimental and numerical results in a similar geometry by Gamboa et al. (2005). This comparison is shown in Figure III, which shows that the difference between the diodicity values is within 30%. Since the diodicity values are low, this difference was considered acceptable and confirms the reliability of the results presented in this paper.

3. Results and Discussion

3.1 Single valve analysis

3.1.1 Effect of α on flow behavior in Tesla valve. - The velocity profiles typically found in a single Tesla valve are shown in Figure IV. The geometry of the valve has an angle α equal to 45°, and flow profiles are shown at two different values of Reynolds numbers. In the case of forward flow, it is seen that the flow mostly takes place in the bottom straight section, and the diversion of fluid into the curved section/branch is minimal. Flow recirculation is observed at the point where the curved section begins, while in the remaining portion of this curved loop, the fluid moves with a low velocity. A small recirculation zone could be seen downstream at the exit of the curved section where the curved and straight sections of the channel reunite, causing flow separation and recirculation (Figures IVa and IVc). When the flow direction is reversed (Figures IVb and IVd), the inlet fluid stream divides into two portions, creating prominent vortex flow in both sections of the valve. As the two flow streams remix at the outlet section of the channel, a much larger recirculation region could again be observed. Comparison of Figures (IVa with IVc) and (IVb with IVd) shows the effect of increasing the Reynolds number. As expected, the flow recirculation in both the curved and exit sections increased and became stronger at a higher Reynolds number value of 2000. The effect of angle α on flow patterns is shown in Figure V. The shape of the valve appears to change from a blunt shape to a relatively streamlined shape as the value of α is increased. Thus, with α = 15°, the fluid in the bottom portion must take a sharp turn before exiting the curved loop, while at α = 60°, it exits the channel relatively smoothly, whether in forward or reverse flow directions. For a moderate angle (α = 30°), significant recirculation regions in the top as well as the bottom branch are observed in the reverse flow. This behavior is similar, as was noticed in Figure IVd for the case of α = 45°. The transient response of pressure drop for four different α (15o, 30o, 45o, 60o) values in forward and reverse flow is presented in Figure VI. The pressure drop values shown in this Figure are taken after some simulation time has elapsed, and a fluctuating but repetitive or constant behavior in property variation is nearly obtained. The plots show that the flow is steady in the forward direction with all the angles considered. However, in the reverse direction, the flow is unsteady, except when α = 60°. The pressure required in reverse flow is found sufficiently larger than the pressure required for forward flow. The quantitative analysis based on time-averaged pressure drop shows that the diodicity [the ratio of pressure drop in reverse flow (Δp_R) to the pressure drop in forward flow (Δp_F)] is maximum when α is 45°.

3.1.2 Effect of β on flow behavior in Tesla valve. - The effect of variation of β, defined as the angle of inclination of the left portion of the curved section, is also studied when α is kept constant at 45°. As illustrated in Figure VII, for forward flow, an increase of β results in a slightly increased flow recirculation at the entrance of the curved section. In other regions, the velocity profiles are almost the same. In the case of reverse flow, at higher values of β (such as 60° or 75°), the forward fluid motion in the bottom section faces considerable resistance from the returning fluid flowing in the curved section. This leads to the formation of a major stagnant zone in which the velocity magnitude is nearly zero (Figures VIIf and VIIh). The pressure drop variation with time for different values of β is shown in Figure VIII. Like in the previous cases, in which the effect of angle α was discussed, the flow is steady in forward flow, whereas it is unsteady when the flow is reversed. The pressure drop remains between 6000-7000 Pa, showing an insignificant effect of β in forward flow. In reverse flow, the pressure drop is greater than 10,000 Pa for all the geometries, with much significant pressure drops for β = 60° or 75°.

3.1.3 Pressure drop, diodicity and mass flow distribution. - A comparison of the time-averaged pressure drop and diodicity values obtained for the different valve geometries considered in this study is given in Table I. The results show that when α is 15°, in forward flow, the pressure drop is higher than the other valves. This results in the lowest diodicity values with this valve at both the Reynolds numbers. Among the four tested valve geometries (while fixing β = 8.5), the geometry with α equal to 45° leads to maximum diodicity. The variation of β from 30°-75° while keeping α

= 45°, indicates that there is no appreciable change in pressure drop for forward flow. However, for reverse flow, the pressure drops are higher for large β angles. The comparison provided in Table 1 shows that valve geometry with α = 45° and β = 60° has maximum diodicity and is considered as the most suitable design among the tested valve shapes. The influence of geometry on mass flow in the two sections of the valve is also determined. The mass flow in the bottom (straight) and the top (curved) sections is represented by m_1 and m_2, respectively. The bar plot in Figure IXa shows that the mass flow rate in the top section is less than 10% of the inlet flow in forward flow. In addition, the mass flow rate in the top section (m_2) decreases with an increase in Reynolds number, indicating that the fluid entry into the curved section is further reduced at higher flow velocities. The ratio of mass flow also depends on the valve geometry, and it is noticed that increasing α increases the m_2/m_1 ratio. This is due to the streamlined shape at higher values of α, which allows more fluid to move through the top curved section. The m_2/m_1 ratios are also found to be low for different values of β during forward flow. As seen in Figure IXb, this ratio remains in the range 0.04-0.07 at Re = 1000 and between 0.02-0.05 at Re = 2000. In the reverse flow, the fluid entry to the curved section is fairly smooth, which allows sufficient mass of the fluid to move through this section. Thus, for reverse flow, m_2/m_1 is mostly greater than 1.

3.1.4 Transient flow features. - As observed earlier in Figures VI and VIII in terms of pressure drop, the flow in the forward direction is steady, while the flow in the reverse direction is usually transient at Re = 2000. The flow patterns in a Tesla valve are now discussed in further detail with the help of instantaneous velocity contours. The contours shown in Figure X are for the valve which has maximum diodicity. The results show that in the outlet section, the high velocity zone not only changes in magnitude but also in size and shape. This zone appears to be of extended size at one instant (for example, at 0.2 or 0.8 ms) and is found to split into multiple zones at other instants (0.6 and 1.2 ms). The changes that occur in the high velocity region lead to the movement of low velocity flow recirculation regions formed near the top and bottom walls of the outlet section.

The instantaneous flow structures can also be explained by tracking the velocity changes in time at specified locations in different sections of the valve. It is observed in Figure XI that at points ‘A’ and ‘B’, which are placed in the outlet section, the variation in velocity is significant. At point A, the x-velocity remains negative, which means the flow is moving towards the outlet section (towards the left). On the other hand, at point B, the x-velocity is positive, which indicates that flow recirculation is taking place at this point. At points ‘C’ and ‘D’, the fluctuation in velocity is small, showing that the flow is steady in the top and bottom sections.

3.2 Performance of multi-stage valves. - To further increase the system’s performance, multiple valves can be connected in series. Thus, the flow behavior in the valve, which has maximum diodicity (α = 45°, β = 60°), is examined with two and three stages. It is found from the time-averaged velocity profiles (not shown here) that the locations of high and low velocity regions are the same and repeat in different stages. The unsteady behavior, however, significantly changes as the number of stages is increased. A comparison is made in Figure XII in terms of the root mean square (RMS) values of velocity variation in time for the two and three-stage Tesla valves. The contour plots of Figure XIIa show that for the forward flow with two stages, the flow is steady. For a three-stage valve, near the exit section of the third stage, the velocity is found to vary considerably, showing flow unsteadiness. In reverse flow, the flow is unsteady in both the two-stage and the three-stage Tesla valves. In a two-stage valve, unsteadiness is more in the second stage when compared with the first stage, whereas in a three-stage valve, unsteadiness is more prominent in the exit section of the third stage and a common region formed by the second stage exit and the third stage inlet. The results thus show that the flow is steady in the beginning but becomes transient as it travels a certain distance inside the valve.

The flow instabilities in a multistage Tesla valve may also be attributed to the varying mass flow rates in the straight and curved sections of the valve. The mass flow rate is calculated at different time intervals in the straight and curved sections of the three-stage valve, and its variation is plotted in Figure XIII. A comparison of mass flow in the straight sections A, C and E shows that the mass flow rate at A has less variation, showcasing the flow’s quasi-steady nature, while at location C, the variation increased, but its value remained negative, indicating that the flow is still in the reverse direction. However, at location E, which lies in the third stage, the mass flow rate turned positive for a portion of the time interval and remained negative for the rest of the interval. This shows that the flow direction is continuously reversing in the straight section of the third stage. Since the total flow rate is constant, an increase in flow in the straight

section decreases flow in the curved section. Like the straight section, the flow rate is less fluctuating in the first stage and more fluctuating in the third stage. The diodicity for two and three-stage valves is calculated and summarized in Table II. The results show that for both Reynolds numbers, the diodicity increases with the increase in the number of stages. The number of stages can therefore be adjusted, based on the pressure/mass flow rate requirements in practical applications.

4. Conclusions. - The numerical work presented in this paper examines the fluid flow, pressure drop, diodicity and mass flow distribution in Tesla valves for Reynolds numbers up to 2000. When flow is in the forward direction, the fluid mostly takes a straight path, and less than 10% of the total inlet flow enters the curved section. In the reverse direction, a significant amount of fluid moves in the curved section. The ratio of mass flow rates in the two sections, for reverse flow, varies from 0.3 to 2.2, depending on the Tesla valve angles. The mixing of the fluid stream in a curved section with the stream in a straight section at the exit junction is often abrupt. This causes increased pressure drop, particularly in reverse flow. The effect of variation of angle α shows that for small angles (e.g., α = 15°), the fluid takes sharp turns, thus resulting in increased pressure drop in reverse as well as forward flow. On the other hand, when α is large, such as 60°, the streamlined shape of the valve reduces pressure loss in both forward and reverse directions. The diodicity values are therefore lower when α = 15° and 60°. For β = 8.5°, the valve with α = 45° results in maximum diodicity. The variation of β indicates that an increase in this angle does not affect the pressure drop in forward flow. In reverse flow, however, its larger values are found to increase pressure drop and hence diodicity. Multiple stages for the Tesla valve are considered, and flow patterns are examined in various stages. It is noticed that, though the time-averaged velocities are the same in different stages, the unsteadiness in flow is increased in the latter stages. The present work performs fluid flow analysis of the Tesla valve and examines its performance in terms of pressure drop/diodicity. Future work, in addition to fluid dynamics, will include the study of the Tesla valve for systems involving other phenomena such as heat transfer and phase changes.

List of Symbols

dh	hydraulic diameter (m)
Di	Diodicity (-)
h	height (m)
m_1	mass flow rate in bottom/straight section (kg/s)
m_2	mass flow rate in top/curved section (kg/s)
p	pressure (Pa)
Δp_F	pressure drop in forward direction (Pa)
Δp_R	pressure drop in reverse direction (Pa)
Re	Reynolds number (-)
t	time (s)
u	x-component of velocity (m/s)
v	y-component of velocity (m/s)
x	horizontal / x-direction (m)
y	vertical / y-direction (m)
α	angle made by the left portion of the curved branch with the horizontal (°)
β	angle made by the right portion of the curved branch with the horizontal (°)
μ	viscosity (kg/m.s)
ν	kinematic viscosity (m2/s)
ρ	density (kg/m3)

Acknowledgement: The authors acknowledge support provided by NED University of Engineering and Technology, Karachi for this work.

Data Availability Statement: The paper includes findings from CFD simulations performed on the commercial code Ansys Fluent. The simulation files are available from the authors. The description of the Tesla valve can be found in the patent (U.S. Patent 1329559A). The details of the code/software are available in software Ansys Fluent user guide.

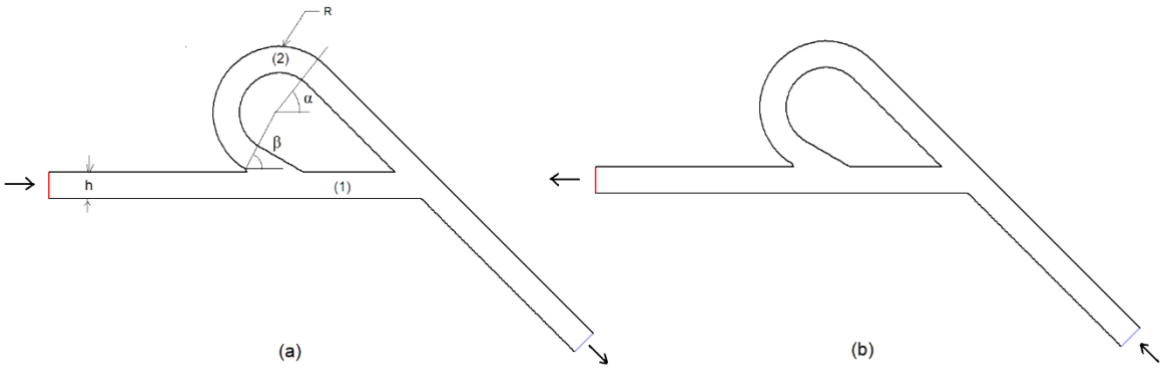

Figure I. Geometry of Tesla valve considered with (a) forward (b) reverse direction

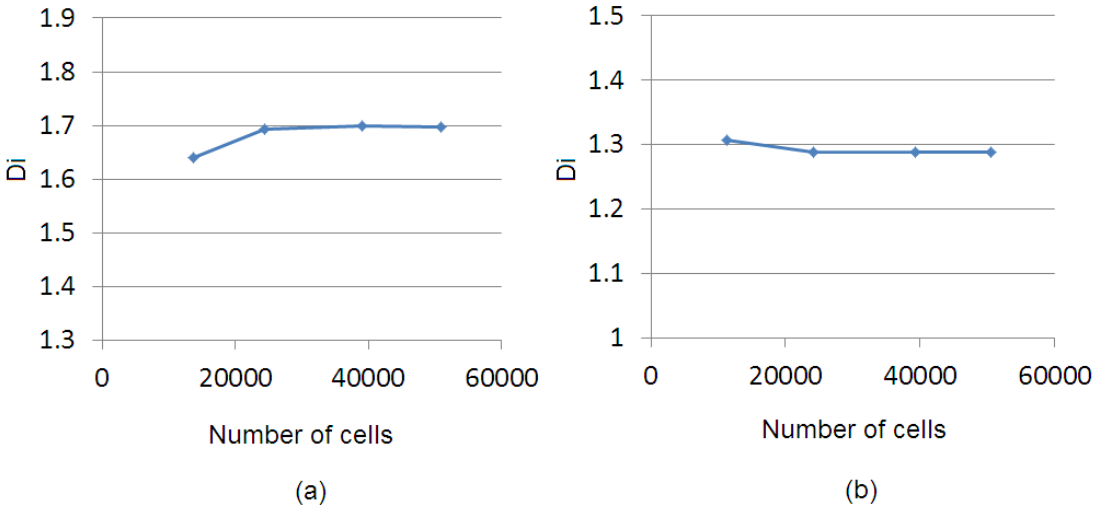

Figure II. Diodicity versus number of cells (a) α = 45° (b) α = 60°, β = 8.5°, Re = 2000.

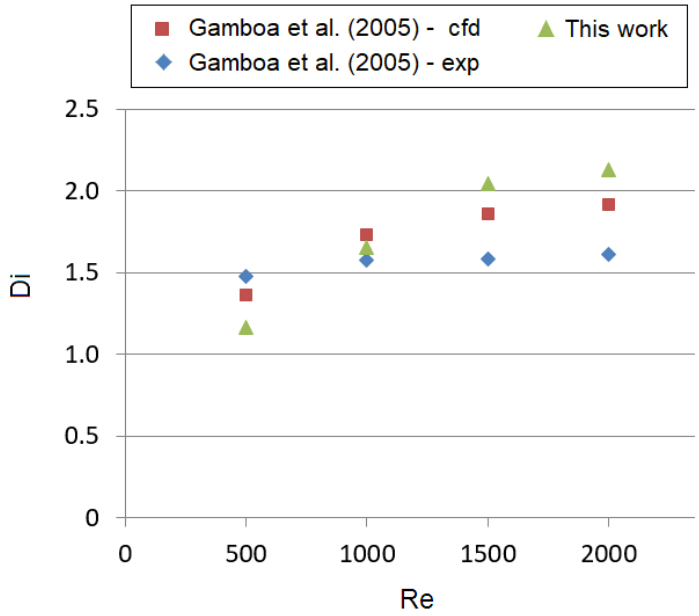

Figure III. Comparison of present CFD results with previous literature (α = 45°, β = 75°)

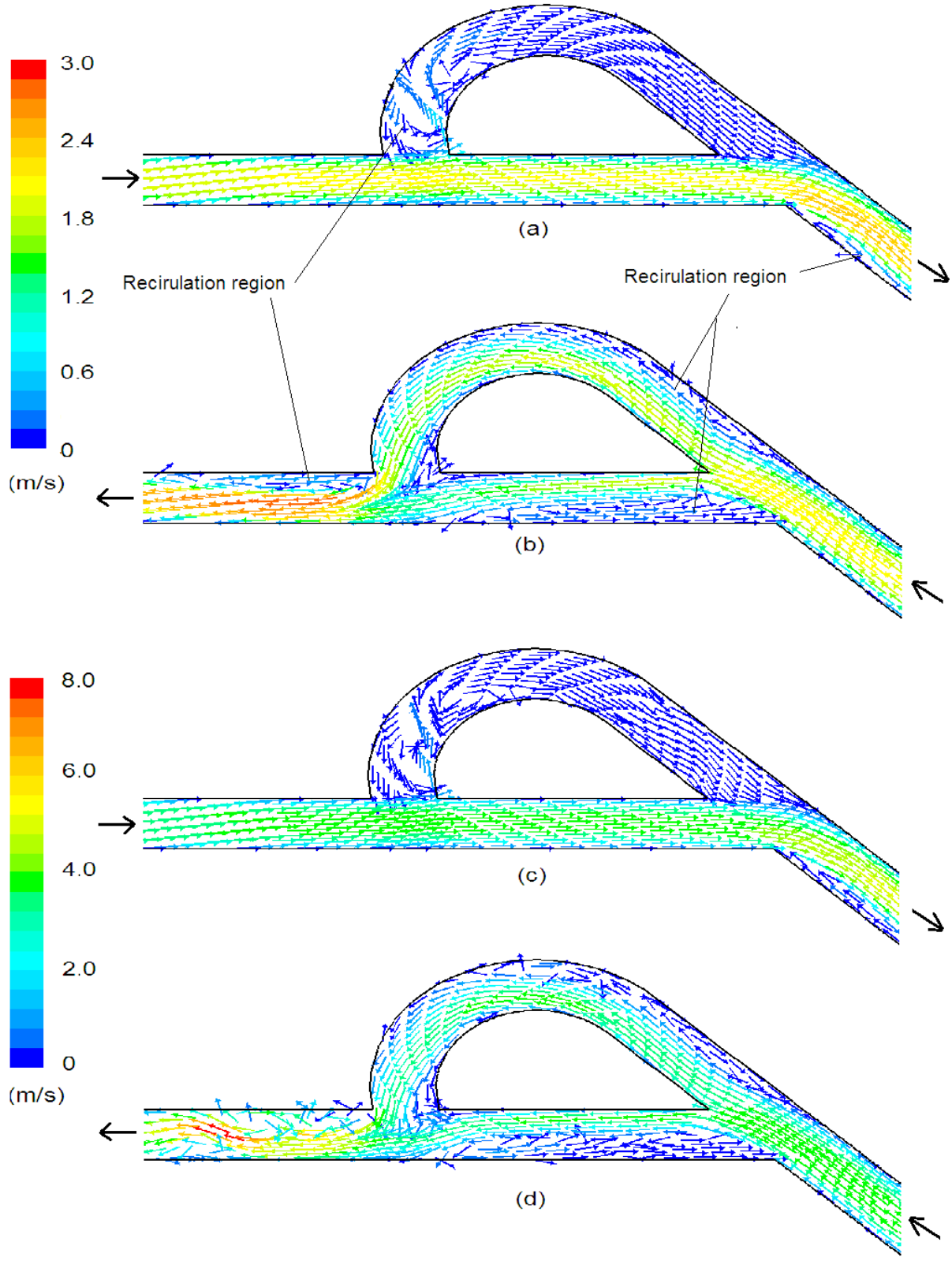

Figure IV. Flow pattern in Tesla valve α = 45°, β = 8.5° (a) Re = 1000, forward flow (b) Re = 1000, reverse flow (c) Re = 2000, forward flow (d) Re = 2000, reverse flow

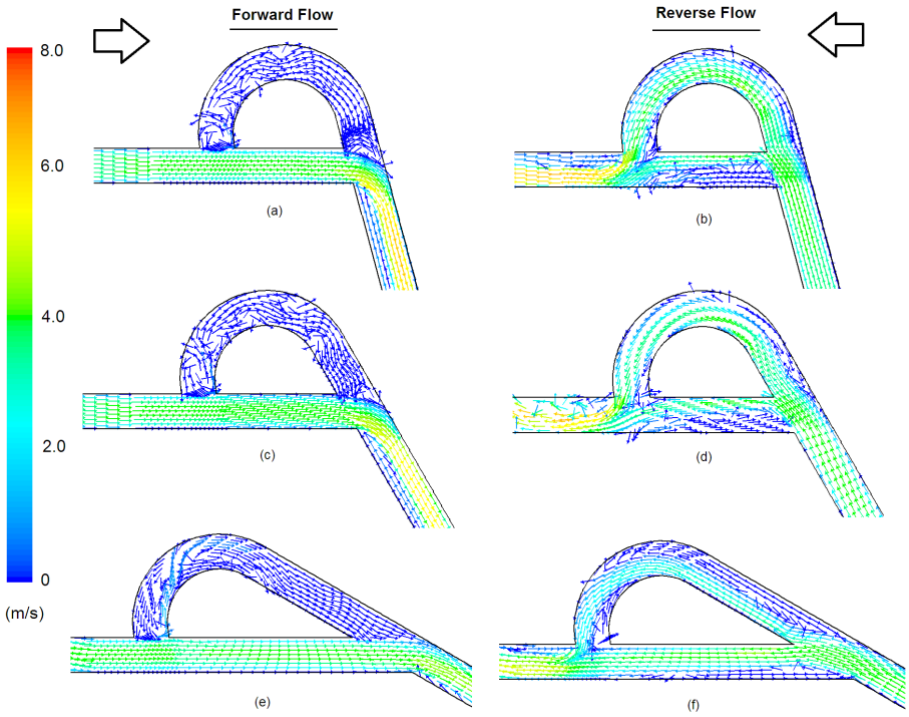

Figure V. Velocity Vectors in Tesla valve (a) α = 15°, forward flow (b) α = 15°, reverse flow (c) α = 30°, forward flow (d) α = 30°, reverse flow (e) α = 60°, forward flow (f) α = 60°, reverse flow (Re = 2000, β = 8.5°).

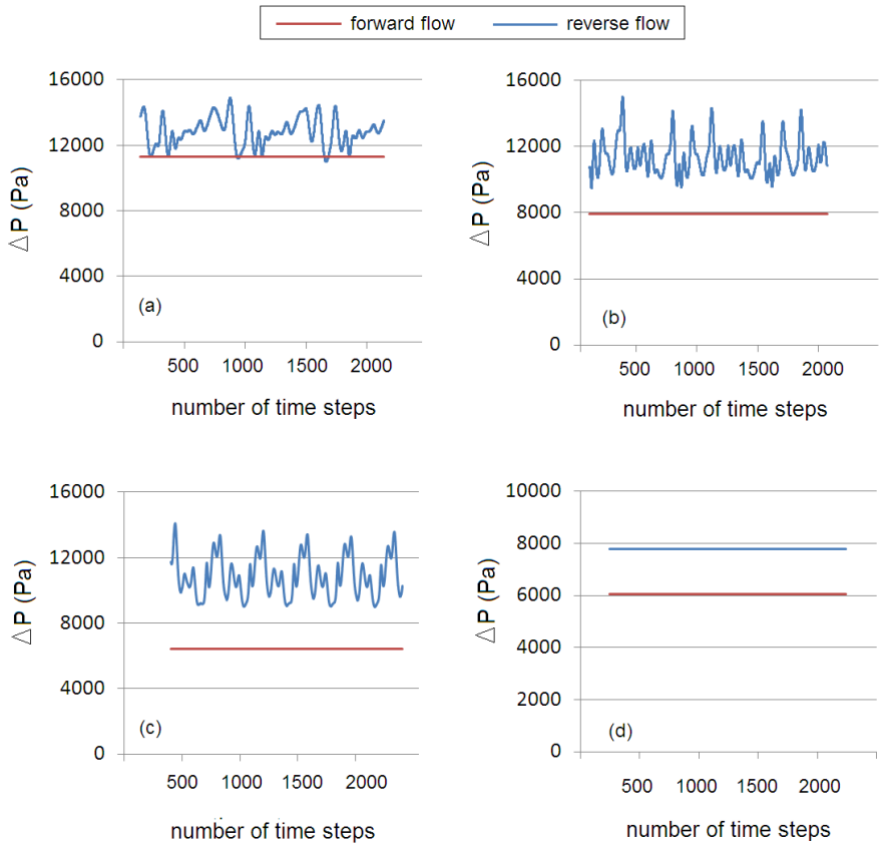

Figure VI. Pressure drop with forward and reverse flow in Tesla valve (a) α = 15° (b) α = 30° (c) α = 45° (d) α = 60° (Re = 2000, β = 8.5°).

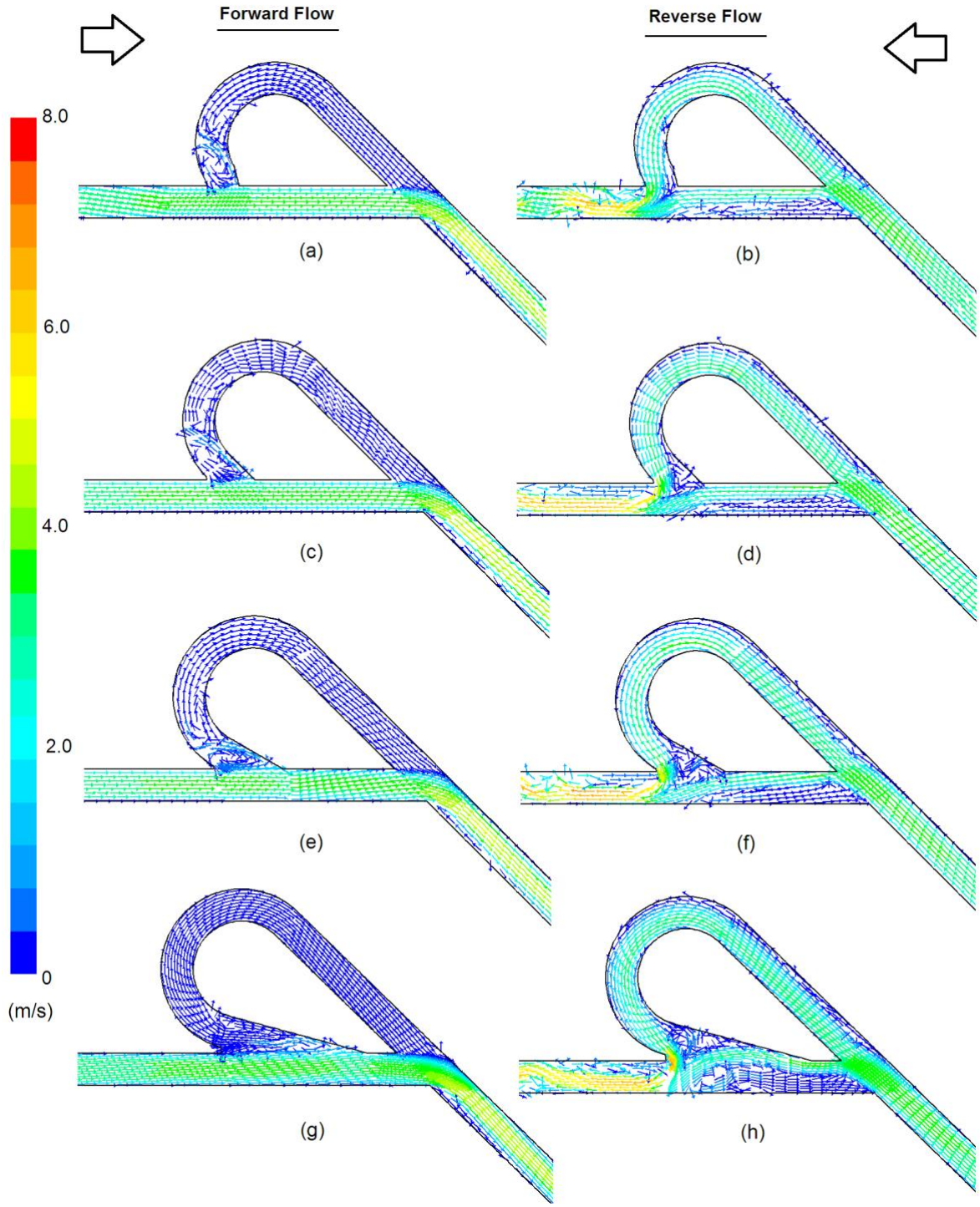

Figure VII Flow pattern in Tesla valve (a) β = 30°, forward flow (b) β = 30°, reverse flow (c) β = 45°, forward flow (d) β = 45°, reverse flow (e) β = 60°, forward flow (f) β = 60°, reverse flow (g) β = 75°, forward flow (h) β = 75°, reverse flow (α = 45°, Re = 2000).

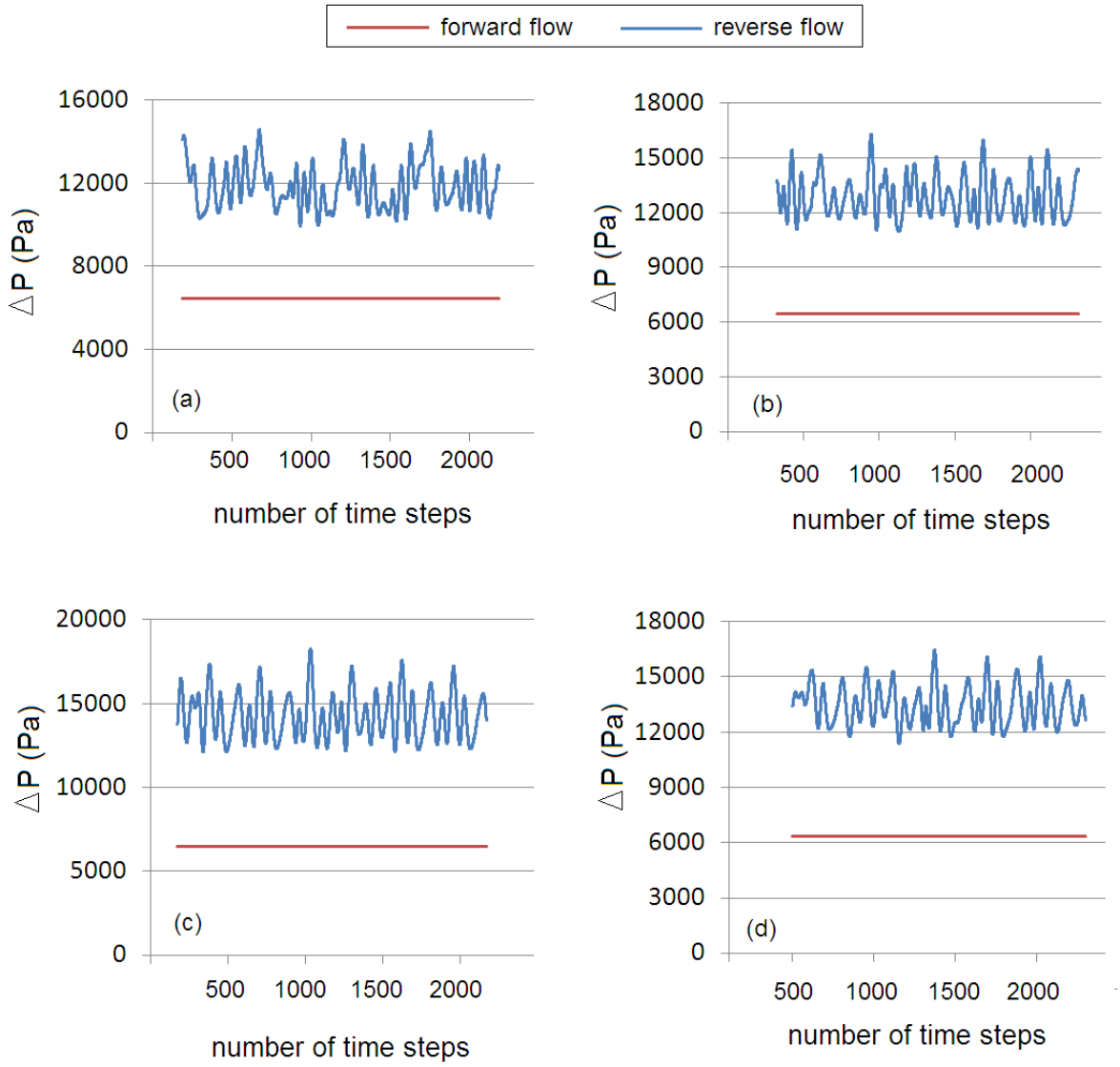

Figure VIII *Pressure drop with forward and reverse flow in Tesla valve (a) β = 30° (b) β = 45° (c) β = 60° (d) β = 75° (α = 45°, Re = 2000).*

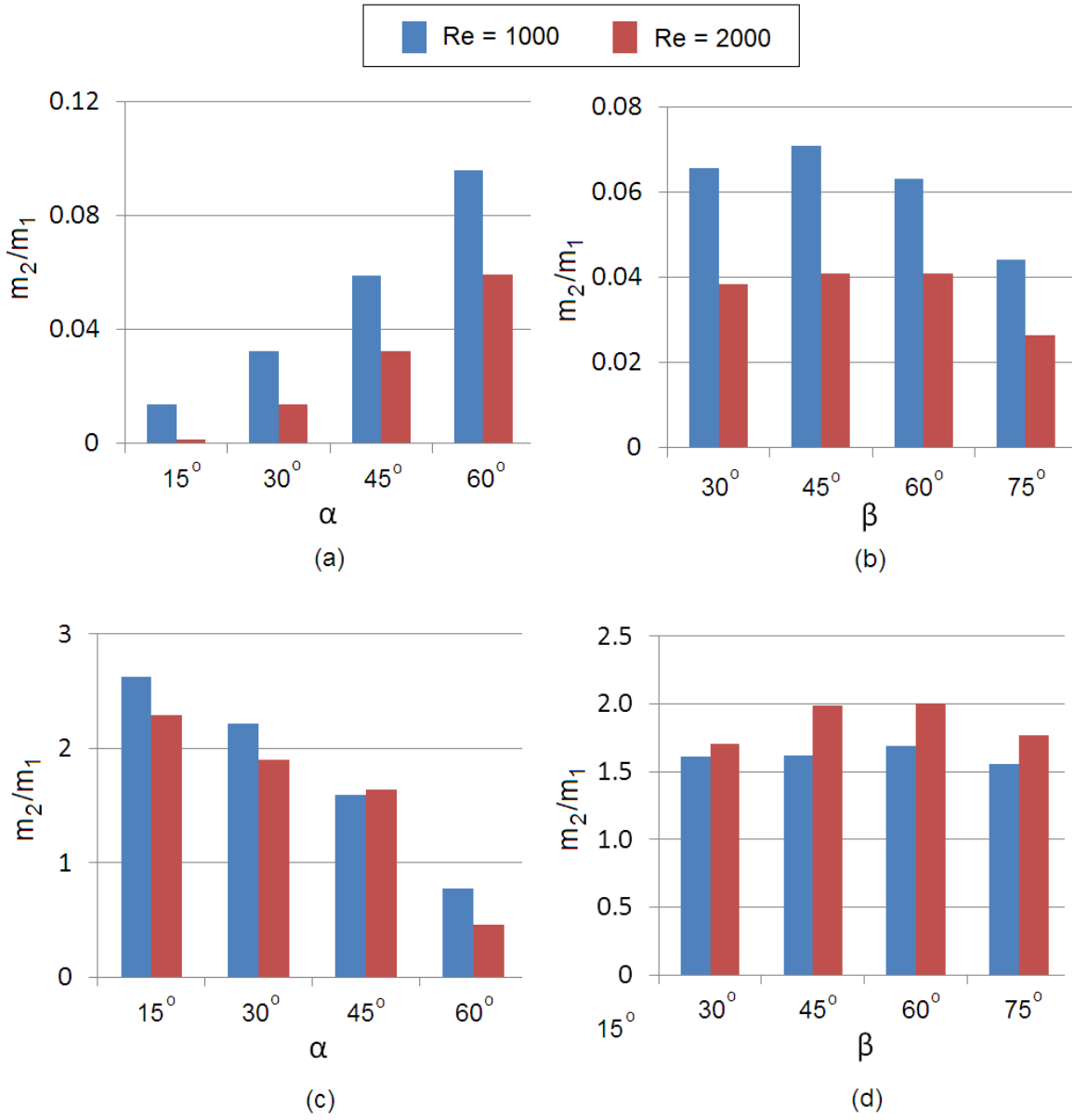

Figure IX. Mass flow rate ratio versus (a) α, forward flow (b) β, forward flow (c) α, reverse flow (d) β, reverse flow (Re = 2000).

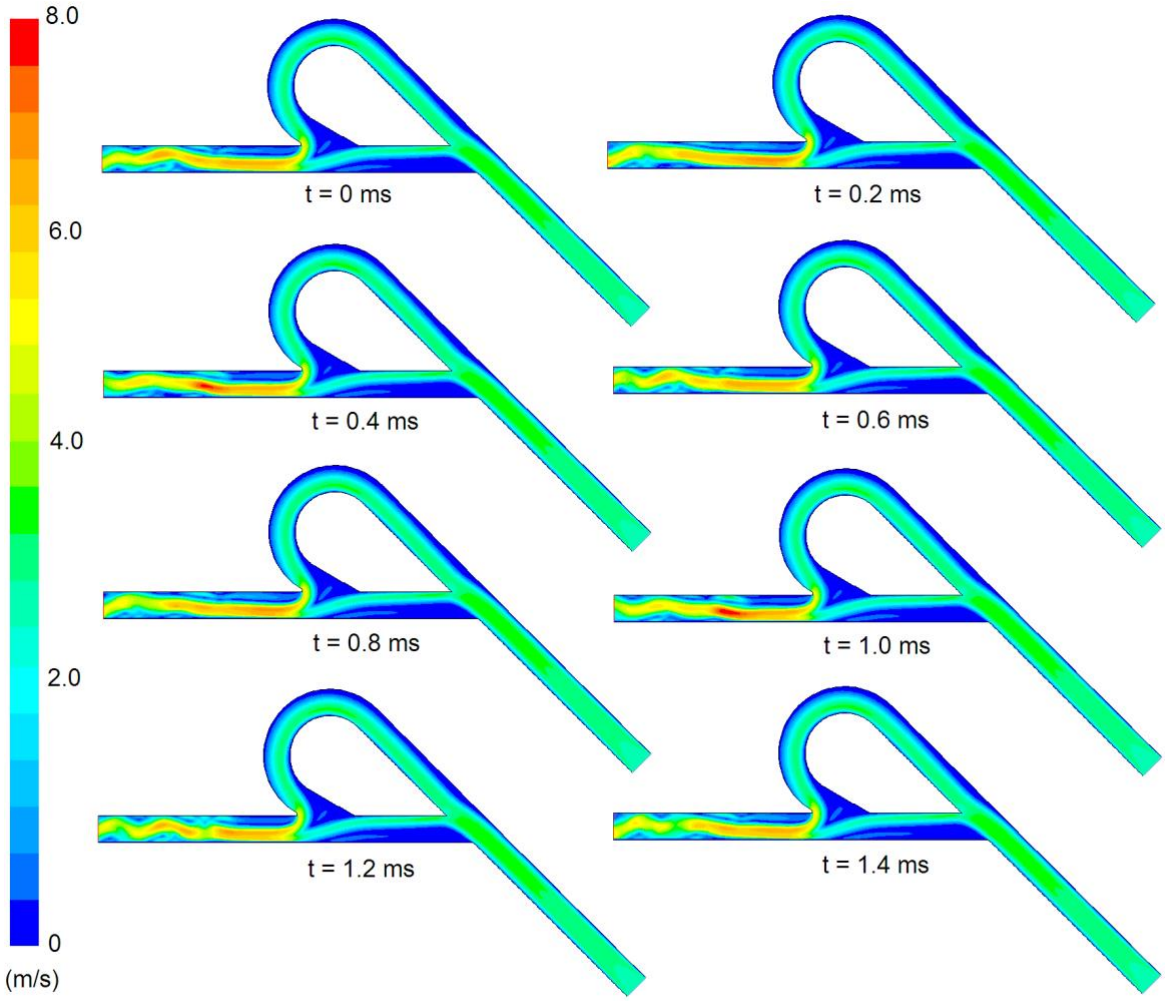

Figure X. Unsteady velocity profiles in time at Re = 2000 (α = 45°, β = 60°).

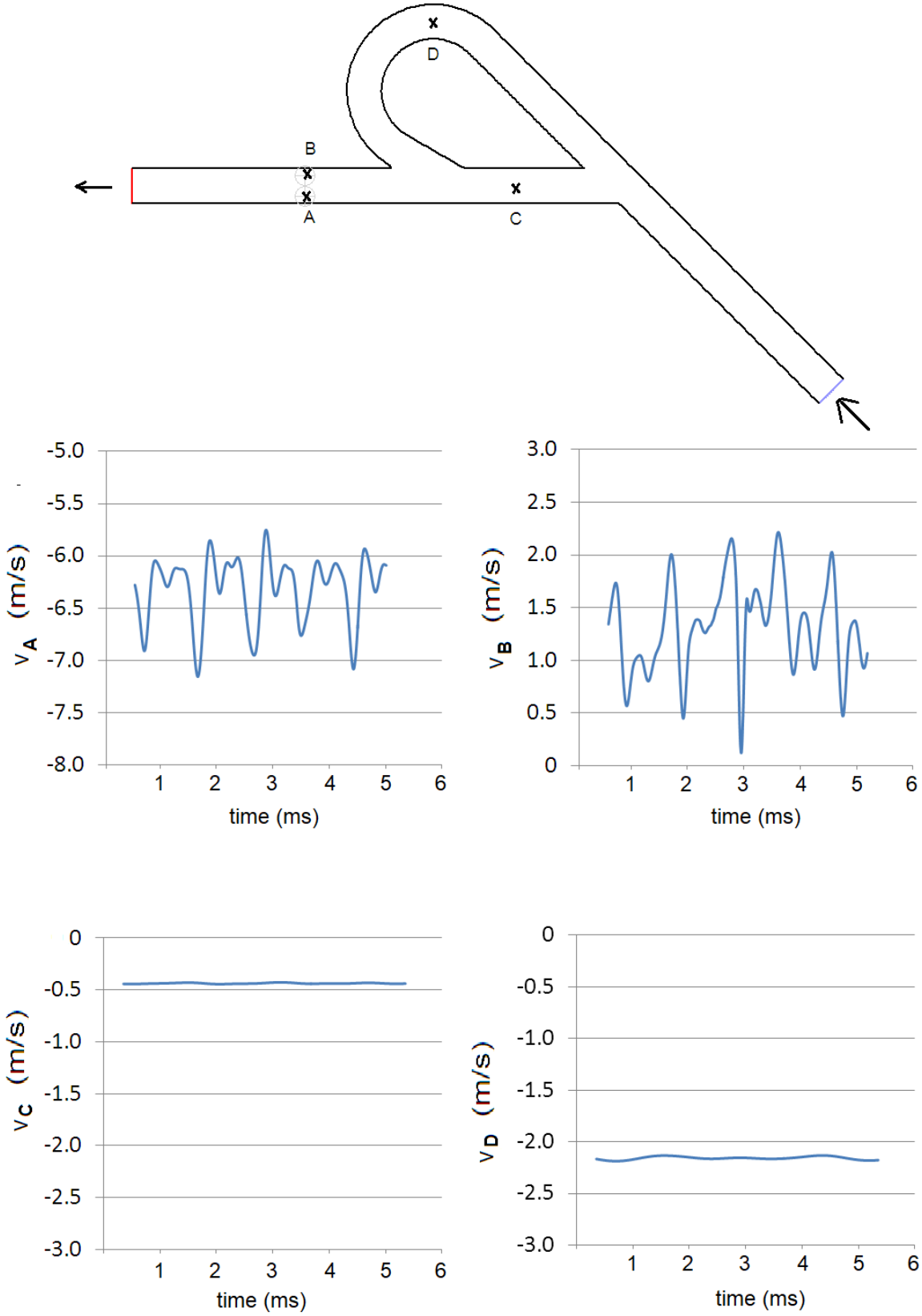

Figure XI. x-velocity plot versus time at Re = 2000 (α = 45°, β = 60°).

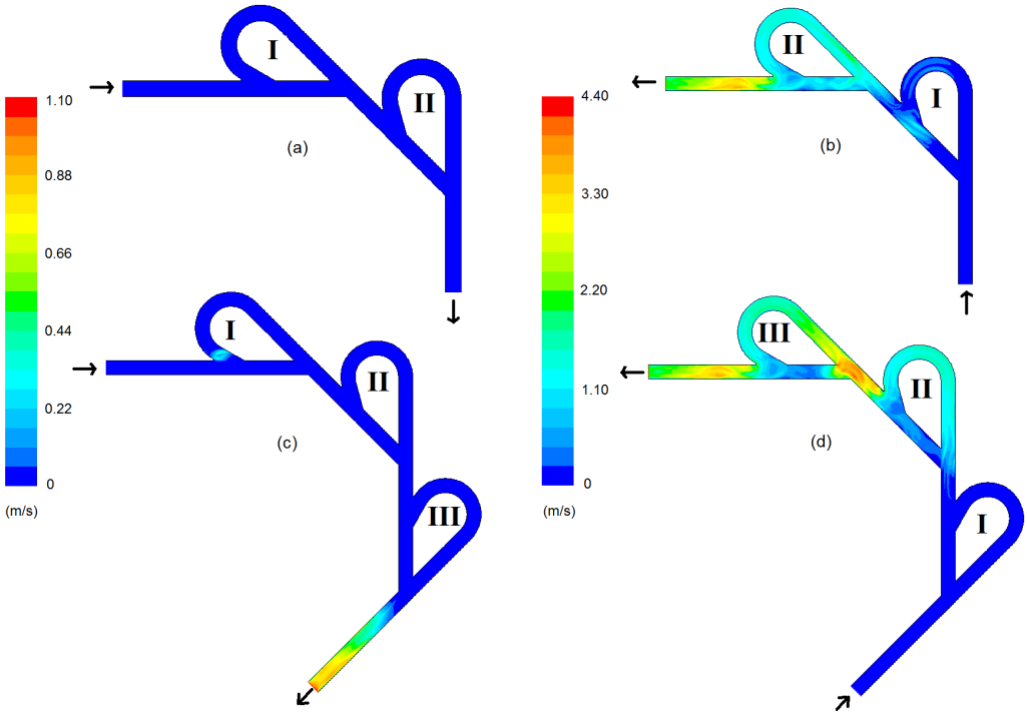

Figure XII. RMS of velocity fluctuation in time (a) two stage valve, forward flow (b) two stage valve, reverse flow (c) three stage valve, forward flow (d) three stage valve, reverse flow (α = 45°, β = 60°, Re = 2000)

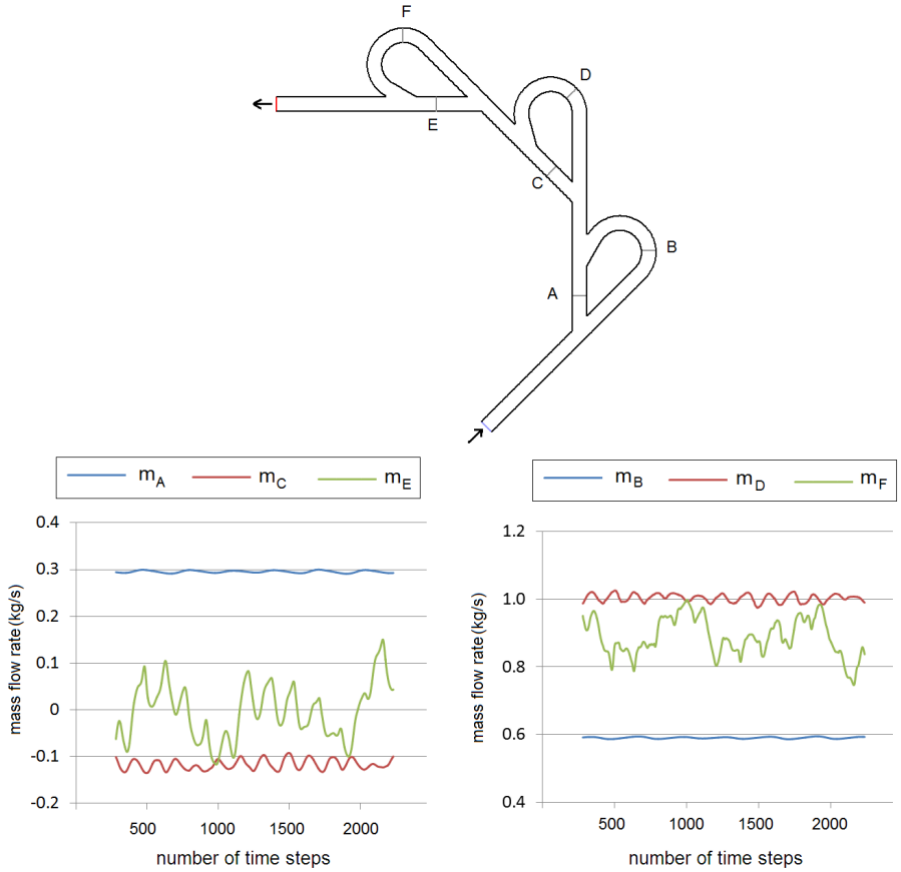

Figure XIII. Mass flow rate variation at monitoring lines in straight sections (A,C and E) and curved sections (B,D and F), (α = 45°, β = 60°, Re = 2000)

		Re = 1000			*Re* = 2000		
α (°)	β (°)	Δp_F (Pa)	Δp_R (Pa)	*Di*	Δp_F (Pa)	Δp_R (Pa)	*Di*
15	8.5	2816.5	3419.7	1.21	11318.8	12856.5	1.14
30	8.5	2432.1	3353.1	1.38	7922.1	11343.2	1.43
45	8.5	2215.7	3114.0	1.41	6416.9	10864.4	1.69
60	8.5	2283.1	2786.6	1.22	6050.5	7797.9	1.29
45	30	2226.3	3371.3	1.51	6472.9	11857.5	1.83
45	45	2242.0	3550.3	1.58	6466.3	12878.6	1.99
45	60	2255.0	3807.6	1.69	6485.2	14248.5	2.20
45	75	2222.2	3677.5	1.65	6342.8	13485.8	2.13

Table I. Effect of geometric parameters of Tesla valve on pressure drop and diodicity at Re = 1000 and 2000.

	Two-stage valve			**Three-stage valve**		
Re	Δp_F (Pa)	Δp_R (Pa)	*Di*	Δp_F (Pa)	Δp_R (Pa)	*Di*
1000	2938.1	9791.1	3.33	3750.4	15116.9	4.03
2000	9555.2	35384.3	3.70	12074.2	53653.9	4.44

Table II. Pressure drop and diodicity for two and three-stage valves at Re =2000 (α = 45°, β= 60°)

References

[1] Chen, M., & Li, Z. (2025). Conceptional design of passive system-level battery fire prevention device based on Tesla valve channel and phase change material. *Journal of Energy Storage*, *107*, Article e114942. https://doi.org/10.1016/j.est.2024.114942

[2] Chen, W.H., Zhing, M.H., Nguyen, T.B., Sharma, A.K., & Li, C.G. (2025). Hydrogen production in reverse tesla valve reactor combining ethanol steam reforming and water gas shift reaction. *Energy*, *318*, Article e134783. https://doi.org/10.1016/j.energy.2025.134783

[3] Chou, C.Y., Kuo, G.C., & Chueh, C.C. (2024). Numerical analysis of thermal-hydraulic influence of geometric flow baffles on multistage Tesla valves in printed circuit heat exchangers. *Applied Thermal Engineering*, *251*, Article e123601. https://doi.org/10.1016/j.applthermaleng.2024.123601

[4] Du, G., Alsenani, T.R., Kumar, J., Alkhalaf, S., Alkhalifah, T., Alturise, F., Almujibah, H., Znaidia, S., & Deifalla, A. (2023) Improving thermal and hydraulic performances through artificial neural networks: An optimization approach for Tesla valve geometrical parameters. *Case Studies in Thermal Engineering*, *52*, Article e103670. https://doi.org/10.1016/j.csite.2023.103670

[5] Gamboa, A.R., Morris, C.J., & Forster, F.K. (2005) Improvements in Fixed-Valve Micropump Performance Through Shape Optimization of Valves. *Journal of Fluids Engineering*, *127(2)*, 339–346. https://doi.org/10.1115/1.1891151

[6] Hai, T., Rahman, M.A., Aksoy, M., Zhou, J., Alenazi, M.J.F., Singh, N.S.S., Zain, J.M., & Jawawi, D.N.A. (2024). Investigating the performance of the Tesla valve channel in a photovoltaic thermal system through numerical simulation: Evaluation from the standpoint of thermodynamic laws. *International Communications in Heat and Mass Transfer*, *159*, Article e108197. https://doi.org/10.1016/j.icheatmasstransfer.2024.108197.

[7] Han, Q., Liu, Z., Yang, S., Han, J., Wang, Z., Miao, J., & Li, W. (2024). The role of Tesla valves in microchannel flow boiling. *International Journal of Heat and Mass Transfer*, *234*, Article e126148. https://doi.org/10.1016/j.ijheatmasstransfer.2024.126148

[8] Huang, F., Ren, L., Xie, S., Leng, M., & Liao, P (2024). Numerical study of flow characteristics and heat transfer mechanism in Tesla valve tube. *Results in Engineering*, *21*, Article e101795. https://doi.org/10.1016/j.rineng.2024.101795

[9] Jiang, E., Wang, W., Miao, J., & Zhang, H. (2025). Effect of the Tesla Valve on the heat transfer performance and the suppression of pressure drop oscillation in a liquid cooling loop. *International Journal of Thermal Sciences, 207*, Article e109356. https://doi.org/10.1016/j.ijthermalsci.2024.109356

[10] Khabarova, D.F, Podzerko, A.V., & Spiridonov, E.K. (2017). Experimental Investigation of Fluidic Diodes. *Procedia Engineering. 206*, 93–98. https://doi.org/10.1016/j.proeng.2017.10.443

[11] Liu, Z., Shao, W.Q., Sun, Y., & Sun, B.H. (2022). Scaling law of the one-direction flow characteristics of symmetric Tesla valve. *Engineering Applications of Computational Fluid Mechanics*, *16(1)*. 441–452. https://doi.org/10.1080/19942060.2021.2023648

[12] Nobakht, A.Y., Shahsavan, M., & Paykani, A. (2013). Numerical Study of Diodicity Mechanism in Different Tesla-Type Microvalves. *Journal of Applied Research and Technology*. *11(6)*, 876–885. https://doi.org/10.1016/S1665-6423(13)71594-3

[13] Purwidyantri, A., & Prabowo, B.A. (2023). Tesla Valve Microfluidics: The Rise of Forgotten Technology. *Chemosensors*, *11(4*), 256–277. https://doi.org/10.3390/ chemosensors11040256)

[14] Tesla, N. (1920). *Valvular Conduit* (U.S. Patent 1329559A, 3 February 1920) [Google Scholar]
Zhang, X., Cao, Z., Fang, K., & Yang, X. (2024). Study on the influence of different structural parameters on the performance of Tesla valve. *Journal of Physics*, *2707*, Article e012092, https://doi.org/10.1088/1742-6596/2707/1/012092

[15] Zhao, Y., Wang, R., Gao, D., Chen, H., & Zhang, H. (2024). Numerical investigation and optimization of a multi-stage Tesla-valve channel based photovoltaic/thermal module. *Renewable Energy*, *228*, Article e120573. https://doi.org/10.1016/j.renene.2024.120573

[16] Zhao, Y.J., Tong, J.B., Zhang, Y.L., Xu X.W., & Tong, L.H. (2024). Hydraulic loss experiment of straight-through Tesla valve in forward and reverse directions. *Science Progress, 107(3)* Article e39285767 https://doi.org/10.1177/00368504241269433.

Author contribution:

1. Conception and design of the study

2. Data acquisition

3. Data analysis

4. Discussion of the results

5. Writing of the manuscript

6. Approval of the last version of the manuscript

MS has contributed to: 1, 2, 3, 4.

MEuH has contributed to: 4, 5 and 6.

SMFH has contributed to: 5 and 6.

Acceptance Note: This article was approved by the journal editors Dr. Rafael Sotelo and Mag. Ing. Fernando A. Hernández Gobertti.

Investigating Tensile & Impact Properties of Recycled Polypropylene, Polyvinyl Chloride, Polyamide & Polyethylene

Investigación de las propiedades de tracción e impacto del polipropileno, cloruro de polivinilo, poliamida y polietileno reciclados

Investigação das propriedades de tração e impacto de polipropileno, cloreto de polivinila, poliamida e polietileno reciclados

Eylia Abbas Jafri [1(*)], Atif Shazad [2], Ifrah Asif [3], Arqam Ahmed Hashmi [4], Umer Nadeem Abdullah [5]

Recibido: 15/05/2025 Aceptado: 23/07/2025

Summary. - Although Pakistan has an abundance of natural resources, it also faces a significant challenge with plastic waste, producing 3.3 million tons annually. This environmental issue demands immediate action, especially due to the increased demand for personal protective equipment (PPE) during the pandemic. Our research aims to make thermoplastics more environmentally friendly by focusing on the properties of recycled polypropylene (PP) enhanced with elastomers and calcium carbonate. Despite a modest loss in tensile properties and impact strength, recycled PP retains key characteristics. Adding calcium carbonate notably increases density, from 908 kg/m³ for stabilized recycled PP to 1029 kg/m³ for a 20% calcium carbonate blend. The total deformation analysis of both recycled and virgin PVC further supports our findings, revealing higher deformation in recycled PVC, which indicates its superior ductility. Additionally, this study examined the effects of aramid short fibers and thermoplastic polyurethane (TPU) additives on recycled polyamide-12 (PA-12). The inclusion of TPU decreased the modulus while increasing tensile strain and energy at break, whereas aramid fibers increased the modulus. Deformation analysis revealed significant strain concentrations in the central sections of these specimens, underscoring the impact of these additives on mechanical behavior. For example, PA-12 with 20% TPU exhibited higher maximum deformation, reflecting its enhanced tensile properties. Moreover, our deformation studies on Poly Butylene terephthalate with 0% HDPE and a blend containing 10% HDPE demonstrated the influence of HDPE content on elastic strain distribution and total deformation. The findings showed that the central region experiences substantial elastic deformation, which is critical for understanding stress distribution in these materials.

Keywords: Environmental sustainability, Thermoplastics, Elastomers, Mechanical Behaviors, Resource Conservation, Technological applications.

[1] Lecturer, National University of Sciences & Technology (Pakistan), eylia@pnec.nust.edu.pk, ORCID iD: https://orcid.org/0009-0009-0859-4134
[2] Lecturer, NED University of Engineering and Technology (Pakistan), ifrahasif@neduet.edu.pk, ORCID iD: https://orcid.org/0000-0001-7551-2199
[3] Research Scholar, NED University of Engineering and Technology (Pakistan), atifshahzad@cloud.neduet.edu.pk, ORCID iD: https://orcid.org/0000-0002-3277-7901
[4] Student, NED University of Engineering and Technology (Pakistan), arqamhashimi201@gmail.com, ORCID iD: https://orcid.org/0009-0004-5601-3262
[5] Student, NED University of Engineering and Technology (Pakistan), umernadeem810@gmail.com, ORCID iD: https://orcid.org/0009-0001-2368-8229

Memoria Investigaciones en Ingeniería, núm. 29 (2025). pp. 74-94
https://doi.org/10.36561/ING.29.6
ISSN 2301-1092 • ISSN (en línea) 2301-1106 – Universidad de Montevideo, Uruguay
Este es un artículo de acceso abierto distribuido bajo los términos de una licencia de uso y distribución CC BY-NC 4.0. Para ver una copia de esta licencia visite http://creativecommons.org/licenses/by-nc/4.0/

Resumen. - *Aunque Pakistán cuenta con abundantes recursos naturales, también enfrenta un importante desafío con los residuos plásticos, generando 3,3 millones de toneladas anuales. Este problema ambiental exige medidas inmediatas, especialmente debido al aumento de la demanda de equipos de protección personal (EPP) durante la pandemia. Nuestra investigación busca lograr que los termoplásticos sean más ecológicos, centrándonos en las propiedades del polipropileno (PP) reciclado mejorado con elastómeros y carbonato de calcio. A pesar de una ligera disminución en las propiedades de tracción y resistencia al impacto, el PP reciclado conserva características clave. La adición de carbonato de calcio aumenta notablemente la densidad, de 908 kg/m³ para el PP reciclado estabilizado a 1029 kg/m³ para una mezcla con un 20 % de carbonato de calcio. El análisis de deformación total del PVC reciclado y virgen respalda aún más nuestros hallazgos, revelando una mayor deformación en el PVC reciclado, lo que indica su mayor ductilidad. Además, este estudio examinó los efectos de las fibras cortas de aramida y los aditivos de poliuretano termoplástico (TPU) en la poliamida-12 (PA-12) reciclada. La inclusión de TPU disminuyó el módulo, pero aumentó la deformación por tracción y la energía de rotura, mientras que las fibras de aramida incrementaron el módulo. El análisis de deformación reveló concentraciones significativas de deformación en las secciones centrales de estas muestras, lo que subraya el impacto de estos aditivos en el comportamiento mecánico. Por ejemplo, el PA-12 con un 20 % de TPU presentó una mayor deformación máxima, lo que refleja sus mejores propiedades de tracción. Además, nuestros estudios de deformación en tereftalato de polibutileno con un 0 % de HDPE y una mezcla con un 10 % de HDPE demostraron la influencia del contenido de HDPE en la distribución de la deformación elástica y la deformación total. Los resultados mostraron que la región central experimenta una deformación elástica sustancial, lo cual es fundamental para comprender la distribución de tensiones en estos materiales.*

Palabras clave: *Sostenibilidad ambiental, termoplásticos, elastómeros, comportamiento mecánico, conservación de recursos, aplicaciones tecnológicas.*

Resumo *. -* *Embora o Paquistão possua abundância de recursos naturais, também enfrenta um desafio significativo com o lixo plástico, produzindo 3,3 milhões de toneladas anualmente. Essa questão ambiental exige ação imediata, especialmente devido ao aumento da demanda por equipamentos de proteção individual (EPI) durante a pandemia. Nossa pesquisa visa tornar os termoplásticos mais ecológicos, concentrando-se nas propriedades do polipropileno (PP) reciclado, aprimorado com elastômeros e carbonato de cálcio. Apesar de uma pequena perda nas propriedades de tração e resistência ao impacto, o PP reciclado mantém características importantes. A adição de carbonato de cálcio aumenta notavelmente a densidade, de 908 kg/m³ para o PP reciclado estabilizado para 1029 kg/m³ para uma mistura com 20% de carbonato de cálcio. A análise da deformação total do PVC reciclado e do PVC virgem corrobora nossos resultados, revelando maior deformação no PVC reciclado, o que indica sua ductilidade superior. Além disso, este estudo examinou os efeitos de fibras curtas de aramida e aditivos de poliuretano termoplástico (TPU) na poliamida-12 (PA-12) reciclada. A inclusão de TPU diminuiu o módulo de elasticidade, ao mesmo tempo que aumentou a deformação por tração e a energia de ruptura, enquanto as fibras de aramida aumentaram o módulo. A análise de deformação revelou concentrações significativas de deformação nas seções centrais dessas amostras, ressaltando o impacto desses aditivos no comportamento mecânico. Por exemplo, o PA-12 com 20% de TPU apresentou maior deformação máxima, refletindo suas propriedades de tração aprimoradas. Além disso, nossos estudos de deformação em poli(tereftalato de butileno) com 0% de HDPE e em uma mistura contendo 10% de HDPE demonstraram a influência do teor de HDPE na distribuição da deformação elástica e na deformação total. Os resultados mostraram que a região central sofre deformação elástica substancial, o que é crucial para a compreensão da distribuição de tensões nesses materiais.*

Palavras-chave: *Sustentabilidade ambiental, Termoplásticos, Elastômeros, Comportamento mecânico, Conservação de recursos, Aplicações tecnológicas.*

1. Introduction. - Plastic, which first emerged in the mid-20th century, has become a cornerstone of our modern economy, growing from a novel material to an indispensable component in countless applications [1]. A study performed to evaluate blends of post-consumer recycled polypropylene (PPr) and virgin PP (PPv) at 25%, 50%, 75%, and 100% PPr to assess processability, thermal stability, oxidative resistance, and mechanical performance. Increasing PPr improved fluidity and inert-condition stability but reduced oxidation resistance and ductility. Extrusion homogenization enhanced oxidative stability of recycled PP by 22%, supporting its use in circular economy applications. [2]. Plastic encompasses a broad spectrum of materials with unmatched properties and extraordinary diversity, finding applications across various sectors. Among these, engineering thermoplastics and advanced engineering thermoplastics, also known as ultra-polymers, are particularly noteworthy for their unique characteristics and exceptional performance [3]. Recent advancements in dynamic covalent chemistry have spurred interest in polymer networks that mimic traditional cross-linked materials while retaining thermoplastic qualities [4].

Blending polybutylene terephthalate (PBT) with polycarbonate (PC) to enhance thermo-chemical and mechanical resistance remains challenging due to phase blockages leading to material segregation [5]. A significant hurdle for polyethylene (PE) pipe-grade resin manufacturers is identifying viable applications for recycled high-density polyethylene (HDPE), especially in pressure pipes [6]. This study explores data-driven modeling to predict tensile strength and modulus of extruded film containing recyclates. Die pressure proved a key quality indicator, correlating with viscosity and degradation. Including melt flow rate, shear viscosity, and feedstock type greatly improved prediction accuracy, with Generalized Additive Models reaching to 85.7% for tensile strength. Results highlight the need for better recyclate classification and larger datasets to enhance industrial predictive modeling.7]. The properties of recycled polypropylene blends, including shape, thermal characteristics, and fracture behavior, have been studied using calorimetry and microscopic examination [8].

Microplastics, often linked to environmental pollutants, can attract materials such as metals, drugs, and polycyclic aromatic hydrocarbons in aquatic environments [9]. The difficulty in combining PBT and PC for enhanced thermo-chemical and mechanical resistance is compounded by phase boundary coalescence during melting, leading to unwanted material segregation [10]. Developing applications for recycled plastics that are as functional as those made from virgin polymers remains a significant challenge, particularly when integrating recycled HDPE into PE pipe-grade resins used for pressure pipes [11]. Virgin polypropylene (Mosten TB 003) was mechanically reprocessed up to 18 times to simulate recycling cycles, with mechanical, thermal, and molecular properties evaluated. Reprocessing caused chain shortening, ~30% molecular weight loss, reduced thermal stability, and yellowing. HS-SPME/GC–MS detected fewer volatiles in highly reprocessed PP, with key compounds identified at 120 °C. [12].

This innovative method enables the incorporation of various reinforcements and polymeric materials into thermoset and thermoplastic matrices [13]. Recycling, especially through tertiary strategies like chemical recycling, is the optimal approach for minimizing waste and recovering valuable materials, with a focus on the fundamental chemistry of each recycling pathway [14]. Additionally, this study examines the composition, thermal properties, and fracture surface characteristics of recycled polypropylene through calorimetry and microscopic analysis, providing valuable insights into blended recycled polypropylene [15]. It also compares the mechanical and processing qualities of virgin pipe-grade PVC with recycled PVC from bottles and pipes, emphasizing the importance of particle size and re-stabilization in achieving consistent and reliable mechanical properties in virgin/recycled PVC blends [16,17].

Within the realm of polyurethane, thermoplastic polyurethane (TPU), a segmented block copolymer classified as a thermoplastic elastomer (TPE), is widely used across numerous industrial domains [18,19]. The pervasive use of plastic polyolefins, polyesters, and polystyrene, which constitute 80% of the global plastic market, has turned waste disposal into a significant environmental issue. Consequently, environmental protection organizations and plastics manufacturers are continually researching innovative methods to recycle and upcycle waste plastics into sustainable new products [20]. The advent of thermoplastic composites has leveraged the remelting and remolding capabilities of thermoplastic matrices while preserving the thermomechanical properties of embedded fibers [21].

Notably, thermoplastic polymers, with their low density, high strength, and corrosion resistance, are increasingly favored over conventional materials like metals or aluminum [22-24]. In composite materials, plastics often serve as matrices reinforced with fibers for enhanced strength in specific directions [25,26]. These materials, which exhibit greater strength compared to simple plastics, are commonly used in constructing industrial pressure tanks, offering high stress-bearing capability while reducing weight [27,28].

Mechanical properties between virgin high impact polypropylene, injected, and recycled one was compared by Fernandes and Shazad [29,30]. Two mixtures, one composed of 30% recycled PP and 70% virgin PP, and other one of 50% recycled PP and 50% virgin PP were assessed to investigate the impact of recycling on mechanical properties. They observed that the tensile properties (ultimate tensile strength, yield strength and strain) did not vary, however, the impact resistance only for samples with up to 30% recycled PP was acceptable for automotive use. Samples above this percentage (50% and 100% recycled PP) showed a significant reduction in impact strength. For comparative purposes, the virgin PP had an impact resistance of 78.7 kJ / m² and the PP 100% recycled 19.7 kJ/m².

The literature review indicates that a wide variety of plastics are used across numerous applications, from household items to industrial products. After their initial use, many of these plastics become waste; however, thermoplastics offer the advantage of being reusable. In local industries, such plastics are often recycled to manufacture various products, though their strength is rarely evaluated against that of virgin materials. Consequently, it is important to investigate how recycling affects the mechanical properties of these materials. A simulation-based approach can help analyze their behavior under loading conditions and provide a basis for comparison with experimental findings. This study examines the tensile and impact properties of widely used plastics such as polyethylene, polypropylene, polyamide, and polyvinyl chloride. In particular, polypropylene recycling was simulated through multiple injection molding cycles to reshape the material. The primary objective is to determine whether recycled polymers—especially recycled PP—maintain mechanical properties comparable to virgin polymers, thereby assessing their suitability for similar applications.

2. Methodology. - The major focus of this study was mechanical properties evaluation of recycled plastics commonly used at domestic and industrial level. Four polymers were selected for recycling purpose due to their extensive use. These selected polymers are listed below:

a. Recycled polypropylene (PPr)
b. Recycled poly vinyl chloride (PVCr)
c. Recycled polyamide (PAr)
d. Recycled polybutylene terephthalate (PBTr)

Recycling process was performed by using a Central co-rotating twin-screw extruder as shown in Figure I with 800 mm long screws (25 mm diameter). The temperature of the barrels changed between 180°C and 215°C while the output rate remained constant at 100 g/min. Calcium Carbonate ($CaCO_3$) was added to enhance mechanical properties, Calcite type crystals in 2-3 micrometer range were added while recycling. The use of these recycled plastics includes an extensive examination of their viability for eco-friendly and sustainable applications, providing insightful information on the industrial utilization of these recycled materials.

Figure I. Recycling of Plastics.

Using ASTM D638 for tensile testing and ASTM D256 for impact testing of recycled materials, mechanical properties were assessed, providing an understanding of the way extrusion parameters affect material qualities for industrial applications. Tensile tests were performed at room temperature, 20°C, and 60°C in accordance with ISO 527 standards. When the stress reached 5 MPa, the testing speed was increased to 50 mm/min from 1 mm/min. The data was sampled at a rate of 50 hertz. According to ISO 179 specifications, notched impact tests were conducted at 20°C using a Rosand Instrumented Falling Weight Tester (type 4). Before testing, specimens were pre-conditioned for 30 minutes within the temperature chamber. Recycling of PP was performed by using different recycling percentages with virgin PP as mentioned in Table I.

Sample	Virgin (%)	Recycled (%)
PPv100	100	-
PPr10	90	10
PPr20	80	20
PPr30	70	30
PPr100	-	100

Table I. Composition of recycled and virgin polypropylene.

To guarantee equal dispersion, a primary batch of polypropylene and stabilizers was created. The additives were added as stabilizers to PPv for evaluating impact of additives to mechanical properties. Two types of stabilizers named Hindered Amine Light Stabilizers (HALS) and Antioxidant (Irganox B215) were added in a constant proportion to PPv and PPr. Eight samples with different blending of additives were produced as shown in Table II, Recycled polypropylene was double blended for blends with EOR and $CaCO_3$. A Batten Feld BSKM 45/20 HY or DSM micro extruder/injection mold was used to create test specimens that were 2 mm thick at 23°C. Following that, 48 hours of conditioning at 23 °C and 50% humidity took place on all samples before testing. Elastomers such as ethylene-propylene rubber (EPR) were mixed in different proportions to enhance toughness and impact resistance but have the side effect of also reducing the yield strength and young's modulus as illustrated by Fernandes [25]. This drawback was countered by addition of inorganic fillers such as Calcium carbonate, $CaCO_3$ which provides increased impact energy, improved hardness, and higher modulus and tensile strength, while lowering the cost. Higher molecular weight PVC having K value approx. 75 was utilized as Virgin pipe-grade PVC (VPPVC) with standard pipe composition, contains 2.4% $CaCO_3$ powder and 2% stabilizer/lubricant. Normal bottles after consumed (RBPVC) was granulated

into 9mm, 5mm, and 3mm pieces. Rigid PVC pipes (RPPVC) after extensive utilization were selected as a recycled material and pelletized through a 3mm screen. Qualitative analyses revealed a higher $CaCO_3$ level (about 5%) and trace amounts of rubber. Table III comprised of different mixing compositions, Virgin with recycled bottle material (VRB) and Virgin with recycled pipe material (VRP).

Sample	Stabilizers (S) (%)	ELASTOMER (E) (%)	$CaCO_3$ (C) (%)
PP+S	0.3	-	-
PP+S+E	0.3	5	-
PP+S+E+C	0.3	5	10
PPr+S+ E+ C	0.3	5	20
PP+S+E+C	0.3	10	10
PPr+S+E+C	0.3	10	20
PP+S+C	0.3	-	10
PPr+S+C	0.3	-	20

Table II. Polypropylene composition with different additives.

Sample Code	Composition (%)
VRB20	VPPVC 83, RBPVC 17
VRB40	VPPVC 71, RBPVC 29
VRB60	VPPVC 62, RBPVC 38
VRB80	VPPVC 56, RBPVC 44
VRB100	VPPVC 50, RBPVC 50
VRP20	VPPVC 83, RPPVC 17
VRP40	VPPVC 71, RPPVC 29
VRP60	VPPVC 62, RPPVC 38
VRP80	VPPVC 56, RPPVC 44
VRP100	VPPVC 50, RPPVC 50

Table III. Formulation of PVC for beverage bottles.

Samples	Composition (%)	
	PBT	HDPE

H0	100	0
H5	95	5
H10	90	10
H15	85	15
H100	0	100

Table IV. Composition of testing samples.

Initiating with the PA-12 sample preparation derived from waste produced during Selective Laser Sintering (SLS) operations, this research promotes environmentally friendly Additive Manufacturing (AM) procedures. The main objective is to turn excess polymer powder, which is often discarded, into a useful raw material. The idea is to promote a cradle-to-cradle approach in which waste from one stage forms a foundation for another. This work focuses on developing novel polymeric blends, with a focus on PA-12 usage, to improve the sustainability of 3D printing for the construction of prosthetic limbs utilizing Fused Deposition Modelling (FDM) technology.

The following groups of specimens were prepared:

a. pure PA-12,
b. pure reused PA-12 and mechanically milled TPU pellets,
c. pure reused PA-12 and aramid short fibers,
d. pure reused PA-12 and graphite powder.

Sample details are given in Table IV and for testing recycled thermoplastics such as PPr, PVCr, PAr, and PBTr, specimens should be prepared according to ISO 294-1 injection-molding guidelines. Mechanical characterization typically includes tensile testing in accordance with ASTM D638, impact resistance measured using ASTM D256. Melt flow rate or volume is determined following ASTM D1238, with ISO 1133-2 recommended for moisture-sensitive materials like PA and PBT. All specimens should be conditioned following ASTM D618, typically at 23 ± 2 °C and 50 ± 5 % RH for at least 96 hours, with additional pre-drying or desiccation for hygroscopic resins to prevent moisture-induced degradation. The automotive and construction sectors frequently utilize PBT, a thermoplastic with a reputation for chemical resistance, insulation, and easy processing. Its poor tensile strength and impact resistance are caused by its rapid crystallization. PBT is frequently combined with other polymers to improve its characteristics.

3. Results and Discussions. -

3.1 Testing of Recycled Plastics. -

a. Density variation: The effects of calcium carbonate and elastomers on density and melt flow index show how recycled PP's qualities might potentially be changed for specific applications. Table V shows the density and melt flow index for different recycled polypropylene blends, based on eight tests for each material. Adding calcium carbonate greatly increases density, from 908 kg/m³ for stabilized recycled polypropylene to 1029 kg/m³ for a 20% calcium carbonate blend.

Sample Compositions	Density (kg/m^3)	Melt Flow Rate (g/10min)
PP + S	908	14.6
PP + S + 5%E	906	19.7
PP + S + 5%E + 10%C	968	14.4
PP + S + 5%E + 20%C	1033	14.6

PP + S + 10%E + 10%C	973	16.1
PP + S + 10%E + 20%C	1029	15.8
PP + S +10%C	974	14.3
PP + S +20%C	1038	14.5

Table V. Effect on Density and Melting behavior of Polypropylene.

The melt flow index also rises with elastomer content, from 14.6 g/10 min for a 5% EOR blend to 19.6 g/10 min. Melt flow rate measures how easily a polymer flows when melted, which affects its processability during manufacturing. Density measures mass per unit volume and influences a polymer's mechanical properties. Both values are important for optimizing polymer performance in different applications.

The density values of various PVCr composites which are represented in Table III. 5x samples were tested for evaluation of density fluctuations and mentioned in Table VI. S0 illustrate the minimum amount of recycling and S5 indicate the maximum amount as shown in Table III.

Samples	S0	S1	S2	S3	S4	S5
Density	145	147	151	154	158	161

Table VI. Density variations.

3.2 Melt Viscosity. - The renograms of PVCr composites are characterized in Figure II indicate that recycled polymer matrix results in the reduction of melt viscosity.

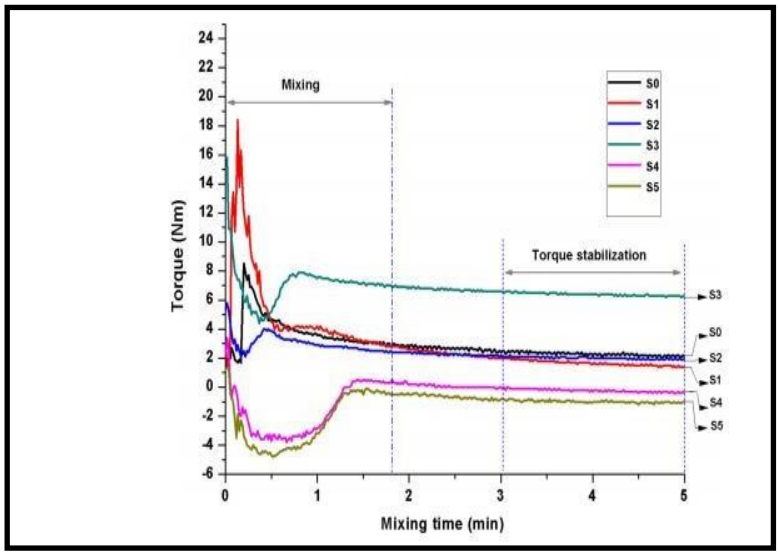

Figure II. Viscosity Variations

b. Tensile strength variations: The study demonstrated that the inclusion of PPr to a blend with PPv had no discernible impact on the yield stress and Young's modulus at room temperature. However, the recycling procedure reduced the impact strength of PP which is the result of additional hardness. The tensile properties of polypropylene were tested at -20°C, 23°C, and 60°C with various calcium carbonate and elastomer compositions are presented in Table VII.

Sample Compositions	Youngs Modulus (MPa)	Yield Stress (MPa)	Yield Strain (%)	Maximum Elongation (%)
Temperature during testing= -20ºC				
PP + S	3400 ± 200	43.8 ± 0.7	3.4 + 0.1	110 + 50
PP + S +5%E	2800 ± 300	43.5 ± 0.6	4.1 + 0.6	95 + 30
PP + S + 5%E + 10%C	3300 ± 600	41.4 ± 0.3	3.6 + 0.3	120 + 30
PP + S + 5%E + 20%C	3100 ± 500	39.0 ± 0.3	3.4 + 0.3	120 + 40
PP + S + 10%E + 10%C	2800 ± 300	39.8 ± 0.6	4.3 + 0.4	160 + 80
PP + S + 10%E + 20%C	3000 ± 700	37.9 ± 0.5	3.9 + 0.4	200 + 100
PP + S +10%C	3300 ± 300	42.4 ± 0.3	2.8 + 0.2	160 + 70
PP + S +20%C	3700 ± 700	40.4 ± 0.6	2.4 + 0.1	120 + 50
Temperature during testing= 23ºC				
PP + S	1010 ± 60	24.6 ± 0.1	6.7 + 0.1	16 to 580
PP + S +5%E	910 ± 30	23.6 ± 0.4	8.9 + 0.7	>150
PP + S + 5%E + 10%C	970 ± 40	22.2 ± 0.9	8.5 + 0.1	>150
PP + S + 5%E + 20%C	1080 ± 120	20.4 ± 0.1	8.3 + 0.1	>150
PP + S + 10%E + 10%C	890 ± 50	20.4 ± 0.2	12.5 + 0.1	>150
PP + S + 10%E + 20%C	960 ± 80	19.5 ± 0.1	9.5 1 1.1	>150
PP + S +10%C	1140 ± 40	22.9 ± 0.1	6.2 # 0.2	>150
PP + S +20%C	1250 ± 60	21.6 ± 0.1	5.6 + 0.2	>150
Temperature during testing= 60ºC				
PP + S	590 ± 140	14.5 + 0.1	10 + 2	>150
PP + S +5%E	390 ± 40	13.1 + 0.1	13.5 + 0.5	>150
PP + S + 5%E + 10%C	410 ± 80	12.7 + 0.2	11 + 2	>150
PP + S + 5%E + 20%C	380 ± 40	12.1 # 0.1	12 # I	>150

PP + S + 10%E + 10%C	320 ± 30	12.2 1 0.2	12 + 4	>150
PP + S + 10%E + 20%C	340 ± 20	11.3 + 0.1	13 + 2	>150
PP + S +10%C	420 ± 70	13.9 # 0.1	11.1 + 0.6	>150
PP + S +20%C	450 ± 60	13.6 + 0.1	9.9 1 0.2	>150

Table VII. Tensile testing results.

At −20 °C and 23 °C, Young's modulus stayed between 1-3 MPa. Increasing calcium carbonate slightly reduced yield stress, while the elastomer had minimal impact. All samples showed necking. Maximum elongation was stable but showed high variation. The stress–strain curves indicate that adding recycled PP to virgin PP has little effect on yield stress. The difference between PPv100 and PPr100 was only 3.87%.

The study examined blends of recycled PVC with virgin pipe-grade PVC to see how they affected mechanical properties and processing. Stress-strain curves in Figure II illustrates that recycled PVC was more ductile and had greater elongation at break than virgin PVC. These results offer guidance for enhancing PVC blend performance.

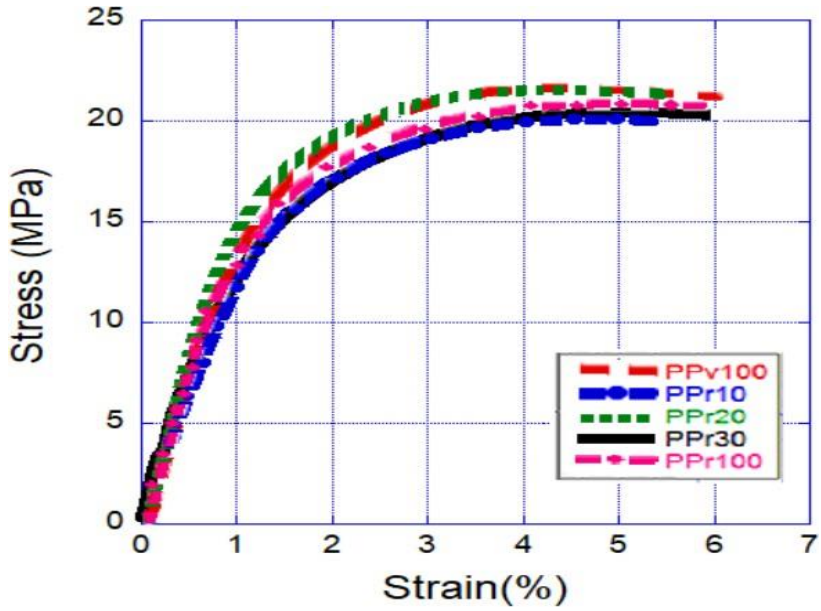

Figure III. Stress-strain curve for PPr.

As a result, the study shows that using 100% recycled PP or blending it with virgin PP has minimal impact on the tensile parameters as shown in Figure III, including yield strength and elastic modulus. However, it is crucial to recognize that the impact strength decreases, demonstrating that the recycling process makes PP extremely stiff and resistant to plastic deformations.

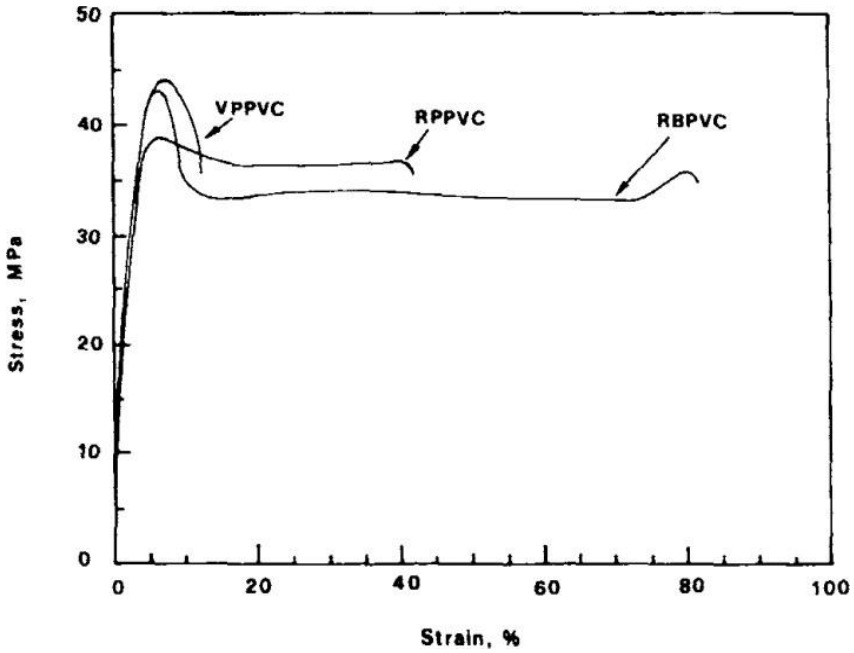

Figure IV. Stress strain curve PVCr.

Stress-strain curves for virgin and recycled PVC are shown in Figure IV. A polymer modifier gives the RBPVC curve its ductility. The VPPVC and RPPVC curves differ. Recycled material shows ductility and high elongation at break, which indicates a modifier is present in the recycled pipes. Recycled PVC from bottles and pipes needs stabilizers because stabilizer loss during manufacturing and use lowers heat resistance. The impact modifier in RBPVC reduces modulus and tensile strength compared to virgin pipe-grade PVC. However, it increases elongation and impact strength. PVC from pipes used for 4-5 years can stretch more before breaking.

Despite having the same modulus, virgin PA-12 performs better than recycled PA-12 powder in terms of elongation at break as depicted in Figure V. The expansion of 10% TPU marginally brings down the modulus however essentially increments ductile strain and energy at break. At 20%, the modulus diminishes to 0.4 GPa, with a further ascent in tensile strain. Aramid filaments upgrade the modulus, with 5% making an unobtrusive difference and 10% prompting a huge ascent to 0.9 GPa, however malleable endure break drops to 36.3%.

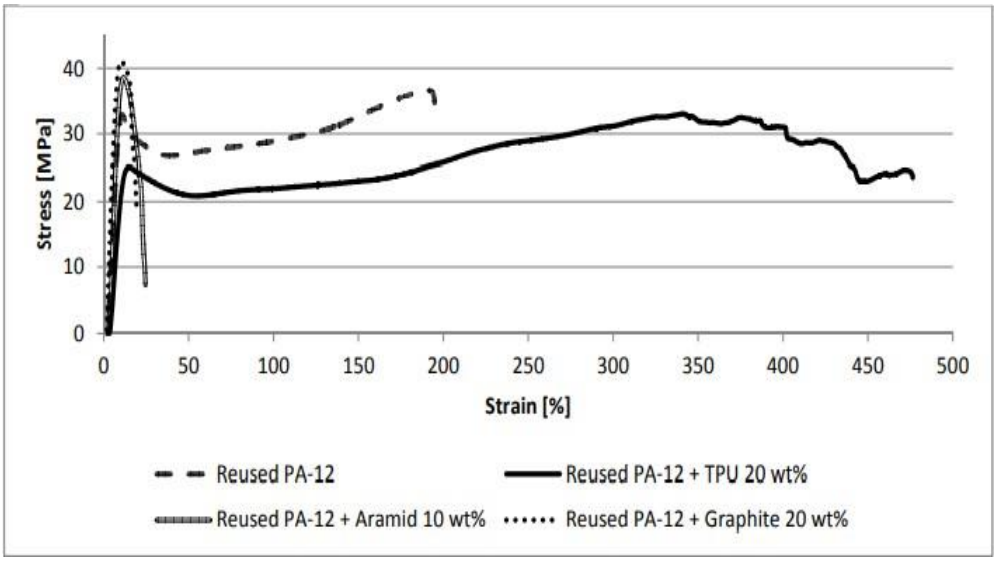

Figure V. Stress strain curve for Polyamide and groups.

Our research on recycled PA-12 looked at the effects of additions such thermoplastic polyurethane (TPU) and aramid short fibers. While aramid fibers enhanced the modulus, TPU lowered the modulus while increasing the tensile strain and energy at break. These results provided useful insights for modifying recycled PA-12's properties for specific engineering applications.

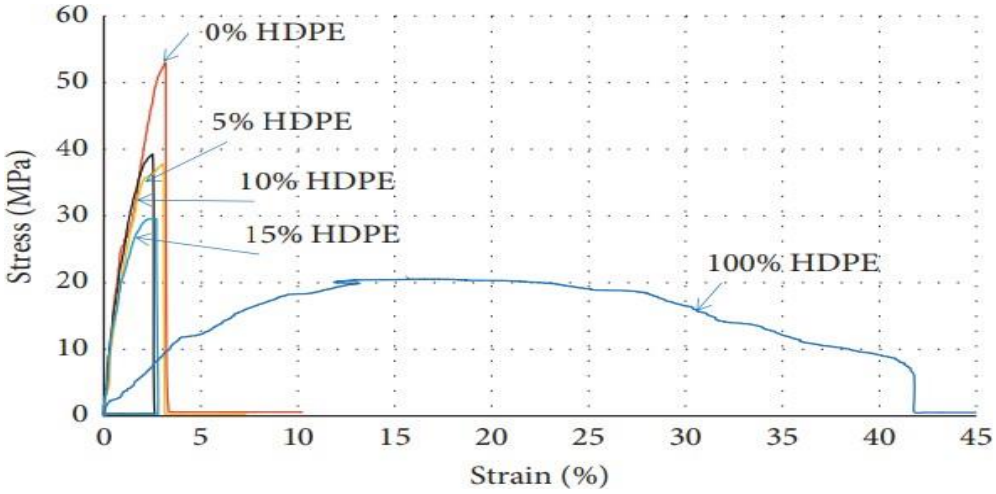

Figure VI. Stress strain curve for PBT mixed with HDPE.

The stress-strain curves of the samples depicted the pure PBT is very brittle with an exceptionally low value of elongation of about 2.5%. Adding HDPE to PBT will lead to a decrease in tensile strength. The tensile strength values of the composite samples are in the middle of pure PBT and HDPE as represented in Figure VI.

c. Impact Testing: According to the Charpy test results at -20°C with six specimens per composition, the inclusion of elastomer and calcium carbonate had no effect on impact energy and maximum force. The fracture mechanism of these samples is also brittle fracture as shown in Table VIII. In general, adding HDPE will reduce tensile strength compared to pure PBT. Because, for incompatible blends such as PBT/HDPE, incompatibility between the two components can result in weaker bonding between the components, poorer mechanical properties, and other problems such as welding line failure in the injection molding process.

Sample Compositions	Energy (KJ/m^2)	Max Force (N)
PP + S	2.0 ± 0.3	270 ± 34
PP + S +5%E	1.7 ± 0.2	275 ± 21
PP + S + 5%E + 10%E	2.2 ± 0.2	270 ± 35
PP + S + 5%E + 20%E	1.8 ± 0.1	280 ± 11
PP + S + 10%E + 10%E	2.5 ± 0.9	280 ± 26
PP + S + 10%E + 20%E	2.0 ± 0.3	330 ± 32
PP + S +10%E	2.1 ± 0.3	270 ± 69
PP + S +20%E	2.0 ± 0.3	3700 ± 33

Table VIII. Impact test Results.

Insights into the tensile and impact behavior of recycled PP, PVC, PA, and PE can serve as a foundation for shaping effective manufacturing and sustainability strategies. In manufacturing, the introduction of performance-based grading systems, standardized processing guidelines, and design-for-recycling principles can enhance material consistency and recyclability. Establishing rigorous quality control measures, including mechanical testing and supplier certification, will strengthen trust in recycled polymers. On the sustainability front, policy measures such as fiscal incentives, eco-label programs, and mandated recycled content thresholds can accelerate adoption. Implementing closed-loop production systems and take-back initiatives can further minimize reliance on virgin plastics. A centralized, publicly accessible database linking mechanical properties with environmental metrics can guide informed material choices. Embedding life cycle assessment requirements into regulations will ensure that both durability and ecological impact are addressed in product development.

d. ANSYS Simulation: ANSYS software was utilized to verify the characteristics of recycled engineering thermoplastic, we ran multiple simulations. Dark blue denotes extremely low stress, light blue denotes low stress, yellow denotes moderate stress, and red denotes high stress. Fracture is caused by an increase in tension during elongation and deformation. In this tensile test simulation of a polymer specimen, one end of the dog-bone sample is fully constrained to prevent displacement or rotation, while a uniaxial displacement or tensile load is applied to the opposite end along the X-axis. The fine mesh consists of a structured hexahedral arrangement in the gauge section to ensure uniform stress distribution, with finer mesh density in the transition regions to capture stress gradients accurately. The element quality appears high, with minimal distortion, ensuring reliable deformation and strain predictions for the polymer material under tensile loading.

Polypropylene (PPr 20): Figure VII depicts the total deformation which is measured in millimeters and is depicted using a color gradient, where blue represents the minimum deformation and red indicates the maximum deformation (2.1305 mm). The specimen exhibits the highest deformation at both ends, with deformation gradually decreasing towards the center, illustrating the stress concentration and distribution along the length of the specimen. The deformation pattern aligns with expectations for the given loading and boundary conditions.

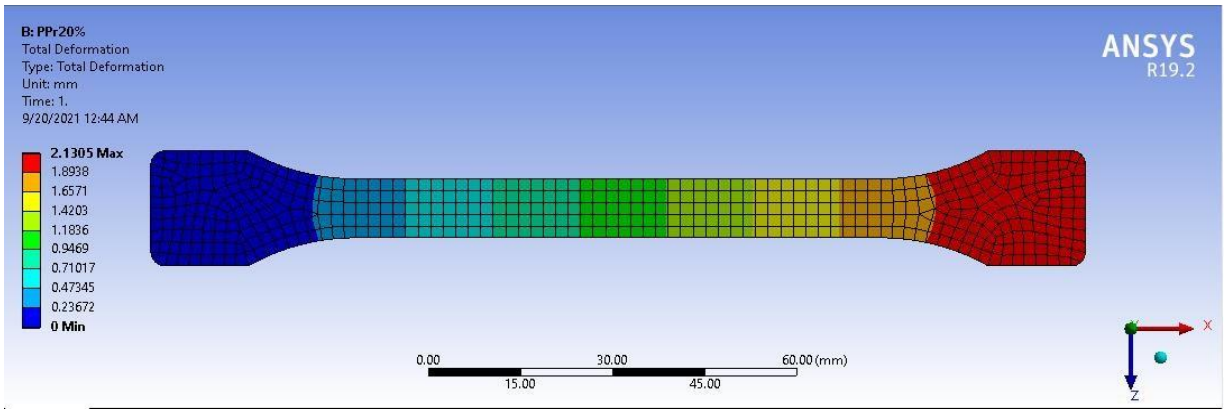

Figure VII. Total Deformation of PPr 20.

Polypropylene (PPr 100): Figure VIII illustrates the total deformation distribution of a 100% recycled polypropylene specimen under a specified loading condition. The deformation is measured in millimeters representing the maximum deformation (1.8824 mm). The highest deformation is observed at one end where tensile force applied to the specimen, with a gradual decrease towards the center, indicating stress concentration and distribution. The total deformation reduced due to increment in recycling percentage.

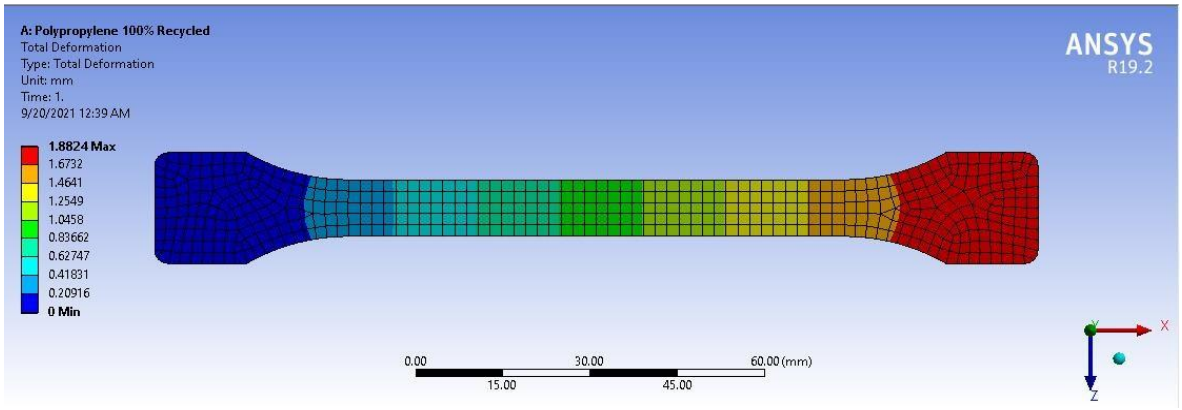

Figure VIII. Total Deformation of PPr 100.

An understanding of how a structure deforms under applied loads or heat impacts may be obtained from these complete deformation simulations. It assists in evaluating structural integrity, load distribution, and design validation by presenting the amount and direction of displacement.

3.3 Recycled PVC. -

3.3.1 Density Test. -

ANSYS Simulation of Recycled Polyvinyl Chloride: The fluctuation in stresses and deformations is investigated to figure out the structural behavior of recycled polyvinyl chloride (PVC) as shown in Figure IX and Figure X. Through critical insights into stress distribution and material reaction, these simulations improved our understanding of the mechanical characteristics of recycled PVC for use in sustainable engineering.

RBPVC:

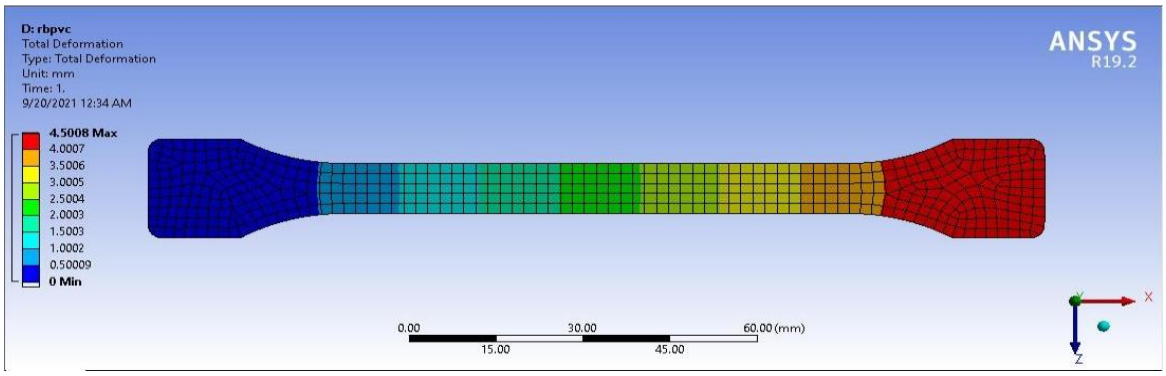

Figure IX. Total deformation for RBPVC.

RPPVC:

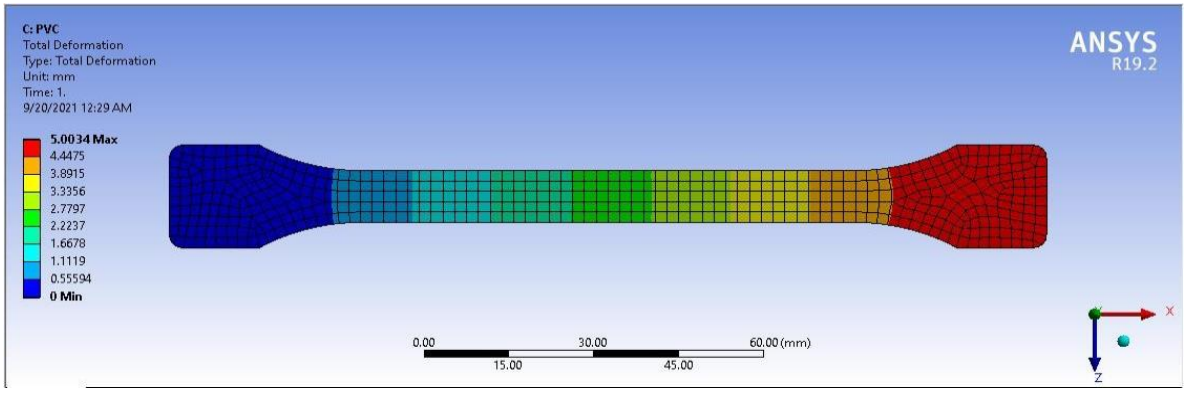

Figure X. Total deformation for RPPVC.

Figure IX depicts the total deformation distribution of a recycled polyvinyl chloride (RBPVC) specimen under a specified loading condition. Maximum deformation (4.5mm) was achieved by applying load at one end. Figure X exhibits a higher maximum deformation value (5.01mm). Both figures demonstrate a similar pattern of maximum deformation at the ends and a gradual decrease towards the centre, indicating consistent stress concentration and distribution along the specimen's length. The higher deformation in the RPPVC specimen suggests a difference in mechanical properties between the virgin RPPVC and recycled RBPVC materials under identical loading conditions. The composites' overall performance was further improved by their increased thermal stability. The material's applicability for many uses in the building industry is reinforced by its notably low water absorption propensity. This composite's added value makes it especially well-suited to produce several goods, such as flooring sheets and tiles, offering a promising path for market use and growth.

ANSYS Simulation of Recycled Polyamide: Recycled polyamide's structural dynamics were studied by conducting simulation of strength analysis and the findings revealed subtleties related to stress, which helped shape a more complex comprehension of its mechanical behavior for applications in sustainable engineering. Figure XI shows the total deformation distribution of a recycled polyamide 12 (PA-12). The major deformation (10.1mm) was observed at one end because force applied at this end. The specimen exhibits the fracture location at the central narrow section due to necking phenomena, indicating a significant stress concentration. The other end of the specimen displays lower deformation value, with the deformation increasing towards the center, demonstrating a pronounced localized deformation pattern typical under such loading conditions.

PAr:

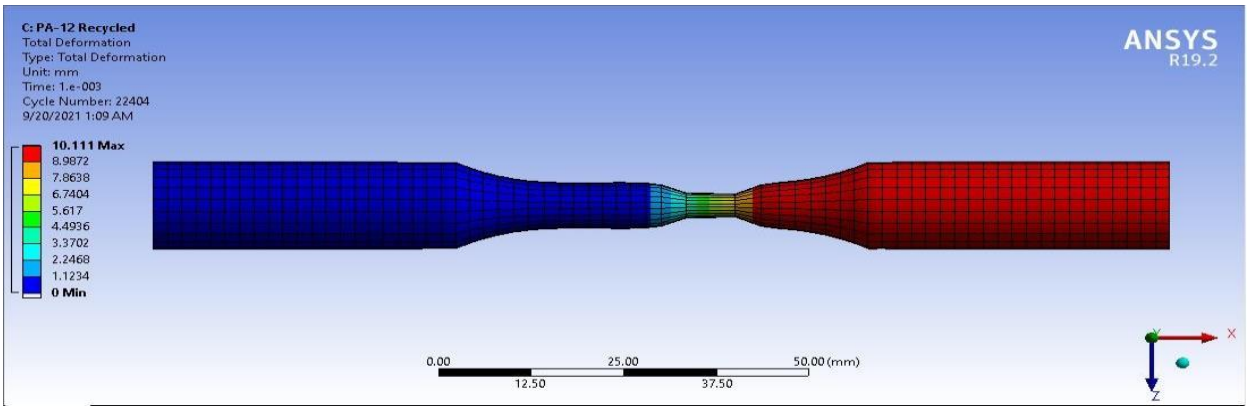

Figure XI. Total deformation for PAr-12.

PAr with TPU:

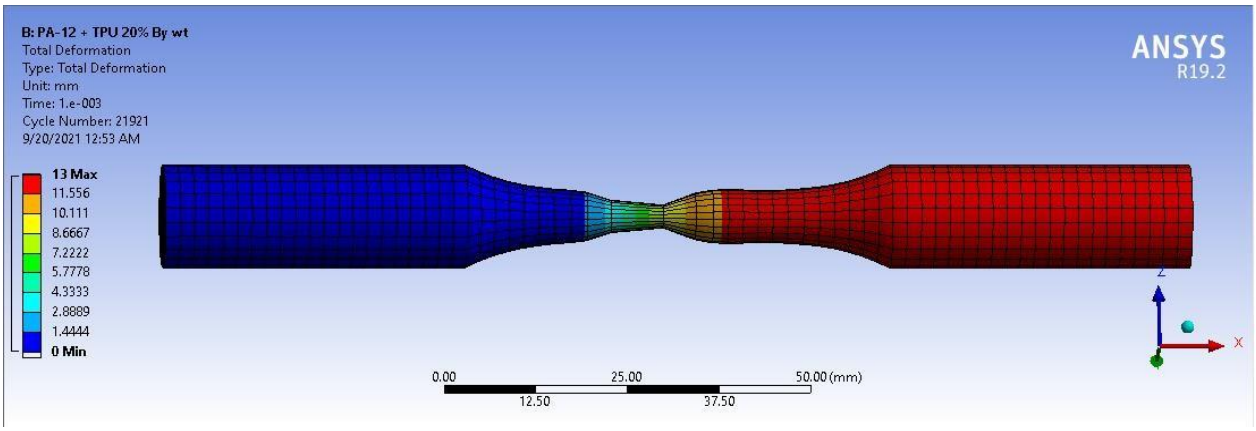

Figure XII. Total deformation for PAr with TPU.

Figure XII depicts the total deformation distribution of a polyamide 12 (PA-12) specimen with 20% TPU by weight. Maximum deformation (13 mm) was observed from loading end towards center. Significant stress concentration was noted towards center which indicate the failure point due to potential necking. The deformation decreases towards the other end of the specimen. The maximum deformation value of 13 mm is higher than that of the recycled PA-12 specimen, suggesting that the addition of TPU affects the mechanical properties and deformation behavior of the material under the applied load.

ANSYS Simulation of PBTr: Structural dynamics of PBT after adding high-density polyethylene (HDPE) were performed and the results provided information on the distribution of stress during deformation as shown in Figure XIV and Figure XV. The behavior of PBT without HDPE is illustrated in Figure XIII in which 3.48mm maximum deformation achieved. This might direct future optimizations for its use in a variety of engineering settings. This method advances our knowledge of the mechanical behavior of HDPE and advances the field of sustainable materials engineering.

PBT + 0% HDPE: Figure XIII displays the total deformation distribution of a PBT specimen with 0% high-density polyethylene (HDPE) under a specified loading condition. The highest deformation occurs at loading end of the specimen, with deformation values decreasing towards the center. Potential failure may occur near center due to less stress bearing area.

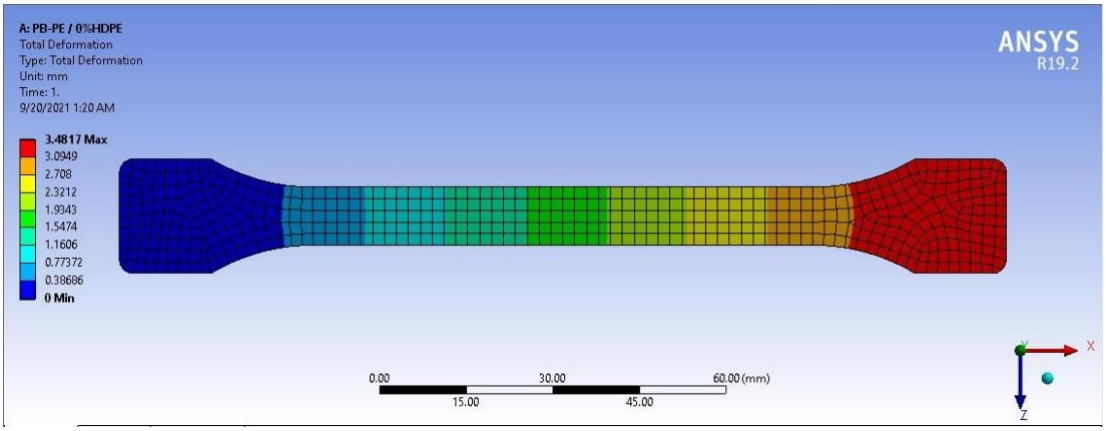

Figure XIII. Total deformation for PBTr.

PBTr + 5% HDPE: Figure XIV illustrates the total deformation distribution of a static structural analysis of a specimen and revealed that maximum deformation (3.2902 mm) was observed at loading end. The highest deformation occurs at one end of the specimen, with a gradual decrease towards the center. This pattern of deformation indicates stress concentration at the extremities and a more uniform deformation in the middle section, reflecting the material's response.

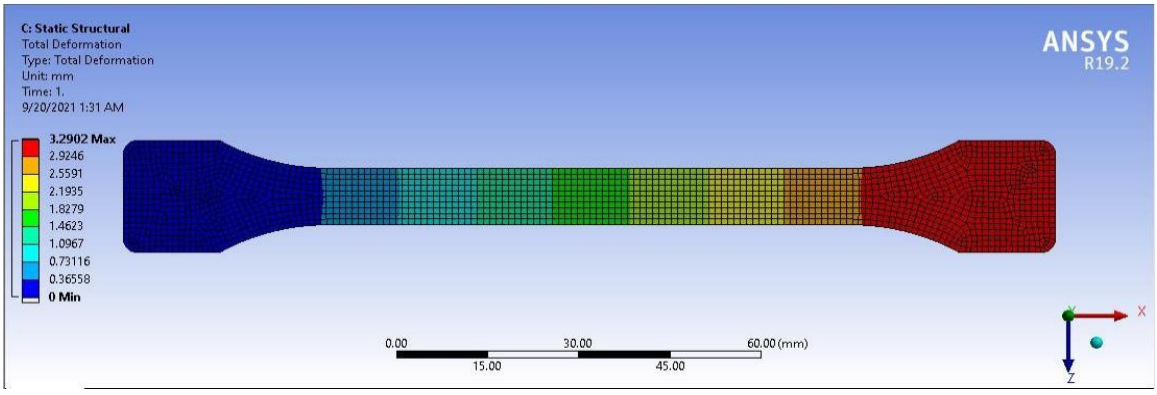

Figure XIV. Total deformation of PBTr after 5% HDPE.

PBTr + 10% HDPE: Figure XV illustrates the equivalent elastic strain distribution of a specimen containing 10% high-density polyethylene under a specified loading condition. The strain is measured in mm/mm and displayed with a color gradient, where blue represents the minimum strain (0.000036008 mm/mm) and red signifies the maximum strain (0.024592 mm/mm). The highest strain is concentrated in the central region of the specimen, while the strain values decrease towards the ends. This pattern indicates that the central section experiences the greatest elastic deformation, reflecting the material's response to the applied load and highlighting areas of potential stress concentration and failure.

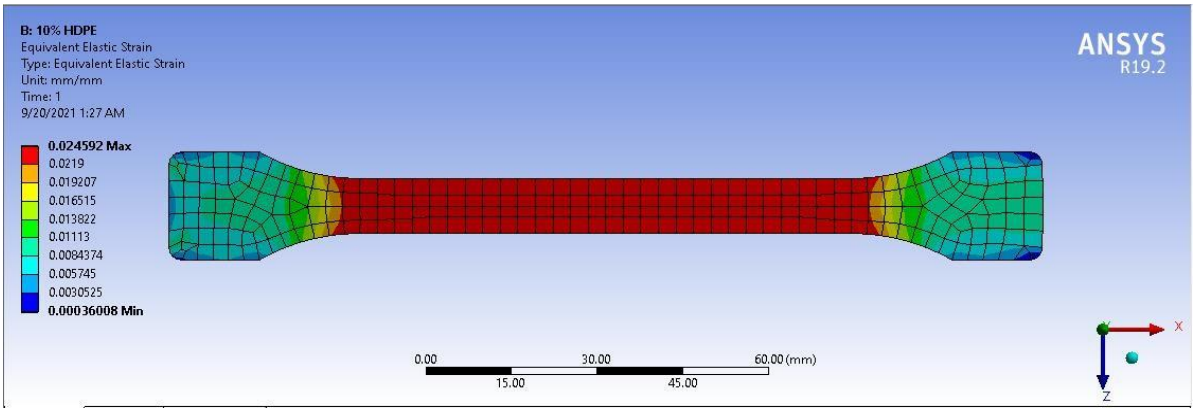

Figure XV. Equivalent elastic strain.

There isn't a single universal standard that dictates a fixed number of permissible recycling cycles for polymers like different materials responded in a change manner to heat such as for PVC, single cycle was opted due to its inclination towards temperature sensitivity. The minimum sample size suggested by the standard was adopted, with five specimens tested for each polymer to ensure a complete analysis because any uncertainty can be easily managed by using these values.

4. Conclusion. - In this engineering approach, a comprehensive study on the characteristics of various recycled plastics was conducted and findings indicate;

i. Addition of polypropylene (PP) with virgin PP does not affect significantly the yield stress and Young's modulus at room temperature.

ii. However, the recycling process makes PPr harder and stiffer, reducing its impact strength. The incorporation of elastomers and calcium carbonate impacts the density and melt flow index, suggesting potential modifications to recycled polypropylene properties for practical applications.

iii. Stress-strain curves demonstrated that recycled PVC outperforms virgin PVC in terms of ductility and elongation at break, providing crucial insights for enhancing PVC mixture performance. The total deformation analysis of recycled PVC and virgin PVC further supports these findings, showing higher deformation in recycled PVC, indicative of its superior ductility.

iv. Additionally, this study investigated the effects of aramid short fibres and thermoplastic polyurethane (TPU) additives on recycled polyamide-12 (PA-12). TPU decreased the modulus while increasing tensile strain and energy at break, whereas aramid fibres enhanced the modulus.

v. Deformation analysis showed significant strain concentrations in the central sections of these specimens, emphasizing the impact of additives on mechanical behaviour. For instance, the PA-12 with 20% TPU exhibited higher maximum deformation, reflecting its improved tensile properties.

vi. The results after blending PB and PE with HDPE showed that the central region experiences significant elastic deformation, which is crucial for understanding stress distribution in these materials.

5. Future recommendation. - Combine mechanical performance data with life cycle assessment and cost analysis to provide a comprehensive framework for industry adoption and policy formulation and more detailed study regarding mechanical properties like creep and fatigue can be performed.

References

[1] M. Delgado-Aguilar, R. Puig, I. Sazdovski, and P. Fullana-i-Palmer, "Polylactic Acid/Polycaprolactone Blends: On the Path to Circular Economy, Substituting Single-Use Commodity Plastic Products," Materials, vol. 13, no. 11, Jan. 2020, doi: 10.3390/ma13112655.

[2] M. Stieglitz, S. Adomeit, M. Müller, K. Hettwer, A. Schlierf, S. Uhlig, S. David, C. Hopmann, and L. Leuchtenberger-Engel, "Model-Based Prediction of the Tensile Properties of Polypropylene Films Made from Recycled Materials," Polymers, vol. 17, art. no. 1044, 2025, doi: 10.3390/polym17081044.

[3] E. N. Peters, "Engineering Thermoplastics—Materials, Properties, Trends," in Applied Plastics Engineering Handbook, 2nd ed., M. Kutz, Ed. William Andrew Publishing, 2017, pp. 3–26, doi: 10.1016/B978-0-323-39040-8.00001-8.

[4] A. S. Pouzada, E. C. Ferreira, and A. J. Pontes, "Friction properties of moulding thermoplastics," Polymer Testing, vol. 25, no. 8, pp. 1017–1023, Dec. 2006, doi: 10.1016/j.polymertesting.2006.06.009.

[5] Z. He, H. Niu, L. Liu, S. Xie, Z. Hua, and Y. Li, "Elastomeric polyolefin vitrimer: Dynamic imine bond cross-linked ethylene/propylene copolymer," Polymer, vol. 229, p. 124015, Aug. 2021, doi: 10.1016/j.polymer.2021.124015.

[6] D. Boyle, A. I. Catarino, N. J. Clark, and T. B. Henry, "Polyvinyl chloride (PVC) plastic fragments release Pb additives that are bioavailable in zebrafish," Environmental Pollution, vol. 263, p. 114422, Aug. 2020, doi: 10.1016/j.envpol.2020.114422.

[7] A. Poláchová, J. Císař, M. Novák, M. Dušánková, and V. Sedlařík, "Effect of repeated thermoplastic processing of polypropylene matrix on the generation of low-molecular-weight compounds," Polymer Degradation and Stability, vol. 238, p. 111337, 2025, doi: 10.1016/j.polymdegradstab.2025.111337.

[8] I.-R. Istrate, R. Juan, M. Martin-Gamboa, C. Domínguez, R. A. García-Muñoz, and J. Dufour, "Environmental life cycle assessment of the incorporation of recycled high-density polyethylene to polyethylene pipe grade resins," Journal of Cleaner Production, vol. 319, p. 128580, Oct. 2021, doi: 10.1016/j.jclepro.2021.128580.

[9] Y. A. Gueche, N. M. Sanchez-Ballester, S. Cailleaux, B. Bataille, and I. Soulairol, "Selective Laser Sintering (SLS), a New Chapter in the Production of Solid Oral Forms (SOFs) by 3D Printing," Pharmaceutics, vol. 13, no. 8, Aug. 2021, doi: 10.3390/pharmaceutics13081212.

[10] R. Lyons, A. Newell, P. Ghadimi, and N. Papakostas, "Environmental impacts of conventional and additive manufacturing for the production of Ti-6Al-4V knee implant: a life cycle approach," International Journal of Advanced Manufacturing Technology, vol. 112, no. 3, pp. 787–801, Jan. 2021, doi: 10.1007/s00170-020-06367-7.

[11] D. Ruggi, C. Barrès, J.-Y. Charmeau, R. Fulchiron, D. Barletta, and M. Poletto, "A quantitative approach to assess high temperature flow properties of a PA 12 powder for laser sintering," Additive Manufacturing, vol. 33, p. 101143, May 2020, doi: 10.1016/j.addma.2020.101143.

[12] T. Zhiltsova and M. S. A. Oliveira, "Sustainable Polypropylene Blends: Balancing Recycled Content with Processability and Performance," Polymers, vol. 17, no. 11, art. no. 1556, Jun. 2025, doi: 10.3390/polym17111556.

[13] N. Aliyeva, H. S. Sas, and B. Saner Okan, "Recent developments on the overmolding process for the fabrication of thermoset and thermoplastic composites by the integration of nano/micron-scale reinforcements," Composites Part A: Applied Science and Manufacturing, vol. 149, p. 106525, Oct. 2021, doi: 10.1016/j.compositesa.2021.106525.

[14] M. Chanda, "Chemical aspects of polymer recycling," Advanced Industrial and Engineering Polymer Research, vol. 4, no. 3, pp. 133–150, Jul. 2021, doi: 10.1016/j.aiepr.2021.06.002.

[15] P. Brachet, L. T. Høydal, E. L. Hinrichsen, and F. Melum, "Modification of mechanical properties of recycled polypropylene from post-consumer containers," Waste Management, vol. 28, no. 12, pp. 2456–2464, Dec. 2008, doi: 10.1016/j.wasman.2007.10.021.

[16] M. Wenguang and F. P. L. Mantia, "Processing and mechanical properties of recycled PVC and of homopolymer blends with virgin PVC," Journal of Applied Polymer Science, vol. 59, no. 5, pp. 759–767, Jan. 1996, doi: 10.1002/(SICI)1097-4628(19960131)59:5<759::AID-APP12>3.0.CO;2-U.

[17] D. Ignacio, K. N. Tumu, M. Munshi, K. L. Vorst, and G. W. Curtzwiler, "Suitability of MRF Recovered Post-Consumer Polypropylene Applications in Extrusion Blow Molded Bottle Food Packaging," Polymers, vol. 15, no. 16, art. no. 3471, Aug. 2023, doi: 10.3390/polym15163471.

[18] D. Tabuani, F. Bellucci, A. Terenzi, and G. Camino, "Flame retarded Thermoplastic Polyurethane (TPU) for cable jacketing application," Polymer Degradation and Stability, vol. 97, no. 12, pp. 2594–2601, Dec. 2012, doi: 10.1016/j.polymdegradstab.2012.07.011.

[19] W. Zhang, J. Shen, X. Guo, K. Wang, J. Jia, J. Zhao, and J. Zhang, "Comprehensive Investigation into the Impact of Degradation of Recycled Polyethylene and Recycled Polypropylene on the Thermo-Mechanical Characteristics and Thermal Stability of Blends," Molecules, vol. 29, no. 18, art. no. 4499, 2024, doi: 10.3390/molecules29184499.

[20] A. Ghosh, "Performance modifying techniques for recycled thermoplastics," Resources, Conservation and Recycling, vol. 175, p. 105887, Dec. 2021, doi: 10.1016/j.resconrec.2021.105887.

[21] R. Bernatas, S. Dagreou, A. Despax-Ferreres, and A. Barasinski, "Recycling of fiber reinforced composites with a focus on thermoplastic composites," Cleaner Engineering and Technology, vol. 5, p. 100272, Dec. 2021, doi: 10.1016/j.clet.2021.100272.

[22] M. E. Grigore, "Methods of Recycling, Properties and Applications of Recycled Thermoplastic Polymers," Recycling, vol. 2, no. 4, Dec. 2017, doi: 10.3390/recycling2040024.

[23] A. Shazad, M. Uzair, and M. Tufail, "Impact of blending of phase change material for performance enhancement of solar energy storage," Renewable Energy, vol. 227, p. 120530, 2024.

[24] A. Shazad, M. Uzair, T. Jamil, and N. Muhammad, "A Comparative Study on the Joint Hardness and tensile properties of Dissimilar Aluminum Alloy using Tungsten Inert Gas (TIG) Welding," in Proc. 4th Int. Conf. Key Enabling Technologies (KEYTECH 2024), Dec. 2024, pp. 173–178.

[25] J. Jadoon, A. Shazad, M. Muzamil, M. Akhtar, and M. Sattar, "Finite Element Analysis of Composite Pressure Vessel Using Reduced Models," Tecciencia, vol. 17, no. 33, Jul. 2022.

[26] F. Xie, "Sustainable polymer composites: functionality and applications," Functional Composite Materials, vol. 2, no. 1, p. 15, Oct. 2021.

[27] S. Kangishwar, N. Radhika, A. A. Sheik, A. Chavali, and S. Hariharan, "A comprehensive review on polymer matrix composites: material selection, fabrication, and application," Polymer Bulletin, vol. 80, no. 1, pp. 47–87, Jan. 2023.

[28] A. Shazad, J. Jadoon, M. Uzair, and M. Muzammil, "Material modelling and failure study of different fiber reinforced composites for pressure vessel," Memoria Investigaciones en Ingenieria, no. 24, pp. 92–104, Jun. 2023.

[29] B. L. Fernandes and A. J. Domingues, "Mechanical characterization of recycled polypropylene for automotive industry," Polímeros, vol. 17, pp. 85–87, 2007.

[30] F. Khan, A. Shakoor, M. B. Afzal, and A. Shazad, "Multi-Infill Strategies for Optimizing Tensile Properties in FDM-Printed PLA+ Components," Journal of Xi'an Shiyou University, Natural Science Edition, vol. 21, 2021.

Author contribution:

1. Conception and design of the study

2. Data acquisition

3. Data analysis

4. Discussion of the results

5. Writing of the manuscript

6. Approval of the last version of the manuscript

EAJ has contributed to: 1, 2, 3, 4, 5 and 6.

AS has contributed to: 1, 2, 3, 4, 5 and 6.

IA has contributed to: 1, 2, 3, 4, 5 and 6.

AAH has contributed to: 1, 2, 3, 4, 5 and 6.

UNA has contributed to: 1, 2, 3, 4, 5 and 6.

Acceptance Note: This article was approved by the journal editors Dr. Rafael Sotelo and Mag. Ing. Fernando A. Hernández Gobertti.

Smart and Sustainable IoT-Driven Vertical Farming Solution for Agricultural Challenges in Pakistan

Solución de agricultura vertical inteligente y sostenible basada en IoT para los desafíos agrícolas en Pakistán

Solução de agricultura vertical inteligente e sustentável baseada em IoT para desafios agrícolas no Paquistão

Sadiq Ur Rehman [1(*)], Muhammad Adeel Mannan [2], Muhammad Ahsan Shaikh [3], Muhammad Uzair [4]

Recibido: 15/05/2025 Aceptado: 23/07/2025

Summary. - Agriculture in Pakistan faces critical challenges such as water scarcity, inefficient resource use, and climate change impacts, particularly in urban and peri-urban areas. This study presents a smart, solar-powered vertical farming system designed to address these issues by integrating capacitive soil moisture sensors, temperature and humidity sensors (DHT22), and light sensors (BH1750), controlled via Raspberry Pi 4. The off-grid system, powered by a 100-watt solar panel and battery, features intelligent irrigation driven by a Random Forest algorithm to optimize water use. Over a six-week trial cultivating cherry tomatoes, the system achieved a 60–65% yield increase, 40% energy savings, and a 28.57% reduction in water consumption compared to traditional methods. While promising, limitations include the small trial size and lack of long-term environmental impact data. Scalability challenges such as cost, maintenance, and local constraints must be addressed for wider adoption. Future work will focus on expanding crop varieties, enhancing AI integration, and improving accessibility for small-scale farmers to support sustainable urban agriculture and food security in Pakistan.

Keywords: Agriculture, Vertical Farming, Sustainable Agriculture, Water Efficiency, Solar Energy.

[1] Ph.D., Associate Professor, Faculty of Engineering Science and Technology, IQRA University (Pakistan), sadiq.rehman@iqra.edu.pk, ORCID iD: https://orcid.org/0000-0002-6308-450X

[2] Ph.D., Associate Professor, Bahria School of Engineering and Applied Sciences, Bahria University (Pakistan), madeelmannan.bukc@bahria.edu.pk, ORCID iD: https://orcid.org/0000-0002-0811-4753

[3] Ph.D., Assistant Professor, Faculty of Engineering Science and Technology, Hamdard University (Pakistan) muhammad.ahsan@hamdard.edu.pk, ORCID iD: https://orcid.org/0000-0003-2408-5689

[4] Ph.D., Associate professor, Electrical Engineering Department, Faculty of Engineering, Islamic University of Madinah (Saudi Arabia) muzair@iu.edu.sa, ORCID iD: https://orcid.org/0000-0003-1063-9476

Memoria Investigaciones en Ingeniería, núm. 29 (2025). pp. 95-108
https://doi.org/10.36561/ING.29.7
ISSN 2301-1092 • ISSN (en línea) 2301-1106 – Universidad de Montevideo, Uruguay
Este es un artículo de acceso abierto distribuido bajo los términos de una licencia de uso y distribución CC BY-NC 4.0. Para ver una copia de esta licencia visite http://creativecommons.org/licenses/by-nc/4.0/

Resumen. - *La agricultura en Pakistán enfrenta desafíos críticos como la escasez de agua, el uso ineficiente de los recursos y los impactos del cambio climático, particularmente en áreas urbanas y periurbanas. Este estudio presenta un sistema de cultivo vertical inteligente alimentado con energía solar, diseñado para abordar estos problemas mediante la integración de sensores capacitivos de humedad del suelo, sensores de temperatura y humedad (DHT22) y sensores de luz (BH1750), controlados mediante Raspberry Pi 4. El sistema autónomo, alimentado por un panel solar de 100 vatios y una batería, cuenta con riego inteligente impulsado por un algoritmo de Bosque Aleatorio para optimizar el uso del agua. Durante un ensayo de seis semanas cultivando tomates cherry, el sistema logró un aumento del 60-65% en el rendimiento, un ahorro de energía del 40% y una reducción del 28,57% en el consumo de agua en comparación con los métodos tradicionales. Si bien es prometedor, las limitaciones incluyen el pequeño tamaño del ensayo y la falta de datos de impacto ambiental a largo plazo. Es necesario abordar los desafíos de escalabilidad, como el costo, el mantenimiento y las restricciones locales, para una adopción más amplia. El trabajo futuro se centrará en ampliar las variedades de cultivos, mejorar la integración de la IA y mejorar la accesibilidad para los pequeños agricultores para apoyar la agricultura urbana sostenible y la seguridad alimentaria en Pakistán.*

Palabras clave: *Agricultura impulsada por el IoT, agricultura vertical, agricultura sostenible, eficiencia hídrica, energía solar*

Resumo. ***-*** *A agricultura no Paquistão enfrenta desafios críticos, como a escassez de água, a utilização ineficiente dos recursos e os impactos das alterações climáticas, particularmente nas áreas urbanas e periurbanas. Este estudo apresenta um sistema de agricultura vertical inteligente, alimentado a energia solar, concebido para lidar com estas questões, integrando sensores capacitivos de humidade do solo, sensores de temperatura e humidade (DHT22) e sensores de luz (BH1750), controlados através do Raspberry Pi 4. O sistema off-grid, alimentado por um painel solar de 100 watts e bateria, possui uma irrigação inteligente acionada por um algoritmo Random Forest para otimizar a utilização da água. Ao longo de um teste de seis semanas de cultivo de tomate-cereja, o sistema obteve um aumento de 60–65% na produtividade, 40% de poupança de energia e uma redução de 28,57% no consumo de água em comparação com os métodos tradicionais. Embora promissor, as limitações incluem o pequeno tamanho do teste e a falta de dados de impacto ambiental a longo prazo. Os desafios de escalabilidade, como o custo, a manutenção e as restrições locais, devem ser abordados para uma adoção mais ampla. O trabalho futuro irá focar-se na expansão das variedades de culturas, na melhoria da integração da IA e na melhoria da acessibilidade para os pequenos agricultores para apoiar a agricultura urbana sustentável e a segurança alimentar no Paquistão.*

Palavras-chave: *Agricultura orientada por IoT, agricultura vertical, agricultura sustentável, eficiência hídrica, energia solar.*

1. Introduction. - The global population has been growing at an increasingly rapid pace, which has led to several challenges, such as the strain on land available for agriculture and the growing need for fresh water to meet both drinking and agricultural demands [1]. Experts predict that by 2050, the world's population could reach 9 billion, further intensifying the pressure on land resources needed for living spaces [2]. With only 10% of the land being suitable for farming, it is becoming increasingly difficult to grow enough crops to meet the needs of a growing population. Furthermore, an enormous number of crops are wasted due to natural disasters such as earthquakes, droughts, heavy rainfall, and flooding [3]. Moreover, the crops that make it to the market are often not fresh, as the farming and agricultural lands are located far from cities and residential areas. Pakistan is one of the developing countries whose economy heavily depends on agriculture [4]. However, rapid urbanization has made it difficult for this sector to grow enough food to meet demand. Traditional farming [5] in Pakistan is still widely practiced but faces many challenges, including high water use and vulnerability to environmental degradation (see Table I).

Challenge	Description
Water Scarcity	Low rainfall and over-extraction of groundwater
Energy Shortage	Frequent power outages, especially in rural áreas
Land Constraints	Urban sprawl reduces arable land availability
Climate Variability	Increasing droughts, floods, and heatwaves
Inefficient Irrigation	High water loss due to outdated techniques
Crop Loss & Decay	Delays from rural farms to markets reduce freshness

Table I. Challenges in Traditional Agriculture in Pakistan

Vertical farming [6] offers a promising solution to these challenges by maximizing agricultural space through stacked beds that grow crops vertically in controlled environments. This method optimizes the use of arable land and allows for more efficient water and energy use. By carefully monitoring and controlling factors like light, temperature, humidity, and soil moisture, vertical farming can create ideal growing conditions with fewer resources. Importantly, vertical farming isn't just about saving space, it also addresses critical sustainability issues around water and energy. Using smart sensors to water plants only when needed helps cut down on wasted water, while integrating solar power reduces dependence on unreliable grid electricity. This combination makes the system not only smarter but also much more environmentally friendly and sustainable, something particularly vital for resource-limited countries like Pakistan.

In this study, we propose a practical and fully autonomous vertical farming system that integrates IoT [7-8] sensors, machine learning algorithms [9], and solar power. This combination not only allows precise control of environmental conditions but also reduces reliance on conventional electricity grids by harnessing renewable energy, making it a realistic and sustainable solution for the challenges faced by agriculture in Pakistan and similar regions. Table II presents a comparison between vertical farming and traditional farming methods, showing measurable improvements in space efficiency, water savings, and environmental impact. While traditional farming requires large land areas and often wastes water through inefficient irrigation, vertical farming can reduce water use by up to 90% and increase yield per square foot. Our approach builds on these advantages by incorporating IoT and machine learning to optimize irrigation and lighting further, backed by solar energy to ensure sustainable power supply.

Aspect	Vertical Farming	Traditional Farming
Space Efficiency	High crops grow in stacked layers, maximizing space.	Low; requires large land areas for planting.
Water Usage	Reduced by up to 90% due to efficient irrigation methods (e.g., hydroponics).	High, especially in water-scarce regions with inefficient irrigation systems.
Energy Usage	High, but can be offset with renewable energy (e.g., solar power).	Generally low but dependent on external power sources.
Yield	Significantly higher per square foot compared to traditional methods.	Relatively low per unit area, especially in urban or degraded soils.

Environmental Impact	Lower carbon footprint due to local production and reduced transportation.	Higher due to transportation and potential soil degradation.

Table II. Comparison Between Vertical Farming and Traditional Farming Systems

The rest of the paper is organized as follows: Section II provides a literature review, Section III details the methodology of the proposed system, Section IV presents the results and discussion, and finally, Section V concludes with a summary of key findings and possible future directions.

2. Literature Review. - The world's economic stability is increasingly threatened by challenges such as infectious diseases and rapid population growth, which directly impact agricultural land availability and food security [10]. In countries like Pakistan, where agriculture is a major economic driver, these pressures are intensified by urbanization and climate change, leading to decreased arable land and freshwater scarcity. This calls for innovative farming solutions that maximize productivity within limited resources.

The proposed system seeks to address these challenges by combining vertical farming with modern technologies such as IoT, machine learning (ML), and solar power. The focus is on creating an easy-to-use internal farming platform with shelving units to grow crops efficiently indoors. Before detailing the system design, it is essential to critically review relevant technologies and their current limitations.

2.1 IoT in Agriculture. - IoT technologies have transformed agricultural monitoring by enabling real-time data collection on environmental factors like soil moisture, temperature, and humidity [11-12]. These systems improve water efficiency through automated irrigation and enable precise crop management [13-14]. However, many existing IoT applications focus primarily on data gathering rather than integrating predictive analytics or full automation, limiting their optimization potential.

Furthermore, IoT integration in vertical farming remains nascent. Vertical farms require more sophisticated control over multiple environmental variables simultaneously, which complicates IoT deployment and data processing. Studies rarely address system scalability or robustness in challenging field conditions, especially in developing countries where infrastructure may be unreliable.

2.2 Vertical Farming vs. Traditional Farming. - Vertical farming, characterized by stacking plants in multi-layered structures, offers substantial benefits over traditional farming, including higher space utilization and significant water savings (up to 90% reduction) due to methods like hydroponics and aeroponics [15-16]. While vertical farming promises efficiency gains, it is important to highlight its main challenges. Energy consumption is notably high due to artificial lighting and climate control requirements, which can limit its practicality in energy-constrained regions [15]. Additionally, the upfront costs and technical complexity can be prohibitive, especially for small-scale farmers in developing countries. Hence, integrating renewable energy sources such as solar power becomes critical but is still underdeveloped in current literature.

2.3 Solar Energy in Agriculture. - Solar energy presents a promising solution to reduce reliance on unreliable electrical grids in agriculture, particularly in countries like Pakistan with high solar insolation [17]. Solar-powered irrigation and greenhouse systems have demonstrated reduced operational costs and lower environmental impact [18]. Despite this, solar integration into vertical farming remains limited. Vertical farming's high continuous energy demands require efficient energy storage and management solutions that are often overlooked.

Additionally, the intermittent nature of solar power poses challenges for maintaining the consistent environmental conditions vertical farms need. Most studies do not address how to mitigate this intermittency or evaluate the economic feasibility of incorporating solar power at scale.

2.4 Machine Learning in Agriculture. - Machine learning has shown significant promise in enhancing agricultural decision-making by analyzing sensor data to predict irrigation needs, crop health, and yield [19-20]. For example, Random Forest algorithms have effectively optimized irrigation schedules, reducing water waste [21]. However, many ML models are trained on limited datasets and have not been extensively validated across diverse crops or

environments.

Moreover, there is a lack of studies integrating ML with IoT in real-time vertical farming environments to create closed-loop systems for dynamic resource management. Bridging this gap is critical to developing intelligent farms that can autonomously optimize water and energy use.

Study	Technology/Method	Key Findings	Limitations
[13]	IoT-based agriculture	Improved water use and crop yield via soil monitoring.	Focused on monitoring, limited automation and predictive control.
[14]	IoT smart irrigation	Demonstrated water-saving potential with soil moisture sensors.	Prototype scale, lack of scalability analysis.
[15]	Hydroponics/Aeroponics	Efficient space use and water savings demonstrated.	High setup costs and energy needs.
[17],[18]	Solar energy in agriculture	Reduced energy costs and grid dependency shown.	Limited focus on integration with high-demand vertical farming.
[21]	ML for irrigation and yield prediction	Improved irrigation scheduling and yield forecasting.	Limited real-world validation and integration with IoT.

Table III. Comparative Analysis of Technological Interventions in Smart and Sustainable Agriculture Systems

The literature indicates clear potential in combining vertical farming, IoT, solar power, and ML. However, a holistic system that integrates these components efficiently, addresses energy constraints, and is tailored to developing country contexts remains elusive. Our research addresses these gaps by proposing a smart vertical farming system that leverages IoT and ML for automated irrigation, powered sustainably by solar energy.

3. Methodology. - The system was implemented on a practical small scale inside a 12x12-foot room, featuring a two-tiered iron frame structure approximately 45 inches tall, enclosed by transparent acrylic sheets (see Figure. I). This setup created a mini-greenhouse effect, optimizing vertical space by stacking growing beds, which is ideal for urban or space-constrained environments. While cherry tomatoes were the primary crop cultivated during this trial, the system is designed to support a diverse range of crops such as leafy greens, herbs, and peppers, which will be explored in future extended studies to validate broader applicability.

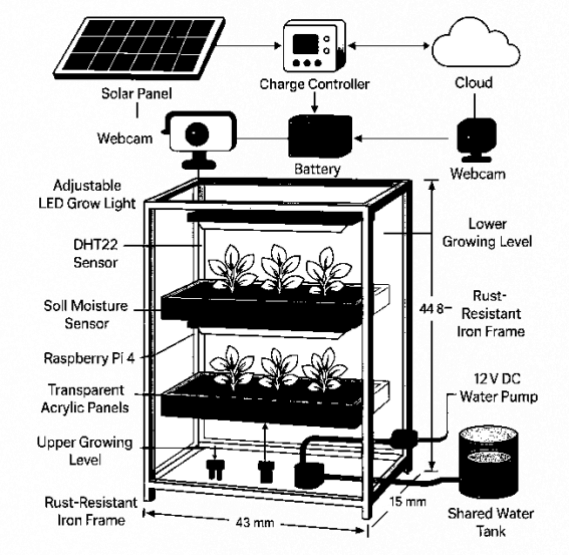

Figure I. Structure Diagram.

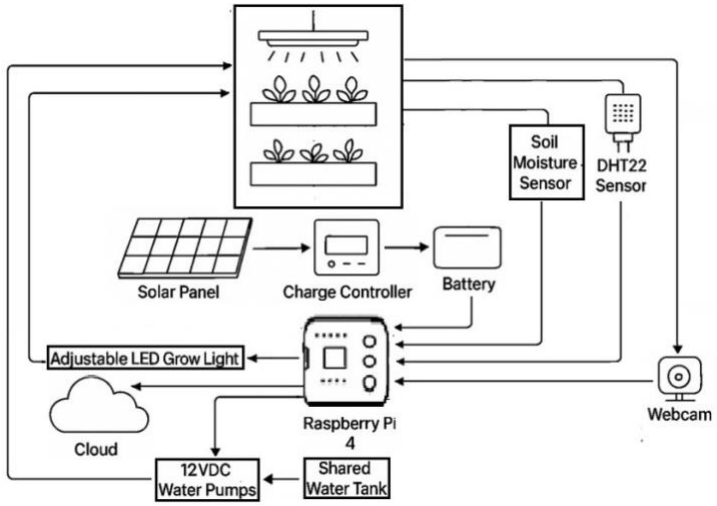

Figure II. System Block Diagram.

Each growing bed was equipped with sensors to continuously monitor environmental and soil conditions, enabling precise control to optimize crop growth. Capacitive soil moisture sensors measured water content, triggering irrigation only when moisture levels fell below 30% to conserve water efficiently. Temperature and humidity were monitored using DHT22 sensors, maintaining the target ranges of 29°C to 34°C and 58% to 68% humidity, respectively. The BH1750 light sensor ensured that plants received adequate light by activating energy-efficient LED grow lights whenever ambient light dropped below 3000 lux. The system architecture is illustrated in Figure II.

The core processing was handled by a Raspberry Pi 4, which collected sensor data every 5 minutes to maintain real-time control of irrigation, lighting, and environmental conditions. The system was powered by a 100-watt solar panel connected to a battery bank via a charge controller, ensuring energy autonomy even during night hours or cloudy conditions. A 12V DC water pump delivered irrigation for approximately 30 seconds per activation, based on sensor readings.

Remote monitoring and manual control were enabled through the Red-Note software dashboard, which presented real-time environmental data and system status to users, facilitating easy intervention if necessary.

To enhance irrigation precision and reduce water waste, a Random Forest regression model was implemented to predict optimal irrigation durations. The model was trained using a dataset comprising 3,200 records collected from preliminary trials. Features included temperature, humidity, soil moisture, and light intensity, while the target variable was irrigation time in seconds. The dataset was split into 80% training and 20% testing partitions. The model achieved an R^2 score of 0.91, indicating strong predictive capability. Predictions were generated every 15 minutes and cross-checked against real-time conditions. When the forecasted irrigation time deviated significantly from the baseline, the machine learning output overrode the rule-based logic, ensuring that water delivery was adapted to actual environmental needs.

Parameter	**Value**
Dataset Size	3,200 points
Training/Test Split	80% / 20%
Features	Temp, Humidity, Moisture, Light
Target	Irrigation Time (sec)
Evaluation Metric	RMSE, MAE, R^2
Model Accuracy	$R^2 = 0.91$

Table IV. Random Forest Model Configuration

To manage energy efficiently, the charge controller prevented battery overcharging, and the system reduced power consumption by limiting non-essential functions during periods of low sunlight, prioritizing critical operations like data logging and irrigation. This adaptive energy management strategy ensured uninterrupted operation while maximizing the use of solar power.

Component	Description	Essential Parameters
Soil Moisture Sensor (FC-28)	Measures the moisture content of the soil to optimize irrigation.	Moisture Range: 0% - 100%
		Threshold: 30% for irrigation trigger
		Accuracy: ±3% to ±10%
Temperature and Humidity Sensor (DHT22)	Monitors the ambient temperature and humidity in the growing environment.	Temperature Range: -40°C to 80°C
		Humidity Range: 0% - 100%
		Accuracy: ±0.5°C for temp
		Accuracy: ±2% for humidity
Light Intensity Sensor (BH1750)	Measures the ambient light intensity to control LED grow lights.	Light Intensity Range: 0 to 65535 lux
		Threshold: 3000 lux for LED activation
Raspberry Pi 4 (Central Controller)	Acts as the main controller for the system, processing sensor data and making decisions.	Processor: Quad-core ARM Cortex-A72
		RAM: 2GB/4GB/8GB
		Connectivity: Wi-Fi, Ethernet
Solar Panel (100W)	Powers the entire system through solar energy, reducing grid dependence.	Power Output: 100W
		Efficiency: Variable based on sunlight intensity
		Voltage: 12V DC
Battery and Charge Controller	Stores energy for night-time use and manages charging of the battery.	Battery Capacity: 12V, 12Ah
		Charge Controller: Protects from overcharging, efficient energy management
DC Water Pump (12V)	Delivers water to the plants based on the moisture level.	Voltage: 12V DC
		Flow Rate: 4-6 liters/min
		Power Consumption: 3- 5W
LED Grow Lights	Provides artificial light to support plant photosynthesis when natural light is insufficient.	Power: 20W-30W per panel
		Color Temperature: 6000-6500K (Daylight)
Cloud-based Dashboard	A web-based interface for remote monitoring and management of the system.	Real-time Monitoring: Temperature, humidity, light, and moisture levels
		User Control: Manual override available

Table V. Components used in the system along with their essential parameters

4. Results and Discussion. - This section discusses the results obtained from the IoT-powered vertical farming system, tested with cherry tomato crops over a 6-week trial period. The key parameters analyzed include water usage efficiency, energy consumption, crop yield, temperature and humidity control, and light intensity. While the system shows promising improvements compared to traditional farming, the scope of the experiment is limited, and statistical analysis has been added to strengthen validity.

Figure III. Assembled hardware of the proposed system model.

4.1 Water Usage Efficiency. - Water efficiency is critical for sustainable farming, especially for crops like cherry tomatoes that require precise irrigation. Using soil moisture sensors integrated with a Random Forest model, the system automated irrigation to maintain soil moisture between 40%-45%, compared to 33%-38% in traditional farming (see Figure V). This resulted in average water savings of 28.6% (±2.3% standard deviation), as shown in Table VI.

Parameter	Traditional Farming	Vertical Farming with IoT	Improvement (%)
Average Soil Moisture (%)	35.5 ± 2.1	42.5 ± 1.8	-
Water Usage (liters)	10.5 ± 0.7	7.5 ± 0.5	28.6 ± 2.3

Table VI. Water Usage Efficiency and Soil Moisture Comparison

Figure IV. Reading of FC-28 on the user interface

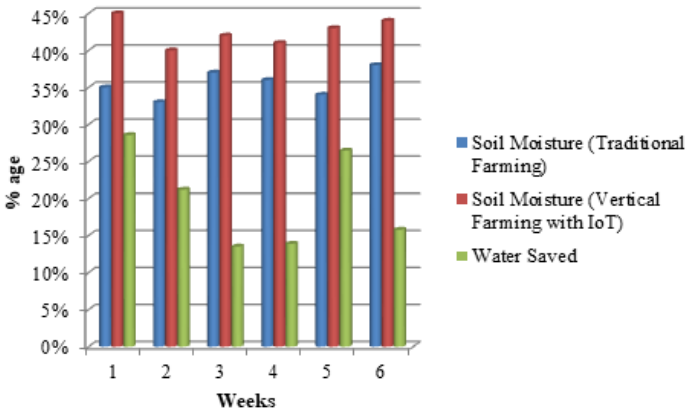

Figure V. Soil Moisture Readings.

4.2 Energy Consumption. - Energy consumption was monitored weekly, comparing the solar-powered vertical farming system with traditional farming relying on grid electricity. Vertical farming consumed between 2.9 to 3.3 kWh per week, significantly less than traditional methods (4.8 to 5.2 kWh). Solar panel efficiency ranged from 35.3% to 40% (see Table VII). Energy savings averaged 39.1% (±1.5%). Figure 6 includes error bars showing weekly consumption variance.

Week	Traditional Energy (kWh)	Vertical Farming Energy (kWh)	Energy Efficiency (%)	Std. Dev (Efficiency)
1	5.0 ± 0.1	3.0 ± 0.1	40	±1.2
2	4.8 ± 0.2	2.9 ± 0.1	39.6	±1.3
3	5.2 ± 0.1	3.1 ± 0.2	40.4	±1.5
4	5.0 ± 0.1	3.2 ± 0.1	36	±1.1
5	4.9 ± 0.2	3.0 ± 0.1	38	±1.4
6	5.1 ± 0.1	3.3 ± 0.2	35.3	±1.6

Table VII. Weekly Energy Consumption and Solar Panel Efficiency

4.3 Crop Yield. - The vertical farming system yielded 60-65% more cherry tomatoes per plant compared to traditional farming (Table VIII). Specifically, plants produced an average of 9 (±1.2) fruits versus 5.5 (±1.0) in the traditional setup. While promising, the limited crop variety and short 6-week trial restrict broader applicability.

Parameter	Traditional Farming (4 Plants)	Vertical Farming (4 Plants)	Yield Increase (%)
Average Fruits per Plant	5.5 ± 1.0	9.0 ± 1.2	63.6 ± 5.4
Total Fruits (6 Weeks)	22 ± 4	36 ± 5	-

Table VIII. Comparison of Crop Yield between Traditional and IoT-Driven Vertical Farming

4.4 Temperature and Humidity Control. - Stable environmental conditions are vital for crop health. The vertical farming system-maintained temperatures between 29°C and 34°C (±1.2°C) and humidity between 58% and 68% (±3%) as can be seen in Figure VI, whereas traditional farming saw wider fluctuations (31°C-36°C, ±2°C; 52%-60%, ±4%). This controlled environment improved plant health and fruit quality.

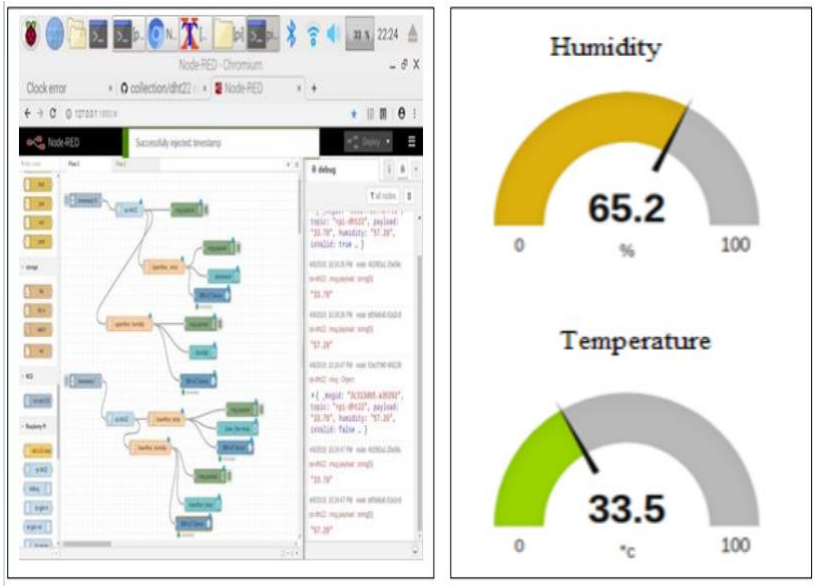

Figure VI. Temperature and Humidity level of a system

Week	Temp Traditional (°C)	Temp Vertical (°C)	Humidity Traditional (%)	Humidity Vertical (%)
Avg ± SD	33.0 ± 1.5	31.5 ± 1.2	57 ± 4	63 ± 3

Table IX. Average Temperature and Humidity Comparison with Variability

4.5 Light Intensity and Growth Conditions. - Light intensity was consistently higher and more stable in the vertical system, ranging from 1150 to 1300 lux, compared to 950 to 1050 lux outdoors. This represents a 22.5% ± 2.1% increase in light availability, promoting better photosynthesis and growth (Table X).

Week	Light Intensity Traditional (lux)	Light Intensity Vertical (lux)	Increase (%)
Avg ± SD	1005 ± 40	1225 ± 55	22.5 ± 2.1

Table X. Light Intensity Comparison

4.6 Baseline Comparison with Other Smart Farming Systems. - To provide broader context for our system's performance, Table XI compares key metrics such as water savings, yield improvement, and energy use against other smart farming solutions reported in the literature. While some field-based IoT irrigation systems demonstrate higher water savings due to starting from less efficient traditional methods, our vertical farming system achieves competitive water efficiency alongside a notably higher yield increase, thanks to its controlled environment. Additionally, the integration of solar power enhances sustainability by reducing reliance on grid electricity an aspect often unreported in other studies. This comparison highlights the practical benefits and unique strengths of our approach within the landscape of smart agriculture technologies.

System Type	Water Savings vs Traditional	Yield Increase	Energy Use Notes
Our Vertical Farm (IoT + Solar)	28.6 ± 2.3 %	63.6 ± 5.4 %	~3.0 kWh/week (solar powered)
[22]	~50 %	~35 %	Not reported
[23]	47.8 %	~34.9 %	Not reported
[24]	~35 %	~24–30 %	—

Table XI. Benchmark Comparison with Other Smart Farming Systems

5. Conclusion and Future Work. - This study successfully developed a smart, solar-powered vertical farming system tailored to the unique agricultural challenges of Pakistan. By integrating real-time environmental monitoring, automated irrigation, and machine learning (Random Forest), the system significantly improved resource efficiency and crop productivity compared to traditional farming. Over a six-week trial, it reduced water use by 28.57%, cut energy consumption by 40%, and increased cherry tomato yield by 60–65%. Its off-grid, solar-powered design ensured reliable operation while maintaining ideal growing conditions, something hard to achieve in open-field farming.

However, this study has some limitations. The experimental scope was limited to a single crop and a short trial period, which restricts the generalizability of the findings. Additionally, long-term environmental impacts and system durability were not assessed, indicating the need for extended studies. Scalability challenges also remain, such as the initial cost of setup, ongoing maintenance requirements, and adapting the system to diverse local conditions and crop types. Addressing these issues will be critical to ensuring wider adoption.

Looking forward, future work should focus on scaling the system for commercial use, expanding to a broader variety of crops, and integrating more advanced AI models for further optimization. Efforts to reduce costs and simplify maintenance will enhance accessibility for small-scale farmers. Moreover, long-term field studies evaluating environmental and economic impacts are essential. With supportive policies and investments, this innovation could play a vital role in driving sustainable agriculture and improving food security in Pakistan.

References

[1] Al Meselmani, Moaed Ali. "Hydroponics: The Future of Sustainable Farming." In Hydroponics: The Future of Sustainable Farming, pp. 101-122. New York, NY: Springer US, 2024. https://doi.org/10.1007/978-1-0716-3993-1_6

[2] Angel, S., Parent, J., Civco, D. L., Blei, A., & Potere, D. (2011). The dimensions of global urban expansion: Estimates and projections for all countries, 2000–2050. Progress in Planning, 75(2), 53–107. https://doi.org/10.1016/j.progress.2011.04.001

[3] Sivakumar, M. V. K. (2005). Impacts of natural disasters in agriculture, rangeland and forestry: An overview. In Natural disasters and extreme events in agriculture: Impacts and mitigation (pp. 1–22). https://doi.org/10.1007/3-540-28307-2_1

[4] Mahmood, G. G., Liberatori, S., & Mazzetto, F. (2025). Agricultural mechanization perspective in Pakistan: Present challenges and digital future. Journal of Agricultural Engineering. https://doi.org/10.4081/jae.2025.1636

[5] Hamadani, H., Rashid, S. M., Parrah, J. D., Khan, A. A., Dar, K. A., Ganie, A. A., Gazal, A., Dar, R. A., & Ali, A. (2021). Traditional farming practices and its consequences. In Microbiota and biofertilizers, Vol. 2: Ecofriendly tools for reclamation of degraded soil environs (pp. 119–128). https://doi.org/10.1007/978-3-030-61010-4_6

[6] Shi, X., Shi, C., Tablada, A., Guan, X., Cui, M., Rong, Y., Zhang, Q., & Xie, X. (2025). A review of research progress in vertical farming on façades: Design, technology, and benefits. Sustainability, 17(3), 921. https://doi.org/10.3390/su17030921

[7] Rehman, S. U., Khan, I. U., Moiz, M., & Hasan, S. (2016). Security and privacy issues in IoT. International Journal of Communication Networks and Information Security, 8(3), 147.

[8] Rehman, S. U., Mustafa, H., & Larik, A. R. (2021). IoT based substation monitoring & control system using Arduino with data logging. In 2021 4th International Conference on Computing & Information Sciences (ICCIS) (pp. 1–6). IEEE. https://doi.org/10.1109/ICCIS54243.2021.9676384

[9] Botero-Valencia, J., García-Pineda, V., Valencia-Arias, A., Valencia, J., Reyes-Vera, E., Mejia-Herrera, M., & Hernández-García, R. (2025). Machine learning in sustainable agriculture: Systematic review and research perspectives. Agriculture, 15(4), 377. https://doi.org/10.3390/agriculture15040377

[10] Saravanan, S., Akay, Y. M., Chen, T., & Akay, M. (2025). Impacts of climate change on global health: A review of preparedness, infectious disease, and excessive heat. Health and Technology, 15(1), 7–14. https://doi.org/10.1007/s12553-024-00927-7

[11] Rehman, S. U., Khan, I., Rehman, N. U., & Hussain, A. (2022). Low-cost smart home automation system with advanced features. Quaid-E-Awam University Research Journal of Engineering Science and Technology Nawabshah, 20(01), 74–82. https://doi.org/10.52584/QRJ.2001.10

[12] Rehman, S. U., & Khan, A. (2023). Integrating IoT technology for improved distribution transformer monitoring and protection. Electrical, Control and Communication Engineering, 19(1), 22–28. https://doi.org/10.2478/ecce-2023-0004

[13] Chew, K.-M., Tan, S. C.-W., Loh, G. C.-W., Bundan, N., & Yiiong, S.-P. (2020). IoT soil moisture monitoring and irrigation system development. In Proceedings of the 2020 9th International Conference on Software and Computer Applications (pp. 247–252). https://doi.org/10.1145/3384544.3384595

[14] Obaideen, K., Yousef, B. A. A., AlMallahi, M. N., Tan, Y. C., Mahmoud, M., Jaber, H., & Ramadan, M. (2022). An overview of smart irrigation systems using IoT. Energy Nexus, 7, 100124. https://doi.org/10.1016/j.nexus.2022.100124

[15] Verma, S., Kumar, A., Kumari, M., Kumar, N., Hansda, S., Saurabh, A., Poonia, S., & Rathore, S. D. (2024). A review on hydroponics and vertical farming for vegetable cultivation: Innovations and challenges. Journal of Experimental Agriculture International, 46(12), 801–821. https://doi.org/10.9734/jeai/2024/v46i123190

[16] Banerjee, C., & Adenaeuer, L. (2014). Up, up and away! The economics of vertical farming. Journal of Agricultural Studies, 2(1), 40–60. http://dx.doi.org/10.5296/jas.v2i1.4416

[17] Hassanien, R. H. E., Li, M., & Lin, W. D. (2016). Advanced applications of solar energy in agricultural greenhouses. Renewable and Sustainable Energy Reviews, 54, 989–1001. https://doi.org/10.1016/j.rser.2015.10.095

[18] Abdelhamid, M. A., Abdelkader, T. K., Sayed, H. A. A., Zhang, Z., Zhao, X., & Atia, M. F. (2025). Design and evaluation of a solar powered smart irrigation system for sustainable urban agriculture. Scientific Reports, 15(1), 11761. https://doi.org/10.1038/s41598-025-94251-3

[19] Haider, W., & Rehman, A. (2019). Knowledge based soil classification towards relevant crop production. International Journal of Advanced Computer Science and Applications, 10(12), 488–501. https://doi.org/10.14569/IJACSA.2019.0101266

[20] Haider, W., Rehman, A., Durrani, N. M., & Rehman, S. U. (2021). A generic approach for wheat disease classification and verification using expert opinion for knowledge-based decisions. IEEE Access, 9, 31104–31129. https://doi.org/10.1109/ACCESS.2021.3058582

[21] Jegan, D., Surendran, R., & Madhusundar, N. (2024). Hydroponic using deep water culture for lettuce farming using random forest compared with decision tree algorithm. In 2024 8th International Conference on Electronics, Communication and Aerospace Technology (ICECA) (pp. 907–914). IEEE. https://doi.org/10.1109/ICECA63461.2024.10800972

[22] Zia, H., Rehman, A., Harris, N. R., Fatima, S., & Khurram, M. (2021). An experimental comparison of IoT-based and traditional irrigation scheduling on a flood-irrigated subtropical lemon farm. Sensors, 21(12), 4175. https://doi.org/10.3390/s21124175

[23] Ragab, M. A., Badreldeen, M. M. M., Sedhom, A., & Mamdouh, W. M. (2022). IOT based smart irrigation system. International Journal of Industry and Sustainable Development, 3(1), 76-86. https://doi.org/10.21608/ijisd.2022.148007.1021

[24] Zafar, U., Arshad, M., Masud Cheema, M. J., & Ahmad, R. (2020). Sensor based drip irrigation to enhance crop yield and water productivity in semi-arid climatic region of Pakistan. Pakistan Journal of Agricultural Sciences, 57(5). https://doi.org/10.21162/PAKJAS/20.83

Author contribution:

1. Conception and design of the study

2. Data acquisition

3. Data analysis

4. Discussion of the results

5. Writing of the manuscript

6. Approval of the last version of the manuscript

SUR has contributed to: 1, 2, 3 and 4.

MAM has contributed to: 4, 5 and 6.

MAS has contributed to: 6.

MU has contributed to: 6.

Acceptance Note: This article was approved by the journal editors Dr. Rafael Sotelo and Mag. Ing. Fernando A. Hernández Gobertti.

Occupational Hazard Assessment And Risk Mitigation In The Gluing And Lapping Section Of A Gas Meter Manufacturing Plant

Evaluación de riesgos laborales y mitigación de riesgos en la sección de encolado y lapeado de una planta de fabricación de medidores de gas

Avaliação de riscos ocupacionais e mitigação de riscos na seção de colagem e lapidação de uma planta de fabricação de medidores de gás

Ammar Zulfikar [1(*)], S. M. Muhib Hussain Naqvi [2], Imran Sikandar [3],
Muhammad Azam [4], Muhammad Hamid [5], Hamza Ahmed [6]

Recibido: 24/05/2025 Aceptado: 24/07/2025

Summary. - Occupational health is fundamental aspect of work force management to ensure healthy and secure working environment especially in production environments where life threatening hazards are commonplace. This study implements Hazard Identification and Risk Assessment (HIRA) within a gas meter manufacturing facility's gluing and lapping shop and compares pre-existing conditions with ISO 45001 (Occupational Health and Safety), ISO 9001 (Quality Management), and ISO 14001 (Environmental Management) standards. Hazards are systematically identified by onsite workplace inspections, incident data analysis, and employee interview and input. Evaluated risk levels are made into standardized risk matrixes and control measures are suggested in line with ISO standards to minimize risk levels. The risk mitigation strategy is developed with established hierarchy of controls, emphasizing elimination, substitution, and engineering controls before administrative measures and personal protective equipment are suggested. Parameters such as temperature, noise, and lighting in the workplace are evaluated, these environmental factors are benchmarked against ISO-defined permissible exposure limits to ensure compliance and safeguard worker well-being. The findings yield actionable recommendations aimed at improving occupational safety, operational efficiency, and regulatory conformity of the gas meter manufacturing plant's gluing and lapping shop. By addressing these challenges, the research contributes to safer and more sustainable industrial practices in gas meter manufacturing. Future works in this field should in cooperate the integration of IOT and sensors to achieve real time monitoring and IOT based controls integrating Mechatronics and IOT with Health safety.

Keywords: Occupational Health and Safety, HIRA, Risk Analysis, ISO 14001, ISO 9001, ISO 45001, Gas meter manufacturing, Mechanical Hazards, Workplace Risk Management, Hierarchy of Control.

[1] Mechanical Engineer, Department of Mechanical Engineering, NED University of Engineering & Technology (Pakistan), zulfikar4401532@cloud.neduet.edu.pk, ORCID iD: https://orcid.org/0009-0000-4484-9362
[2] Final Year Student (BE), Department of Mechanical Engineering, NED University of Engineering & Technology (Pakistan), naqvi4400260@cloud.neduet.edu.pk, ORCID iD: https://orcid.org/0009-0002-2602-2542
[3] Assistant Professor, Department of Mechanical Engineering, NED University of Engineering & Technology (Pakistan), isikandar@neduet.edu.pk, ORCID iD: https://orcid.org/0009-0006-3418-5148
[4] Lecturer, Department of Mechanical Engineering, NED University of Engineering & Technology (Pakistan), muhammadazam239@cloud.neduet.edu.pk, ORCID iD: https://orcid.org/0009-0007-1238-8961
[5] Mechanical Engineer, Department of Mechanical Engineering, NED University of Engineering & Technology (Pakistan), hamid4403139@cloud.neduet.edu.pk, ORCID iD: https://orcid.org/0009-0008-0911-2494
[6] Mechanical Engineer, Department of Mechanical Engineering, NED University of Engineering & Technology (Pakistan), ahmed4404825@cloud.neduet.edu.pk, ORCID iD: https://orcid.org/0009-0005-9948-8898

Memoria Investigaciones en Ingeniería, núm. 29 (2025). pp. 109-130
https://doi.org/10.36561/ING.29.8
ISSN 2301-1092 • ISSN (en línea) 2301-1106 – Universidad de Montevideo, Uruguay
Este es un artículo de acceso abierto distribuido bajo los términos de una licencia de uso y distribución CC BY-NC 4.0. Para ver una copia de esta licencia visite http://creativecommons.org/licenses/by-nc/4.0/

Resumen. - *La salud ocupacional es un aspecto fundamental de la gestión de la fuerza laboral para garantizar un entorno de trabajo saludable y seguro, especialmente en entornos de producción donde los peligros que amenazan la vida son comunes. Este estudio implementa la Identificación de Peligros y la Evaluación de Riesgos (HIRA) dentro del taller de encolado y lapeado de una planta de fabricación de medidores de gas, y compara las condiciones preexistentes con las normas ISO 45001 (Salud y Seguridad Ocupacional), ISO 9001 (Gestión de Calidad) e ISO 14001 (Gestión Ambiental). Los peligros se identifican sistemáticamente mediante inspecciones en el lugar de trabajo, análisis de datos de incidentes y entrevistas y comentarios de los empleados. Los niveles de riesgo evaluados se convierten en matrices de riesgo estandarizadas y se sugieren medidas de control de acuerdo con las normas ISO para minimizar los niveles de riesgo. La estrategia de mitigación de riesgos se desarrolla con una jerarquía establecida de controles, enfatizando la eliminación, la sustitución y los controles de ingeniería antes de sugerir medidas administrativas y equipo de protección personal. Se evalúan parámetros como la temperatura, el ruido y la iluminación en el lugar de trabajo. Estos factores ambientales se comparan con los límites de exposición permisibles definidos por la norma ISO para garantizar el cumplimiento normativo y proteger el bienestar de los trabajadores. Los hallazgos generan recomendaciones prácticas para mejorar la seguridad laboral, la eficiencia operativa y la conformidad normativa del taller de encolado y lapeado de la planta de fabricación de medidores de gas. Al abordar estos desafíos, la investigación contribuye a prácticas industriales más seguras y sostenibles en la fabricación de medidores de gas. Los trabajos futuros en este campo deberían cooperar con la integración del Internet de las Cosas (IoT) y sensores para lograr la monitorización en tiempo real y controles basados en el IoT que integren la mecatrónica y el IoT con la seguridad sanitaria.*

Palabras clave: *Salud y seguridad ocupacional, HIRA, análisis de riesgos, ISO 14001, ISO 9001, ISO 45001, fabricación de medidores de gas, riesgos mecánicos, gestión de riesgos en el lugar de trabajo, jerarquía de control.*

Resumo. - *A saúde ocupacional é um aspecto fundamental da gestão da força de trabalho para garantir um ambiente de trabalho saudável e seguro, especialmente em ambientes de produção onde riscos de risco à vida são comuns. Este estudo implementa a Identificação de Perigos e Avaliação de Riscos (HIRA) em uma oficina de colagem e lapidação de uma fábrica de medidores de gás e compara as condições preexistentes com as normas ISO 45001 (Saúde e Segurança Ocupacional), ISO 9001 (Gestão da Qualidade) e ISO 14001 (Gestão Ambiental). Os perigos são sistematicamente identificados por inspeções no local de trabalho, análise de dados de incidentes e entrevistas e informações com funcionários. Os níveis de risco avaliados são transformados em matrizes de risco padronizadas e medidas de controle são sugeridas em conformidade com as normas ISO para minimizar os níveis de risco. A estratégia de mitigação de riscos é desenvolvida com uma hierarquia de controles estabelecida, enfatizando a eliminação, a substituição e os controles de engenharia antes que medidas administrativas e equipamentos de proteção individual sejam sugeridos. Parâmetros como temperatura, ruído e iluminação no local de trabalho são avaliados, e esses fatores ambientais são comparados com os limites de exposição permitidos definidos pela ISO para garantir a conformidade e salvaguardar o bem-estar dos trabalhadores. Os resultados produzem recomendações práticas que visam melhorar a segurança ocupacional, a eficiência operacional e a conformidade regulatória da oficina de colagem e lapidação da fábrica de medidores de gás. Ao abordar esses desafios, a pesquisa contribui para práticas industriais mais seguras e sustentáveis na fabricação de medidores de gás. Trabalhos futuros nesta área devem cooperar com a integração de IoT e sensores para alcançar monitoramento em tempo real e controles baseados em IoT, integrando Mecatrônica e IoT com a segurança da saúde.*

Palavras-chave: *Saúde e Segurança Ocupacional, HIRA, Análise de Riscos, ISO 14001, ISO 9001, ISO 45001, Fabricação de medidores de gás, Riscos Mecânicos, Gestão de Riscos no Local de Trabalho, Hierarquia de Controle.*

1. Introduction. - Workplace safety is a critical concern, where hazards hide in plain sight and pose significant risks to employees, work operations, and the environment. This project focuses on implementing HIRA in a meter manufacturing plant, aligning our work and findings with international standards such as ISO 45001 (Occupational Health and Safety Management), ISO 9001 (Quality Management), and ISO 14001 (Environmental Management).

Gas meters are manufactured in Seven processing shops Starting with Machining shop to gluing and lapping followed by paint shop, PPM shop and Assembly finally the meters are calibrated and tested in the calibration shop than sent to packaging. Manufacturing environments, particularly those involving precision engineering and assembly, pose various risks, including mechanical hazards, chemical exposure, electrical risks, and ergonomic concerns. Gas meters play a crucial and prominent role in ensuring safe and accurate gas distribution, maintaining a safe and efficient production facility ensure the quality of meter produced and the safety of workers who produce it. A high-risk environment of the gas meter manufacturing plant is the crucial sealing step of its manufacturing process, the gluing and lapping shop.

Manufacturing plants in Pakistan have many hazards, including but not limited to machinery-related injuries, exposure to toxic chemicals, electrical risks, ergonomic issues, fires and explosion, biological hazards like dust and poor sanitation. As well as Inadequate safety training, lack of proper protective equipment, and weak enforcement of regulations further increase risks and the risks potential danger. Poor ventilation, excessive noise, and repetitive tasks contribute to long-term health issues manifesting as chronic injuries and illnesses either immediately or after long years in workers, to maintain worker safety and operational efficiency It is necessary to address these risks by implementing of strict safety regulations, proper worker training, risk assessments analysis, and protective measures.

This study aims to identify potential hazards within the gluing and lapping shop of this plant, assessing their impact on workers and production processes, and propose strategies that are in line with industry practices and occupational health and safety regulations to maximize safety and production. The findings will help improve workplace safety, reduce the likelihood of accidents, and enhance overall operational efficiency.

A systematic process crucial for ensuring workplace safety, operational efficiency, and regulatory compliance is Hazard Identification and Risk Assessment (HIRA), particularly in high-risk industries like gas meter manufacturing [1]. Hazards such as chemical exposure and mechanical injuries are mostly common, making it an essential tool for proactive risk management [2]. The process involves identifying, assessing, and prioritizing hazards to implement targeted controls, thereby minimizing risks to employees, assets, and the environment [3]. For this instance, in gas meter manufacturing, mechanical hazards from presses and cutting machines, can be mitigated through engineering solutions and personal protective equipment (PPE) [4].

The application of HIRA in gas meter manufacturing is identical to other industries with high-risk, including foundries and power plants, proving to be highly productive [5]. Risks posed by flammable materials can be overcome by use of Chemical and fire safety measures, including proper ventilation and fire suppression systems [6]. Use of the hierarchy of controls comprises of substituting hazardous chemicals with safer alternatives [7], while mechanical injuries are minimized by drafting and adopting machine guarding procedures [8]. Environmental controls for airborne contaminants include dust extraction systems and waste management protocols that help adhere to environmental regulations [10].

It's incorporation with ISO standards—9001, 14001, and 45001—allows the developing of an enhanced safety and operational efficiency-based framework [11]. ISO 9001 encourages the enhancement of product reliability and process efficiency through risk-based thinking [12]. Meanwhile, ISO 14001 focuses on the negative aspects of the environment, such as harmful chemical spills or emissions, and works to reduce them [13]. In the same manner, ISO 45001 requires HIRA to be part of the system, thus ensuring active worker involvement and legal aspects of occupational safety and health [14]. Compliance with these standards allows gas meter producers to balance safety, quality, and environmental objectives, thereby facilitating compliance and strengthening resilience [15].

Various methodologies and tools including risk matrices for prioritizing hazards are available for gas meter manufacturing plants, based on severity and likelihood [16], process failures including leaks in meter calibration systems can be identified using Process Failure Modes and Effects Analysis (PFMEA [17]. Thermal and noise safety measures, such as Thermal Work Limit (TWL) indices for assessing heat stress and noise monitoring systems for protecting workers from permanent hearing loss which enhance workplace safety [18]. Lemmens et al. (2022) [12] came up with a risk matrix approach as a tool based on decision-making for checking probability and impact when preventive and diagnostic interventions are implemented. This Research aims for quantitative risk assessment methodologies, Karanikas et al. (2022) [13] examined ISO 45001:2018 [17] while identifying new features of systems in occupational health and safety management, which strengthened the structured approaches of earlier HIRA methodologies.

It's evolution alongside risk assessment methodologies demonstrates a gradual shift between qualitative hazard identification and structured, standardized approaches incorporating risk matrices and management frameworks. The integration of ISO standards and industry-based applications highlight the ongoing development of risk assessment strategies for improvising workplace safety and operational efficiency.[15][16][17]

Yousefinezhadi et al. (2015) conducted a systematic review examining how quality management systems particularly ISO 9001 and the EFQM (European Foundation for Quality Management) model [9] affect hospital performance. From a HIRA (Hazard Identification and Risk Assessment) perspective, the study shows that these structured frameworks help healthcare organizations systematically identify operational hazards, evaluate risks, and implement ongoing improvements. [9]

It studies within textile industries mark out factors such as noise, dust, heat, chemicals and unguarded machinery as extreme high priority hazards [21]. Qualitative data from interviews and focus groups most hazard identification was informal and reactive, and use of PPE has been limited with minimal training. The study by Hussain and T. Jamali in 2019 highlights vulnerability among workers especially young workers new to the industry and women in the field. They also identify specific hazards such as heat stress, fire risks, and mechanical injuries, and points to the absence of structured risk evaluations or preventive strategies. This study done in Pakistan highlights the emerging need for HIRA protocols within the countries growing industrial sector for it to develop and prosper. [21]

The study by Ho and Tenkate (2024) highlights significant challenges in the readability and suitability of Safety Data Sheets (SDSs) as hazard communication tools. Even after modifications to address comprehensibility, SDSs still fell short of being adequate. Key issues included dense technical jargon, inconsistency between sections, and a lack of clarity in hazard communication. These findings underscore the need for SDSs to be simplified and standardized to ensure they are accessible to workers with varying literacy levels, thereby improving workplace safety. [22]

Necessary HIRA for Workshops Environmental Features: Thermal risks in industrial settings effect both worker safety and productivity as well as morale. The Thermal Work Limit (TWL) and other heat stress indices help evaluate sustainable work rates in extreme heat. [3]

Thermal Work Limit (TWL) determines the maximum sustainable work rate by considering Dry Bulb Temperature (DBT), Wet Bulb Temperature (WBT), Globe Temperature (GT) and Atmospheric Pressure (AP). Unlike WBGT, TWL accounts for hydration, acclimatization, and skin area effect of clothing, making it a more precise heat stress predictor. [3]
TWL is widely used in mining, construction, and workshops for heat management and work-rest cycle planning. [4]
TWL in HIRA for Workshops is essential for workplace safety by:

- Identifying heat stress hazards. [3]
- Setting safe work-rest schedules. [3]
- Implementing engineering controls (ventilation, cooling stations). [3]
- Enforcing administrative controls (hydration programs, shift rotations).[3]

Lighting Safety in HIRA

Proper lighting is essential for workplace safety, Lighting safety in workshops is evaluated through:

- Illuminance (Lux) Calculations: Ensuring compliance with standards (e.g., 300–500 lux for general workshops, 750 lux for detailed tasks). [5]
- Light Distribution and Shadow Control: Optimizing uniformity to prevent vision-related hazards. [5]

Noise Safety in HIRA

- Excessive noise exposure can lead to hearing loss and decreased concentration. Noise safety assessments involve:
- Decibel (dB) Level Monitoring: OSHA recommends an exposure limit of 85 dB over an 8-hour shift. [7]
- Noise Dose Calculation: Evaluating cumulative exposure using Time-Weighted Average (TWA) measurements. [7]
- Engineering Controls: Implementing noise barriers, dampening materials, and silent machinery. [7]
- Personal Protective Equipment (PPE): Using earplugs or earmuffs for workers exposed to high noise levels. [3]

Based on the conducted literature review, it is evident that a significant research gap exists in the application of Hazard Identification and Risk Assessment (HIRA) within gas meter manufacturing plants. Although HIRA methodologies have been widely utilized across various industrial sectors including chemical, petroleum, and general manufacturing, there is a notable absence of focused studies that address the distinct risks and operational hazards inherent to gas meter production. This gap underscores the need for a specialized analysis that accounts for the specific materials, processes, and safety challenges unique to this sector. The present study seeks to address this gap by performing a comprehensive HIRA tailored to the gas meter manufacturing's gluing and lapping shop. By systematically identifying hazards and evaluating associated risks, this research aims to offer practical recommendations for improving workplace safety, mitigating operational risks, and contributing valuable insights to the broader field of industrial risk management.

2. Research Methodology. - Here is the outline of the systematic approach applied for this research to identify hazard, identify risks, and propose control measures for the gas meter manufacturing plant in alignment with ISO Standards. The process is divided into the following parts:

- Hazard Identification
- Risk Assessment
- Risk Evaluation
- Recommendation of Control Measures
- Compliance with ISO Standards

Each stage is executed systematically across the gluing and lapping of the meter manufacturing plant and utmost importance, and focus is implemented in ensuring that the process is in alignment with the principles of ISO standards.

2.1 Hazard Identification. - The first step involves identifying potential hazards in various departments. This step combines observational and analytical techniques and information from relevant research articles. The following methods are employed:

- Site Surveys and Inspections
- Analysis of Historical Data
- Employee Interviews and Feedback

2.1.1 Risk Assessment. - After identifying hazards, risks associated with each hazard are quantified using various approach including the risk matrix method.

2.1.2 Risk Evaluation. - Risk evaluation is the process of analyzing and prioritizing potential hazards based on their likelihood of occurrence and the severity of their consequences. This systematic approach helps in determining the level of risk associated with various activities and guides decision-making to mitigate or eliminate hazards effectively. It is an essential step in ensuring workplace safety and compliance with standards like ISO 45001. [1] [19]

Risk Priority	Definitions of Priority
High	Situation is considered critical; stop work immediately or consider cessation of this operation/task.
Medium	Must be fixed as soon as possible; Zonal HSE team leader should take immediate action.
Low	Very important—must be fixed within two weeks. Zonal HSE team leader considers short-term and/or long-term actions. Can also be addressed via scheduled maintenance. If a quick/easy fix exists, resolve immediately. Otherwise, manage through routine procedures.

Table I. Risk Priority Table defining urgency levels (High/Medium/Low) for hazard mitigation, with corresponding response protocols for HSE teams.

2.1.3 Recommendation of Control Measures & their compliance with ISO Standards. - On the basis of previous evaluation, certain control measures are suggested in order to curtail the maximum hazard that is possible in the workplace. These controls are suggested based on the hierarchy of controls. [4]
After deducing the controls, their acquiescence is validated with previously stated ISO standards and the discrepancies are removed.

2.2 Calculations and comparison of measured and calculated Environmental parameters with standards. -
2.2.1 Noise. - The methodology involves calculating the combined noise levels of machines using logarithmic addition based on decibel differences. Identical machines are combined first, and incremental contributions from other machines are determined using values from a reference table (Table 2) for specific dB differences. [3]

Difference between two decibel levels to be added (dB)	Amount to be added to larger level to obtain decibel sum (dB)
0	3.0
1	2.6
2	2.1
3	1.8
4	1.4
5	1.2
6	1.0
7	0.8
8	0.6
9	0.5
10	0.4
11	0.3
12	0.2

Table II. Decibel summation reference chart showing correction values to add when combining two noise levels of differing intensities.

2.2.2 Lighting. - Lighting levels are assessed in accordance with ISO 8995-1:2002, which provides illumination standards for workplaces. Measurements are taken using a lux meter, and results are compared with ISO-recommended values.

Work Area	**Recommended Illuminance (lux)**
General Offices	300-500
Precision Assembly	1000-2000
Industrial Workspaces	300-750
Warehouse Areas	100-300
Laboratories	500-1000
Control Rooms	150-300

Table III. Recommend Lighting Levels (lux) for different areas according to ISO standards.

Proper lighting is essential for reducing eye strain, improving accuracy, and enhancing overall workplace safety. If measured values are below ISO standards, corrective actions such as additional lighting fixtures, LED upgrades, or task lighting adjustments are recommended.

2.2.3 Wet Bulb Globe Temperature (WBGT), Humidex and Thermal Work Limit (TWL). - Humidex is a measure used to describe how hot the weather feels to the average person, taking into account both temperature and humidity. It is primarily used to understand how heat and moisture together affect human comfort and health. Humidex here is calculated through the formula

$$HX = \mathrm{Ta} + \frac{5}{9}(\rho - 10) \quad [18]$$

$$\rho = 6.11 * e^{\frac{5417.753}{\frac{1}{237.16} - \left(\frac{1}{Td}\right)}} \quad [18]$$

$$T_{dew} = T - \frac{(100 - RH)}{5} \quad [18]$$

Where;
air temperature Ta (C); T_d is dew point temperature (K); Wet-bulb temperature (T_x); Globe thermometer temperature (T_s); ρ is vapors pressure of water (in hPa); specific humidity q; surface air pressure Ps (Pa); HX is Humidex; WBGT is Wet Bulb Globe Temperature.

WBGT takes a more comprehensive approach, incorporating several factors like air temperature, humidity, wind speed, and radiant heat from the sun or other sources.

$$\mathrm{WBGT} = 0.7 \times T_x + 0.3 \times T_s \quad [4]$$

Where;
Wet-bulb temperature (T_x); Globe thermometer temperature (T_s); Thermal Work limit (TWL).

The TWL (Thermal Work Limit) is another critical index used to evaluate the safety of working conditions in heat, particularly in hot and humid environments

$$TWL = 410.33 - 6.97T - 0.95RH \quad [20]$$

Where;
Air temperature (T); Relative Humidity (RH).

a. Material Chemical property and Safety Analysis

2.2.4 Material data and safety data sheet. - Safety data sheets (SDSs) are hazard communication materials that accompany chemicals/Hazardous products in the workplace. Many SDSs contain dense, technical text, which places

considerable comprehension demands on workers, especially those with lower literacy skills, such as technicians and line workers. Thus, there is a need for simplified and to-the-point data represented in an organized manner to help facilitate workers and make it easier to highlight chemical hazards and harmful actions emerges.

2.2.5 Analyzing chemical work protocol. - The following chemical compound check sheet is designed to act a s a structured to standardize and ensure safe handling, storage, and exposure control for various chemicals used in the workplace. It outlines essential information such as the specific storage requirements, permissible exposure duration, required personal protective equipment (PPE), and recommended handling protocols for each chemical. Additionally, it indicates the current level of training or awareness provided to personnel as well as recommended level.

Chemical	Storage	Exposure Time	Assigned PPE	Handling Protocol	Training / Awareness	Recommended level of Training

Table IV. Chemical compound check sheet example.

2.2.6 Safety analysis. - The chemical compound check Sheet shown above will serve as our fundamental tool for various safety analysis related to all chemicals encountered or worked with in any manufacturing industry. This acts as a support to our Hazard Identification and Risk Assessment (HIRA) by allowing us to quantize and categorize the risk and hazard associated with workplace chemicals, whilst considering factors like exposure duration, storage conditions, and required PPE. A PPE Gap Analysis can also be performed by comparing the listed PPE with what's in actual use, identifying mismatches or deficiencies in protection. The sheet's "Training/Awareness" column highlights areas lacking proper instruction, allowing for a Training Needs Analysis to plan targeted safety sessions. Furthermore, it can be utilized during compliance audits and safety inspections to verify that chemicals are stored correctly, labeled accurately, and handled according to safety protocols, ensuring compliance with standards such as ISO 45001.

2.4 Implementation of Control Measures. - Hierarchy of Risk Control should use when assessing the adequacy of existing controls and introducing new controls. The health and safety management system ISO 45001 states that the organization shall establish a process for achieving risk reduction based upon the following hierarchy. [17]

2.4.1 Elimination. - The first way to control an issue or hazard is to eliminate it. This can be achieved by changing design and physically solving the issue of hazard. Elimination is the most effective way to control hazards. For example, replacing sharp-edged tools with ergonomically designed alternatives to prevent cuts or hand injuries, replacing a solvent containing volatile organic compounds (VOCs) with water-based solutions to prevent inhalation risks and fire hazards, installing electric motors instead of diesel engines to reduce workplace noise exposure, and minimizing hearing damage risks. [17]

2.4.2 Substitution. - Substitution is the process of replacing hazardous materials or practices with safer alternatives. This is often applied in industries that handle toxic chemicals, dangerous equipment, or high-risk procedures. When implementing substitution, it is essential to evaluate the substitute thoroughly to ensure that it does not create new hazards, such as untested chemical reactions or other environmental concerns. For example, in a painting process, substituting solvent-based paints with water-based alternatives reduces workers' exposure to volatile organic compounds (VOCs), which can cause respiratory issues. Similarly, in manufacturing, replacing carcinogens like asbestos with synthetic, non-hazardous fibers significantly reduces long-term health risks. Substitution can also involve switching from manual handling to automated systems to minimize ergonomic risks. [17]

2.4.3 Engineering Controls. - Engineering controls aim to redesign or modify equipment or processes to remove hazards at the source or reduce the likelihood of exposure. This process is more commonly carried out in industries with the help of new technologies; especially the use of IOT bases systems for monitoring and controlling. [17]

2.4.4 Administrative Controls. - Administrative controls involve altering how work is performed to reduce risks. These measures include establishing safety policies, enforcing regular maintenance schedules, and training workers to recognize hazards. [15]

2.4.5 Personal Protective Equipment. - PPE is considered a last-resort control measure when other methods cannot fully mitigate risks. It includes items such as gloves, helmets, goggles, and respirators designed to protect individuals from specific hazards. [15] [16] [17]

3. Results. - Prior to identify hazard potential in gas meter manufacturing plant gluing and lapping production process, the manufacturing processes should be known first. The plant produces 2 major Models. Model A is made for lower altitude and higher temperature climates for cities such as Karachi. Model is made for the Sindh province of Pakistan. Model B is designed for Higher altitude climates and lower temperatures. They both serve the same purpose to measure gas flow rate and have some differences in the design, but our focus is the processes that are present for their manufacturing.

Below is a birds eye view Schematic of the Shop in review

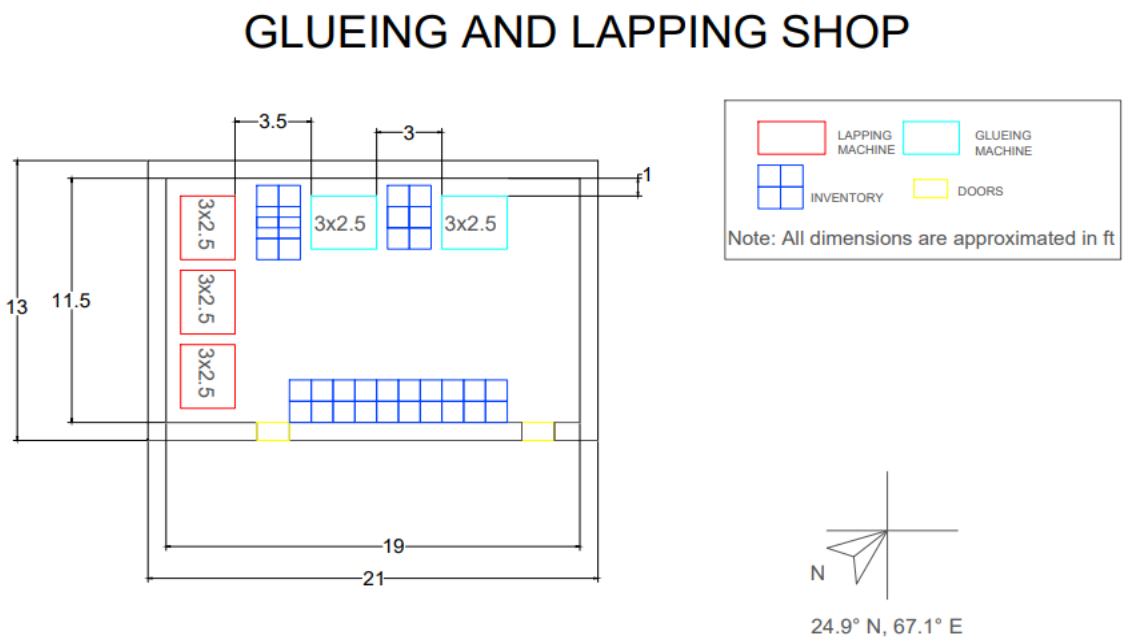

Figure I. Gluing Shop top-down view schematic drawing.

The processes and work operations occurring in the gas meter manufacturing plant's gluing and lapping are:
1. Adhesive Application – Application of adhesive at designated points on to the main body of the meter using pneumatic dispensers to ensure uniform bonding on the sealing areas between metal body and plastic jig panel.
2. Gluing and Curing – Components are placed in dedicated jigs within 10 high stacks on pallets, after adhesive application to maintain alignment and ensure proper bonding during curing. Curing time varies from 4 to 8 hours depending on temperature and weather.
3. Lapping Operation – Lapping of critical sealing surfaces using Lap Master machines with abrasive compounds (black sic) to achieve required flatness and surface finish to ensure plastic plates lay flat on the metal body.
4.Stacking and Handling – Finished parts are stacked in trolleys or crates with proper spacing and tagging to prevent damage and ensure batch traceability and shipped forward to next section.
After thoroughly analyzing the production process, a comprehensive Hazard Identification and Risk Assessment (HIRA) was conducted to systematically identify potential hazards, evaluate associated risks, and determine appropriate

control measures. Before proceeding with risk ranking, it is essential to establish clear criteria to accurately assess the seriousness of identified hazards and their associated risk levels, it is necessary to formulate criterion of seriousness or risk ranking degree. Likelihood (L) is the possibility of accidents occurrence (Table 4). Severity or Consequences (C) is the seriousness of the injury and working days loss (Table V).

Likelihood Criterion: Likelihood is the probability or possibility of an accident or hazardous event occurring. It is categorized into five levels as follows: [1] [19]

Level	Criteria	Qualitative Description	Semi-Qualitative Description
1	Rarely Occurred	Can be considered, but not only in extreme state	Less than once in ten years
2	Small Possibility	Not yet happened, but usually occurred at a time	Once-in-ten-year occurrence
3	Possible	Should have happened, and maybe have happened elsewhere	One in five years or once a year
4	Great Possibility	Can easily happen, may appear in the most common state	More than once in a year or month
5	Almost Definitely	Frequently happens and is expected in the most common state	More than once in a month

Table V. Likelihood Criterion – Classifying accident or event probabilities from 'Rarely Occurred' to 'Almost Definitely' with qualitative and semi-quantitative descriptors

Consequence Severity Criterion: Severity refers to the seriousness of potential injury, health effects, or property damage resulting from a hazardous event. It is categorized into five levels as follows (Table VI): [1] [19]

Level	Criteria	Qualitative Description	Semi-Qualitative Description
1	Not Significant	Does not cause any damage or injury to humans	No working days lost
2	Small	Causes minor injury, small losses, but does not affect work continuity	Can still work on the same day/shift
3	Moderate	Results in severe injury requiring hospitalization, no permanent disability but financial loss	Losing less than three working days
4	Great	Causes severe injuries and permanent disability, leads to significant financial losses affecting business continuity	Losing three or more working days
5	Disaster	Results in deaths and severe losses, leading to permanent business stoppage	Losing working days forever

Table VI. Consequence Severity Criteria Matrix – Classifying incident impacts from 'Not Significant' to 'Catastrophic' with qualitative and semi-quantitative descriptors

Risk Rating Classification Criterion: This Risk Rating Classification Criterion (Table VII) provides a structured framework for prioritizing workplace hazards based on their calculated Risk Priority Number (RPN). By categorizing

risks into four severity levels—Low (1–4), Medium (5–9), High (10–15), and Critical (16–25), it aligns quantitative risk assessments with actionable mitigation strategies. [1] [19]

Risk Rating (R)	Risk Level	Description
1 – 4	Low	Acceptable risk. No immediate action required.
5 – 9	Medium	Moderate risk. Requires planned action to mitigate.
10 – 15	High	Significant risk. Requires immediate action to mitigate.
16 – 25	Critical	Unacceptable risk. Requires urgent intervention to eliminate or control hazards.

Table VII. Risk Rating Classification Criterion – Categorizing risk levels (Low to Critical) based on calculated RPN scores with corresponding mitigation requirements.

3.1 Hazard Identification and Risk Assessment (HIRA) Table. -

Hazard Identification				Risk Evaluation
	Work activity	Hazard	Possible Accident	Existing Risk Control
1	Stacking of meters	Loose Inventory/Stack	Slipping or falling, leading to fractures, sprains, or head injuries	Fixed number of crates
2	Movement within Pathways	No pathway designated	Collisions, severe injuries	No physical markings on floor.
3	General Housekeeping	Trash Heap in Corner	Fire risk, pest infestation, slips/trips	Occasional cleanups
4	Working with Electrical Systems	Bare Wirings	Electrical shock, electrocution, sparks, fire hazards	Protective covers (Inadequate as wires are still bare),
5	Accessing Heights for Stacking	Use of unstable or inappropriate platforms (like crates) for elevation	Falls from height causing serious injury	No existing control

Table VIII. Hazard Identification and Risk Assessment (HIRA) table outlining workplace hazards, potential accidents, and existing control measures for various operational activities.

3.1.1 Risk Priority Number (RPN) Calculations. -

Hazard Identification			Risk Evaluation		
	Work activity	Hazard	Severity	Likelihood	RPN
1	Stacking of meters	Loose Inventory/Stack	3	4	12
2	Movement within Pathways	No pathway designated	3	3	9

3	General Housekeeping	Trash Heap in Corner	4	3	12
4	Working with Electrical Systems	Bare Wirings	4	3	12
5	Accessing Heights for Stacking	Use of unstable or inappropriate platforms (like crates) for elevation	4	4	16

Table IX. Risk Priority Number (RPN) calculations for identified workplace hazards, evaluating severity and likelihood to prioritize risk mitigation.

3.1.2 Risk Ranking Matrix. - The risk prioritization matrix offers a structured visualization of identified hazards by categorizing them based on their likelihood of occurrence and the severity of their impact, as determined through the preceding HIRA (Hazard Identification and Risk Assessment) analysis. This matrix supports a systematic approach to risk ranking, enabling focused and effective mitigation efforts aligned with the assessed risk levels according to calculated RPN in table 8 and classified according to Table 6 Risk Rating Classification Criterion.

Risk Ranking Matrix		**Very Likely**	**Likely**	**Possibly**	**Unlikely**	**Highly unlikely**
		5	**4**	**3**	**2**	**1**
Catastrophic	**5**					
Significant	**4**		Accessing Heights for Stacking	General Housekeeping, Working with Electrical Systems		
Harmful	**3**		Stacking of meters	Movement within Pathways		
Minor	**2**					
Negligible	**1**					

Figure II. Risk Ranking Matrix evaluating workplace hazards by likelihood and severity, highlighting critical risks like passage blockage and moving part contact.

3.1.3 Additional Control Suggestions and Improved Risk Priority Number (RPN) score. -

Hazard Identification			**Risk Control**				
Work activity		Hazard	Additional Controls	Hierarchy of controls	Severity	Likelihood	RPN*
1	Stacking of meters	Loose Inventory/ Stack	Restrict stack height Conduct daily checks. Set maximum load signs Conduct stacking training	Engineering controls, Administrative Controls	2	2	4

2	Movement within Pathways	No pathway designated Tripping Hazard	Clear Floor markings. Provide movement safety training.	Engineering controls, Administrative Controls.	2	1	2
3	General Housekeeping	Trash Heap in Corner Flammable	Regular and schedule cleanups Fireproof bins. Spot checks, assigned disposal duties.	Engineering controls, Administrative Controls.	2	2	4
4	Working with Electrical Systems	Bare Wirings – Electrical Fire	Protective enclosures/conduits for all bare wires. Lockout/Tagout procedures for electrical work. Audit wiring layout regularly Restrict access to electrical areas.	Engineering controls, Administrative Controls	1	2	2
5	Accessing Heights for Stacking	Use of unstable or inappropriate platforms (like crates) for elevation - Fall Hazard	Stop using crates as steps. Use step stools or ladders. Place items within reach or use adjustable platforms. Train on safe reaching and lifting.	Engineering controls, Administrative Controls.	2	2	4

Table X. Recalculated Risk Priority Number (RPN) calculations for identified workplace hazards, evaluating severity and likelihood to prioritize risk mitigation after the implementation of suggested controls.

3.1.4 Risk Action Priority Matrix. - The Risk Action Priority matrix is a structured analytical tool used to determine and visualize the urgency and sequence of risk control measures implementation. The systematic ranking of identified hazards based on criterions such as severity, likelihood, and exposure time allows this matrix to categorizes risks into action tiers, from immediate action to scheduling controls in the near future or setting up routine monitoring. It is designed with recognized safety standards in mind, including ISO 12100 (Safety of Machinery), ensuring adherence to the hierarchy of risk controls.

Color Key for Risk Action Priority Matrix (Figure 3)

Risk Action Priority Matrix	Very Likely	Likely	Unlikely	Very Unlikely
Catastrophic	Bare Wirings Electrical Fire	Trash Heap in Corner - Flammable		
Significant	Loose Inventory/Stack	Heat Stress Summer	Heat Stress Winter	
Harmful	Accessing Heights for Stacking – Fall Hazard	No Pathway Designated – Tripping Hazard		INSUFFICIENT LIGHTING

Figure III. Risk Action Priority Matrix – Mapping workplace hazards by severity and probability to guide mitigation efforts, with drilling operations and passage blockage flagged as highest priority.

Hazard Level	Action
	No need to act immediately, but keep inspecting
	Perform reparation/control maintenance in the next one year.
	Take action in the next three months.
	Take reparation/ control maintenance action within one month ahead.
	Take action immediately/Emergency protocol - possible use restriction.

Figure IV. Hazard Response Timeline Guide – Color-coded action priorities from emergency protocols (immediate) to routine monitoring (no urgent action).

3.2 Environmental Conditions Analysis. - Noise, light intensity, temperature, and humidity were measured using dedicated mobile applications that leverage the smartphone's built-in sensors. The details are as follows:

- Noise Measurement: Conducted using a Noise Meter app - Sound meter developed by Smart Tools Co, utilizing a MEMS (Micro-Electro-Mechanical Systems) microphone to capture sound pressure levels in decibels (dB).
- Light Intensity Measurement: Conducted using a Lux Meter app – Illuminance - light luxmeter. Developed by Phuongpn, relying on a photodiode-based ambient light sensor to measure illumination levels in lux (lx).
- Temperature and Humidity Measurement: Conducted using a climate monitoring app - Room temperature Thermometer Dev by Master Texhnologis, using a combination of capacitive humidity sensors and silicon bandgap temperature sensors for ambient readings.

To ensure accuracy, reliability and repeatability, all sensors were calibrated against known reference values, and multiple readings were taken at different times over an extended period. This approach enabled a more consistent and representative dataset for calculating environmental indices

3.2.1 Noise Level Comparison. - A comparison between the measured noise level within the work area and the permissible limit established by ISO 45001 can be seen in the following bar graph
standards. The recorded noise level in the facility is approximately 79 dB, which is in the range of the ISO 45001 prescribed limit of 85 dB.

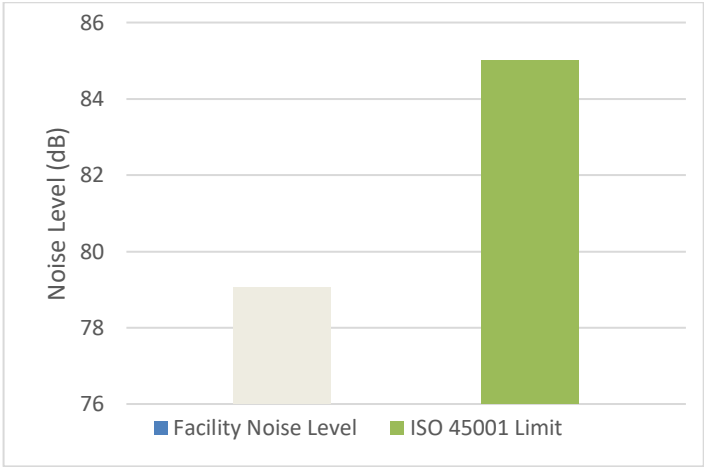

Figure V. Facility noise level (dB) assessment compared to ISO 45001 occupational exposure limits, highlighting compliance gaps.

This deviation is non-compliant with occupational health and safety guidelines, suggesting that workers are exposed to potentially harmful noise levels. Prolonged exposure to these conditions will lead to hearing damage, putting an emphasizing on the need for immediate intervention.

3.2.2 Light Level Comparison. - The bar graph is based on the comparison between the measured light level in the facility and the recommended standard according to ISO guidelines. The measured illumination within the area is

approximately 150 lux, which is significantly below the ISO workshop standard of 300 lux. This indicates inadequate lighting conditions in the current workspace, which can negatively impact workers' visibility, productivity, and safety. Insufficient lighting can lead to eye strain, increased error rates, and a higher risk of accidents.

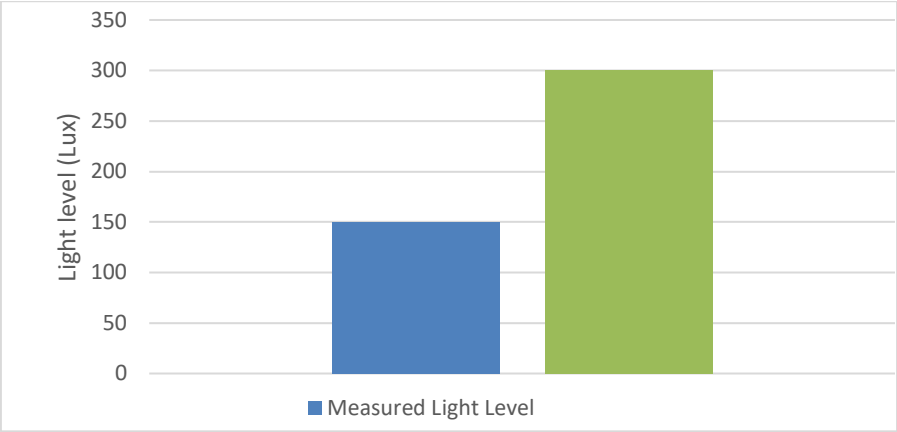

Figure VI. Workspace illumination analysis comparing measured light levels against OSHA/NIOSH recommended standards for workshop safety.

3.2.3 Heat Stress Level Comparison. - The following bar graph depicts the Calculated Thermal Work Limit (TWL), which is a real-time or site-specific measurement of the risk of heat stress, against the ISO Standard TWL. Showing close alignment between the two, though the calculated value is slightly higher. This indicates that the working environment is safe.

The next set of bar graphs compare WBGT and humidex with their ISO standard values. These supportive metrics underline the need for bolt various barometric stresses along in conjunction with the above evaluation.

These indicators hot stress measured standards at these values may be alluded to records, that the surrounding conditions verged on or approach the internationally accepted thresholds within minimum safety standards when it comes to thermal exposure. The compliance support lifts exact guidelines prove the dependability of the measurements

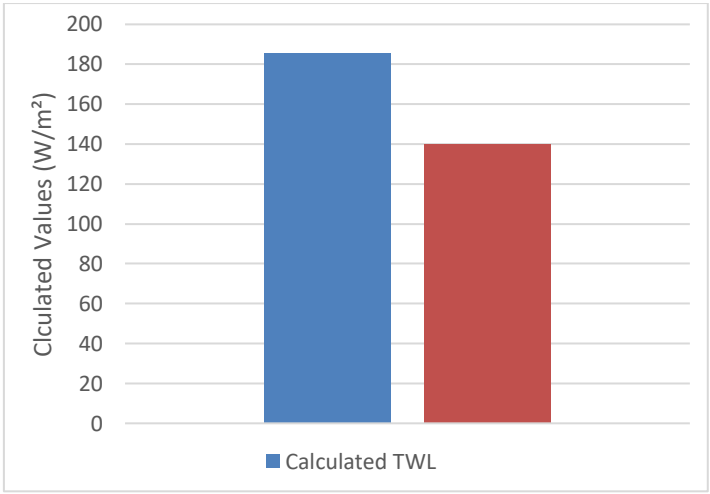

Figure VII. Thermal Work Limit (TWL) assessment showing measured heat stress risk (0.07 kW) against ISO safety thresholds for industrial environments.

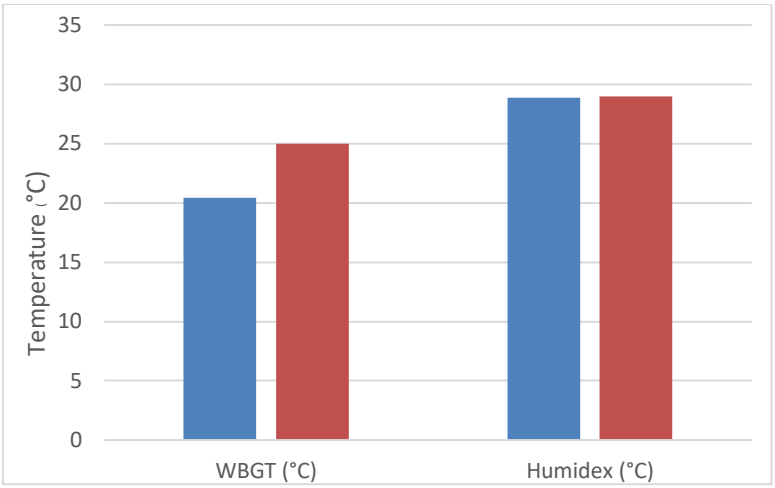

Figure VIII. Heat stress exposure analysis comparing measured Wet Bulb Globe Temperature (WBGT) and Humidex values against ISO safety thresholds.

3.3 Material and chemical safety analysis. - The following table highlights all current data and protocols in

Chemical Compound Check Sheet					
Chemical	Storage	Expose time	Assigned PPE	Handling Protocol	Training/Awareness
Silica flex 221	Store in a dry place at room temperature; avoid moisture. Keep containers sealed.	8 hours (avoid prolonged dust inhalation)	Gloves	Minimize skin contact	None
Black Sic	dry, cool place; keep away from oxidizing agents	8 hours (limit dust exposure)	Gloves	Minimize skin contact	None

Table XI. Basic information extracted from MSDS for the mentioned chemicals used in the workplace.

3.4 Safety protocols updates and recommendations. - In-depth analysis of SDS allow for following new improved protocols to be suggested. We have updated the Chemical Component Check Sheet to align with SDS hazard data by adding required PPE (respirators, eye protection), enhancing handling protocols (ventilation, wet methods), and mandating hazard-specific training, ensuring compliance with safety standards like ISO 45001

Chemical Compound Check Sheet					
Chemical	Storage	Expose time	Assigned PPE	Handling Protocol	Training/Awareness
Silica flex 221	Store in a dry place at room temperature; avoid moisture. Keep containers sealed.	8 hours (avoid prolonged dust inhalation). Risk: Respiratory irritation	- Nitrile gloves - NIOSH-certified N95 respirator - Safety goggles	- Use local exhaust ventilation - Avoid dust generation - Wash hands after handling	Mandatory training: - Dust control measures - Proper PPE use - Emergency procedures
Black Sic	dry, cool place; keep away from oxidizing agents	8 hours (limit dust exposure). Risk: Carcinogen (H350)	- Nitrile gloves - NIOSH-certified respirator (P100 for dust/fibers)	- Handle in fume hood/ventilated area - No dry sweeping (use wet methods) - Static charge precautions	Mandatory training: - Carcinogen hazards - Spill response

			- Lab coat + eye protection		- Medical surveillance requirements

Table XII. updated information for previously extracted data taken from MSDS for the mentioned chemicals used in the workplace.

4. Improvement Proposals and Result Discussions. - Based on the expected goals which fit the data and its processing results presented, conclusions are made as follows;

1. The skin contact of the worker with the coolant needs to be monitored, and the risk level should be mitigated by use of either substitution with lesser toxic and work-efficient coolant or by use of adequate PPEs.
2. Automated sensors must be introduced or the use of and, or gates-based technological devices that help optimize the present machinery and reduce chances of contact with moving parts during operation. This applies to all drilling machines and rotating machines within the shop.
3. Reinforcement of worker training programs. Along with periodic safety audits and continuous monitoring of key environmental parameters, such as noise and ventilation, for maintaining a safe and compliant work environment.
4. The Light intensity levels in the workplace needs to be improved in order to match the ISO standard of 300 Lx by use of energy energy-efficient LED-based lighting system in order to counter visibility issues.
5. Continuous monitoring of temperature and humidity levels along with proper inspection of ventilation equipment during various times and seasons throughout the year, to eradicate the effects of humidity and high temperatures that are measured through the previously calculated parameters.
6. The integration of ISO 45001, ISO 14001, and ISO 9001 standards contributed to a structured approach to occupational safety, environmental management, and quality control. Compliance with these standards ensured a systematic risk management process, improving worker safety, reducing environmental impact, and enhancing overall operational efficiency.
7. An efficient workplace management system needs to be developed and reinstated in order to facilitate the flux of raw material and finished products, which would otherwise lead to the blocking of passages serving as an obstacle to movement and would in turn increase safety risks for the workers.
8. Providing Personal Protective Equipment to the workers, which aligns with D. P. Restuputri and M. Fakhri (2015), namely:
    - Ear Plugs/Muffs to reduce the effect of harmful noise.
    - Respirators or Dust Masks that protect the lungs from harmful dust, fumes, and vapors generated by processes like grinding, cutting, and welding.
    - Safety Goggles for avoiding contact with chips and other small flying metal pieces from shop operations.
    - Safety Gloves that reduce damage in case of contact with rotating parts and reduce skin contact time with coolant.
    - Safety Shoes (Steel-Toed Boots) that reduce damage from falling objects such as gas meters stacked in piles and other tools being used.
    - Specialized Work clothing's (Coveralls, Aprons) such as fire-resistant coveralls or aprons, protects the body from hot surfaces, sparks, and chemicals while preventing loose clothing from getting caught in machinery.
    - Hair Protection (Hairnets or Caps) that prevent hair from getting caught in machines.

5. Conclusions. - The results suggest the importance of HIRA, HSE, and environmental conditions analysis, these are integral to a safe working environment.

Despite all of these findings and suggestions to maintain HSE standards it is implicative that HIRA is conducted on a regular basis and older findings are updated with more newer data especially for the section environmental conditions

analysis as environmental conditions are changing at a considerable pace across the world due to global warming and extreme temperature shifts have been seen in the last decade.

Future work should focus on integrating advanced technologies like Internet of Things (IoT) and Artificial Intelligence (AI) based monitoring systems for real-time hazard detection, developing industry specific risk models, and creating adaptive HIRA frameworks. Emphasis should also be placed on incorporating human factors, supporting lifecycle based environmental assessments, and aligning practices with international safety and environmental standards.

Conflict of interest. - There are no significant competing financial, professional, or personal interests that might have affected the performance.

Acknowledgment. - The researchers acknowledge all people who participated in this study for their efforts. We gratefully acknowledge the developers of the mobile applications used in this study for their role in ensuring reliable environmental data collection. The Noise Meter app by Smart Tools Co., the Lux Meter app by Phuongpn, and the Room Temperature Thermometer app by Master Technologies provided accurate and consistent measurements of noise, light, temperature, and humidity. These tools were essential to our calibrated data gathering and greatly enhanced the validity of our analysis. The research team acknowledge the support provided by ChatGPT by OpenAI for the formulations and enhancement for literature review and research abstracts and its significant role in enhancing the linguistic quality of our work.

Glossary:

- ISO: International Organization for Standardization for risk and safety standards.
- HIRA: Hazard Identification and Risk Assessment – a process for potential hazards and evaluate risks.
- IRA: Individual Risk Assessment – focused on risks to individual personnel.
- Humidity: Refers to the environmental moisture level, a factor in thermal stress.
- Noise: Environmental hazard affecting hearing and concentration.
- Severity: Refers to the extent of potential harm from a hazard.
- Likelihood: Probability of occurrence of a hazard.
- Identification: The Process of recognizing potential hazards.
- Risk: The combination of the probability of an event and its consequences.
- Hazard: A source or situation with the potential to cause harm.
- Artificial Intelligence (AI): a pattern based on human intelligence process followed by machines, especially computer systems for tasks such as decision-making, pattern recognition, and automation.
- Information Technology (IT): study or use of computers, networks, and other electronic systems for storing and processing information.
- TWL: The sustainable metabolic rate under specific environmental conditions for a human body.
- WBGT: estimates the effect of temperature, humidity, wind speed, and solar radiation.
- PPE: Personal Protective Equipment Gear designed to be worn to minimize exposure to hazards or the damage caused by them.
- M3 Tapping Machine: Tapping machine that creates 3mm diameter internal threads via tapping tool into predrilled holes.
- M13 Tapping Machine: Tapping machine that creates 13mm diameter internal threads via tapping tool into predrilled holes.
- M5 Tapping Machine: Tapping machine that creates 5mm diameter internal threads via tapping tool into predrilled holes.

List of Symbols:

- TWL: Thermal Work Limit (W/m²)
- WBGT: Wet Bulb Globe Temperature (°C)
- GT: Globe Temperature – Part of WBGT calculation.
- Ta: air temperature(C)
- Td Is dew point temperature (K)
- T_x:Wet-bulb temperature
- T_s: Globe thermometer temperature
- ρ: Vapour pressure of water (in hPa)
- q꞉specific humidity
- Ps꞉surface air pressure (Pa)
- HX : Humidex
- WBGT: Is Wet Bulb Globe Temperature
- Q: Heat dissipation rate
- SA : Skin area
- ΔT : temperature gradient
- T: Air temperature
- RH: Relative Humidity

References

[1] D. P. Restuputri and M. Fakhri, "The analysis of health and safety aspects by using hazard identification and risk assessment (HIRA) method," in Proc. 8th Int. Seminar Ind. Eng. Manage., 2015, pp. ER-37–ER-43.

[2] S. Choudhary and V. Shukla, "Analysis of risk and occupational hazards in foundry," Int. J. Sci. Res. Eng. Trends, vol. 4, no. 4, pp. 628–631, 2018.

[3] V. S. Miller and G. P. Bates, "The thermal work limit is a simple, reliable heat index for the protection of workers in thermally stressful environments," Ann. Occup. Hyg., 2007.

[4] Y. Epstein and D. S. Moran, "Thermal comfort and the heat stress indices," Ind. Health, vol. 44, 2006.

[5] I. Q. Al Saffar and A. W. Ezzat, "Qualitative risk assessment of combined cycle power plant using hazards identification technique," Dept. Mech. Eng., Univ. Baghdad, Iraq, 2020.

[6] M. Lukić, M. Peceľ, B. Protić, and D. Filipović, "An evaluation of summer discomfort in Niš (Serbia) using Humidex," in Proc. Int. Conf. Climate Studies.

[7] N. Shah, "Assessment of the workplace conditions and health and safety situation in chemical and textile industries of Pakistan," Sci. J. Public Health, vol. 3, no. 6, p. 857, 2015, doi: 10.11648/j.sjph.20150306.20.

[8] V. S. Miller and G. P. Bates, "The thermal work limit is a simple reliable heat index for the protection of workers in thermally stressful environments," School of Public Health, Curtin Univ. Technol., Western Australia, 2007.

[9] T. Yousefinezhadi, E. Mohamadi, H. Safari Palangi, and A. Akbari Sari, "The effect of ISO 9001 and the EFQM model on improving hospital performance: A systematic review," Iran Red Crescent Med. J., vol. 17, no. 12, Dec. 2015, doi: 10.5812/ircmj.23010.

[10] K. H. Sherwani, A. Demir, and L. Maroof, "Way to achieve sustainable benefits of ISO 9001 practices," Int. J. Qual. Rel. Manage., Sep. 2024, doi: 10.1108/IJQRM-01-2023-0023.

[11] M. A. Shaikh, S. Weiguo, M. U. Shahid, H. Ayaz, and M. Ali, "An assessment of hazards and occupational health & safety practices for workers in the textile industry: A case study," Int. J. Acad. Res. Bus. Soc. Sci., vol. 8, no. 10, pp. 817–829, 2018.

[12] S. M. P. Lemmens, V. A. Lopes Van Balen, Y. C. M. Röselaers, H. C. J. Scheepers, and M. E. A. Spaanderman, "The risk matrix approach: A helpful tool weighing probability and impact when deciding on preventive and diagnostic interventions," BMC Health Serv. Res., vol. 22, no. 1, p. 218, Dec. 2022, doi: 10.1186/s12913-022-07484-7.

[13] N. Karanikas, D. Weber, K. Bruschi, and S. Brown, "Identification of systems thinking aspects in ISO 45001:2018 on occupational health & safety management," Saf. Sci., vol. 148, p. 105671, Apr. 2022, doi: 10.1016/j.ssci.2022.105671.

[14] A. C. Ahmad, I. N. Mohd Zin, M. K. Othman, and N. H. Muhamad, "Hazard identification, risk assessment and risk control (HIRARC) accidents at power plant," MATEC Web Conf., vol. 66, p. 00105, 2016, doi: 10.1051/matecconf/20166600105.

[15] ISO, ISO 9001: Quality management systems – Requirements. Int. Org. Standardization, 2015.

[16] ISO, ISO 14001: Environmental management systems – Requirements with guidance for use. Int. Org. Standardization, 2015.

[17] ISO, ISO 45001: Occupational health and safety management systems – Requirements with guidance for use. Int. Org. Standardization, 2018.

[18] E. Diaconescu, H. Sankare, K. Chow, T. Q. Murdock, and A. J. Cannon, "A short note on the use of daily climate data to calculate Humidex heat-stress indices," Int. J. Climatol., doi: 10.1002/joc.7833.

[19] A. Giovanni, L. D. Fathimahhayati, and T. A. Pawitra, "Risk analysis of occupational health and safety using hazard identification, risk assessment and risk control (HIRARC) method (case study in PT Barokah Galangan Perkasa)," UJEM (Indonesian J. Ind. Eng. Manage.), vol. 4, no. 2, pp. 198–211, Jun. 2023.

[20] H. O. Ahmed, J. A. Bindekhain, M. I. Alshuweihi, M. A. Yunis, and N. R. Matar, "Assessment of thermal exposure level among construction workers in UAE using WBGT, HSI, and TWL indices," Ind. Health, vol. 58, no. 2, pp. 170–181, 2020, doi: 10.2486/indhealth.2018-0259.

[21] N. Hussain, M. M. Kadir, A. A. Nafees, R. Karmaliani, and T. Jamali, "Needs assessment regarding occupational health and safety interventions among textile workers: A qualitative case study in Karachi, Pakistan," Int. J. Occup. Environ. Health, vol. 25, no. 4, pp. 223–230, 2019, doi: 10.1080/10773525.2019.1681197.

[22] K. Ho and T. Tenkate, "Safety data sheets as a hazard communication tool: An assessment of suitability and readability," Saf. Health Work, vol. 15, pp. 192–199, 2024, doi: 10.1016/j.shaw.2024.01.006.

[23] SILICON CARBIDE, powder Safety Data Sheet SIS6959.0, Version 1.0, Date of issue: Jan. 23, 2017.

[24] PRODUCT DATA SHEET Sikaflex®-221, Version 04.01, Nov. 2023, en_GH 012001202210001000.

Author contribution:

1. Conception and design of the study
2. Data acquisition
3. Data analysis
4. Discussion of the results
5. Writing of the manuscript
6. Approval of the last version of the manuscript

AZ has contributed to: 1, 2, 3 4 and 5.

MA has contributed to: 4, 5 and 6.

IS has contributed to: 5 and 6.

MHN has contributed to: 5 and 6.

MH has contributed to: 4, 5 and 6.

HA has contributed to: 4, 5 and 6.

Acceptance Note: This article was approved by the journal editors Dr. Rafael Sotelo and Mag. Ing. Fernando A. Hernández Gobertti.

Optimizing Domestic Refrigerator Performance with Varied Lubricants for R134a Refrigerant: Comparative Analysis

Optimización del rendimiento del refrigerador doméstico con lubricantes variados para el refrigerante R134a: un análisis comparativo

Otimização do desempenho de refrigeradores domésticos com diferentes lubrificantes para o refrigerante R134a: análise comparativa

Muhammad Ehtesham ul Haque [1(*)], Abdul Samad Khan [2], Adeel Ahmed Khan [3], Muhammad Anus Irshad [4]

Recibido: 28/05/2025 Aceptado: 24/07/2025

Summary. - The efficiency and performance of domestic refrigerators don't only depend on refrigerant but also on lubricating oil used in the refrigerator compressor. The lubricant of the compressor is responsible for the absorption of heat energy evolved during the compressor work. The primary objective of this study is to examine and compare the effects of two distinct lubricating oils utilized with the refrigerant R134a on various performance metrics of the domestic refrigerator compressor, including evaporator capacity, compressor power consumption, and the coefficient of performance (COP) of the refrigerator. These performance parameters were compared for two different cases, viz., domestic refrigerator having R134a as a refrigerant with Mineral oil (MO) and Polyol ester oil (POE), and for two different methods such as manually by using R134a ph chart and EES software. The tests were conducted on a 329-liter refrigerating capacity double-door refrigerator. The effect of changing oil from MO to POE resulted in the increment of evaporator capacity from 1.81 kW to 1.99 kW and COP from 4.9 to 5.7 while the compressor power consumption reduced from 370 watts to 340 watts which concluded that POE oil is the better lubricant in the domestic compressor as compared to MO.

Keywords: Lubricants, Polyol ester oil, Mineral oil, R-134a, EES, Domestic refrigerator.

[1] Assistant Professor, Department of Mechanical Engineering, NED University of Engineering & Technology (Pakistan), mailto:mehaque@neduet.edu.pk, ORCID iD: https://orcid.org/0000-0001-8751-348X

[2] Lecturer, Department of Mechanical Engineering, NED University of Engineering & Technology (Pakistan), abdulsamadkhan@neduet.edu.pk, ORCID iD: https://orcid.org/0009-0005-5449-635X

[3] Assistant Professor, Department of Mechanical Engineering, NED University of Engineering & Technology (Pakistan), adeelahmedk@neduet.edu.pk, ORCID iD: https://orcid.org/0009-0004-6790-8176

[4] Lecturer, Department of Mechanical Engineering, NED University of Engineering & Technology (Pakistan), mailto:muhammadanus@neduet.edu.pk, ORCID iD: https://orcid.org/0009-0006-8193-4287

Memoria Investigaciones en Ingeniería, núm. 29 (2025). pp. 131-151
https://doi.org/10.36561/ING.29.9
ISSN 2301-1092 • ISSN (en línea) 2301-1106 – Universidad de Montevideo, Uruguay
Este es un artículo de acceso abierto distribuido bajo los términos de una licencia de uso y distribución CC BY-NC 4.0. Para ver una copia de esta licencia visite http://creativecommons.org/licenses/by-nc/4.0/

Resumen. - *La eficiencia y el rendimiento de los refrigeradores domésticos no solo dependen del refrigerante, sino también del aceite lubricante utilizado en el compresor. El lubricante del compresor es responsable de la absorción de la energía térmica desarrollada durante el trabajo del compresor. El objetivo principal de este estudio es investigar y comparar el efecto de dos aceites lubricantes diferentes utilizados con el refrigerante R134a en varios parámetros de rendimiento del compresor del refrigerador doméstico, como la capacidad del evaporador, el consumo de energía del compresor y, por último, pero no menos importante, el COP del sistema de refrigeración. Estos parámetros de rendimiento se compararon para dos casos diferentes: un refrigerador doméstico con R134a como refrigerante, aceite mineral (MO) y aceite de polioléster (POE), y para dos métodos diferentes, como el manual mediante el uso de una tabla de pH del R134a y el software EES. Las pruebas se realizaron en un refrigerador de doble puerta con capacidad de refrigeración de 329 litros. El efecto de cambiar el aceite de MO a POE resultó en el incremento de la capacidad del evaporador de 1,81 kW a 1,99 kW y el COP de 4,9 a 5,7 mientras que el consumo de energía del compresor se redujo de 370 vatios a 340 vatios, lo que concluyó que el aceite POE es el mejor lubricante en el compresor doméstico en comparación con MO.*

Palabras clave: *Lubricantes, Aceite de polioléster, Aceite mineral, R-134a, EES, Refrigerador doméstico.*

Resumo. ***-*** *A eficiência e o desempenho de refrigeradores domésticos dependem não apenas do refrigerante, mas também do óleo lubrificante utilizado no compressor. O lubrificante do compressor é responsável pela absorção da energia térmica liberada durante o funcionamento do compressor. O principal objetivo deste estudo é examinar e comparar os efeitos de dois óleos lubrificantes distintos, utilizados com o refrigerante R134a, em diversas métricas de desempenho do compressor de um refrigerador doméstico, incluindo a capacidade do evaporador, o consumo de energia do compressor e o coeficiente de desempenho (COP) do refrigerador. Esses parâmetros de desempenho foram comparados em dois casos diferentes: um refrigerador doméstico com R134a como refrigerante, utilizando óleo mineral (MO) e óleo de éster de poliol (POE), e por dois métodos distintos: manualmente, utilizando a tabela de pH do R134a, e por meio do software EES. Os testes foram realizados em um refrigerador de duas portas com capacidade de refrigeração de 329 litros. A mudança do óleo de MO para POE resultou no aumento da capacidade do evaporador de 1,81 kW para 1,99 kW e do COP de 4,9 para 5,7, enquanto o consumo de energia do compressor reduziu de 370 watts para 340 watts, concluindo-se que o óleo POE é um lubrificante melhor para compressores domésticos em comparação com o MO.*

Palavras-chave: *Lubrificantes, óleo éster de poliol, óleo mineral, R-134a, EES, refrigerador doméstico.*

1. Introduction. - There are many challenges facing energy conservation and environmental protection today, and how energy is supplied and consumed, both practices require major changes (Allouhi et al., 2015). Energy conservation has recently emerged as an important social issue. It involves efforts to reduce energy consumption by utilizing less energy-intensive services and ensuring more efficient equipment management (Ollukkaran & Sreedharan, 2023). According to the Montreal and Kyoto treaties, home refrigerators are the main source of emissions of the fluorine and chlorine gases which are present in refrigerants. These emissions contribute significantly to the degradation of the ozone layer and the acceleration of global warming. The release of chlorofluorocarbons (CFCs) and hydrofluorocarbons (HFCs) from these appliances leads to increased ultraviolet radiation reaching the Earth's surface. This not only harms ecosystems and human health but also exacerbates climate change by trapping heat in the atmosphere. . Nowadays, Ozone Depletion (OD) and Global Warming (GW) are increasing day by day (Khan, ul Haque, Khan, Obaidullah, & Khan, 2024), and refrigerant compounds such as chlorofluorocarbons (CFCs), hydrochlorofluorocarbons (HCFCs), and hydrofluorocarbons (HFCs) are responsible (Damola S. Adelekan et al., 2017). Previously, refrigeration systems commonly used hydrochlorofluorocarbon (HCFC) refrigerants such as R12 (dichlorodifluoromethane) and R22 (chlorodifluoromethane). However, their use is now prohibited due to their ozone-depleting effects (Tada et al., 2016).

Researchers (D. S. Adelekan et al., 2021) examined the performance of an altered household refrigerator under varying mass charges of R600a refrigerant, TiO2 nanoparticle concentrations, and ambient temperature conditions. The refrigerator's energy consumption at 0.2 g/L and 0.4 g/L concentrations of TiO2 nanolubricant was lowered by 0.13 to 14.09% in comparison to the baseline concentration (0 g/L). Utilizing 0.2 g/L of nanolubricant in the refrigerator, the greatest coefficient of performance was reached with a 60g charge of R600a and at ambient temperature of 22°C.

A domestic refrigerator using R134a and LPG as the refrigerant was studied in 2018 with two different lubricants, including POE, MO. It also investigated nano-oils comprising of TiO2, SiO2, and Al2O3, nanoparticles in combination with MO. The results showed that compressor power consumption was 15.87% lower and the COP was 56.32% higher than calculated for R134a/POE lubricant (Gill, Singh, Ohunakin, & Adelekan, 2018). In 2019, an experiment was carried out to investigate the performance of a refrigeration system using an R134a/PAG oil mixture and R134a/PAG/Al2O3 (R134a/nano-oil) mixture which shows that COP was increased by 6.5% after the addition of the nanoparticles in the compressor (Nair, Parekh, & Tailor, 2020).

In 2019, an Energy analysis of a domestic refrigerator system with Artificial neural network (ANN) using different concentration combinations of LPG/TiO2 – lubricant as a replacement for R134a was used and the findings revealed that compressor power consumption and pressure ratio using LPG with nano-oil was 3.20–18.1 and 2.33–8.45% respectively lower and the cooling capacity and COP was around 18.74–32.72 and 10.15–61.49% respectively higher in comparison with R134a as a refrigerant (Gill, Singh, Ohunakin, & Adelekan, 2019). In 2019, hexagonal boron nitride (h-BN) was used as a solid nanoparticle in POE with R134a as a refrigerant and the findings showed that using 3 vol% of h-BN nanoparticle improved the energy saving by 60% in comparison with pure POE oil (Harichandran, Paulraj, Maha Pon Raja, & Kalyana Raman, 2019). In 2021, the performance of a domestic refrigerator was investigated via R134a with POE and R600a with nano-oil (MO with Al2O3) which resulted in an improvement of COP and compressor discharge pressure by 37.2% and 8.9% respectively, and a reduction in power consumption and evaporator pressure by 28.7% and 24.7% respectively by using 0.1 wt.% of R600a with nano-oil (MO with Al2O3) as compared to the conventional refrigeration system (Yogesh, Dinesh, & Sandeep, 2021). In 2022, authors investigated the performance of the refrigeration cycle of a domestic refrigerator by adding ZrO2 nanoparticle of concentration 0.2 g/L in R134a refrigerant and found out that by using nano-oil, the refrigeration capacity of the system was increased to 38.7% (Baskaran, Manikandan, Tesfaye, Nagaprasad, & Krishnaraj, 2022).

An experimental comparison of a residential refrigerator's performance analysis using MO oil versus POE oil is needed to determine which lubricant performs the best with R134a. The literature review indicates that there are no or very little studies that compare the thermodynamic performance of home refrigerators using the same refrigerant but two different lubricants, and a comparative analysis using EES. Chlorine in refrigerant compounds such as CFC and HCFC is responsible for OD and GW. However, in this experimental research work, R-134a, which is an HFC compound, is used. It is chlorine-free, making it environmentally feasible for the analysis. This study aims to perform the

thermodynamic analysis experimentally of two different compressor lubricating oils to find the better lube oil which can be used in a domestic refrigerator with the Refrigerant R134a, and comparative analysis was performed with the EES Professional V10.4-3D software. The comparison was made based on performance parameters including COP, compressor power consumption & evaporator cooling capacity.

2. Materials and Methods. -

2.1 Experimental setup. - The experiment conducted by utilization of an experimental setup consists of a double-door domestic refrigerator with a gross capacity of 397 Litres. It includes a hermetic reciprocating type of compressor in which HFC – R134a is used as a refrigerant with a charged mass of 190 grams, a dryer, a capillary tube, an air-cooled condenser, and an evaporator. Table I represents the specification of the experimental setup.

S/N	Refrigerator description	Units
1	Climate Class	Tropical
2	Protection Class	I
3	Storage Volume	329L
4	Freezer Volume	68L
5	Power rating	180W
6	Voltage/frequency rating	200-240V/50 Hz
9	Condenser type	Air cooled
10	Refrigerant type	R134a
11	Mass charge	190 g
12	Freezing Capacity	4kg/24 hr
13	Lamp rating	10 Watt
14	Overall size	620 x 600 x 1700 (mm)
15	Compressor type	Hermetic (HFC)
16	Number of doors	Double

Table I. Specification of the refrigerator.

Figure I shows the pressure gauges installed at the suction & discharge lines of the compressor while Figure II shows temperature sensors at different locations within the refrigerator to record data in the data logger.

Figure I. Pressure gauge installed at compressor's suction & discharge lines.

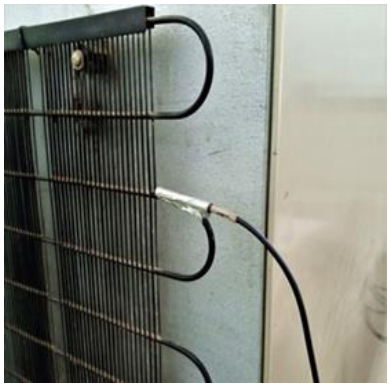

(a)

(b)

Figure II. Temperature sensors installed inside & outside of the refrigerator.

The overall experiment was performed by using two different lubricants that are MO and POE oil with the refrigerant R134a for both oils. Table II represents the range of experimental setups while Table III & Table IV shows the properties of the POE oil & MO.

S/N	Parameter	Range of experiment	
1	Refrigerant name	R – 134a	R – 134a
2	Refrigerant charge	190 g	190 g
3	Compressor Lubricant	MO	POE
4	Lubricant charge	300 ml	300 ml
5	Evaporator type	Air-cooled	Air-cooled

Table II. Range of experimental conditions.

S/N	Lubricating oil characteristics	Units
1	Oil Type	POE
2	Density at 15°C kg/L	0.980
3	Kinematic viscosity @ 40°C	32.0 cSt
4	Kinematic viscosity @ 100°C	5.8 cSt
5	Viscosity index	125
6	Flash Point	235 °C
7	Pour Point	– 48 °C
8	Cu Corrosion @ 100°C x 3 hrs	1a
9	Water ppm	<100

Table III. Characteristics of POE Oil.

S/N	Lubricating oil characteristics	Units
1	Oil Type	MO
2	Density at 15°C kg/L	0.916
3	Kinematic viscosity @ 40°C	55 cSt
4	Kinematic viscosity @ 100°C	5.9 cSt
5	Viscosity index	41
6	Flash Point	179 °C
7	Pour Point	– 35 °C

Table IV. Characteristics of MO.

3. Performance analysis. -

3.1 Evaporator capacity. - The evaporative heat transfer rate through the refrigeration system was calculated separately for the compressor, charged with MO and POE lubricants, respectively. The formula used for the refrigeration effect is given by eq (1):

$$\dot{Q} = \dot{m}\ (h_5 - h_4) \qquad (1)$$

The refrigerant mass flow rate is calculated by eq (2):

$$\dot{m} = \frac{\dot{W}_{comp}}{(h_2 - h_1)} \qquad (2)$$

In eq (1), h_4 & h_5 represents the enthalpies at evaporator inlet and commencement of superheating of the refrigerant. In eq (2), h_1 & h_2 represents the enthalpies at compressor inlet and compressor outlet/condenser inlet while W ̇_comp indicates the compressor power consumption.

3.2 Compressor power consumption. - The data logger which was used to record experimental readings at different locations inside and outside the refrigerator can also measure voltage and current consumed by the compressor during the time interval when the refrigerator was in operation. The power consumed by the compressor can be calculated by the eq (3):

$$Power = voltage\ x\ current\ \ (W) \qquad (3)$$

3.3 COP. - The actual COP values for the VCRS were evaluated using EES software by first charging the compressor with MO, and the same procedure was repeated for POE lubricating oil. The COP values obtained were validated against the COP values calculated using ASHRAE Ph Chart for HFC R – 134a (Handbook, 2017).

To determine the COP for the refrigerator, the temperature sensors were attached at different positions to the refrigerator itself, and the temperature readings were recorded using a data logger. In contrast, the pressure at the suction and discharge of the compressor was noted by operating the two pressure gauges after every five minutes. The temperature and pressure readings were recorded for the entire day, but average values were used in the calculation. Figure III shows the schematic diagram of the refrigerator with a data logger for data measurement.

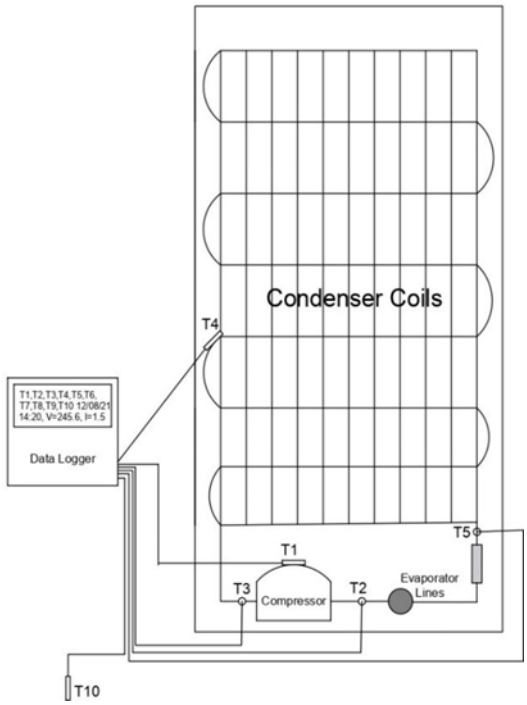

Figure III. Schematic diagram of a refrigerator showing temperature sensors and data logger.

The COP of the domestic refrigerator is given by eq (4):

$$COP = \frac{\dot{Q}}{\dot{W}_{comp}} \qquad (4)$$

3.4 Compressor & evaporator temperatures. - The compressor was charged with two different lubricants, MO, and a synthetic lubricant, each time with the same amount of refrigerant, i.e., HFC R – 134a. To compute the effect on refrigerator performance by using two different lubricating oils, the performance parameters such as compressor suction & discharge pressures & temperatures and compressor dome temperatures were recorded during the time interval when the refrigerator was in operation. In the first step, the compressor was charged with 190 grams of R134a and 300 ml of MO. The compressor was charged again with the same amount of refrigerant for the second run, using 300 ml of POE. Figure IV depicts the placement of the temperature sensors at the compressor dome.

The experimental setup consists of ten DS18B20 digital temperature sensors, each utilized to obtain internal freezer compartment temperatures using the data logger alongside time, voltage, and current. Figure V depicts the placement of temperature sensors. Temperature readings were taken twice for the bottom and right-side walls of the freezer compartment while changing the compressor lubricant from MO to POE oil.

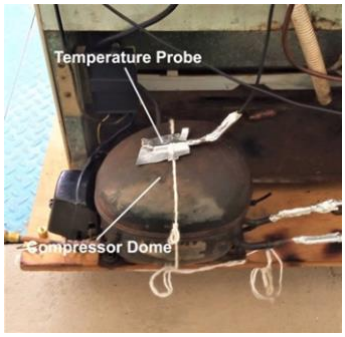

Figure IV. Placement of temperature sensors at compressor dome

(a) (b)

Figure V. Placement of temperature sensors in the freezer compartment

4. Results and Discussion. - The investigation involved a double-door domestic refrigerator which used two different lubricants, mineral oil (MO) and polyolester (POE) oil. HFC R-134a performance was evaluated using the ASHRAE pressure-enthalpy (P-h) chart and Engineering Equation Solver (EES) software.

4.1 Calculation of COP by using P-h chart. - The refrigeration cycle was hand-drawn on the R134a Ph chart by using the average values of temperature and pressure recorded during the experiments. The COP is then calculated and listed in Table V for both lubricating oils. Figure VI depicts the calculated COP values while Figure VII & Figure VIII represents the refrigeration cycle on the R134a Ph chart for MO & POE oil respectively.

S/N	Refrigerant	Lubricating oil	COP
1	HFC R134a	MO	4.958
2		POE	5.795

Table V. COP values for MO & POE lubricants using R134a ph chart.

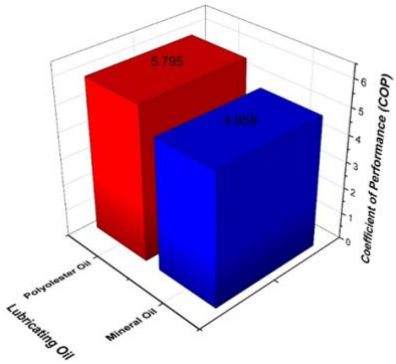

Figure VI. COP (MO vs POE oil).

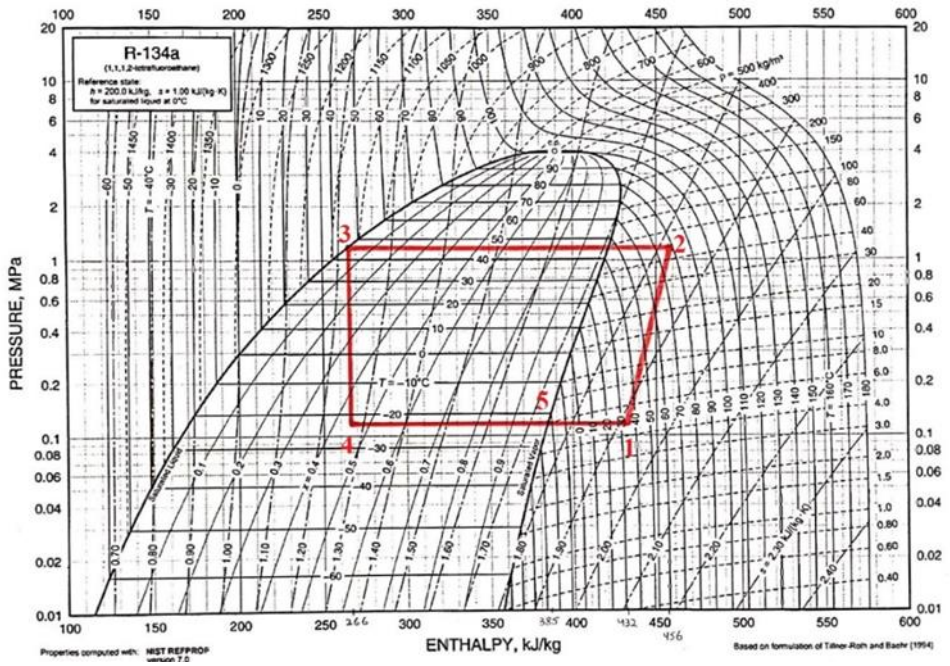

Figure VII. Refrigeration cycle on R134a Ph chart for MO

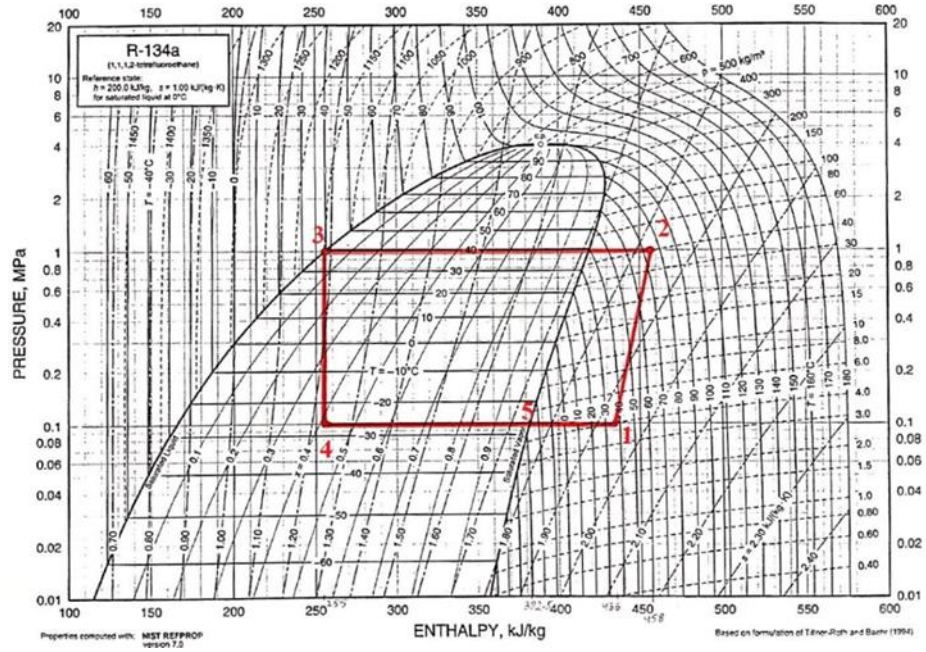

Figure VIII. Refrigeration cycle on R134a Ph chart for POE oil

R-134a and the majority of HFC refrigerants do not mix well with mineral oil. For this reason, the evaporator and pipes retain oil as a result of this poor miscibility. These retained mineral oil acts as an insulator and hinders in the heat transfer (Sundaresan, Judge, Chu, & Radermacher, 1996). On the other hand, POE oil and R-134a mix quite well. By circulating with the refrigerant, it improves heat transfer and lessens oil logging in the evaporator. As a result of this better miscibility of POE oil with R-134, more effective evaporation and condensation occur which improves the COP value.

As compared to mineral oil, POE oil has superior lubricity under high pressure and high temperature condition which is common in the R-134 compressor (Sundaresan, Pate, Doerr, & Ray, 1996).

4.2 Compressor power consumption. - The power consumed by the compressor when it is charged with POE oil came out to be less than it is consumed by the compressor using MO as a lubricant. The compressor voltage and current data were obtained using the data logger. Table VI represents the average current & power consumed by the compressor when using MO & POE oil. Figure IX depicts the compressor power consumption recorded by data logger; Figure X shows the graph representing the current drawn by the compressor while Figure XI depicts the bar chart showing the compressor average power consumption when both the oils were used.

S/N	Refrigerant	Lubricating oil	Average Current (Ampere)	Average Power (Watts)
1	HFC R134a	MO	1.535	370.91
2		POE	1.391	340.62

Table VI. Average Current & Power consumed using MO & POE oil.

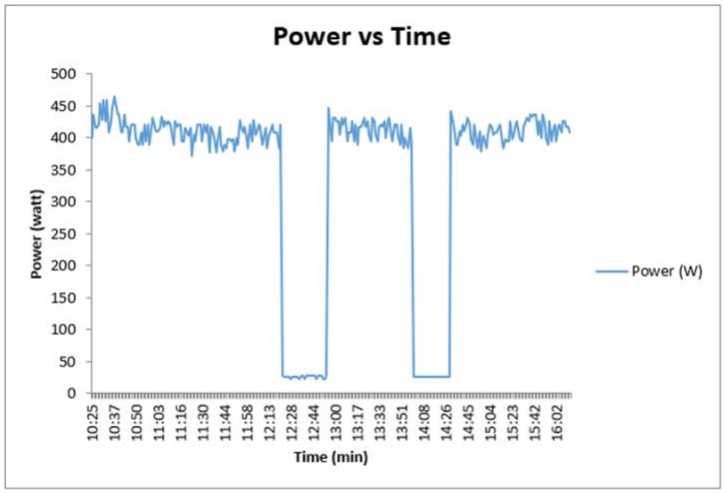

Figure IX. Compressor power consumption.

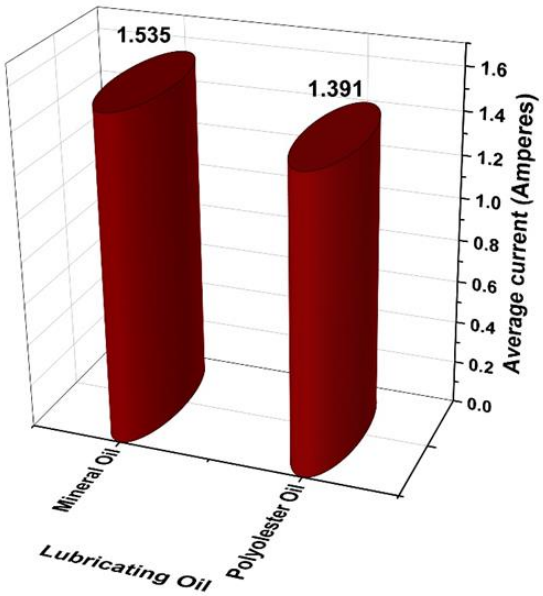

Figure X. Average current drawn (MO vs POE oil).

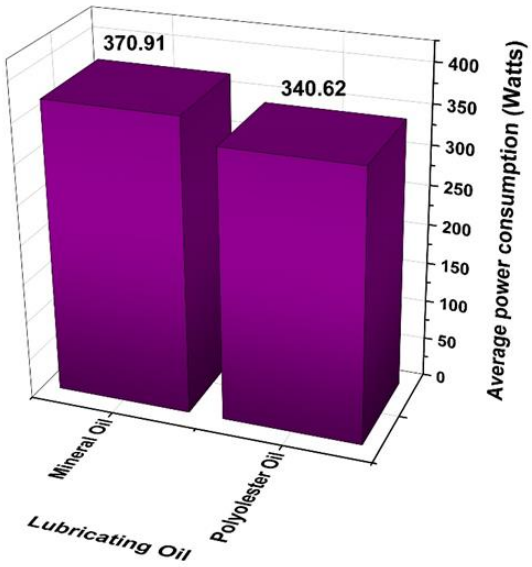

Figure XI. Average power consumption (MO vs POE oil).

POE oils are outstanding lubricants in high-temperature, high-pressure environments, which are typical in HFC systems. This characteristic results in reduced mechanical friction and weir losses in the compressor. A lower frictional loss reduces the power requirement of the compressor and hence higher COP values are achieved.

4.3 Evaporator capacity. - By using eq (1) & eq (2), the mass flow rate and refrigeration effect of the refrigerant can be calculated easily which is also shown in Table VII. Figure XII depicts the bar chart representing the evaporator capacities when both the oils i.e., POE and MO were used in the experiment.

S/N	Refrigerant	Lubricating oil	Mass flowrate (kg/s)	Evaporator capacity (Kilowatts)
1	HFC R134a	MO	0.0152	1.8171
2		POE	0.0156	1.9992

Table VII. Evaporator cooling capacity using MO & POE oil.

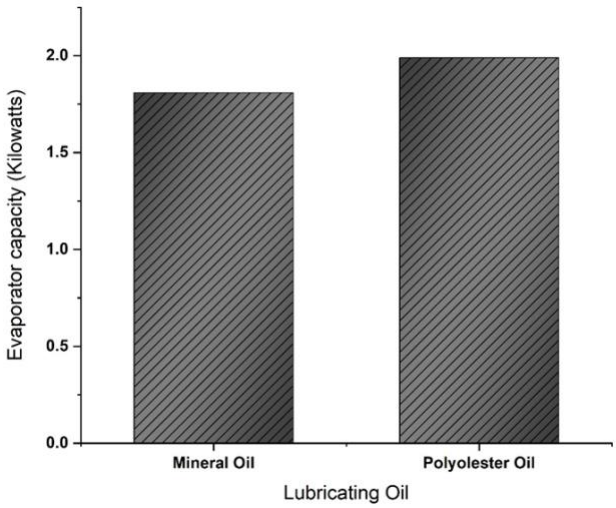

Figure XII. Evaporator cooling capacity (MO vs POE oil).

4.4 Compressor & evaporator temperatures. - Table VIII represents the thermophysical properties of MO and POE lubricants. The temperature and pressure were measured several times, and the average readings were used for calculations. The DS18B20 temperature sensors used in this setup have a measurement range of -55°C to 125°C with an accuracy of ±0.5 °C.

S/N	Lube oil	Viscosity at 40 ºC (cSt)	Viscosity at 100 ºC (cSt)	Flash point (ºC)	Density at 15ºC (kg/L)
1	MO	55	5.9	179	0.916
2	POE	32	5.8	235	0.980

Table VIII. Thermophysical properties for MO and POE lubricants.

Table IX shows average experimental data using MO and POE lubricants. It is evident that POE has a lower compressor temperature difference leading to lower compressor ratio which means compressor doesn't have to work as hard to compress the refrigerant. Less heat is generated during compression, leading to lower operating temperatures within the compressor. Cooler operating temperatures help prevent overheating and thermal degradation of compressor components, contributing to increased reliability and longevity.

S/N	Lube oil	Pressure (bar)		Temperature (ºC)		
		Compressor Suction	Compressor discharge	Compressor suction	Compressor discharge	Condenser outlet
1	MO	1.2	12	31.06	83.98	46
2	POE	1	10	36.23	82.98	39.72

Table IX. Experimental data using MO and POE lubricants.

Table X represents the average evaporator temperatures and compressor dome temperature using MO & POE lubricating oils. Figure XIII, Figure XIV and Figure XV represent the graphs of evaporator right and bottom side walls and compressor dome temperatures recorded by data logger when both the oils were used in the compressor for analysis.

S/N	Lube oil	Temperature (ºC)		
		Evaporator Right side wall	Evaporator Bottom side floor	Compressor dome
1	MO	**1.165**	**-3.560**	89.3
2	POE	**-6.794**	**-6.140**	98.9

Table X. Temperature data using MO & POE lubricating oils.

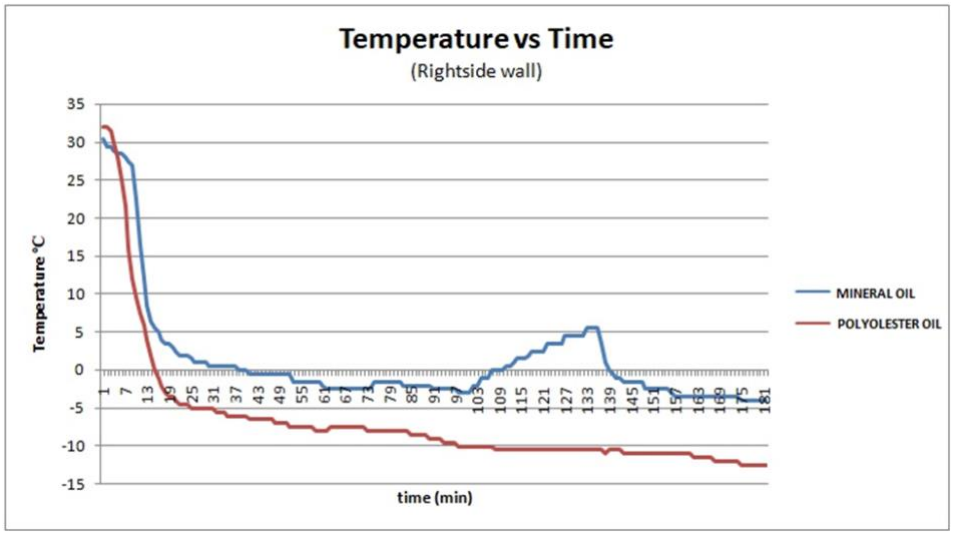

Figure XIII. Evaporator right side wall temperature.

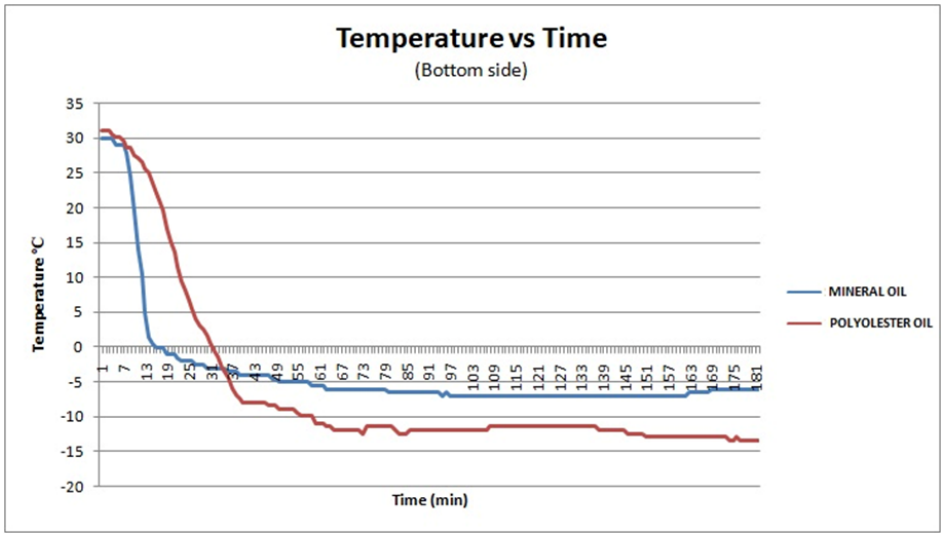

Figure XIV. Evaporator bottom side wall temperature.

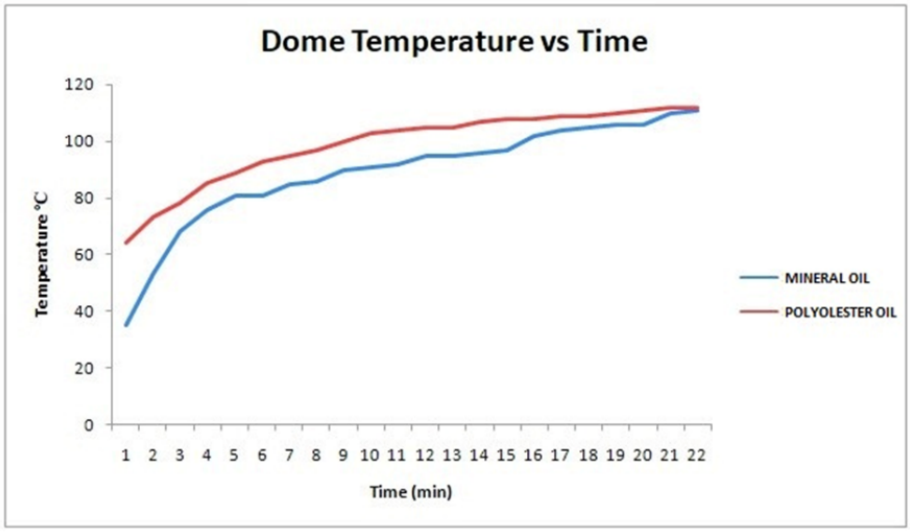

Figure XV. Compressor dome temperature.

The COP of the refrigerator is greater when POE oil is used, as opposed to when mineral oil is used. Because POE oil mixes better with R-134a, decreases heat exchanger oil film development, increases heat transfer, provides dependable oil return, and lowers compressor mechanical losses.

5. Validation by EES Software. -

5.1 Mineral Oil. - The performance analysis results are compared and validated by EES software. Three parameters of the present work, i.e., COP, refrigeration effect, and compressor power are validated with the EES software. Figure XVI shows the validation results i.e., COP, compressor power & evaporator capacity of the refrigeration system when using MO with R134a as a refrigerant. Figure XVII & Figure XVIII shows the ph & T-s plots for MO given by EES.

Unit Settings: SI C bar kJ mass deg

COP = 4.523 $\dot{m}$ = 0.0152 [kg/s] P = 0.4006 [kW] $\dot{Q}$ = 1.812 [kW]

Q_H = 189.5 [KJ/kg] Q_L = 119.2 [KJ/kg] W_c = 26.35 [KJ/kg]

Figure XVI. Validation of MO by EES software.

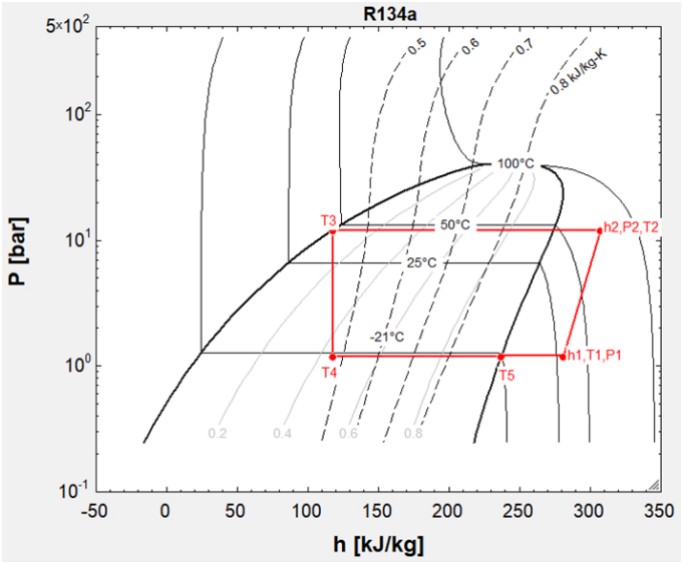

Figure XVII. ph plot for MO by EES software.

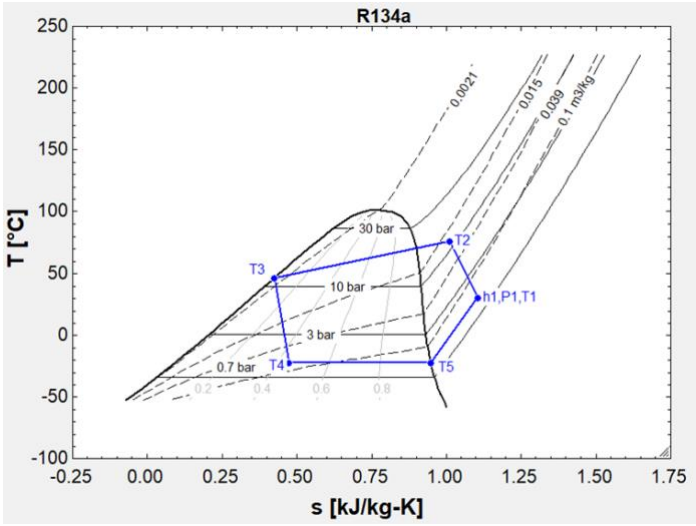

Figure XVIII. T-s plot for MO by EES software.

When compared with the values obtained from the ph chart in tables V, VI, and VII, it is evident that the EES software values validate the values obtained from the ph chart.

5.2 POE Oil. – Figure XIX depicts the validation results i.e., COP, compressor power & evaporator capacity of the refrigeration system when using POE oil with R134a as a refrigerant. Also, Figure XX & Figure XXI shows the ph & T-s plots for POE oil given by EES.

Unit Settings: SI C bar kJ mass deg

COP = 5.781 $\dot{m}$ = 0.0156 [kg/s] P = 0.343 [kW] $\dot{Q}$ = 1.983 [kW]

Q_H = 200.7 [KJ/kg] Q_L = 127.1 [KJ/kg] W_c = 21.99 [KJ/kg]

Figure XIX. Validation of Mineral Oil by EES software.

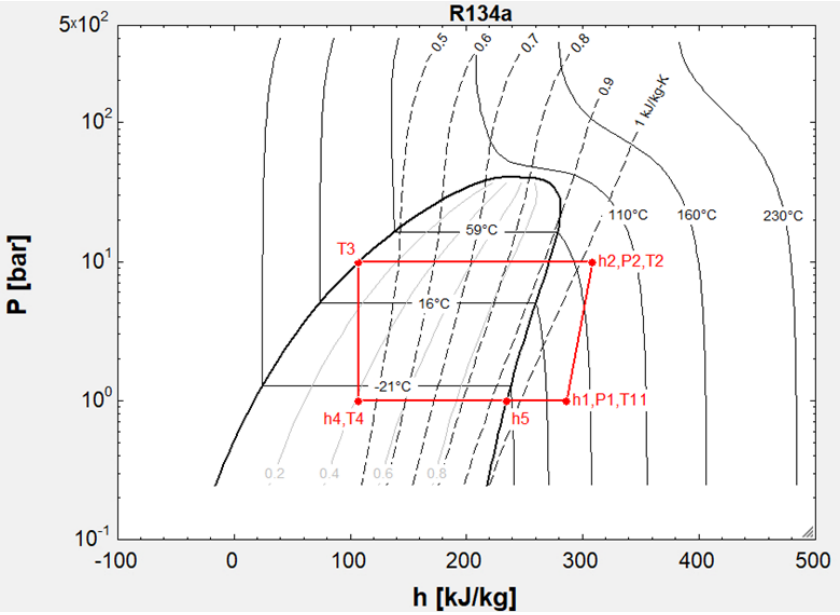

Figure XX. ph plot for POE oil by EES software.

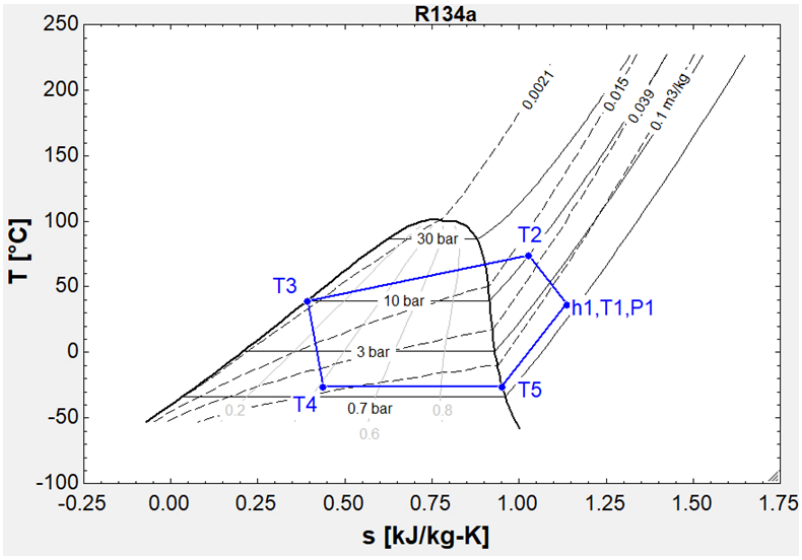

Figure XXI. T-s plot for POE oil by EES software.

5.3 Comparison of the results. - The COP, compressor power consumption & refrigeration effect of the refrigeration system with two different lubricating oils with the same refrigerant R134a using two different methods i.e., EES software and R134a Ph chart are listed in Table XI.

S/N	Compressor Lube oil	COP		Compressor power (kW)		Evaporator capacity (kW)	
		ph chart	EES	ph chart	EES	ph chart	EES
1	MO	4.958	4.523	0.370	0.400	1.8171	1.812
2	POE	5.795	5.781	0.340	0.343	1.9992	1.983

Table XI. Comparison of the performance parameters.

The percentage errors between the two methods i.e by using the R-134a ph chart and EES software for COP, compressor power and evaporator capacity are shown in Table XII.

S/N	Compressor Lube oil	Parameters	% Error
1	MO	COP	9.6
		Compressor Power	7.5
		Evaporator Capacity	0.28
2	POE	COP	0.24
		Compressor Power	0.87
		Evaporator Capacity	0.81

Table XII. Percentage error.

Figure XXII, Figure XXIII, and Figure XXIV represent the 3D graphs showing COP, compressor power consumption, and refrigeration effects when using both oils, i.e., POE and MO, and both methods, R-134a and EES software. This allows for an easy comparison of values at a glance.

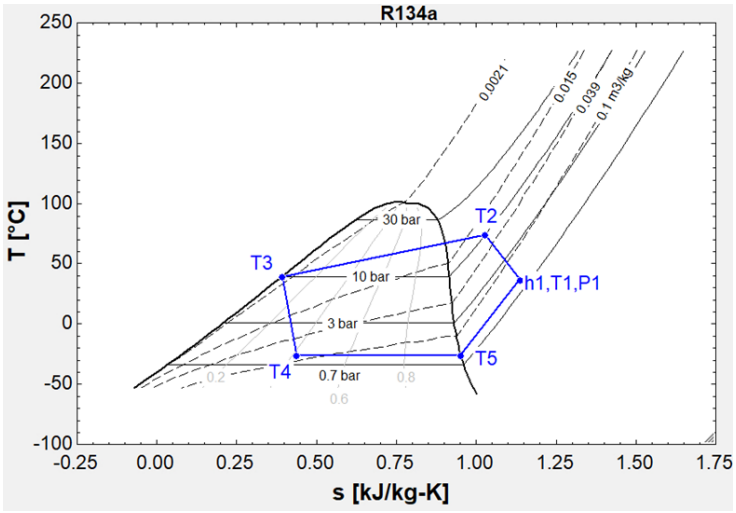

Figure XXII. COP (R134a ph chart vs EES).

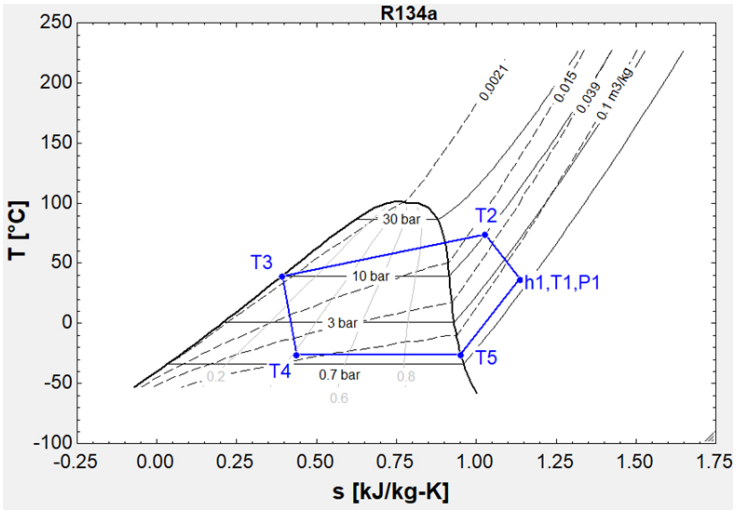

Figure XXIII. Compressor Power consumption (R134a ph chart vs EES).

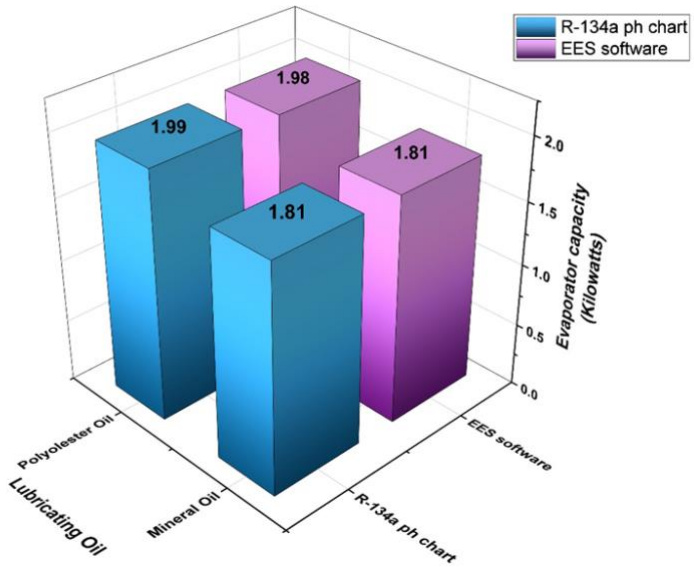

Figure XXIV. Refrigeration effect (R134a ph chart vs EES).

6. Conclusion. - Based on the experimental investigation and performance analysis of the domestic refrigerator using two different compressor lubricating oils i.e., Mineral Oil and POE oil, the following conclusions are noted keeping in mind the comparative analysis of the lubricating oil performance parameters with the same refrigerant R134a:

a. COP (Coefficient of Performance) is used to measure the efficiency of vapor compression refrigeration systems. The COP values were obtained manually using the ASHRAE Ph chart for R134a and validated by the EES program while using two different compressor lubricants, i.e., MO and POE. The error associated with these two methods is very less, as observed in Table XI. From Figure XXII, it is evident that the COP value obtained for MO is significantly less when compared to the COP value for POE; this is because of increased refrigeration effect as shown in Figure XXIV.

b. From Figure XI, it is evident that there is a considerable reduction in compressor power consumption while using POE lubricant. Around 30 watts less power is consumed when the compressor is shifted from MO to POE which is also depicted in Table XI. The difference in power consumed is due to enhanced lubricity. Changing the lubricant has significantly reduced the current consumed by the compressor, which is evident from Figure X.

c. Since refrigerant R134a is miscible with POE oil used, there is an increase in refrigeration from 1.817 KJ/s to 1.999 KJ/s. Moreover, the mass flow rate calculated is approximately the same using two different lubricants. Therefore, the increase in evaporator capacity indicated in Figure XII is due to an increase in the heat transfer rate from the air to the refrigerant in the evaporator.

d. The lubricant's thermophysical properties significantly impact refrigerator performance parameters. The properties of both lubricants are listed in the Table IX depict that MO will be carried along with the refrigerant into the system in more significant amounts, compared to POE, due to its decreased flash point and density. The oil inside the evaporator and condenser significantly decreases the heat transfer rate by creating an insulating effect. In contrast, POE oil has a high return rate to the compressor due to its miscibility with R134a. From Table IX, the increase in compressor suction temperature when POE is used suggests that heat transfer through the evaporator has enhanced. Hence, the refrigerant returned to the compressor has a high temperature. A similar effect can be observed for condenser outlet temperature.

e. The lowest shell temperature, i.e., 111 ºC, is obtained for the compressor charged with R134a and MO mixture indicated in Table X. In contrast, in Figure XV, the comparatively higher temperature curve shown in red is for the compressor charged with POE. The increase in compressor dome temperature is due to more excellent heat dissipation from the shell.

Experimental work and theoretical studies have been carried out in this research to investigate the performance of a VCRS using two different classes of compressor lubricants, namely MO and POE oil. Lubricant effects on system performance are easily measurable, as evidenced by the difference in performance parameters evaluated such as COP, evaporator capacity & compressor power consumption. The miscible POE oil outperformed an immiscible MO with R134a refrigerant. From Table XI, it could be concluded that the COP value obtained is higher for POE oil, implying that the factor of miscibility has positive effects on system performance. System reliability should not be the only priority when selecting a compressor lubricant but also enhanced system performance and efficiency.

References

[1] Adelekan, D. S., Ohunakin, O. S., Babarinde, T. O., Odunfa, M. K., Leramo, R. O., Oyedepo, S. O., & Badejo, D. C. (2017). Experimental performance of LPG refrigerant charges with varied concentration of TiO2 nano-lubricants in a domestic refrigerator. Case Studies in Thermal Engineering, 9, 55-61. doi: https://doi.org/10.1016/j.csite.2016.12.002

[2] Adelekan, D. S., Ohunakin, O. S., Oladeinde, M. H., Jatinder, G., Atiba, O. E., Nkiko, M. O., & Atayero, A. A. (2021). Performance of a domestic refrigerator in varying ambient temperatures, concentrations of TiO2 nanolubricants and R600a refrigerant charges. Heliyon, 7(2), e06156. doi: https://doi.org/10.1016/j.heliyon.2021.e06156

[3] Allouhi, A., El Fouih, Y., Kousksou, T., Jamil, A., Zeraouli, Y., & Mourad, Y. (2015). Energy consumption and efficiency in buildings: current status and future trends. Journal of Cleaner Production, 109, 118-130. doi: https://doi.org/10.1016/j.jclepro.2015.05.139

[4] Baskaran, A., Manikandan, N., Tesfaye, J., Nagaprasad, N., & Krishnaraj, R. (2022). Investigation on the Performance of Domestic Refrigerator with Zirconium Oxide-R134a Nanorefrigerant. Journal of Nanomaterials, 2022, 3668458. doi: https://doi.org/10.1155/2022/3668458

[5] Gill, J., Singh, J., Ohunakin, O. S., & Adelekan, D. S. (2018). Energetic and exergetic analysis of a domestic refrigerator system with LPG as a replacement for R134a refrigerant, using POE lubricant and mineral oil based TiO2-, SiO2- and Al2O3-lubricants. International Journal of Refrigeration, 91, 122-135. doi: https://doi.org/10.1016/j.ijrefrig.2018.05.010

[6] Gill, J., Singh, J., Ohunakin, O. S., & Adelekan, D. S. (2019). Energy analysis of a domestic refrigerator system with ANN using LPG/TiO2–lubricant as replacement for R134a. Journal of Thermal Analysis and Calorimetry, 135(1), 475-488. doi: https://doi.org/10.1007/s10973-018-7327-3

[7] Handbook, A. (2017). Fundamentals, ASHRAE–American society of heating, Ventilating and Air-Conditioning Engineers: ASHRAE.

[8] Harichandran, R., Paulraj, P., Maha Pon Raja, S., & Kalyana Raman, J. (2019). Effect of h-BN solid nanolubricant on the performance of R134a–polyolester oil-based vapour compression refrigeration system. Journal of the Brazilian Society of Mechanical Sciences and Engineering, 41(3), 140. doi: https://doi.org/10.1007/s40430-019-1645-7

[9] Khan, A. S., ul Haque, M. E., Khan, A. A., Obaidullah, S., & Khan, M. U. (2024). Revitalizing Comfort: Designing an Energy–Efficient HVAC System for the University Auditorium. Memoria Investigaciones en Ingeniería (26), 2-37. doi: https://doi.org/10.36561/ING.26.2

[10] Nair, V., Parekh, A. D., & Tailor, P. R. (2020). Experimental investigation of a vapour compression refrigeration system using R134a/Nano-oil mixture. International Journal of Refrigeration, 112, 21-36. doi: https://doi.org/10.1016/j.ijrefrig.2019.12.009

[11] Ollukkaran, B. A., & Sreedharan, S. (2023). Motivational factors for Energy Conservation in the workplace: A Focus from Employees Perspective. GMSARN International Journal, 17, 8-13.

[12] Sundaresan, S., Judge, J., Chu, W., & Radermacher, R. (1996). A comparison of the oil return characteristics of R-22/mineral oil, and its HFC alternatives (R-407C & R-410A) with mineral oil and POE in a residential heat pump.

[13] Sundaresan, S., Pate, M., Doerr, T., & Ray, D. (1996). A Comparison of the Effects of POE and Mineral Oil Lubricants on the In-Tube Evaporation of R-22, R-407C and R-410A.

[14] Tada, A., Okido, T., Shono, Y., Takahashi, H., Shitara, Y., & Tanaka, S. (2016). Tribological Characteristics of Polyol Ester Type Refrigeration Oils under Refrigerants Atmosphere. Tribology Online, 11, 348-353. doi: https://doi.org/10.2474/trol.11.348

[15] Yogesh, J., Dinesh, Z., & Sandeep, J. (2021). Performance investigation of vapor compression refrigeration system using R134a and R600a refrigerants and Al2O3 nanoparticle-based suspension. Materials Today: Proceedings, 44, 1511-1519. doi: https://doi.org/10.1016/j.matpr.2020.11.732

Author contribution:

1. Conception and design of the study

2. Data acquisition

3. Data analysis

4. Discussion of the results

5. Writing of the manuscript

6. Approval of the last version of the manuscript

MEuH has contributed to: 1, 2, 3 4, 5 and 6.

ASK has contributed to: 1, 2, 3 4, 5 and 6.

AAK has contributed to: 1, 2, 3 4, 5 and 6.

MAI has contributed to: 1, 2, 3 4, 5 and 6.

Acceptance Note: This article was approved by the journal editors Dr. Rafael Sotelo and Mag. Ing. Fernando A. Hernández Gobertti.

Analysis of barriers to the massification use of private electric vehicles in urban passenger transport in Lima, Peru

Análisis de las barreras para la masificación del uso de vehículos eléctricos privados en el transporte urbano de pasajeros en Lima, Perú

Análise das barreiras ao uso generalizado de veículos elétricos particulares no transporte urbano de passageiros em Lima, Peru

Russell Nazario Ticse [1(*)], José Ramos Saravia [2], María Quintana Caceda [3], Jorge Wong Kcomt [4], Wilson Arroyo Delgado [5]

Recibido: 14/06/2025 Aceptado: 25/08/2025

Summary. - The study aims to evaluate and understand the general perception of the interest groups involved in the adoption of electric vehicles on the barriers against their massification. Electric vehicles have benefits such as: making the vehicle fleet energy independent from fossil fuel, improving public health, reducing imports and environmental impact; however, the adoption rate of electric vehicles in many countries is relatively low and varies substantially between countries. developed and developing. In emerging markets, stakeholders must know which barriers are most significant to prevent their massification, consequently determine what policy actions could be applied to help the adoption of electric vehicles. The Social Impact Assessment (SIA) has become a key factor to determine the viability of projects, know the population's expectations about projects or programs, carry out a market study and help in decision making. In this study, we propose an approach for SIA using an integrated gray clustering and entropy weighting method (the IGCEW method), In Peru, four interest groups were identified and the three main barriers were evaluated. As a result, the weights of each barrier in the introduction of electric vehicles in an emerging market will be obtained.

Keywords: Electric vehicles; barriers; Adoption of EV; Emerging markets.

[1] Doctor. Universidad Nacional de ingeniería UNI (Perú), rnazariot@uni.pe, ORCID iD: https://orcid.org/0000-0002-6224-0830
[2] Doctor. Universidad de ingeniería y Tecnología UTEC (Perú), jramos@utec.edu.pe, ORCID iD: https://orcid.org/0000-0002-1713-7893
[3] Doctor. Universidad Nacional de ingeniería UNI (Perú), mquintana@uni.edu.pe, ORCID iD: https://orcid.org/0000-0002-2677-6179
[4] Doctor. Association of Energy Engineers (United States of America), jwong@aeecenter.org, ORCID iD: https://orcid.org/0000-0002-1745-4282
[5] Máster en Ingeniería Civil. Universidad Autónoma del Perú (Perú), warroyo@autonoma.edu.pe, ORCID iD: https://orcid.org/0000-0003-2679-5326

Memoria Investigaciones en Ingeniería, núm. 29 (2025). pp. 152-165
https://doi.org/10.36561/ING.29.10
ISSN 2301-1092 • ISSN (en línea) 2301-1106 – Universidad de Montevideo, Uruguay
Este es un artículo de acceso abierto distribuido bajo los términos de una licencia de uso y distribución CC BY-NC 4.0. Para ver una copia de esta licencia visite http://creativecommons.org/licenses/by-nc/4.0/

Resumen. - *El estudio busca evaluar y comprender la percepción general de los grupos de interés involucrados en la adopción de vehículos eléctricos sobre las barreras que impiden su masificación. Los vehículos eléctricos ofrecen beneficios, la mejora de la salud pública, la reducción de las importaciones del petróleo y el impacto ambiental. Sin embargo, la tasa de adopción de vehículos eléctricos en muchos países es relativamente baja y varía considerablemente entre países desarrollados y en desarrollo. En los mercados emergentes, los actores clave deben conocer las barreras más significativas que impiden su masificación para determinar qué políticas podrían implementarse para impulsar su adopción. La Evaluación de Impacto Social (SIA) se ha convertido en un factor clave para determinar la viabilidad de los proyectos, conocer las expectativas de la población sobre proyectos o programas, realizar un estudio de mercado y contribuir a la toma de decisiones. En este estudio, proponemos un enfoque para la SIA utilizando un método integrado de agrupamiento gris y ponderación por entropía (método IGCEW). En Perú, se identificaron cuatro grupos de interés y se evaluaron las tres principales barreras. Como resultado, se obtendrá la ponderación de cada barrera en la introducción de vehículos eléctricos en un mercado emergente.*

Palabras clave: *Vehículos Eléctricos; Barreras; Adopción de VE; Mercados emergentes.*

Resumo. ***-*** *O estudo busca avaliar e compreender a percepção geral dos stakeholders envolvidos na adoção de veículos elétricos quanto às barreiras que impedem seu uso generalizado. Os veículos elétricos oferecem benefícios como independência da frota em relação aos combustíveis fósseis, melhoria da saúde pública e redução de importações e impacto ambiental. No entanto, a taxa de adoção de veículos elétricos em muitos países é relativamente baixa e varia consideravelmente entre países desenvolvidos e em desenvolvimento. Nos mercados emergentes, os principais participantes precisam entender as barreiras mais significativas à adoção generalizada e, consequentemente, determinar quais políticas podem ser implementadas para impulsionar a adoção. As Avaliações de Impacto Social (SIA) se tornaram fatores-chave para determinar a viabilidade de projetos, entender as expectativas do público em relação a projetos ou programas, conduzir pesquisas de mercado e contribuir para a tomada de decisões. Neste estudo, propomos uma abordagem para SIA usando um método integrado de agrupamento de cinzas e ponderação de entropia (método IGCEW). No Peru, quatro grupos de interesse foram identificados e as três principais barreiras foram avaliadas. O resultado será uma ponderação de cada barreira à introdução de veículos elétricos em um mercado emergente.*

Palavras-chave: *Veículos elétricos, Barreiras, Adoção de VE; Mercados emergentes.*

1. Introduction. - In Peru, particularly in Lima, there is a lack of urban planning and territorial organization. This is exacerbated by massive migration from rural provinces to the city. Thus, exponential population growth (people and cars) has resulted in severe problems with traffic, noise, pollution and health. This situation makes the transportation sector the most critical priority for the Peruvian government, just behind public safety. Peru's transportation sector represents 43% of the national energy demand. In addition, vehicles cause 40% of CO2eq emissions from all energy consumers [1], resulting in a 3% GHG annual emission growth rate. This puts Lima in the 22nd place of most polluted cities in the world. According to WHO, in Lima 15,000 people die annually due to respiratory and cardiac diseases caused or aggravated by environmental pollution [2], It can't be overemphasized that chaotic transportation and uncontrolled pollution negatively impact public health and quality of life, as well as public safety, security and business development, including tourism [3]. According to Peru's National Society of Mining, Petroleum and Energy (SNMPE), the trade balance of hydrocarbons for Peru is negative (more imports than exports) and this situation has caused a trade deficit of US$3,587 million in 2017 [4]. This shows Peru is highly dependent on imported oil, weakening its trade balance. This makes Peru a vulnerable country, economically and strategically.

So, it is imperative that the government of Peru urgently focus on developing and implementing viable and sustainable alternatives to the above-described set of intertwined and interdependent demographics transportation, pollution, health, and safety problems. Clearly, a more effective, efficient and environmentally sound transportation system must be implemented as part of a systemic approach. Transport electrification using renewable sources of energy will significantly reduce emissions, improve public health and enhance quality of life. This is a universal concern in urban areas of both developed and developing countries alike [5]. From the energy supply side, Peru's oil production is decreasing year after year. Considering it is a nonrenewable resource that is now harder to obtain locally and more expensive to buy internationally, transport electrification should be an obvious alternative. But, thus far, it is not in Peru. Note Peru has untapped potential in hydro, solar, wind, geothermal and cogeneration (combined heat and power). But oil and gas, addiction and dependency, are hard to quit.

Europe has the transport white paper as a roadmap towards a competitive and efficient transport system in the use of resources, with goals for 2050, the reduction of GHGs in the European Union of between 80 and 95% in 2050 compared to 1990 levels, in addition the use of conventionally fueled cars in urban transport should be reduced by 50% by 2030, and in cities completely eliminated by 2050 [6]. That is to say, in Europe it is already included in the design of energy and transportation policy [7], as well as in the main polluting countries such as China [8] and the United States. [9]. Peru also has a goal of reducing 40% of CO2 emissions by 2030. According to Peru's Ministry of the Environment (MINAM), this means that by 2030 total GHG emissions must not exceed 179 million tons of CO2eq.

To achieve this goal, and to have a more efficient, competitive, sustainable and less-vulnerable energy matrix, many countries are promoting EVs. Thus, Norway is a leading country with the highest per capital sales of EVs, with the aim of using only EVs from 2025 onwards [10]. Japan planned to increase EV and PHEV adoption rate by 15-20% in new cars by 2020 [11]. However, in an International Energy Agency (IEA) report, EV sales in 2020 were less than 1% of total sales. Germany announced a goal to supply 1 million EVs by 2020 [12], but the IEA reports that the country didn't reach half a million in sales in 2020. Therefore, many leading countries have tried ambitious adoption and deployment goals, but the actual adoption rate is much lower than expected. The percentage of EVs sold in the world during 2020 by country is shown in Figure 1.

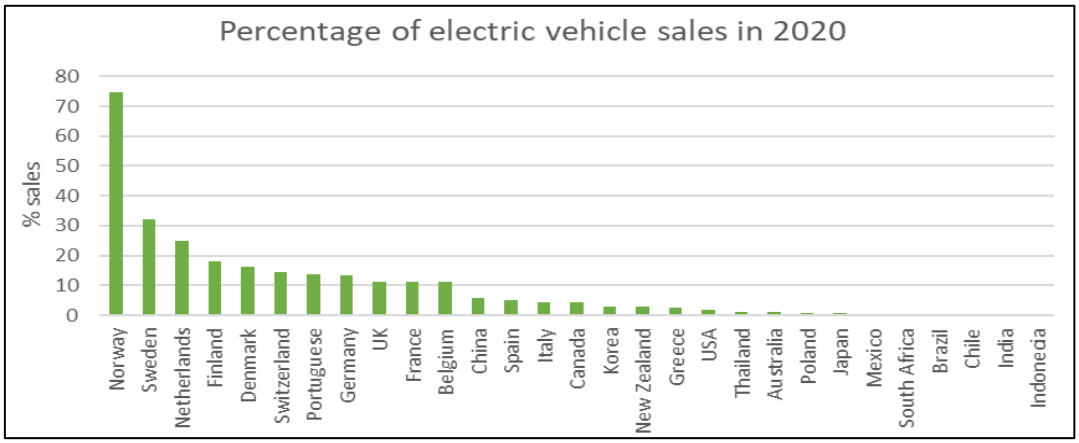

Figure I. 2020 EV Sales in the World [12].

Nevertheless, sales of EVs are slowly increasing everywhere. Consequently, we must insist on better ways to increase adoption and penetration of EVs using public, private and non-government means. Figure 1 clearly shows a big gap between EV adoption in developed versus developing countries. Therefore, in emerging markets, greater efforts should be made to achieve a higher penetration rate of electric vehicles. A market study is needed, because a crucial factor that determines the success or failure of a new technology is user acceptance [13].

Despite the many EV benefits, technological change and sustainable energy conversion are very slow, particularly in developing countries. To accelerate widespread EV adoption, several obstacles must first be overcome. An important barrier is the natural resistance to change of consumers with respect to new technologies, that may be considered foreign or unproven [14]. Thus, seriously considering such attitude is key in first understanding the barrier and eventually in overcoming it. Acceptance by a specific user is hard to predict, and attitudes toward EVs vary greatly between real and potential users [15] for BEV, it is particularly important to acknowledge that entrenched perceptions are affected by historical concerns (often no longer valid) with respect to low performance, poor functionality and safety [16].

It has been shown that it is important to deeply analyze attitudes and perceptions, with respect to widespread adoption [14]. Thus, social impact evaluation, such as SIA, applied to stakeholders at the outset of projects, by integrating technical, social and behavioral perspectives, has been proposed to achieve effective transport decarbonization [17]. Some of the main challenges for adoption include battery technology (capacity/ range/weight), battery cost, and charge infrastructure. However, intrinsic consumer acceptance is important, since many personal and subjective considerations make up ultimate decision criteria [14]. This work focuses on studying the main and most visible barriers to EV adoption, such as cost, range, and charging time. We will quantify with weights each of such barriers as perceived in the Lima, Peru, automotive market. This article contributes in determining what barrier is the most influential and provides a deeper understanding on how EV stake holders make adoption decisions. Such new knowledge should be useful to both public and private organizations.

2. State of the art. -Widespread adoption of EVs has had resistance in countries and cities. Some barriers are more important than others. Barriers often vary by location, market, type of vehicle, vehicle application, culture, economics, geography and energy resources. According to Berkeley et al., 2018, in Europe resistance to adoption is characterized by 12 barriers made of two main groups: “economic uncertainty” and “socio- technical factors.” Economic uncertainty is associated with age and geography, while the socio-technical issues are related to gender [18]. EV sales in 32 European countries identified country economic standing and fuel price [19].

In the Nordic region, common barriers are EV range, price and charge infrastructure in spite of technological progress. It has been shown that many barriers are highly interrelated and, in general, connected to consumer knowledge and experience [20]. In Sweden, new barriers were identified: the number of charge stations and charging preferences [21]. In the UK, the main barrier reported by consumers is EV range [22]. In Ireland, another set of barriers includes lack of sustained promotion and consumer awareness, thus EVs represent only 0.7% of new vehicles in the 2017 market, a

much lower share than those in neighbor countries [23]. In the Netherlands, Amsterdam especially, in 2016, selecting an EV may be impeded by its purchase price and EV residual value uncertainty [24]. In Germany, the defining barriers for private buyers are EV price and range, according to survey data [25] There, high battery cost and immature technology cause only a few BEV and HEV to be considered cost effective without subsidies, when compared to ICEVs [26].

In the UK and Germany, stakeholders report that technology bugs continue to plague EVs' commercial viability. Other barriers are fragmented infrastructure, lack of standards and regulations, and new technology skepticism among consumers [27]. In Switzerland and Finland, a key barrier to widespread adoption is BEV battery capacity, which is the main cause of range anxiety [28]. In Italy, the main barrier is high prices of EVs as compared with conventional cars. In Norway, financial incentives triggered a lower TCO for EVs. In the Netherlands, France and the UK, EV TCO is close to those of ICEVs. In other countries, EV TCOs continue to be higher than conventional cars [29]. Similarly, a study by Palmer shows that in the UK and the US (California and Texas), TOC of every type of electric vehicles (BEV, EVH, and PHEV) is relatively higher than the TOC of ICEV. But the gap has been reduced since the introduction of more EVs in 2015. The gap changed less in the UK, due primarily to the lack of EV subsidies [30]. In France, high cost, lack of charge infrastructure and low promotion are considered the most influential barriers [31]. In Latvia, absence of charge infrastructure and high initial cost are the two defining factors for EV adoption [32]. In the US, early in the process, existing barriers included perceived EV uncertainty and limited range, followed by overall cost [14].

In Asia, a report from Singapore shows that even though EV ownership cost is similar to ICEV's, remaining barriers to adoption are battery technology (range), charge infrastructure, public perception and other related cost factors [33]. In China (Tianjin) public perception barriers to BEV were surveyed, showing that high battery cost topped the barrier list [34]. Other Chinese authors said that in smaller cities with lower income, smaller population and infrastructure limitations, the consumers are more sensitive to purchase price, purchase subsidies and charge station coverage, in contrast to larger cities with more EVs [35]. A different report (He, Zhan, & Hu, 2018) shows that personal norms and consumer personality have a positive influence in proclivity to EV purchasing; specifically, consumers' innovation attitude and environmental concerns were influential. However, environmental concerns are tempered with high external EV cost, including actual purchase cost and perceived complexity [36].

In South America, barriers to implementing a fleet of EV taxis in the city of Cuenca, Ecuador, are broken down as follows: 50% are technological barriers, including range, charge time, charge infrastructure, and certified service personnel; then 25% is vehicle performance; and the remaining 25% is costs (vehicle, battery) and limited potential user knowledge [37]. In Argentina the first barrier is purchase price, next is battery range, third is the lack of public charge infrastructure, and finally the absence of tax incentives [38].

Summarizing this section about barriers, it is clear that a high initial cost continues to be the most important barrier, since it directly affects the total cost of ownership (TCO). Next, lack of better financing mechanisms, lack of charge infrastructure, and range limitation, real or perceived, are often mentioned. There is always some social skepticism and lack of knowledge from most new potential EV consumers [39].

2.1 Objective of the study. - Thus far, the social impact of barriers to EV adoption has been chiefly carried out through qualitative means, resulting in rather subjective interpretations. Consequently, the objective of this work is to apply a quantitative method that should provide more objectivity to the policy- making and decision- making processes, by using the Integrated Grey Clustering and Entropy Weight (IGCEW) method. This research focuses solely on the private light automotive market of Lima, Peru

3. Methodology. -

3.1 Evaluation method. - This section provides a description of the Integrated Grey Clustering and Entropy Weight Method. Both methods are combined in one (IGCEW) to assess the social impact of each barrier listed in Table 1, as a quantitative market research tool.

Criteria	Barriers	Description
C1	Autonomy	How many km can you drive before discharging.
C2	High Price	Expensive compared to a conventional vehicle
C3	Recharge time	Charging time is longer in electric vehicles

Table I. Main Barriers

Social Impact Assessment (SIA) is a method to evaluate project viability where social preferences are key inputs. The key strategy of SIA is to understand peoples' preferences and concerns and also be able to address such preferences and concerns, thus minimizing potential social conflicts, while concurrently influencing both private decision making and public policy making. Similarly, understanding stakeholder drivers is a key success driver in any social project or program that involves significant change [40]. In general, other studies about EV preferences with public participation are based on qualitative methods [41]. To achieve more objectivity in analysis and decision making, this work attempts a more quantitative approach. The grey clustering method is based on the theory of grey systems, originally developed by Deng (1982) [42]. Grey systems is a theory that deals with small samples and limited information [43]. The Grey Clustering approach considers the uncertainty and classifies observed objects in grey classes [43]. Such a methodology has contributed to classifying air quality [44], energy quality [45], and drought risk [46], among others.

Shannon's entropy concept is applied to measure differences among various criteria and is used in decision making [47]. Thus, the weight-entropy method is based on the theory originally developed by Claude E. Shannon [48]. Such a theory has contributed to resolve or clarify diverse issues, such as transport (shared taxi) [49], environmental [50], risk assessment (hazardous materials transportation and handling) [51], social conflicts [43], decision making [52], and others.

3.2 Grey clustering method based on central triangular whitening function. - In this article we use the grey clustering method, based on a central triangular whitening function (CTWF), applied to stakeholder groups as SIA observation objects.

The CTWF function for GREY CLUSTERING

$$f_j^k(x_{ij}) = \begin{cases} 0, & x \notin [\lambda_{k-1}, \lambda_{k+1}] \\ \frac{x-\lambda_{k-1}}{\lambda_k-\lambda_{k-1}}, & x \in [\lambda_{k-1}, \lambda_k] \\ \frac{\lambda_{k+1}-x}{\lambda_{k+1}-\lambda_k}, & x \in [\lambda_k, \lambda_{k+1}] \end{cases} \quad (1)$$

Where $f_j^k(x_{ij})$ is the CTWF of the k-th gray class of the j-th criterion,

Case study:
Our applying IGCEW for SIA was aimed at identifying the most critical barriers to EV widespread adoption in Peru, by observing the attitudes and behaviors of key stakeholders in Lima, Peru.

Stakeholder groups:

- EV Owners (G1). People who have purchased or leased an EV or more.
- Future EV Buyers (G2). People who want to buy an EV and said so.
- EV suppliers and importers (G3). We focused on salespeople who understand consumers' preferences and decision-making process.
- Specialists (G4). These are experts and professionals who are well informed about EVs.

Center points of extended gray classes						
λ_0	λ_1	λ_2	λ_3	λ_4	λ_5	λ_6
0	10	30	50	70	90	100

Table II. Type Extended gray classes in case study

	Very Negative	Negative	Normal	Positive	Very Positive
C_1	$0 \leq x_{11} \leq 20$	$20 \leq x_{21} \leq 40$	$40 \leq x_{31} \leq 60$	$60 \leq x_{41} \leq 80$	$80 \leq x_{51} \leq 100$
C_2	$0 \leq x_{12} \leq 20$	$20 \leq x_{22} \leq 40$	$40 \leq x_{32} \leq 60$	$60 \leq x_{42} \leq 80$	$80 \leq x_{52} \leq 100$
C_3	$0 \leq x_{13} \leq 20$	$20 \leq x_{23} \leq 40$	$40 \leq x_{33} \leq 60$	$60 \leq x_{43} \leq 80$	$80 \leq x_{53} \leq 100$

Table III. Grey Classes for Each Criterion CJ, J=1,2,3

Shannon showed that a function that satisfies the characteristics for measuring entropy or degree of disorder can be:

$$H_{shannon} = -k \sum_i^n p_i * \log(p_i) \quad (2)$$

Where: $0 \leq p_i \leq 1$; for $\sum_i^n p_i = 1$

Step 2: The entropy H_j of each criterion C_j is calculated using Eq. (3)

The normalization matrix, entropy

$$H_j = -k \sum_{i=1}^m p_{ij} * \ln (p_{ij}) \quad (3)$$

Step 3. The degree of divergence div_j, is calculated

$$div_j = 1 - H_j \quad (4)$$

Step 4. The degree of convergence cov_j, is calculated (it is the contribution of the research)

$$cov_j = 1/div_j \quad (5)$$

Step 5. Normalization of each criterion (barrier or policy) w_j is calculated by the equation

$$w_j = \frac{cov_j}{\sum_{i=1}^m cov_j} \quad (6)$$

Step 6. The Weight of the criterion (barrier or policy) w_j is calculated by equation (7)

$$z_{ij} = \sum_{K=1}^S f_i^k(x_{ij}) \bullet \alpha_k \quad (7)$$

Step 7. For our purpose of prioritizing the policies, equation (10) is obtained, obtaining the Weight of the criterion (barrier or policy) w_j^*

$$w_j^* = w_j . z_j \quad (8)$$

4. Results. - Table IV is the X matrix, from stakeholder groups survey output data. Tables V through XIII summarize the results of applying the underlying grey clustering methodology to the data obtained from the survey. Next, we determine the convergence for the data listed in Table XIII.

	C_1	C_2	C_3
G_1	52.14	65.00	67.65
G_2	54.00	74.00	69.00
G_3	47.33	73.53	66.47
G_4	72.50	75.00	72.50

Table IV. Matrix X, Results from Survey to Stakeholder Groups Gi and Criteria Cj

	C_1	C_2	C_3
f11	0.0000	0.0000	0.0000
f21	0.0000	0.0000	0.0000
f31	0.8930	0.2500	0.1175
f41	0.1070	0.7500	0.8825
f51	0.0000	0.0000	0.0000

Table V. CTWF Values for Group 1 Grey Clustering

	C_1	C_2	C_3
f_{12}	0.0000	0.0000	0.0000
f_{22}	0.0000	0.0000	0.0000
f_{32}	0.8000	0.0000	0.0500
f_{42}	0.2000	0.8000	0.9500
f_{52}	0.0000	0.2000	0.0000

Table VI. CTWF Values for Group 2 Grey Clustering.

	C_1	C_2	C_3
f_{13}	0.0000	0.0000	0.0000
f_{23}	0.1335	0.0000	0.0000
f_{33}	0.8665	0.0000	0.1765
f_{43}	0.0000	0.8235	0.8235
f_{53}	0.0000	0.1765	0.0000

Table VII. CTWF Values for Group 3 Grey Clustering

	C_1	C_2	C_3
f_{14}	0.0000	0.0000	0.0000
f_{24}	0.0000	0.0000	0.0000
f_{34}	0.0000	0.0000	0.0000
f_{44}	0.8750	0.7500	0.8750
f_{54}	0.1250	0.2500	0.1250

Table VIII. CTWF Values for Group 4 Grey Clustering

Social impact class	Interval	α_k
Very negative	[20,30]	20
Negative	[30,50]	40
Normal	[50,70]	60
Positive	[70,90]	80
Very positive	[90,100]	100

Table IX. social impact evaluation for groups G1, G2 and G3.

	C_1	C_2	C_3
G_1	62.14	75.00	77.65
G_2	64.00	84.00	79.00
G_3	57.33	83.53	76.47
G_4	82.50	85.00	82.50

Table X. Impact Matrix for Each Combination of Criterion and Stakeholder Group

	C_1	C_2	C_3
G_1	0.23363	0.22899	0.24602
G_2	0.24063	0.25646	0.25030
G_3	0.21555	0.25503	0.24228
G_4	0.310185	0.25952	0.26139

Table XI. Normalized social impact matrix

	C_1	C_2	C_3
H_j	807.1473	1041.0942	994.6186
Div_j	0.71608	0.63379	0.65013
W_j	0.3580	0.3169	0.3251

Table XII. Determination of Divergence of weights for each barrier or Criterion. Values for H_j, div_j and W_j for each Criterion C-j used in the Case Study

	C_1	C_2	C_3
$1/div_j$	1.3965	1.5778	1.5381
Cov_j	0.3095	0.3496	0.3408
Alfa	66.4925	81.882	78.905
W_j^*	20.578	28.631	26.896

Table XIII. Determination of Convergence Values and Weights for each Criterion

5. Discussion of results. -

5.1 Analysis of Convergent Criteria. - EV introduction to a new market or country encompasses a cultural, energy and technological transition. Barriers to adoption are ever present and need to be eliminated or lower to achieve a successful introduction and eventual widespread adoption.

Limited Range. - The range from an EV battery depends on several variables, including battery capacity, drive train efficiency, vehicle aerodynamics, driving habits, loads (carrying and hauling), road quality, geography, etc. This factor is often a defining one for many potential buyers [39]. Such concern has been consistently observed in the US [14], Switzerland and Finland [28]. In Ecuador, range is considered the main barrier [37], as well as in Singapore [33], Germany [25], and the UK [22].

High Price. - The gap between an EV's initial cost and a conventional ICEV's varies between the cost US $6,000 to $8,000 of comparable vehicles. In 32 European countries, the purchasing cost was identified as the main economic barrier [19]. This was shown in France [31], Latvia [32], and the Netherlands [24]. Also, initial cost was the main barrier in China [34] and Argentina [38]. A high initial cost impacts "Overall Cost of Ownership" or TCO, which also depends on the financing options and financial cost available [39]. Countries, regions or cities with lower purchasing power, less population and infrastructure limitations, have consumers that are even more sensitive to the purchasing price of any vehicle, electric or conventional [35].

Charge Time. - Charging (or filling up) a conventional or ICE car is quick and simple. But depending on several factors, charging EVs takes longer, and many users are not willing to wait so long for a full battery charge. This is often a key concern, given the lack of availability of rapid-charging stations. Most users do not want to interrupt and delay their road or city trips with excessive charging times [22], [25], [53]. In addition, charging time relates to range anxiety (smaller batteries can be charged quicker but have shorter EV range). Both factors are serious obstacles for adoption [28]. Thus quicker, more powerful (kW) and more expensive chargers are needed or expected for EVs with larger batteries (more kWh). Such expectations are manifest in Sweden [21], France [31], Singapore [33], Latvia [32], Colombia [54] and Argentina [38]. Technical barriers such as "lack of charge infrastructure," and "real vs. perceived range limitations" are present in most countries. In addition, there is "social skepticism" due to lack of awareness and knowledge by consumers [39]. In Latvia, a larger number of charge stations and free charging policy are appreciated by users [55], while in Switzerland and Finland, consumers demand ease (speed) of charging [28]. In general, commercial users have a higher preference for rapid charging systems, than private users [56].

Barrier ranking. - Social Impact Assessment (SIA) of barriers to adoption was carried out by using qualitative and quantitative approaches. The impact of barriers was measured through weights w for each barrier and criterion. Table XIV lists the ranking of each barrier/criterion pair with the corresponding weight wj*.

Wj*	Criteria	barriers
28.631	C2	High price
26.896	C3	Recharge time
20.578	C1	Autonomy range

*Table XIV. Ranking of barriers/criteria using weights Wj**

6. Conclusions. - We have first identified and then qualitatively evaluated the barriers that impede EV's widespread adoption in Lima, Peru. Next, we have ranked and prioritized such barriers to help define more effective government and business policies that support a transition to EVs. By applying the IGCEW method, we have been able to make sense of qualitative information provided by four (4) stakeholder groups. We found that the first barrier is purchase price (initial cost), next is charging availability (ease of charging), and finally EV/battery range. A higher purchase price is even more important in lower-income towns, while range expectation depends on the intended EV use (urban vs. road). And commercial users give a higher priority to quick charging than private users. What we have learned in this work should help both Peruvian government and automotive businesses develop a more effective and coordinated strategy towards EV introduction, a smoother transition from ICE vehicles and eventual widespread adoption of EVs.

References

[1] Osinergmin, “El Sector Transporte Terrestre, el Uso de la Energía y sus Impactos en el Cambio Climático,” 2014.

[2] DW, “Las capitales y países de América Latina más contaminados”, 16/05/2019, p. www.dw.com/es/, May 2019.

[3] C. McAndrews and E. Deakin, “Public health sector influence in transportation decision- making: The case of health impact assessment,” Case Stud Transp Policy, 2018, doi: 10.1016/j.cstp.2018.02.002.

[4] Gestion.pe, “SNMPE: Déficit de balanza comercial de hidrocarburos del Perú suma US$ 3,587 millones,” diario Gestion, Lima-Peru, Aug. 28, 2018. https://gestion.pe/economia/snmpe- deficit-balanza-comercial- hidrocarburos-peru-suma-us-3-587-millones-242843- noticia/?ref=gesr.

[5] M. Contestabile, M. Alajaji, and B. Almubarak, “Will current electric vehicle policy lead to cost-effective electrification of passenger car transport?,” Energy Policy, vol. 110, no. January,
pp. 20–30, 2017, doi: 10.1016/j.enpol.2017.07.062.

[6] European Commission, Roadmap to a Single European Transport Area– Towards a competitive and resource efficient transport system. 2011. doi: 10.2832/30955.

[7] A. Ajanovic and R. Haas, “Dissemination of electric vehicles in urban areas: Major factors for success,” Energy, vol. 115, pp. 1451–1458, 2016, doi: 10.1016/j.energy.2016.05.040.

[8] X. Zhang, Y. Liang, E. Yu, R. Rao, and J. Xie, “Review of electric vehicle policies in China: Content summary and effect analysis,” Renewable and Sustainable Energy Reviews, vol. 70, no. May 2015, pp. 698–714, 2017, doi: 10.1016/j.rser.2016.11.250.

[9] S. A. Adderly, D. Manukian, T. D. Sullivan, and M. Son, “Electric vehicles and natural disaster policy implications,” Energy Policy, vol. 112, no. November 2017, pp. 437–448, 2018, doi: 10.1016/j.enpol.2017.09.030.

[10] G. Bauer, “The impact of battery electric vehicles on vehicle purchase and driving behavior in Norway,” Transp Res D Transp Environ, vol. 58, pp. 239–258, 2018, doi: 10.1016/j.trd.2017.12.011.

[11] T. Maruyama, A. Division, and M. I. Bureau, “Japan ’ s Initiatives for the diffusion of Next- Generation Vehicles Tomohisa Maruyama , Deputy Director Automobile Division , Manufacturing Industries Bureau , METI Diffusion Targets for Next-Generation Vehicles,” 2014.

[12] W. MacDougall, “Electromobility in Germany: Vision 2020 and Beyond,” Germany Trade & Invest, p. 46, 2013.

[13] F. D. Davis, “User acceptance of computer technology: system characteristics, user perceptions.,” Int. J. Man Mach., vol. Stud. 38, pp. 457–487., 1993.

[14] O. Egbue and S. Long, “Barriers to widespread adoption of electric vehicles: An analysis of consumer attitudes and perceptions,” Energy Policy, vol. 48, no. 2012, pp. 717–729, 2012, doi: 10.1016/j.enpol.2012.06.009.

[15] L. Frank, M. Bradley, S. Kavage, J. Chapman, and T. K. Lawton, “Urban form, travel time, and cost relationships with tour complexity and mode choice,” Transportation, vol. 35, no. 1, pp. 37–54, 2008, doi: 10.1007/s11116-007-9136-6.

[16] S. Carley, R. M. Krause, B. W. Lane, and J. D. Graham, “Intent to purchase a plug-in electric vehicle: A survey of early impressions in large US cites,” Transp Res D Transp Environ, vol. 18, no. 1, pp. 39–45, 2013, doi:

10.1016/j.trd.2012.09.007.

[17] T. Schwanen, D. Banister, and J. Anable, "Scientific research about climate change mitigation in transport: A critical review," Transportation Research Part A: Policy and Practice, vol. 45, no. 10, pp. 993–1006, 2011, doi: 10.1016/j.tra.2011.09.005.

[18] N. Berkeley, D. Jarvis, and A. Jones, "Analysing the take up of battery electric vehicles: An investigation of barriers amongst drivers in the UK," Transp Res D Transp Environ, vol. 63, pp. 466–481, 2018, doi: 10.1016/j.trd.2018.06.016.

[19] C. Münzel, P. Plötz, F. Sprei, and T. Gnann, "How large is the effect of financial incentives on electric vehicle sales? – A global review and European analysis," Energy Econ, vol. 84, no. xxxx, p. 104493, 2019, doi: 10.1016/j.eneco.2019.104493.

[20] L. Noel, G. Zarazua de Rubens, J. Kester, and B. K. Sovacool, "Understanding the socio- technical nexus of Nordic electric vehicle (EV) barriers: A qualitative discussion of range, price, charging and knowledge," Energy Policy, vol. 138, no. October 2019, p. 111292, 2020, doi: 10.1016/j.enpol.2020.111292.

[21] I. Vassileva and J. Campillo, "Adoption barriers for electric vehicles: Experiences from early adopters in Sweden," Energy, vol. 120, pp. 632– 641, 2017, doi: 10.1016/j.energy.2016.11.119.

[22] S. M. Skippon, N. Kinnear, L. Lloyd, and J. Stannard, "How experience of use influences mass-market drivers' willingness to consider a battery electric vehicle: A randomised controlled trial," Transp Res Part A Policy Pract, vol. 92, pp. 26–42, 2016, doi: 10.1016/j.tra.2016.06.034.

[23] E. O'Neill, D. Moore, L. Kelleher, and F. Brereton, "Barriers to electric vehicle uptake in Ireland: Perspectives of car-dealers and policy-makers," Case Stud Transp Policy, vol. 7, no. 1, pp. 118–127, 2019, doi: 10.1016/j.cstp.2018.12.005.

[24] H. Quak, N. Nesterova, and T. Van Rooijen, "Possibilities and Barriers for Using Electric- powered Vehicles in City Logistics Practice," Transportation Research Procedia, vol. 12, no. June 2015, pp. 157–169, 2016, doi: 10.1016/j.trpro.2016.02.055.

[25] P. Plötz, U. Schneider, J. Globisch, and E. Dütschke, "Who will buy electric vehicles? Identifying early adopters in Germany," Transp Res Part A Policy Pract, vol. 67, pp. 96–109, 2014, doi: 10.1016/j.tra.2014.06.006.

[26] P. Letmathe and M. Suares, "A consumer-oriented total cost of ownership model for different vehicle types in Germany," Transp Res D Transp Environ, vol. 57, no. 2017, pp. 314– 335, 2017, doi: 10.1016/j.trd.2017.09.007.

[27] S. Steinhilber, P. Wells, and S. Thankappan, "Socio-technical inertia: Understanding the barriers to electric vehicles," Energy Policy, vol. 60, pp. 531–539, 2013, doi: 10.1016/j.enpol.2013.04.076.

[28] M. A. Melliger, O. P. R. van Vliet, and H. Liimatainen, "Anxiety vs reality – Sufficiency of battery electric vehicle range in Switzerland and Finland," Transp Res D Transp Environ, vol. 65,
pp. 101–115, 2018, doi: 10.1016/j.trd.2018.08.011.

[29] P. Z. Lévay, "The effect of fiscal incentives on market penetration of electric vehicles: A pairwise comparison of total cost of ownership," Energy Policy, vol. 105, no. February, pp. 524– 533, 2017, doi: 10.1016/j.enpol.2017.02.054.

[30] K. Palmer, "Total cost of ownership and market share for hybrid and electric vehicles in the UK, US and Japan," Appl Energy, vol. 209, no. October 2017, pp. 108–119, 2018, doi: 10.1016/j.apenergy.2017.10.089.

[31] E. Windisch, “Driving electric? A financial analysis of electric vehicle policies in France to cite this version: HAL Id: tel-00957749 Université Paris-Est Thèse de doctorat Spécialité Transport Driving electric? A financial assessment of electric vehicle policies,” 2014.

[32] A. Barisa, M. Rosa, and A. Kisele, “Introducing Electric Mobility in Latvian Municipalities: Results of a Survey,” Energy Procedia, vol. 95, pp. 50–57, 2016, doi:0.1016/j.egypro.2016.09.015.

[33] V. Nian, H. M.P., and J. Yuan, “The prospects of electric vehicles in cities without policy support,” Energy Procedia, vol. 143, pp. 33–38, 2017, doi: 10.1016/j.egypro.2017.12.644.

[34] Z. Y. She, Qing Sun, J. J. Ma, and B. C. Xie, “What are the barriers to widespread adoption of battery electric vehicles? A survey of public perception in Tianjin, China,” Transp Policy (Oxf), vol. 56, no. February, pp. 29–40, 2017, doi: 10.1016/j.tranpol.2017.03.001.

[35] Y. Huang and L. Qian, “Consumer preferences for electric vehicles in lower tier cities of China: Evidences from south Jiangsu region,” Transp Res D Transp Environ, vol. 63, pp. 482– 497, 2018, doi: 10.1016/j.trd.2018.06.017.

[36] X. He and W. Zhan, “How to activate moral norm to adopt electric vehicles in China? An empirical study based on extended norm activation theory,” J Clean Prod, vol. 172, pp. 3546– 3556, 2018, doi: 10.1016/j.jclepro.2017.05.088.

[37] W. J. Ordóñez Chillogalli, “Estudio de las barreras que impiden la Introducción del Vehículo Eléctrico en la flota de taxis en la ciudad e Cuenca”,” (Universidad Politécnica Salesiana), Ecuador, 2019.

[38] S. De Luca, R. Di Pace, and F. Storani, “A Study on Users’ Behaviour Towards Electric Vehicles in Immature Markets: The Argentina Case Study,” Proceedings - 2018 IEEE International Conference on Environment and Electrical Engineering and 2018 IEEE Industrial and Commercial Power Systems Europe, EEEIC/I and CPS Europe 2018, pp. 1–6, 2018, doi: 10.1109/EEEIC.2018.8493840.

[39] G. Haddadian, M. Khodayar, and M. Shahidehpour, “Accelerating the Global Adoption of Electric Vehicles: Barriers and Drivers,” Electricity Journal, vol. 28, no. 10, pp. 53–68, 2015, doi: 10.1016/j.tej.2015.11.011.

[40] S. H. Hamilton, S. Elsawah, J. H. A. Guillaume, A. J. Jakeman, and S. A. Pierce, “Environmental Modelling & Software Integrated assessment and modelling: Overview and synthesis of salient dimensions,” Environmental Modelling and Software, vol. 64, pp. 215–229, 2015, doi: 10.1016/j.envsoft.2014.12.005.

[41] B. Tang, S. Wong, and M. C. Lau, “Social impact assessment and public participation in China: A case study of land requisition in Guangzhou,” vol. 28, pp. 57–72, 2008, doi: 10.1016/j.eiar.2007.03.004.

[42] L. Y. Liu Sifeng., Introduction to Grey Systems Theory. In: Grey Systems. Understanding Complex Systems, vol 68. Berlin, Heidelberg., 2010. doi: https://doi.org/10.1007/978-3-642- 16158-2_1.

[43] A. Delgado and I. Romero, “Environmental Modelling & Software Environmental con fl ict analysis using an integrated grey clustering and entropy-weight method: A case study of a mining project in Peru,” Environmental Modelling and Software, vol. 77, pp. 108–121, 2016, doi: 10.1016/j.envsoft.2015.12.011.

[44] A. Delgado, P. Montellanos, and J. Llave, “Air quality level assessment in Lima city using the grey clustering method,” IEEE ICA-ACCA 2018 - IEEE International Conference on Automation/23rd Congress of the Chilean Association of Automatic Control: Towards an Industry 4.0 - Proceedings, pp. 1–4, 2019, doi: 10.1109/ICA-ACCA.2018.8609699.

[45] M. Sacasqui, J. Luyo, and A. Delgado, "A Unified Index for Power Quality Assessment in Distributed Generation Systems Using Grey Clustering and Entropy Weight," 2018 IEEE ANDESCON, ANDESCON 2018 - Conference Proceedings, pp. 1–4, 2018, doi: 10.1109/ANDESCON.2018.8564631.

[46] D. Luo, L. Ye, and D. Sun, "Risk evaluation of agricultural drought disaster using a grey cloud clustering model in Henan province, China," International Journal of Disaster Risk Reduction, vol. 49, no. June, p. 101759, 2020, doi: 10.1016/j.ijdrr.2020.101759.

[47] C. Carlsson, "Fuzzy multiple criteria decision making: Recent developments," Fuzzy Sets Syst, vol. 78, no. 2, pp. 139–153, 1996, doi: 10.1016/0165-0114(95)00165-4.

[48] W. Shannon, C.E., Weaver, "The Mathematical Theory of Communication.," The University of Illinois Press, Urbana., vol. 27, no. 1, pp. 212–214, 1948.

[49] Q. Xiao, R. He, C. Ma, and W. Zhang, "Evaluation of urban taxi- carpooling matching schemes based on entropy weight fuzzy matter- element," Applied Soft Computing Journal, vol. 81, p. 105493, 2019, doi: 10.1016/j.asoc.2019.105493.

[50] R. K. Srivastav and S. P. Simonovic, "An analytical procedure for multi- site, multi-season streamflow generation using maximum entropy bootstrapping," Environmental Modelling and Software, vol. 59, pp. 59– 75, 2014, doi: 10.1016/j.envsoft.2014.05.005.

[51] W. Huang et al., "Historical data-driven risk assessment of railway dangerous goods transportation system: Comparisons between Entropy Weight Method and Scatter Degree Method," Reliab Eng Syst Saf, vol. 205, no. September 2020, p. 107236, 2021, doi: 10.1016/j.ress.2020.107236.

[52] M. Song, Q. Zhu, J. Peng, and E. D. R. Santibanez Gonzalez, "Improving the evaluation of cross efficiencies: A method based on Shannon entropy weight," Comput Ind Eng, vol. 112, pp. 99–106, 2017, doi: 10.1016/j.cie.2017.07.023.

[53] T. Gnann, P. Plötz, A. Kühn, and M. Wietschel, "Modelling market diffusion of electric vehicles with real world driving data - German market and policy options," Transp Res Part A Policy Pract, vol. 77, pp. 95–112, 2015, doi: 10.1016/j.tra.2015.04.001.

[54] J. Restrepo, J. Rosero, and S. Tellez, "Performance testing of electric vehicles on operating conditions in Bogotá DC, Colombia," 2014 IEEE PES Transmission and Distribution Conference and Exposition, PES T and D-LA 2014 - Conference Proceedings, vol. 2014-Octob, 2014, doi: 10.1109/TDC-LA.2014.6955276.

[55] L. Raslavičius, B. Azzopardi, A. Keršys, M. Starevičius, Ž. Bazaras, and R. Makaras, "Electric vehicles challenges and opportunities: Lithuanian review," Renewable and Sustainable Energy Reviews, vol. 42, pp. 786– 800, 2015, doi: 10.1016/j.rser.2014.10.076.

[56] X. H. Sun, T. Yamamoto, and T. Morikawa, "Fast-charging station choice behavior among battery electric vehicle users," Transp Res D Transp Environ, vol. 46, pp. 26–39, 2016, doi: 10.1016/j.trd.2016.03.008

Author contribution:

1. Conception and design of the study
2. Data acquisition
3. Data analysis
4. Discussion of the results
5. Writing of the manuscript
6. Approval of the last version of the manuscript

RNT has contributed to: 1, 2, 3 4, 5 and 6.

JRS has contributed to: 1, 2, 3 4, 5 and 6.

MQC has contributed to: 1, 2, 3 4, 5 and 6.

JWK has contributed to: 1, 2, 3 4, 5 and 6.

WAD has contributed to: 1, 2, 3 4, 5 and 6.

Acceptance Note: This article was approved by the journal editors Dr. Rafael Sotelo and Mag. Ing. Fernando A. Hernández Gobertti.

Aplicaciones Recientes de Tecnologías Digitales en la Agricultura

Recent Applications of Digital Technologies in Agriculture

Aplicações Recentes de Tecnologias Digitais na Agricultura

Lizmarie Camacho [1(*)], José Simmonds [2], Yaliska Moreno-González [3], Marco Vieto-Vega [4], Yarien Moreno [5], Noriel Correa [6], Marciano Santamaría Lezcano [7], Fabiola Mabel Montero González [8]

Recibido: 26/06/2025 Aceptado: 25/08/2025

Resumen. - El sector agrícola enfrenta múltiples desafíos, además de su papel fundamental en el desarrollo económico y la reducción de la pobreza. Entre estos retos, destaca la necesidad de satisfacer la creciente demanda mundial de alimentos mientras se enfrenta a las adversidades del cambio climático, plagas, inundaciones, incendios forestales, conflictos políticos y guerras, entre otros factores. En este contexto, resulta imprescindible el desarrollo y la implementación de tecnologías adaptadas a las condiciones específicas de cada región para optimizar los distintos procesos agrícolas.

En este sentido, la incorporación de tecnologías digitales en la agricultura ha dado lugar al concepto de Agricultura 4.0, el cual, en los últimos años, ha facilitado la transición de los procesos agrícolas hacia el entorno digital. Esta revisión breve tiene como objetivo analizar y destacar las principales características de las tecnologías digitales aplicadas a la agricultura, así como algunas de sus aplicaciones reportadas en el período comprendido entre 2018 y 2024. Adicionalmente, se abordan los desafíos futuros para la mejora continua de los procesos agrícolas mediante el uso de tecnologías digitales.

Palabras clave: IoT, agricultura de precisión, agrotecnología, Aprendizaje Automático, Inteligencia Artificial.

[1] Estudiante. Facultad de Informática, Electrónica y Comunicación, Universidad de Panamá; Centro de Investigaciones en Tecnologías de la Información y Comunicación, Universidad de Panamá; Centro de Investigación con Técnicas Nucleares, Universidad de Panamá (Panamá), lizmarie.camacho@up.ac.pa, ORCID iD: https://orcid.org/0009-0006-5200-4961

[2] Estudiante. Facultad de Informática, Electrónica y Comunicación, Universidad de Panamá; Centro de Investigaciones en Tecnologías de la Información y Comunicación, Universidad de Panamá; Centro de Investigación con Técnicas Nucleares, Universidad de Panamá (Panamá), jose.simmondsg@up.ac.pa, ORCID iD: https://orcid.org/0000-0002-1406-2232

[3] Ingeniera en Producción Animal (MSc). Facultad de Ciencias Agropecuarias, Universidad de Panamá (Panamá), milena2y@gmail.com, ORCID iD: https://orcid.org/0000-0001-6643-7713

[4] Ingeniero en Sistemas y Computación. School of Mathematics and Statistics, Victoria University of Wellington (Nueva Zelandia), mv030790@gmail.com, ORCID iD: https://orcid.org/0009-0009-0752-0205

[5] Investigador. Facultad de Informática, Electrónica y Comunicación; Centro de Investigaciones en Tecnologías de la Información y Comunicación, Universidad de Panamá (Panamá); Centro de Investigación con Técnicas Nucleares; School of Optical and Electronic Information, Huazhong University of Science and Technology (China)
yarien.moreno@up.ac.pa, ORCID iD: https://orcid.org/0000-0002-6646-8162

[6] Investigador. Facultad de Ciencias Naturales, Exactas y Tecnología; Centro de Investigación con Técnicas Nucleares, Universidad de Panamá; Centro de Investigaciones en Tecnologías de la Información y Comunicación, Universidad de Panamá (Panamá).
noriel.correa@up.ac.pa, ORCID iD: https://orcid.org/0000-0002-9991-7868

[7] Profesor. Facultad de Ciencias Naturales, Exactas y Tecnología, Departamento de Física, Centro de Investigación con Técnicas Nucleares, Universidad de Panamá; Centro de Investigaciones en Tecnologías de la Información y Comunicación, Universidad de Panamá (Panamá), marciano.santamaria@up.ac.pa, ORCID iD: https://orcid.org/0000-0002-7081-7273

[8] Profesor Especial I. Facultad de Informática, Electrónica y Comunicación, Departamento de Informática, Universidad de Panamá; Centro de Investigaciones en Tecnologías de la Información y Comunicación, Universidad de Panamá (Panamá), fabiola.monterog@up.ac.pa, ORCID iD: https://orcid.org/0000-0002-4681-9471

Memoria Investigaciones en Ingeniería, núm. 29 (2025). pp. 166-189
https://doi.org/10.36561/ING.29.11
ISSN 2301-1092 • ISSN (en línea) 2301-1106 – Universidad de Montevideo, Uruguay
Este es un artículo de acceso abierto distribuido bajo los términos de una licencia de uso y distribución CC BY-NC 4.0. Para ver una copia de esta licencia visite http://creativecommons.org/licenses/by-nc/4.0/

Summary. - *The agricultural sector faces multiple challenges, in addition to its fundamental role in economic development and poverty reduction. Among these challenges is the need to meet the growing global demand for food while facing the adversities of climate change, pests, floods, forest fires, political conflicts and wars, among other factors.*

In this context, the development and implementation of technologies adapted to the specific conditions of each region is essential to optimize the different agricultural processes. In this sense, the incorporation of digital technologies in agriculture has given rise to the concept of Agriculture 4.0, which, in recent years, has facilitated the transition of agricultural processes towards the digital environment. This brief review aims to analyze and highlight the main characteristics of digital technologies applied to agriculture, as well as some of their applications reported in the period between 2018 and 2024. Additionally, future challenges for the continuous improvement of agricultural processes by digital technologies are addressed.

Keywords: *IoT, precision agriculture, agrotechnology, Machine Learning, Artificial Intelligence.*

***Resumo*. -** *O setor agrícola enfrenta múltiplos desafios, além de seu papel fundamental no desenvolvimento econômico e na redução da pobreza. Entre esses desafios, destaca-se a necessidade de atender à crescente demanda global por alimentos ao mesmo tempo que enfrenta adversidades como mudanças climáticas, pragas, inundações, incêndios florestais, conflitos políticos e guerras, entre outros fatores. Neste contexto, torna-se imprescindível o desenvolvimento e a implementação de tecnologias adaptadas às condições específicas de cada região para otimizar os diversos processos agrícolas.*

Nesse sentido, a incorporação de tecnologias digitais na agricultura deu origem ao conceito de Agricultura 4.0, que nos últimos anos facilitou a transição dos processos agrícolas para o ambiente digital. Esta breve revisão tem como objetivo analisar e destacar as principais características das tecnologias digitais aplicadas à agricultura, bem como algumas das suas aplicações reportadas no período entre 2018 e 2024. Adicionalmente, abordam-se os desafios futuros para a melhoria contínua dos processos agrícolas através do uso de tecnologias digitais.

Palavras-chave: *IoT; agricultura de precisão; agrotecnologia; aprendizado de máquina; inteligência artificial.*

1. Introducción. - El sector agrícola desempeña un papel esencial a nivel global, ya que satisface las crecientes demandas alimentarias de la humanidad y contribuye significativamente al desarrollo económico y la reducción de la pobreza. En este contexto, mejorar la calidad de vida de las comunidades rurales, particularmente en los países en desarrollo, es fundamental para impulsar el progreso agrícola. Esto requiere la formulación constante de estrategias y políticas adecuadas que integren el desarrollo de tecnologías aplicadas a la agricultura, capaces de abordar las necesidades específicas de cada región. Entre estas tecnologías destacan herramientas como los sistemas de posicionamiento global, dispositivos de distribución de riego, técnicas avanzadas de captura y análisis de datos, redes de sensores, y el uso de drones, entre otras [1].

La aplicación de estas innovaciones tecnológicas trasciende áreas específicas de la agricultura y abarca diversas técnicas de cultivo. Por ejemplo, la hidroponía, que permite el cultivo de plantas mediante soluciones minerales sin necesidad de suelo agrícola [2], o la acuaponía, que integra el cultivo de peces con sistemas hidropónicos para la producción de plantas [3], la agricultura vertical representa una solución innovadora, al cultivar plantas en capas verticales, optimizando el espacio disponible y permitiendo la producción de cosechas durante todo el año en entornos urbanos o interiores. Estas prácticas no solo impulsan la sostenibilidad y la eficiencia, sino que también ofrecen soluciones concretas a los desafíos globales de la seguridad alimentaria.

La agricultura vertical constituye una innovación dentro de un enfoque más amplio conocido como agricultura urbana, definida como el proceso de aprovechar pequeñas áreas para la producción de cultivos, la cría de especies menores e incluso la obtención de productos medicinales [4]. Esta técnica ha sido implementada con éxito, particularmente en países con limitaciones de espacio físico, como Japón y Singapur, ya que ofrece una solución sostenible y eficiente para optimizar la producción agrícola y las diversas etapas de la cadena de suministro de alimentos [5], [6]. Además, al desarrollarse en un entorno controlado, la agricultura vertical minimiza el desperdicio de cultivos ocasionado por condiciones climáticas adversas o plagas imprevistas [7].

La relevancia de esta técnica radica en la integración de tecnologías avanzadas, como sistemas de automatización, almacenamiento de datos y monitoreo en tiempo real, que permiten la medición precisa de variables físicos clave para el cultivo, como temperatura ambiental, presión atmosférica y humedad relativa. Estas herramientas contribuyen significativamente al aumento de la productividad agrícola mediante la adopción de tecnologías emergentes, tales como la Automatización Industrial, Big Data, Computación en la Nube, Ciencia de Datos, Internet de las Cosas (IoT), Inteligencia Artificial (IA) y Aprendizaje Automático, entre otras [8].

Por otro lado, las agrotecnologías, también conocidas como Agricultura 4.0, representan implementaciones tecnológicas que ofrecen un amplio abanico de posibilidades para el desarrollo y seguimiento de proyectos de alto rendimiento en el sector agrícola. Entre las principales ventajas de estas tecnologías se encuentran la optimización del espacio destinado al cultivo, la toma de decisiones informadas basadas en el análisis de datos recolectados mediante redes soportadas por tecnología IoT, y el empleo de Inteligencia Artificial para monitorear el estado de los cultivos a través del análisis de imágenes. Asimismo, estas tecnologías permiten la categorización y predicción de las propiedades del suelo mediante técnicas avanzadas de aprendizaje automático, entre otros beneficios, lo cual permite la mejora constante de los distintos procesos agrícolas [9].

Figura I. Concepto de Agricultura Inteligente. Adaptada de [10].

En la Figura I se observa cómo el concepto de "Agricultura Inteligente" se integra dentro del marco de la Industria 4.0. Este enfoque aprovecha tecnologías emergentes como drones, análisis de datos, Internet de las Cosas (IoT), robótica, entre otras, para optimizar y aumentar la producción agrícola, contribuyendo así de manera eficiente y sostenible a la seguridad alimentaria. Asimismo, estas innovaciones no solo mejoran la productividad agrícola, sino que también generan nuevas oportunidades laborales y fomentan el desarrollo y la investigación en el sector [10].

Por otro lado, la Agricultura 4.0 no se limita únicamente a la producción agrícola directa, sino que también impacta sectores clave relacionados, como el energético, el meteorológico y el hídrico, que influyen directa e indirectamente en el crecimiento de los cultivos [11], [12]. Esto amplía significativamente las posibilidades para desarrollar e implementar aplicaciones basadas en tecnologías emergentes, con un impacto positivo en el crecimiento del sector agrícola. Sumado a ello, en los últimos años, se ha registrado un aumento considerable en la adopción de agrotecnologías a nivel mundial, con la ejecución de numerosos proyectos que han tenido un impacto directo e indirecto en la economía de diversos países [13], [14], [15]. En este contexto, el presente trabajo ofrece una revisión breve de las aplicaciones de tecnologías digitales orientadas a abordar los múltiples desafíos actuales en diversos sectores de la agricultura.

2. Metodología. - Esta investigación se basa en una revisión de alcance con síntesis narrativa sobre la contribución de las tecnologías digitales al desarrollo del sector agrícola. Se buscaron estudios publicados entre 2018 y 2024, en español e inglés, en Scopus, Web of Science, IEEE Xplore, ACM Digital Library, ScienceDirect, SpringerLink y Wiley Online Library; Google Scholar se empleó de forma complementaria para ampliar hallazgos/localizar DOI y ResearchGate no se usó como fuente primaria. Las búsquedas combinaron términos como Agricultura de Precisión, smart/precision agriculture, IoT, Wireless Sensor Network, Agrotechnology y Agriculture 4.0, entre otros. Se emplearon cadenas booleanas con operadores AND/OR y comillas; por ejemplo: ("precision agriculture" OR "smart agriculture" OR "Agricultura de Precisión") AND (IoT OR "wireless sensor network" OR WSN) AND ("machine learning" OR "computer vision" OR "edge computing"), aplicando en todas las bases el filtro temporal 2018–2025. La selección de estudios siguió un flujo de cuatro etapas: (i) identificación de registros, (ii) eliminación de duplicados, (iii) cribado por título y resumen, y (iv) evaluación del texto completo para determinar la inclusión final, registrando los conteos y motivos de exclusión. Criterios de inclusión: trabajos revisados por pares con aplicaciones agrícolas y métricas reportadas. Exclusión: preprints no revisados, literatura gris no verificable, reseñas sin datos, ámbitos no agrícolas y duplicados. La calidad y el riesgo de sesgo se valoraron con una lista de chequeo específica para este estudio. La extracción estandarizada recopiló año, país/región, cultivo/escenario, sensores/datos, tamaño de datos, modelo/algoritmo, métricas, baseline, resultados y limitaciones. La síntesis agrupó hallazgos por dominio (riego,

sanidad vegetal, rendimiento, logística) y por tecnología, incluyendo una tabla transversal. Se respetaron licencias al adaptar figuras y se reconocieron limitaciones por sesgos de indexación/idioma y por la heterogeneidad de métricas.

A continuación, se presentan diversas aplicaciones de tecnologías digitales en la agricultura, con sus principales características y su impacto en el desarrollo del sector.

3. Aplicaciones recientes de tecnologías digitales en los procesos agrícolas

3.1. Aprendizaje Automático e Inteligencia Artificial. - Actualmente, la aplicación del Aprendizaje Automático en la agricultura ha experimentado un crecimiento constante, y el desarrollo de estas aplicaciones puede clasificarse en diversas áreas. Una de las clasificaciones más relevantes fue reportada en 2018 por Liakos et al., quienes identificaron cuatro grandes áreas de aplicación del Aprendizaje Automático en la agricultura: manejo de la cosecha, manejo del ganado, manejo del agua y manejo de la tierra [16].

No obstante, las aplicaciones del Aprendizaje Automático y la Inteligencia Artificial se extienden a otros subsectores. En esta sección, se presentan algunas aplicaciones recientes de estas tecnologías orientadas a la Agricultura 4.0. La Figura II ilustra algunas de las técnicas de Aprendizaje Automático (ML por sus siglas en inglés) empleadas para optimizar la agricultura, según lo reportado por [17]. En este estudio, se implementaron ocho modelos de ML en diferentes áreas. Entre ellos, las Redes Neuronales Artificiales (ANN, por sus siglas en inglés) fueron las más utilizadas para la gestión de cultivos, mientras que las Máquinas de Soporte Vectorial (SVM, por sus siglas en inglés) destacaron en la gestión del ganado. Además, se emplearon modelos de ML para optimizar el manejo del agua y del suelo, demostrando su versatilidad en el sector agrícola.

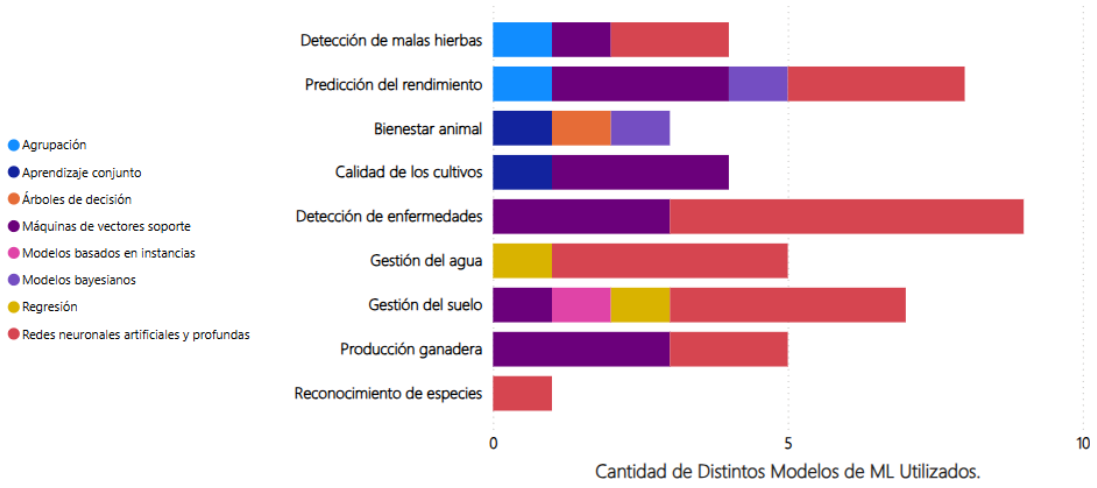

Figura II. Número total de modelos de ML según cada subcategoría, adaptado de [17].

Entre los trabajos destacados en el sector agrícola sobresale el reporte de [18], quienes utilizaron algoritmos basados en Aprendizaje Automático (Machine Learning, ML) para predecir el contenido de materia orgánica y el pH en campos de arroz. En este estudio se aplicaron técnicas como la regresión por mínimos cuadrados parciales (PLSR, por sus siglas en inglés), la máquina de vectores de soporte por mínimos cuadrados (LS-SVM), la máquina de aprendizaje extremo (ELM) y el modelo de árboles de decisión Cubista, logrando resultados significativos en términos de precisión en las predicciones. De igual manera, se ha informado sobre el uso de técnicas de ML en el control de plagas en cultivos. Por ejemplo [19] utilizaron métodos basados en aprendizaje automático e imagenología para identificar enfermedades en hojas de plantas de té, consiguiendo mejoras considerables en la detección temprana y precisión diagnóstica. Ese mismo año, Muthoni et al. reportaron en [20] analizaron la variación espaciotemporal en los mapas de rendimiento de cultivos de maíz en países del sur de África, incluyendo Mozambique, Zambia, Malawi y Zimbabue. Este análisis permitió identificar zonas específicas con bajos rendimientos agrícolas, ofreciendo así información valiosa para implementar

estrategias focalizadas de manejo agrícola y mejorar la seguridad alimentaria en la región. De igual forma, en 2021, [21] desarrollaron un modelo de Aprendizaje Profundo para estimar el contenido de clorofila en hojas de tomate. Su trabajo incluyó la recopilación de datos y el diseño de una arquitectura de red neuronal, logrando resultados satisfactorios en su propuesta.

Un año más tarde, Herrera et al. propusieron un modelo basado en técnicas de Machine Learning (ML) para la predicción espacial de sequías en el departamento del Magdalena, Colombia. Este modelo empleó técnicas como Random Forest (RF), que utiliza múltiples árboles de decisión para mejorar la precisión de predicción, y árboles de decisión (Decision Tree Classifier, DTC), que clasifican los datos mediante reglas lógicas simples, facilitando así la identificación precisa de zonas susceptibles a sequías en la región [22].

De igual forma en 2023, Kong et al., reportaron en [23] un modelo predictivo para señales SAR en campos de remolacha azucarera en Noord-Brabant, Países Bajos. Utilizando variables biológicas de cultivo como el índice de área foliar, el peso de la parte superior de la planta y los niveles de humedad del suelo superficial y radicular, implementaron un modelo de Regresión de Bosque Aleatorio junto con un simulador de crecimiento agrícola. Este modelo permitió predecir las observaciones SAR en las bandas co-pol y cross-pol C de Sentinel-1 [23]. Ese mismo año, Ghatrehsamani et al. presentaron una revisión sobre herramientas tecnológicas y métodos basados en Inteligencia Artificial para la gestión de malas hierbas resistentes a herbicidas. Entre las técnicas analizadas se encuentran métodos basados en Aprendizaje Automático (Machine Learning), específicamente Aprendizaje Profundo (Deep Learning) mediante Redes Neuronales Convolucionales (CNN), además de técnicas de clasificación, mapeo e imagenología térmica[24]. Adicionalmente en 2023, Wei et al. propusieron un sistema innovador de monitoreo de seguridad para la producción agrícola, basado en redes de sensores, nube e Inteligencia Artificial. Este sistema superó a los métodos tradicionales en eficiencia, precisión y velocidad. El algoritmo DV-Hop mostró un mejor rendimiento, con una alta tasa de captura de datos, alcanzando un 99% en las pruebas más exigentes, y demostró una notable confiabilidad en la transferencia de datos, velocidad y latencia [25].

Un año más tarde, en un ámbito relacionado, pero centrado en la producción animal, Vieto y Moreno, presentaron una revisión del uso de distintas técnicas de Aprendizaje Automático aplicadas a la mejora de los distintos procesos relacionados con la ganadería. Entre las aplicaciones se encuentran la detección de anemia en cabras y ovejas, detección de enfermedades, y monitoreo de bienestar animal. La revisión comprende el uso de múltiples técnicas de Aprendizaje Automático como algoritmos K-means, Bosques Aleatorios, Modelos Bayesianos, Arboles de Decisión, entre otras [26]. En el contexto agrícola, en 2024, El-Kenawy et al estudiaron modelos predictivos avanzados para estimar el rendimiento de cultivos de papa mediante algoritmos de aprendizaje automático como K-vecinos más cercanos (K-Nearest Neighbors, KNN), potenciación del gradiente (Gradient Boosting) y potenciación extrema del gradiente (Extreme Gradient Boosting, XGBoost), junto con modelos de aprendizaje profundo como redes neuronales de grafos (Graph Neural Networks, GNN), memoria a largo plazo (Long Short-Term Memory, LSTM) y unidades recurrentes cerradas (Gated Recurrent Units, GRU). El rendimiento de estos modelos se evaluó mediante métricas estadísticas como el error cuadrático medio (Mean Squared Error, MSE), raíz del error cuadrático medio (Root Mean Squared Error, RMSE) y error absoluto medio (Mean Absolute Error, MAE). Los resultados indicaron que las redes neuronales de grafos (GNN) mostraron el mejor desempeño, con un MSE de 0.02363 y un coeficiente de determinación (R^2) de 0.51719, seguidas por las LSTM y GRU. Este desempeño superior sugiere una capacidad significativa de las GNN para capturar patrones complejos en los datos agrícolas, destacando su potencial para mejorar la toma de decisiones y promover prácticas agrícolas más sostenibles en comparación con otros métodos evaluados [27].

En el mismo año, Wang et al. realizaron una revisión exhaustiva sobre la integración de la teledetección y el Aprendizaje Automático en la agricultura de precisión. El estudio destacó que, debido a sus características diversas, los distintos tipos de datos de teledetección tienen un impacto variado en la agricultura de precisión, siendo la teledetección hiperespectral la más utilizada, seguida por el uso de vehículos aéreos no tripulados (Unmanned Aerial Vehicles, UAVs), los cuales presentan un notable potencial en crecimiento. En cuanto a los algoritmos de Aprendizaje Automático, la Máquina de Vectores de Soporte (SVM, por sus siglas en inglés) fue la técnica más empleada, seguida

por el algoritmo de Bosque Aleatorio (Random Forest). Juntos, estos dos métodos representan el 38% de los más utilizados, contribuyendo significativamente al avance de la agricultura de precisión [28].

Estos trabajos evidencian cómo los avances en Aprendizaje Automático e Inteligencia Artificial están transformando los procesos agropecuarios desde diversos enfoques. La implementación de la "Agricultura Inteligente" (Figura I) integra estas tecnologías, permitiendo que, a través del monitoreo constante de los cultivos (Figura II), se generen soluciones basadas en áreas de Inteligencia Artificial, como el Aprendizaje Automático, haciendo posible que mediante los datos se logre optimizar tiempos de producción, mejorar la calidad de los cultivos, incrementando la eficiencia y precisión en la gestión agrícola, a través de soluciones tecnológicas para los desafíos actuales, como la seguridad alimentaria, la escasez de recursos y el cambio climático.

3.2. Uso de Vehículo aéreo no tripulado. - En los últimos años, el uso de drones en el sector agrícola ha experimentado un crecimiento significativo, impulsado por los avances tecnológicos en esta área. Estos dispositivos no tripulados ofrecen una opción económica y eficiente como herramienta de análisis de datos y robot móvil. Entre sus aplicaciones más frecuentes destacan la detección y control de plagas, la vigilancia y el monitoreo de cultivos. La Figura III muestra los resultados reportados por [29], en los que se detalla, en porcentaje, la implementación de vehículos no tripulados en la agricultura de precisión. Asimismo, la Figura III evidencia más de 50 años de investigación sobre el uso de drones en este sector, demostrando una trayectoria de desarrollo tecnológico y el crecimiento continuo de esta tecnología en los procesos agrícolas.

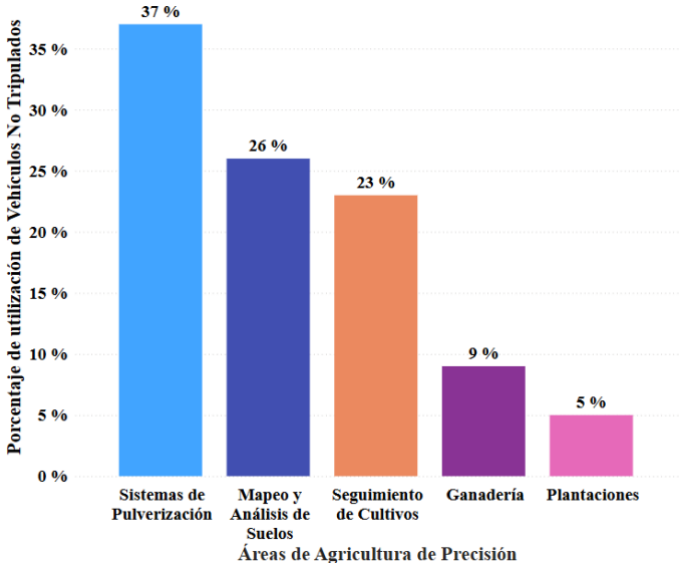

Figura III. Porcentaje de Vehículos no Tripulados en Distintas Áreas de la Agricultura de Precisión, adaptado de [29].

Entre los estudios destacados, podemos mencionar el realizado en 2018, por Dian Bah et al. quienes propusieron un método automático basado en Redes Neuronales Convolucionales con datos no supervisados para la detección de malezas mediante imágenes obtenidas por UAV. Los resultados, comparables al etiquetado supervisado tradicional, mostraron diferencias de precisión del 1.5% en campos de espinacas y del 6% en campos de judías [30]. Un año más tarde, en 2019, Yeom et al. analizaron en [31], los efectos de la labranza sobre la salud de las plantas mediante índices de vegetación calculados a partir de imágenes de drones de alta resolución, encontrando consistentemente índices más altos en campos de labranza cero.

En un desarrollo paralelo, en 2020, Kasper et al. publicaron en [32] un método para cartografiar el estado de las copas de macadamia utilizando imágenes multiespectrales capturadas por UAV y satélites WorldView-3, logrando una precisión de clasificación superior al 98.5%. Ese mismo año, Meng et al. investigaron cómo los parámetros operativos

de UAV influían en la distribución de gotas en árboles frutales, optimizando rutas de vuelo y frecuencia de pulverización para durazneros con diferentes configuraciones [33].

Más adelante, en 2021, Parthasarathy et al. revisaron técnicas avanzadas de vigilancia y gestión de plagas mediante UAV, destacando la integración de tecnologías aéreas, satelitales y de teledetección para la detección temprana de enfermedades en cultivos [34]. Poco después, en 2022, Vélez et al. emplearon drones Phantom 4 y cámaras RGB para crear una base de datos confiable de agricultura de precisión en cultivos de pistacho, utilizando mapeo de ortomosaicos y rutas de vuelo optimizadas [35].

Luego, en 2023, Singh y Sharma desarrollaron un sistema que combina dispositivos IoT y drones multirrotor para vigilancia y fumigación, optimizando rutas de vuelo y mejorando la eficiencia de redes de sensores integradas [36]. Además, ese mismo año, Chin et al. llevaron a cabo una revisión sistemática sobre el uso de drones para la detección de enfermedades en plantas. Identificaron que el tizón es la enfermedad más comúnmente estudiada, el hongo el patógeno más relevante, y las imágenes en color infrarrojo (CIR) las más utilizadas para tareas de clasificación en Aprendizaje Automático [37].

Posteriormente en 2024, García-Gil et al. propusieron un método eficiente en términos de energía para el despliegue y migración de microservicios en redes de UAV, utilizando un modelo de Programación Lineal Entera Mixta (MILP). Este enfoque optimiza la duración de las baterías distribuyendo equitativamente la carga de trabajo entre los UAV, lo que maximiza el tiempo de vuelo y minimiza el consumo de batería. Al descomponer las aplicaciones IoT en microservicios, cada UAV es capaz de gestionar servicios específicos, superando las limitadas capacidades computacionales y de batería. El modelo MILP también facilita la migración de microservicios para reducir el consumo energético, extendiendo así la vida útil del servicio. Este enfoque aprovecha las redes de UAV para ofrecer soluciones efectivas en aplicaciones como la gestión ganadera [38]. Ese mismo año, Guebsi et al. y Hawashin et al. realizaron revisiones significativas sobre el uso de tecnologías avanzadas en los sistemas UAV y su impacto en sectores como la agricultura de precisión. Guebsi et al. abordaron los avances en plataformas aéreas, sensores multiespectrales e hiperespectrales, y sistemas de navegación, destacando aplicaciones clave como el monitoreo de cultivos y la siembra asistida por drones. Además, subrayaron los desafíos regulatorios, tecnológicos y económicos, resaltando la necesidad de estandarizar las regulaciones para vuelos BVLOS (Beyond Visual Line Of Sight) y mejorar el acceso económico para los pequeños agricultores, al tiempo que proponían oportunidades de investigación futura, como el uso de enjambres de drones. Por su parte, Hawashin et al. exploraron el potencial de la tecnología Blockchain en los sistemas UAV, destacando su capacidad para mejorar la trazabilidad de los datos en las cadenas de suministro y optimizar la gestión de las operaciones de vuelo, lo que mejora la eficiencia operativa y la integridad de los datos. También subrayaron cómo Blockchain puede potenciar la transparencia, el control de acceso y el rendimiento de los sistemas UAV, identificando retos como la descentralización y proponiendo áreas para futuras investigaciones. Ambas revisiones resaltan el impacto transformador de estas tecnologías y las oportunidades de investigación para avanzar en la sostenibilidad y eficiencia de las operaciones en agricultura de precisión [39], [40].

Estos estudios destacan el papel transformador de los drones y las tecnologías emergentes en la agricultura y ganadería, posicionándolos como herramientas esenciales para enfrentar desafíos críticos como la sostenibilidad, la eficiencia y la seguridad alimentaria a nivel global. Su implementación reduce costos operativos, optimiza el uso de recursos naturales, como agua y fertilizantes, y adicionalmente minimiza el impacto ambiental al reducir el uso de agroquímicos. Además, estas tecnologías permiten un monitoreo en tiempo real, favorecen la detección temprana de plagas y enfermedades, y mejoran la toma de decisiones informadas, lo que se traduce en un mayor control sobre los cultivos y una gestión más eficiente de los procesos agrícolas.

3.3 Big Data. - El Big Data en la agricultura abarca la gestión de datos estructurados, semiestructurados y no estructurados, provenientes de diversas fuentes como repositorios, hojas de cálculo, imágenes satelitales, videos y encuestas. Su objetivo principal es mejorar los procesos agrícolas mediante la toma de decisiones informadas, optimizando el crecimiento de los cultivos, reduciendo costos y fomentando cadenas de suministro sostenibles

respaldadas por tecnologías digitales y análisis de datos [41]. En este contexto, múltiples organizaciones como CGIAR y el Instituto Internacional de Investigación sobre Políticas Alimentarias (IFPRI) han procesado grandes volúmenes de datos para desarrollar plataformas de Big Data destinadas a mejorar la investigación agrícola a nivel internacional [42]. De igual forma, la Organización de las Naciones Unidas para la Alimentación y la Agricultura (FAO) implementó, durante la pandemia de COVID-19, una herramienta para recopilar información en tiempo real sobre agricultura y cadenas de suministro, facilitando la adopción de medidas específicas en cada país [43]. Estos esfuerzos han impulsado el aumento de aplicaciones relacionadas con la integración del Big Data en los procesos agrícolas.

Entre las aplicaciones destacadas, se encuentra la reportada por Zhang y Liu en 2019, quienes desarrollaron un sistema basado en Internet de las Cosas (IoT) para la adquisición de datos agrícolas, utilizando sensores, imágenes y datos meteorológicos transmitidos mediante GPRS y redes 3G. Su modelo mostró una precisión superior al 99% en la predicción de datos agrícolas [44]. Un año después, [45] exploraron el uso de Big Data y Aprendizaje Profundo para la detección de enfermedades en cultivos, logrando una precisión del 72% en la identificación de hojas infectadas, destacando la importancia de la detección temprana en la Agricultura Inteligente. Por otra parte, en 2021, Lokhande et al. demostraron cómo el Análisis de Datos y la Minería de Datos pueden mejorar la producción de cultivos en India, utilizando técnicas de preprocesamiento, Arboles de Decisión y Regresiones Lineales para obtener predicciones de rendimiento agrícola con resultados satisfactorios. Los resultados mostraron un coeficiente de determinación (R^2) de 0.658, indicando que el modelo explicó aproximadamente el 66% de la variabilidad en la producción del cultivo. Además, el estudio sugirió que la precisión de las predicciones podría aumentar aún más al incrementar la cantidad y variedad de los datos analizados, subrayando así el potencial del Big Data para mejorar significativamente las decisiones agrícolas y aumentar la productividad [46]. Posteriormente, en 2022, Li et al. analizaron cómo el Big Data puede transformar la toma de decisiones organizacionales, mostrando mejoras significativas en la calidad de las decisiones gracias a las capacidades avanzadas de análisis de datos [47]. En el contexto agrícola, esta capacidad analítica permite gestionar grandes volúmenes de información provenientes de diversas fuentes, tales como sensores, imágenes satelitales y registros históricos, facilitando decisiones más informadas sobre el manejo eficiente de recursos, optimización de cosechas, prevención de enfermedades y plagas, así como la planificación estratégica del cultivo. En la misma línea, Ouafiq et al. propusieron SFOBA, una arquitectura de Big Data orientada a la Agricultura Inteligente, que combina IoT y sistemas basados en conocimiento para garantizar la resiliencia a largo plazo, monitorear la calidad de los datos y transformar requisitos comerciales en soluciones analíticas significativas [48]. Un año más tarde en 2023, Ngo et al. propusieron los Registros Electrónicos Agrícolas (EAR), un sistema que integra datos agrícolas mediante tecnologías como Elasticsearch y Hive, ofreciendo recomendaciones precisas para la gestión de fertilizantes en diversos entornos [49]. Ese mismo año, Wu et al. presentaron un estudio sobre la integración de operaciones de maquinaria agrícola con Big Data, promoviendo decisiones más científicas y eficientes en la gestión de maquinaria para modernizar la producción agrícola [50]. Luego en 2024, Rana et al. emplearon Apache Spark para predecir los precios de la espinaca en Pakistán durante el periodo de 2007 a 2022, evaluando diversos modelos como ARIMA, Random Forest y LSTM. El modelo LSTM destacó por su capacidad para identificar patrones temporales complejos con alta precisión, superando a los demás modelos evaluados. El estudio resalta que la integración de fuentes de datos adicionales, como información climática y análisis de sentimientos del mercado, podría optimizar la precisión de las predicciones y ofrecer una visión más completa de los factores que influyen en los precios agrícolas [51]. Por otro lado, Stephen et al. analizaron cuatro arquitecturas de Redes Neuronales Convolucionales preentrenadas para el monitoreo de la salud de las plantas de algodón: ResNet18, GoogLeNet, InceptionV3 y MobileNetV3 Large. En donde el modelo MobileNetV3 Large obtuvo el mejor desempeño, con una exactitud del 93.9%, una especificidad del 96.12% y una precisión del 97.48%, utilizando imágenes en tiempo real obtenidas a través de una aplicación Android en áreas agrícolas de la India, logrando clasificar 11 regiones de la planta de algodón y ofrecer información sobre la cosecha y el rendimiento [52]. Del mismo modo, en 2024, Giannakopoulos et al. realizaron la relación entre los índices agroeconómicos y la analítica de marketing digital en empresas agrícolas, utilizando análisis de regresión, correlación y modelos de redes neuronales, demostrando una relación entre dichos índices y distintas métricas de marketing digital [53].

En conjunto, estos estudios reflejan una tendencia emergente hacia la aplicación del Big Data en la agricultura, con un impacto significativo en la toma de decisiones, la optimización de la gestión de datos y la modernización de la

producción. Adicionalmente los estudios resaltan la importancia del análisis de Big Data junto con la integración de diversas tecnologías para enfrentar los retos del sector agrícola y fomentar su desarrollo sostenible.

3.4 Cloud Computing y Cloud Storage. - La computación en la nube, definida como el almacenamiento y acceso a datos y programas a través de Internet, se ha convertido en un componente clave para la modernización de la agricultura. Este modelo permite a los usuarios acceder a archivos y aplicaciones desde cualquier dispositivo conectado a Internet, proporcionando flexibilidad y conveniencia [54]. En el ámbito agrícola, el modelo Cloud-Fog-Edge ha sido propuesto como una arquitectura integrada para la Agricultura Inteligente. Este enfoque utiliza la capa Cloud para almacenar y analizar datos a gran escala, cargar algoritmos en nodos Fog y realizar copias de seguridad. La capa Fog, instalada localmente, procesa datos en tiempo real para tomar decisiones inmediatas, mientras que la capa Edge recolecta y transfiere datos a las capas superiores. Aunque estas tecnologías presentan ventajas significativas, también enfrentan desafíos en su implementación y desarrollo futuro [55].

Entre las aplicaciones más relevantes de la computación en la nube a la agricultura, en 2019 Li et al. desarrollaron un sistema de monitoreo basado en IoT con un esquema de almacenamiento híbrido que integra bases de datos NoSQL, DynamoDB, Oracle y Amazon S3. Este sistema mejoró el rendimiento y la escalabilidad en la gestión de datos agrícolas [56]. Ese mismo año, otro estudio de Li et al. exploró el uso de robots móviles para monitorear invernaderos, utilizando computación en la nube para calcular rutas de movimiento optimizadas [57]. Posteriormente, en 2020, Paludo et al. implementaron el algoritmo Simple Non-Iterative Clustering (SNIC) y un modelo de aprendizaje supervisado Naive Bayes para mapear cultivos de maíz y soya en Brasil. El sistema propuesto basado en la nube logró altos niveles de precisión en la identificación de áreas cultivadas [58]. Adicionalmente, Hsu et al. reportaron el uso de Cloud Fog Computing para analizar datos de grandes extensiones agrícolas, optimizando la supervisión de cultivos y el manejo de plagas en áreas con recursos limitados de red [59].

Un año más tarde, Phasinam et al. diseñaron un sistema de riego inteligente basado en IoT, con análisis de datos en la nube para proporcionar a los agricultores información precisa sobre la humedad del suelo y el ambiente [60]. De igual forma, en 2021, Idoje et al. presentaron una visión general de las tecnologías utilizadas en la Agricultura 4.0 (A4.0), incluyendo aplicaciones en la producción de cultivos y animales, así como en la gestión postcosecha [61]. Por otro lado, Islam et al. exploraron casos de uso de IoT y UAVs en la Agricultura Inteligente, destacando sus ventajas en la supervisión y manejo de cultivos [62]. Luego, en 2022, Kheir et al. reportaron un sistema basado en la nube para optimizar estrategias de fertilización y manejo del suelo, utilizando algoritmos de reconocimiento de patrones en una base de conocimiento [63].

Posteriormente, en 2023, se presentaron varias aplicaciones como:

- Utilización de imágenes multiespectrales procesadas en Google Earth Engine para predecir propiedades del suelo en el Valle del Mantaro, Perú, logrando modelos adaptativos de monitoreo de suelos [64].
- Calibración de un sistema inteligente para medir evapotranspiración de referencia (ETo) y controlar riego mediante IoT, demostrando alta precisión en sus mediciones [65].
- Desarrollo de una red de sensores inalámbricos basada en IoT y LoRa (Long Range, tecnología inalámbrica de largo alcance y bajo consumo energético) integrados con controladores lógicos programables (PLC) para gestionar múltiples procesos agrícolas con bajo costo y consumo energético [66].

Seguidamente en 2024, se desarrollaron diversos sistemas innovadores, tal es el caso de Morchid et al. e Ivanochko et al. quienes presentaron soluciones de Agricultura Inteligente que utilizan IoT y computación en la nube para potenciar la sostenibilidad y eficiencia en el sector agrícola. El sistema propuesto por Morchid et al. se centra en un riego inteligente que optimiza el consumo de agua mediante sensores y monitoreo en tiempo real, complementado con alertas por correo electrónico para facilitar la gestión del recurso hídrico [67]. Por otro lado, Ivanochko et al. desarrollaron una aplicación para Android que permite a los agricultores supervisar las condiciones de sus cultivos y ganado, enfocándose especialmente en el control de la humedad [68]. Adicionalmente ese mismo año Lee et al. reportaron un modelo de

clasificación de imágenes utilizando Redes Neuronales para Agricultura Inteligente, optimizado para dispositivos de computación en la nube, logrando predecir el estado de salud de las plantas, mejorando la eficiencia y reduciendo costos al utilizar Fog-computing [69].

Estos estudios reflejan cómo la computación en la nube y sus tecnologías asociadas están transformando la agricultura por medio de la optimización de procesos agrícolas, la mejora en la toma de decisiones basada en datos, y el incremento de la eficiencia en la gestión de recursos. A través de soluciones innovadoras como el almacenamiento y análisis de datos en tiempo real, la integración de IoT, la implementación de modelos predictivos y el monitoreo remoto.

3.5 Redes de Sensores Inalámbricos (WSN). - Las Redes de Sensores Inalámbricos (WSN, por sus siglas en inglés) han ganado popularidad como herramientas esenciales para la monitorización y recopilación de datos en lugares remotos o de difícil acceso. Estas redes están compuestas por nodos sensores que se comunican de manera inalámbrica para recolectar información del entorno y transmitirla de manera eficiente para evaluar su desempeño y efectividad, los investigadores recurren a herramientas y simuladores específicos, que facilitan el análisis y optimización de las WSN en diversas aplicaciones [70].

La Tabla I presenta un resumen de las principales aplicaciones de las Redes de Sensores Inalámbricos en la agricultura durante los últimos cinco años, evidenciando su impacto en áreas clave del sector.

Año	Resumen	Ref.
2019	Desarrollaron un sistema de alimentación inteligente para cerdos utilizando sensores y tecnología de decisión que permite identificar y alimentar a cada cerdo de manera precisa y remota.	[71]
2019	Investigaron la maximización de la vida útil de redes WSN mediante la captación de energía solar. La simulación mostró que la vida útil de la red se extendió significativamente, de 5,75 días a 115,75 días, con un ciclo de trabajo del 25% o más.	[72]
2020	Resaltaron la importancia de la agricultura en Afganistán y propusieron el uso de técnicas de Agricultura Inteligente basadas en IoT para mejorar la eficiencia y gestión agrícola.	[73]
2020	Utilizaron sensores inalámbricos en invernaderos con la tecnología LoRaWan para transmitir datos a largas distancias con bajo consumo de energía, destacando la importancia de la temperatura y humedad para mediciones precisas.	[74]
2021	Implementaron un sistema de agricultura inteligente para el monitoreo de campos de maíz utilizando IoT, sensores y drones, eliminando la necesidad de comunicación a larga distancia entre sensores.	[75]
2021	Presentaron un sistema de monitoreo climático basado en IoT con sensores de temperatura, humedad y niveles de gas, conectados a una placa Arduino, demostrando su efectividad en el monitoreo de varios parámetros del aire.	[76]
2022	Revisaron estudios y tecnologías relacionadas con la agricultura de precisión, destacando sus beneficios en la mejora del rendimiento de cultivos, la eficiencia de recursos y la toma de decisiones en agricultura.	[77]
2023	Crearon una red de redes de sensores inalámbricos (WSN) y dispositivos de bajo costo como el ESP8266 y Arduino para la monitorización continua de la salud de las vacas lecheras, permitiendo a los ganaderos rastrear de manera remota los signos vitales a través de aplicaciones móviles.	[78]
2023	Implementaron un protocolo de autenticación de tres factores para redes inalámbricas en campos agrícolas, mejorando la seguridad y privacidad mediante técnicas fotográficas.	[79]
2023	Diseñaron una red de sensores inalámbricos para invernaderos basada en el protocolo Zigbee mejorado (EMP-ZBR), que mostró menor latencia, alta tasa de entrega de paquetes y baja sobrecarga de control, mejorando el rendimiento del sistema de monitoreo agrícola.	[80]

2024	Reportaron un protocolo de enrutamiento seguro y optimizado para redes WSN en agricultura inteligente, integrando Blockchain y utilizando Mapas Cognitivos Difusos Distribuidos (DFCM) para la selección de Cabezas de Clúster (CHs), con el fin de equilibrar el consumo energético de la red.	[81]
2024	Señalaron algunos de los principales desafíos actuales de las redes WSN en la agricultura, proponiendo soluciones innovadoras para optimizar la eficiencia energética y mejorar el rendimiento de estos sistemas, utilizando técnicas como la recolección de energía y protocolos inalámbricos.	[82]
2024	Introdujeron un sistema para clasificar comportamientos en ganado usando Redes de Sensores Inalámbricos (WSN), con configuraciones óptima y restringida, mejorando el rendimiento en un 9% y 6% respectivamente y alcanzó una precisión superior al 70% en distintas actividades como caminar, pastar y descansar, destacándose por sus innovaciones en configuraciones y ahorro energético.	[83]

Tabla I. Aplicaciones de redes de sensores inalámbricos en la agricultura.

Como se muestra en la Tabla I, las Redes de Sensores Inalámbricos han experimentado un crecimiento significativo en términos de velocidad y cobertura. Este avance resalta la importancia de continuar investigando y desarrollando esta tecnología para asegurar que, en el futuro, las redes sean más eficientes y puedan cubrir las demandas cada vez mayores de los usuarios. Asimismo, es crucial garantizar su adaptabilidad a distintos entornos y desafíos, mejorando tanto su rendimiento como su eficiencia energética. Además, al combinar las redes de sensores inalámbricos con tecnologías emergentes, como el Internet de las Cosas (IoT), la Inteligencia Artificial y el Blockchain, permitirá ampliar sus aplicaciones. Esta sinergia puede contribuir al desarrollo de una agricultura más sostenible y a una gestión más eficiente de los recursos naturales.

3.6 IoT. - La incorporación de tecnologías digitales en los sistemas de producción agrícola ha impulsado significativamente el desarrollo del sector, facilitando la creación de cadenas digitales y alimentarias más funcionales y eficientes. Estas herramientas no solo simplifican el acceso y la distribución de información, sino que también promueven la investigación, el desarrollo, la innovación y la transferencia tecnológica en el ámbito agrícola. Al aprovechar estas tecnologías, los agricultores pueden obtener datos en tiempo real, mejorar la gestión de sus recursos, optimizar las prácticas de cultivo y aumentar la productividad, lo que contribuye al desarrollo sostenible de la agricultura y a fortalecer la seguridad alimentaria [84].

Figura IV. Arquitectura de sistema de agricultura inteligente. Adaptada de [78], [85].

Tal como se muestra en la Figura IV, la arquitectura de los sistemas basados en IoT está conformada por varias secciones fundamentales. En primer lugar, la capa de adquisición de datos utiliza redes de sensores y actuadores para capturar información directamente del entorno físico. Posteriormente, la capa de computación en la niebla se encarga del procesamiento inicial y la organización local de estos datos, preparando la información para un análisis más profundo. Además, la puerta de enlace de comunicaciones facilita la transferencia eficiente de los datos entre los dispositivos y la infraestructura en la nube, empleando distintos medios de comunicación como satélites, fibra óptica y microondas. Finalmente, la capa de computación en la nube ofrece servicios avanzados de almacenamiento, análisis detallado y visualización mediante aplicaciones web. Finalmente, la sección de almacenamiento y computación en la nube permite guardar los datos recopilados y procesarlos para facilitar su acceso y análisis en el futuro. Esta arquitectura posibilita una gestión eficiente y optimizada de la información, facilitando la toma de decisiones en tiempo real e impulsando la productividad en aplicaciones agrícolas, motivo por el cual los sistemas IoT han experimentado una adopción creciente en el sector agrícola, como lo destacan diversos autores [86], [87]. En ese sentido, la Tabla II presenta un resumen de las aplicaciones de IoT recientemente desarrolladas en la agricultura.

Año	Resumen	Ref.
2018	Presentaron una plataforma para gestionar información sobre cultivos agrícolas recopilada mediante UAV multirrotor, utilizando el framework Django para recoger información de los cultivos y la posición de los UAV en tiempo real.	[88]
2019	Propusieron el uso de programadores de riego automatizados de bajo costo con Arduino, basados en mediciones del aire y el sustrato para asegurar el crecimiento óptimo de las plantas y el uso eficiente del agua.	[89]
2020	Investigaron los protocolos de mensajería IoT más utilizados en aplicaciones de agricultura inteligente, identificando y evaluando siete protocolos (MQTT, CoAP, XMPP, AMQP, DDS, REST-HTTP y WebSocket) según sus indicadores de rendimiento.	[90]
2021	Plantearon un sistema basado en IoT para la agricultura urbana que determina la necesidad de riego según la condición del terreno y parámetros como temperatura y humedad, permitiendo el monitoreo y control remoto.	[91]
2021	Implementaron un sistema de acuaponía adaptable mediante la integración de tecnologías digitales y Aprendizaje Automático, presentando resultados empíricos sobre la eficacia de enfoques basados en datos para la toma de decisiones.	[92]
2022	Reportaron una estrategia innovadora de optimización con tecnología Blockchain para invernaderos, que incluye predicción, optimización y control. Usaron el algoritmo de filtro de Kalman para anticipar datos de los sensores del invernadero durante la fase de predicción.	[93]
2022	Propusieron un sistema de predicción de plagas basado en lógica difusa que puede predecir y prevenir plagas potenciales, determinando la relación entre temperatura, humedad, precipitaciones y la reproducción de plagas en cultivos de arroz y mijo.	[94]
2022	Diseñaron una WSN con nodos de sensores de bajo costo y consumo energético, alimentados por paneles fotovoltaicos, capaces de recolectar datos sobre condiciones ambientales y parámetros del suelo.	[95]

2023	Propusieron el uso de Inteligencia Artificial (IA) e Internet de las Cosas (IoT) para analizar y comprender áreas de la vida contemporánea, especialmente en la cría de ganado, con el objetivo de mejorar la comprensión del comportamiento animal, gestionar enfermedades y optimizar las decisiones económicas de los agricultores.	[96]
2023	Estudiaron el uso de energía solar para desarrollar un sistema de bombas de agua para el riego agrícola, utilizando un sensor de flujo de agua controlado por NodeMCU ESP8266 y mostrando los datos en la aplicación Blynk.	[97]
2023	Desarrollaron un sistema inteligente de monitoreo forestal basado en IoT que previene accidentes al identificar cambios ambientales y reducir riesgos con una alta precisión 99.2%. Además, el sistema muestra un gran potencial para mejorar la seguridad contra incendios en otros contextos, como industrias y parques.	[98]
2024	Presentaron una plataforma de detección de plagas basada en IoT que integra una trampa inteligente para insectos y un clasificador CNN, alcanzando una precisión del 97.5% y un recall del 98.92%, superando a otros modelos de ML y Aprendizaje Profundo (DL) empleados en la clasificación de plagas y el monitoreo agrícola.	[99]
2024	Reportaron un sistema IoT impulsado por Raspberry Pi, que automatiza la supervisión y gestión del riego, la temperatura, la humedad y la iluminación, mediante una aplicación móvil, validando su eficacia en el desarrollo de plantas, destacando su potencial en la agricultura actual.	[100]

Tabla II. Aplicaciones recientes del Internet de las Cosas (IoT) en la agricultura.

Como se observa en la Tabla II, estas aplicaciones basadas en diversas tecnologías digitales han logrado responder eficazmente a las distintas demandas del sector agrícola. Su implementación ha facilitado tanto la adquisición de datos para su posterior análisis como el desarrollo de sistemas automatizados para procesos clave, como la gestión del riego, el monitoreo de cultivos y la detección temprana de plagas. Además, estas innovaciones promueven una agricultura más sostenible al reducir el desperdicio de recursos y aumentar la productividad. Adicionalmente la expansión de sistemas basados en el Internet de las Cosas (IoT) ha evidenciado la necesidad de seguir integrando nuevos dispositivos y tecnologías, ya que todo está interconectado y funciona en sinergia. Esta interconexión permite una mayor eficiencia y precisión en la toma de decisiones, lo que se traduce en una optimización de los recursos y una mejora continua en los procesos agrícolas.

4. Conclusiones. - Este estudio, fundamentado en una revisión breve de investigaciones científicas recientes, examina el impacto de las distintas tecnologías digitales como el Internet de las Cosas, Big Data, la Computación en la Nube, la Inteligencia Artificial, los drones y el Aprendizaje Automático, en los múltiples procesos de la agricultura moderna, incluyendo el mapeo digital de suelos, la detección temprana de enfermedades en cultivos, la optimización del riego, la planificación agrícola y la gestión eficiente de recursos. La revisión resalta como estos avances han sido fundamentales para generar un modelo agrícola más eficiente y sostenible, capaz de abordar la serie de desafíos globales existentes como el cambio climático, la seguridad alimentaria y el aumento de la demanda de alimentos.

Del mismo modo, la revisión destaca, mediante el reporte de distintas aplicaciones, el rol crucial de la Inteligencia Artificial y el Aprendizaje Automático en la optimización de recursos críticos, como cultivos, ganado, agua y suelos, a través de modelos avanzados como Redes Neuronales y Máquinas de Soporte Vectorial. Así mismo, la incorporación de drones y tecnologías de percepción remota ha mejorado significativamente la precisión en el monitoreo y la rápida detección de situaciones para la temprana toma de decisiones, particularmente en extensas áreas agrícolas. Por su parte,

las redes de sensores inalámbricos y el IoT han optimizado la recopilación y uso eficiente de datos agrícolas, mientras que la integración de Big Data y la Computación en la Nube ha robustecido los procesos de toma de decisiones basados en el análisis de datos. Sin embargo, este informe está limitado por la ventana temporal 2018-2024, el lenguaje e indexación de las posibles partes y la heterogeneidad de las mediciones que evitan el metaanálisis comparable; Además, la aprobación a corto plazo se domina brevemente y hay poca repetición abierta. Estos siguen siendo desafíos con escalabilidad, compatibilidad y disponibilidad, lo que enfatiza la necesidad de una investigación continua, marcos legislativos claros y programas de capacitación de adopción. En el futuro, es aconsejable estandarizar las mediciones y las líneas base, publicar datos y código y validar en una escala. También debe estudiar Edge/TinyML, aprendizaje federal, fusión multimodal y gestión de datos/datos cibernéticos. La evaluación, la sostenibilidad (accidente cerebrovascular) y la aceptación socioeconómica de los beneficios de costos serán la clave para facilitar la implementación real. A pesar de las restricciones, el equilibrio es positivo: el impacto económico y operativo observado muestra que el éxito a largo plazo depende de la cooperación efectiva entre los participantes públicos, privados y académicos para consolidar el modelo agrícola flexible y prepararse para desafíos futuros.

References

[1] J. Paneque-Gálvez, M. K. McCall, B. M. Napoletano, S. A. Wich, y L. P. Koh, "Small drones for community-based forest monitoring: An assessment of their feasibility and potential in tropical areas", Forests, vol. 5, núm. 6, pp. 1481–1507, 2014, doi: 10.3390/F5061481.

[2] Aema, "TECNICAS HIDROPONICAS - AEMA Hispanica". Consultado: el 12 de julio de 2022. [En línea]. Disponible en: https://aemahispanica.com/actualidad/tecnicas-hidroponicas/

[3] C. Saavedra-Gualtero, A. Cárdenas-Forero, y F. Freyle-Corro, "Implementación de un sistema de acuaponía sustentable modular. DImplementation of a modular sustainable aquaponics system".

[4] T. Van Gerrewey, N. Boon, y D. Geelen, "Vertical Farming: The Only Way Is Up?", Agronomy, vol. 12, núm. 1, p. 2, dic. 2021, doi: 10.3390/agronomy12010002.

[5] Olabimpe Banke Akintuyi, "Vertical farming in urban environments: A review of architectural integration and food security", Open Access Research Journal of Biology and Pharmacy, vol. 10, núm. 2, pp. 114–126, abr. 2024, doi: 10.53022/oarjbp.2024.10.2.0017.

[6] M. H. M. Saad, N. M. Hamdan, y M. R. Sarker, "State of the Art of Urban Smart Vertical Farming Automation System: Advanced Topologies, Issues and Recommendations", Electronics (Basel), vol. 10, núm. 12, p. 1422, jun. 2021, doi: 10.3390/electronics10121422.

[7] S. Oh y C. Lu, "Vertical farming - smart urban agriculture for enhancing resilience and sustainability in food security", J Hortic Sci Biotechnol, vol. 98, núm. 2, pp. 133–140, mar. 2023, doi: 10.1080/14620316.2022.2141666.

[8] N. Elbeheiry y R. S. Balog, "Technologies Driving the Shift to Smart Farming: A Review", IEEE Sens J, vol. 23, núm. 3, pp. 1752–1769, feb. 2023, doi: 10.1109/JSEN.2022.3225183.

[9] G. Mohyuddin, M. A. Khan, A. Haseeb, S. Mahpara, M. Waseem, y A. M. Saleh, "Evaluation of Machine Learning approaches for precision Farming in Smart Agriculture System - A comprehensive Review", IEEE Access, 2024, doi: 10.1109/ACCESS.2024.3390581.

[10] R. Abbasi, P. Martinez, y R. Ahmad, "The digitization of agricultural industry – a systematic literature review on agriculture 4.0", 2022. doi: 10.1016/j.atech.2022.100042.

[11] C. Yang, X. Ji, C. Cheng, S. Liao, B. Obuobi, y Y. Zhang, "Digital economy empowers sustainable agriculture: Implications for farmers' adoption of ecological agricultural technologies", Ecol Indic, vol. 159, p. 111723, feb. 2024, doi: 10.1016/J.ECOLIND.2024.111723.

[12] B. Petrović, R. Bumbálek, T. Zoubek, R. Kuneš, L. Smutný, y P. Bartoš, "Application of precision agriculture technologies in Central Europe-review", J Agric Food Res, vol. 15, p. 101048, mar. 2024, doi: 10.1016/J.JAFR.2024.101048.

[13] R. Zulfikhar, A. Z. A. Alaydrus, S. Sutiharni, A. Nanjar, y H. Hartati, "Utilization of Smart Agricultural Technology to Improve Resource Efficiency in Agro-industry", West Science Agro, vol. 2, núm. 01, pp. 28–34, feb. 2024, doi: 10.58812/WSA.V2I01.656.

[14] P. Chetri, U. Sharma, y P. Vigneswara Ilavarasan, "Weather information, farm-level climate adaptation and farmers' adaptive capacity: Examining the role of information and communication technologies", Environ Sci Policy, vol. 151, p. 103630, ene. 2024, doi: 10.1016/J.ENVSCI.2023.103630.

[15] I. A. Lakhiar et al., "A Review of Precision Irrigation Water-Saving Technology under Changing Climate for Enhancing Water Use Efficiency, Crop Yield, and Environmental Footprints", Agriculture 2024, Vol. 14, Page 1141, vol. 14, núm. 7, p. 1141, jul. 2024, doi: 10.3390/AGRICULTURE14071141.

[16] K. G. Liakos, P. Busato, D. Moshou, S. Pearson, y D. Bochtis, "Machine learning in agriculture: A review", Sensors (Switzerland), vol. 18, núm. 8, ago. 2018, doi: 10.3390/S18082674.

[17] A. Cravero, S. Pardo, S. Sepúlveda, y L. Muñoz, "Challenges to Use Machine Learning in Agricultural Big Data: A Systematic Literature Review", Agronomy, vol. 12, núm. 3, p. 748, mar. 2022, doi: 10.3390/agronomy12030748.

[18] M. Yang, D. Xu, S. Chen, H. Li, y Z. Shi, "Evaluation of machine learning approaches to predict soil organic matter and pH using vis-NIR spectra", Sensors (Switzerland), vol. 19, núm. 2, ene. 2019, doi: 10.3390/S19020263.

[19] G. Yashodha y D. Shalini, "An integrated approach for predicting and broadcasting tea leaf disease at early stage using IoT with machine learning – A review", Mater Today Proc, vol. 37, núm. Part 2, pp. 484–488, ene. 2021, doi: 10.1016/J.MATPR.2020.05.458.

[20] F. Muthoni, C. Thierfelder, B. Mudereri, J. Manda, M. Bekunda, y I. Hoeschle-Zeledon, "Machine learning model accurately predict maize grain yields in conservation agriculture systems in Southern Africa", 2021 9th International Conference on Agro-Geoinformatics, Agro-Geoinformatics 2021, jul. 2021, doi: 10.1109/AGRO-GEOINFORMATICS50104.2021.9530335.

[21] M. I. Khoshrou, P. Zarafshan, M. Dehghani, G. Chegini, A. Arabhosseini, y B. Zakeri, "Deep Learning Prediction of Chlorophyll Content in Tomato Leaves", 9th RSI International Conference on Robotics and Mechatronics, ICRoM 2021, pp. 580–585, 2021, doi: 10.1109/ICROM54204.2021.9663468.

[22] D. M. Herrera Posada y E. Aristizábal, "Modelo de inteligencia artificial y aprendizaje automático para la predicción espacial y temporal de eventos de sequía en el departamento del Magdalena, Colombia.", Inge CuC, vol. 18, núm. 2, pp. 249–265, nov. 2022, doi: 10.17981/ingecuc.18.2.2022.20.

[23] F. Kong, "MODELING SENTINEL-1 OBSERVABLES FOR SUGARBEET FIELDS USING MACHINE LEARNING A STUDY ABOUT SAR ASSIMILATION TECHNIQUE".

[24] S. Ghatrehsamani et al., "Artificial Intelligence Tools and Techniques to Combat Herbicide Resistant Weeds—A Review", Sustainability 2023, Vol. 15, Page 1843, vol. 15, núm. 3, p. 1843, ene. 2023, doi: 10.3390/SU15031843.

[25] Y. Wei, C. Han, y Z. Yu, "An environment safety monitoring system for agricultural production based on artificial intelligence, cloud computing and big data networks", Journal of Cloud Computing, vol. 12, núm. 1, pp. 1–17, dic. 2023, doi: 10.1186/s13677-023-00463-1.

[26] M. Vieto-Vega, "Machine Learning en la detección y predicción de enfermedades del ganado", Memoria Investigaciones en Ingeniería, núm. 27, pp. 46–59, dic. 2024, doi: 10.36561/ING.27.4.

[27] E.-S. M. El-Kenawy, A. A. Alhussan, N. Khodadadi, S. Mirjalili, y M. M. Eid, "Predicting Potato Crop Yield with Machine Learning and Deep Learning for Sustainable Agriculture", Potato Res, jul. 2024, doi: 10.1007/s11540-024-09753-w.

[28] J. Wang, Y. Wang, G. Li, y Z. Qi, "Integration of Remote Sensing and Machine Learning for Precision Agriculture: A Comprehensive Perspective on Applications", Agronomy, vol. 14, núm. 9, p. 1975, sep. 2024, doi: 10.3390/agronomy14091975.

[29] M. H. M. Ghazali, A. Azmin, y W. Rahiman, "Drone Implementation in Precision Agriculture – A Survey", International Journal of Emerging Technology and Advanced Engineering, vol. 12, núm. 4, pp. 67–77, abr. 2022, doi: 10.46338/IJETAE0422_10.

[30] M. Dian Bah, A. Hafiane, y R. Canals, "Deep Learning with Unsupervised Data Labeling for Weed Detection in Line Crops in UAV Images", Remote Sensing 2018, Vol. 10, Page 1690, vol. 10, núm. 11, p. 1690, oct. 2018, doi: 10.3390/RS10111690.

[31] J. Yeom et al., "Comparison of Vegetation Indices Derived from UAV Data for Differentiation of Tillage Effects in Agriculture", Remote Sensing 2019, Vol. 11, Page 1548, vol. 11, núm. 13, p. 1548, jun. 2019, doi: 10.3390/RS11131548.

[32] K. Johansen et al., "Mapping the condition of macadamia tree crops using multi-spectral UAV and WorldView-3 imagery", ISPRS Journal of Photogrammetry and Remote Sensing, vol. 165, pp. 28–40, jul. 2020, doi: 10.1016/J.ISPRSJPRS.2020.04.017.

[33] Y. Meng, J. Su, J. Song, W.-H. Chen, y Y. Lan, "Experimental evaluation of UAV spraying for peach trees of different shapes: effects of operational parameters on droplet distribution".

[34] F. Al-Turjman y H. Altiparmak, "Smart agriculture framework using UAVs in the Internet of Things era", Drones in Smart-Cities: Security and Performance, pp. 107–122, ene. 2020, doi: 10.1016/B978-0-12-819972-5.00007-0.

[35] S. Vélez, R. Vacas, H. Martín, D. Ruano-Rosa, y S. Álvarez, "High-Resolution UAV RGB Imagery Dataset for Precision Agriculture and 3D Photogrammetric Reconstruction Captured over a Pistachio Orchard (Pistacia vera L.) in Spain", Data (Basel), vol. 7, núm. 11, nov. 2022, doi: 10.3390/DATA7110157.

[36] P. K. Singh y A. Sharma, "An intelligent WSN-UAV-based IoT framework for precision agriculture application", Computers and Electrical Engineering, vol. 100, p. 107912, may 2022, doi: 10.1016/J.COMPELECENG.2022.107912.

[37] R. Chin, C. Catal, y A. Kassahun, "Plant disease detection using drones in precision agriculture", Precis Agric, vol. 24, núm. 5, pp. 1663–1682, oct. 2023, doi: 10.1007/S11119-023-10014-Y.

[38] S. García-Gil, D. Ramos-Ramos, J. Berrocal, J. M. Murillo, y J. Galán-Jiménez, "Microservices migration: A pathway to improved energy efficiency in UAV networks", Internet of Things, vol. 30, p. 101463, mar. 2025, doi: 10.1016/j.iot.2024.101463.

[39] R. Guebsi, S. Mami, y K. Chokmani, "Drones in Precision Agriculture: A Comprehensive Review of Applications, Technologies, and Challenges", Drones, vol. 8, núm. 11, p. 686, nov. 2024, doi: 10.3390/drones8110686.

[40] D. Hawashin et al., "Blockchain applications in UAV industry: Review, opportunities, and challenges", Journal of Network and Computer Applications, vol. 230, p. 103932, oct. 2024, doi: 10.1016/j.jnca.2024.103932.

[41] S. S. Kamble, A. Gunasekaran, y S. A. Gawankar, "Achieving sustainable performance in a data-driven agriculture supply chain: A review for research and applications", 2020. doi: 10.1016/j.ijpe.2019.05.022.

[42] I. C. for T. Agriculture, I. F. P. R. Institute, y C. P. for B. D. in Agriculture, "CGIAR Big Data Coordination Platform Full Proposal", 2016, Consultado: el 28 de agosto de 2023. [En línea]. Disponible en: https://cgspace.cgiar.org/handle/10947/4303

[43] "FAO's Big Data tool on food chains under the COVID-19 pandemic | UN-SPIDER Knowledge Portal". Consultado: el 15 de marzo de 2023. [En línea]. Disponible en: https://un-spider.org/links-and-resources/covid-19/fao%E2%80%99s-big-data-tool-food-chains-under-covid-19-pandemic

[44] C. Zhang y Z. Liu, "Application of big data technology in agricultural Internet of Things", Int J Distrib Sens Netw, vol. 15, núm. 10, oct. 2019, doi: 10.1177/1550147719881610.

[45] A. H. Basori, A. B. F. Mansur, y H. Y. Riskiawan, "SMARF: Smart Farming Framework Based on Big Data, IoT and Deep Learning Model for Plant Disease Detection and Prevention", Communications in Computer and Information Science, vol. 1174 CCIS, pp. 44–56, 2020, doi: 10.1007/978-3-030-38752-5_4.

[46] S. A. Lokhande, "Effective use of big data in precision agriculture", 2021 International Conference on Emerging Smart Computing and Informatics, ESCI 2021, pp. 312–316, mar. 2021, doi: 10.1109/ESCI50559.2021.9396813.

[47] L. Li, J. Lin, Y. Ouyang, y X. (Robert) Luo, "Evaluating the impact of big data analytics usage on the decision-making quality of organizations", Technol Forecast Soc Change, vol. 175, p. 121355, feb. 2022, doi: 10.1016/J.TECHFORE.2021.121355.

[48] E. M. Ouafiq, R. Saadane, y A. Chehri, "Data Management and Integration of Low Power Consumption Embedded Devices IoT for Transforming Smart Agriculture into Actionable Knowledge", Agriculture 2022, Vol. 12, Page 329, vol. 12, núm. 3, p. 329, feb. 2022, doi: 10.3390/AGRICULTURE12030329.

[49] V. M. Ngo, T. V. T. Duong, T. B. T. Nguyen, C. N. Dang, y O. Conlan, "A big data smart agricultural system: recommending optimum fertilisers for crops", International Journal of Information Technology (Singapore), vol. 15, núm. 1, pp. 249–265, ene. 2023, doi: 10.1007/S41870-022-01150-1.

[50] C. Wu et al., "China's agricultural machinery operation big data system", Comput Electron Agric, vol. 205, p. 107594, feb. 2023, doi: 10.1016/J.COMPAG.2022.107594.

[51] H. Rana, M. U. Farooq, A. K. Kazi, M. A. Baig, y M. A. Akhtar, "Prediction of Agricultural Commodity Prices using Big Data Framework", Engineering, Technology & Applied Science Research, vol. 14, núm. 1, pp. 12652–12658, feb. 2024, doi: 10.48084/ETASR.6468.

[52] A. Stephen, P. Arumugam, y C. Arumugam, "An efficient deep learning with a big data-based cotton plant monitoring system", International Journal of Information Technology, vol. 16, núm. 1, pp. 145–151, ene. 2024, doi: 10.1007/s41870-023-01536-9.

[53] N. T. Giannakopoulos, M. C. Terzi, D. P. Sakas, N. Kanellos, K. S. Toudas, y S. P. Migkos, "Agroeconomic Indexes and Big Data: Digital Marketing Analytics Implications for Enhanced Decision Making with Artificial Intelligence-Based Modeling", Information, vol. 15, núm. 2, p. 67, ene. 2024, doi: 10.3390/info15020067.

[54] L. Abualigah y M. Alkhrabsheh, "Amended hybrid multi-verse optimizer with genetic algorithm for solving task scheduling problem in cloud computing", J Supercomput, vol. 78, núm. 1, pp. 740–765, ene. 2022, doi: 10.1007/s11227-021-03915-0.

[55] Y. Kalyani y R. Collier, "A Systematic Survey on the Role of Cloud, Fog, and Edge Computing Combination in Smart Agriculture.", Sensors (Basel), vol. 21, núm. 17, sep. 2021, doi: 10.3390/s21175922.

[56] X. Li, Z. Ma, X. Chu, y Y. Liu, "A Cloud-Assisted Region Monitoring Strategy of Mobile Robot in Smart Greenhouse", 2019, doi: 10.1155/2019/5846232.

[57] X. Li, Z. Ma, X. Chu, y Y. Liu, "A Cloud-Assisted Region Monitoring Strategy of Mobile Robot in Smart Greenhouse", Mobile Information Systems, vol. 2019, 2019, doi: 10.1155/2019/5846232.

[58] A. Paludo, W. R. Becker, J. Richetti, L. C. D. A. Silva, y J. A. Johann, "Mapping summer soybean and corn with remote sensing on Google Earth Engine cloud computing in Parana state – Brazil", vol. 13, núm. 12, pp. 1624–1636, 2020, doi: 10.1080/17538947.2020.1772893.

[59] T. C. Hsu, H. Yang, Y. C. Chung, y C. H. Hsu, "A Creative IoT agriculture platform for cloud fog computing", Sustainable Computing: Informatics and Systems, vol. 28, p. 100285, dic. 2020, doi: 10.1016/J.SUSCOM.2018.10.006.

[60] K. Phasinam et al., "Application of IoT and Cloud Computing in Automation of Agriculture Irrigation", J Food Qual, vol. 2022, pp. 1–8, ene. 2022, doi: 10.1155/2022/8285969.

[61] G. Idoje, T. Dagiuklas, y M. Iqbal, "Survey for smart farming technologies: Challenges and issues", Computers & Electrical Engineering, vol. 92, p. 107104, jun. 2021, doi: 10.1016/J.COMPELECENG.2021.107104.

[62] N. Islam, M. M. Rashid, F. Pasandideh, B. Ray, S. Moore, y R. Kadel, "A Review of Applications and Communication Technologies for Internet of Things (IoT) and Unmanned Aerial Vehicle (UAV) Based Sustainable Smart Farming", Sustainability 2021, Vol. 13, Page 1821, vol. 13, núm. 4, p. 1821, feb. 2021, doi: 10.3390/SU13041821.

[63] A. M. S. Kheir, K. A. Ammar, A. Amer, M. G. M. Ali, Z. Ding, y A. Elnashar, "Machine learning-based cloud computing improved wheat yield simulation in arid regions", Comput Electron Agric, vol. 203, p. 107457, dic. 2022, doi: 10.1016/J.COMPAG.2022.107457.

[64] S. Pizarro et al., "Implementing Cloud Computing for the Digital Mapping of Agricultural Soil Properties from High Resolution UAV Multispectral Imagery", Remote Sensing 2023, Vol. 15, Page 3203, vol. 15, núm. 12, p. 3203, jun. 2023, doi: 10.3390/RS15123203.

[65] A. A. Junior, T. J. A. da Silva, y S. P. Andrade, "Smart IoT lysimetry system by weighing with automatic cloud data storage", Smart Agricultural Technology, vol. 4, p. 100177, ago. 2023, doi: 10.1016/J.ATECH.2023.100177.

[66] M. Saban et al., "A Smart Agricultural System Based on PLC and a Cloud Computing Web Application Using LoRa and LoRaWan", Sensors 2023, Vol. 23, Page 2725, vol. 23, núm. 5, p. 2725, mar. 2023, doi: 10.3390/S23052725.

[67] A. Morchid, R. Jebabra, H. M. Khalid, R. El Alami, H. Qjidaa, y M. Ouazzani Jamil, "IoT-based smart irrigation management system to enhance agricultural water security using embedded systems, telemetry data, and cloud computing", Results in Engineering, vol. 23, p. 102829, sep. 2024, doi: 10.1016/J.RINENG.2024.102829.

[68] I. Ivanochko, M. J. Greguš, y O. Melnyk, "Smart Farming System Based on Cloud Computing Technologies", Procedia Comput Sci, vol. 238, pp. 857–862, ene. 2024, doi: 10.1016/J.PROCS.2024.06.103.

[69] S. Lee et al., "Image Processing for Smart Agriculture Applications Using Cloud-Fog Computing", Sensors 2024, Vol. 24, Page 5965, vol. 24, núm. 18, p. 5965, sep. 2024, doi: 10.3390/S24185965.

[70] P. Alvarado-Medellin et al., "Sistema dinámico para el monitoreo y control de redes inalámbricas de sensores que operan bajo el protocolo de comunicación ZigBee", Ingeniería, investigación y tecnología, vol. 20, núm. 1, pp. 0–0, ene. 2019, doi: 10.22201/fi.25940732e.2019.20n1.003

[71] W. Ma, J. Fan, C. Zhao, y H. Wu, "The realization of pig intelligent feeding equipment and network service platform", IFIP Adv Inf Commun Technol, vol. 546, pp. 473–484, 2019, doi: 10.1007/978-3-030-06179-1_47.

[72] H. Sharma, A. Haque, y Z. A. Jaffery, "Maximization of wireless sensor network lifetime using solar energy harvesting for smart agriculture monitoring", Ad Hoc Networks, vol. 94, p. 101966, nov. 2019, doi: 10.1016/J.ADHOC.2019.101966.

[73] B. Sharma, N. Kumar, M. W. Rasooli, y B. Bhushan, "Applicability Of Wireless Sensor Networks & Iot In Saffron & Wheat Crops: A Smart Agriculture Perspective", Article in International Journal of Scientific & Technology Research, vol. 9, p. 2, 2020, Consultado: el 17 de febrero de 2024. [En línea]. Disponible en: www.ijstr.org

[74] R. K. Singh, M. Aernouts, M. De Meyer, M. Weyn, y R. Berkvens, "Leveraging LoRaWAN Technology for Precision Agriculture in Greenhouses", Sensors 2020, Vol. 20, Page 1827, vol. 20, núm. 7, p. 1827, mar. 2020, doi: 10.3390/S20071827.

[75] M. Cicioğlu y A. Çalhan, "Smart agriculture with internet of things in cornfields", Computers & Electrical Engineering, vol. 90, p. 106982, mar. 2021, doi: 10.1016/J.COMPELECENG.2021.106982.

[76] J. Mabrouki, M. Azrour, D. Dhiba, Y. Farhaoui, y S. El Hajjaji, "IoT-based data logger for weather monitoring using arduino-based wireless sensor networks with remote graphical application and alerts", Big Data Mining and Analytics, vol. 4, núm. 1, pp. 25–32, mar. 2021, doi: 10.26599/BDMA.2020.9020018.

[77] A. Z. Bayih, J. Morales, Y. Assabie, y R. A. de By, "Utilization of Internet of Things and Wireless Sensor Networks for Sustainable Smallholder Agriculture", Sensors 2022, Vol. 22, Page 3273, vol. 22, núm. 9, p. 3273, abr. 2022, doi: 10.3390/S22093273.

[78] J. G. Rajendran, M. Alagarsamy, V. Seva, P. M. Dinesh, B. Rajangam, y K. Suriyan, "IoT based tracking cattle healthmonitoring system using wireless sensors", Bulletin of Electrical Engineering and Informatics, vol. 12, núm. 5, pp. 3086–3094, oct. 2023, doi: 10.11591/eei.v12i5.4610.

[79] M. Noor Fatima, P. Basin, with the King Abdullah, K. Mahmood, T. Roc, y M. Faizan Ayub, "Privacy-Preserving Three-Factor Authentication Protocol for Wireless Sensor Networks Deployed in Agricultural Field", 2023, doi: 10.1145/3607142.

[80] R. Tang, N. K. Aridas, y M. S. Abu Talip, "Design of Wireless Sensor Network for Agricultural Greenhouse Based on Improved Zigbee Protocol", Agriculture 2023, Vol. 13, Page 1518, vol. 13, núm. 8, p. 1518, jul. 2023, doi: 10.3390/AGRICULTURE13081518.

[81] A. K. Rao, K. K. Nagwanshi, y M. K. Shukla, "An optimized secure cluster-based routing protocol for IoT-based WSN structures in smart agriculture with blockchain-based integrity checking", Peer Peer Netw Appl, vol. 17, núm. 5, pp. 3159–3181, sep. 2024, doi: 10.1007/s12083-024-01748-1.

[82] K. Aggarwal, G. Sreenivasula Reddy, R. Makala, T. Srihari, N. Sharma, y C. Singh, "Studies on energy efficient techniques for agricultural monitoring by wireless sensor networks", Computers and Electrical Engineering, vol. 113, p. 109052, ene. 2024, doi: 10.1016/j.compeleceng.2023.109052.

[83] J. Navarro, R. R. Fernández, V. Aceña, A. Fernández-Isabel, C. Lancho, y I. M. de Diego, "Real-time classification of cattle behavior using Wireless Sensor Networks", Internet of Things, vol. 25, p. 101008, abr. 2024, doi: 10.1016/J.IOT.2023.101008.

[84] J. Xu, B. Gu, y G. Tian, "Review of agricultural IoT technology", Artificial Intelligence in Agriculture, vol. 6, pp. 10–22, 2022, doi: 10.1016/j.aiia.2022.01.001.

[85] M. S. Farooq, S. Riaz, A. Abid, K. Abid, y M. A. Naeem, "A Survey on the Role of IoT in Agriculture for the Implementation of Smart Farming", IEEE Access, vol. 7, pp. 156237–156271, 2019, doi: 10.1109/ACCESS.2019.2949703.

[86] J. Xu, B. Gu, y G. Tian, "Review of agricultural IoT technology", Artificial Intelligence in Agriculture, vol. 6, pp. 10–22, ene. 2022, doi: 10.1016/J.AIIA.2022.01.001.

[87] A. K. Vishwakarma, S. Chaurasia, K. Kumar, Y. N. Singh, y R. Chaurasia, "Internet of things technology, research, and challenges: a survey", Multimed Tools Appl, may 2024, doi: 10.1007/s11042-024-19278-6.

[88] M. E. E. Alahi, N. Pereira-Ishak, S. C. Mukhopadhyay, y L. Burkitt, "An Internet-of-Things Enabled Smart Sensing System for Nitrate Monitoring", IEEE Internet Things J, vol. 5, núm. 6, pp. 4409–4417, dic. 2018, doi: 10.1109/JIOT.2018.2809669.

[89] Y. A. Rivas-Sánchez, M. F. Moreno-Pérez, y J. Roldán-Cañas, "Environment Control with Low-Cost Microcontrollers and Microprocessors: Application for Green Walls", Sustainability 2019, Vol. 11, Page 782, vol. 11, núm. 3, p. 782, feb. 2019, doi: 10.3390/SU11030782.

[90] D. Glaroudis, A. Iossifides, y P. Chatzimisios, "Survey, comparison and research challenges of IoT application protocols for smart farming", Computer Networks, vol. 168, p. 107037, feb. 2020, doi: 10.1016/J.COMNET.2019.107037.

[91] A. K. Podder et al., "IoT based smart agrotech system for verification of Urban farming parameters", Microprocess Microsyst, vol. 82, p. 104025, abr. 2021, doi: 10.1016/J.MICPRO.2021.104025.

[92] A. Ghandar, A. Ahmed, S. Zulfiqar, Z. Hua, M. Hanai, y G. Theodoropoulos, "A decision support system for urban agriculture using digital twin: A case study with aquaponics", IEEE Access, vol. 9, pp. 35691–35708, 2021, doi: 10.1109/ACCESS.2021.3061722.

[93] F. Jamil, M. Ibrahim, I. Ullah, S. Kim, H. K. Kahng, y D. H. Kim, "Optimal smart contract for autonomous greenhouse environment based on IoT blockchain network in agriculture", Comput Electron Agric, vol. 192, p. 106573, ene. 2022, doi: 10.1016/J.COMPAG.2021.106573.

[94] R. P. Sharma, D. Ramesh, P. Pal, S. Tripathi, y C. Kumar, "IoT-Enabled IEEE 802.15.4 WSN Monitoring Infrastructure-Driven Fuzzy-Logic-Based Crop Pest Prediction", IEEE Internet Things J, vol. 9, núm. 4, pp. 3037–3045, feb. 2022, doi: 10.1109/JIOT.2021.3094198.

[95] G. Patrizi, A. Bartolini, L. Ciani, V. Gallo, P. Sommella, y M. Carratu, "A Virtual Soil Moisture Sensor for Smart Farming Using Deep Learning", IEEE Trans Instrum Meas, vol. 71, 2022, doi: 10.1109/TIM.2022.3196446.

[96] S. Mishra y S. K. Sharma, "Advanced contribution of IoT in agricultural production for the development of smart livestock environments", Internet of Things, vol. 22, p. 100724, jul. 2023, doi: 10.1016/J.IOT.2023.100724.

[97] W. L. Prasetya, A. Ma'arif, H. M. Marhoon, R. Alayi, y A.-N. Sharkawy, "Monitoring of Water Flow on Solar-Powered Pump for IoT-Based Agriculture", Journal of Science in Agrotechnology, vol. 1, núm. 1, pp. 23–35, may 2023, doi: 10.21107/JSA.V1I1.6.

[98] M. Krishnamoorthy, Md. Asif, P. P. Kumar, R. S. S. Nuvvula, B. Khan, y I. Colak, "A Design and Development of the Smart Forest Alert Monitoring System Using IoT", J Sens, vol. 2023, núm. 1, ene. 2023, doi: 10.1155/2023/8063524.

[99] S. Ahmed et al., "IoT based intelligent pest management system for precision agriculture", Sci Rep, vol. 14, núm. 1, p. 31917, dic. 2024, doi: 10.1038/s41598-024-83012-3.

[100] G. Krishnan et al., "A Raspberry Pi-Powered IoT Smart Farming System for Efficient Water Irrigation and Crop Monitoring", Malaysian Journal of Science and Advanced Technology, vol. 4, núm. 2, pp. 149–158, mar. 2024, doi: 10.56532/MJSAT.V4I2.295.

Nota contribución de los autores:

1. Concepción y diseño del estudio
2. Adquisición de datos
3. Análisis de datos
4. Discusión de los resultados
5. Redacción del manuscrito
6. Aprobación de la versión final del manuscrito

LC ha contribuido en: 1, 2, 3 4, 5 y 6.

JS ha contribuido en: 1, 2, 3 4, 5 y 6.

YMG ha contribuido en: 1, 2, 3 4, 5 y 6.

MVV ha contribuido en: 1, 2, 3 4, 5 y 6.

YM ha contribuido en: 1, 2, 3 4, 5 y 6.

NC ha contribuido en: 1, 2, 3 4, 5 y 6.

MSL ha contribuido en: 1, 2, 3 4, 5 y 6.

FMMG ha contribuido en: 1, 2, 3 4, 5 y 6.

Acceptance Note: This article was approved by the journal editors Dr. Rafael Sotelo and Mag. Ing. Fernando A. Hernández Gobertti.

Computational study of the direct impact of a 200 kA lightning strike on external floating roof tanks

Estudio computacional del impacto directo de un rayo de 200 kA sobre tanques externos de techo flotante

Estudo computacional do impacto direto de uma descarga atmosférica de 200 kA em tanques externos de teto flutuante

Juan David Losada Losada [1(*)], Darwin Marín Yépez [2], Camilo Younes Velosa [3]

Recibido: 09/08/2025 Aceptado: 14/10/2025

Summary. - This study investigates the electromagnetic behavior of external floating roof tanks subjected to a direct 200 kA lightning strike. Using computational electromagnetics, electric and magnetic fields were calculated for two scenarios: with and without the use of bypass conductors, as recommended by API RP-545. Simulation results revealed that electric field values at the junction between the tank wall and the floating roof exceed 200 kV/m in the absence of bypass conductors, increasing the risk of ignition. The implementation of bypass conductors significantly reduced the field intensity, indicating their effectiveness in mitigating fire hazards in flammable storage environments.

Keywords: Lightning; floating roof tank; computational electromagnetism.

[1] Docente. Facultad de Ciencias e Ingeniería de la Universidad de Manizales (Colombia), jlosada@umanizales.edu.co, ORCID iD: https://orcid.org/0000-0001-9935-9977

[2] Docente. Facultad de Ciencias e Ingeniería de la Universidad de Manizales (Colombia), dmariny@unal.edu.co, ORCID iD: https://orcid.org/0000-0002-2709-361X

[3] Docente. Facultad de Ingeniería y Arquitectura de la Universidad Nacional de Colombia (Colombia), cyounesv@unal.edu.co, ORCID iD: https://orcid.org/0000-0002-9685-8196

Memoria Investigaciones en Ingeniería, núm. 29 (2025). pp. 190-204
https://doi.org/10.36561/ING.29.12
ISSN 2301-1092 • ISSN (en línea) 2301-1106 – Universidad de Montevideo, Uruguay
Este es un artículo de acceso abierto distribuido bajo los términos de una licencia de uso y distribución CC BY-NC 4.0. Para ver una copia de esta licencia visite http://creativecommons.org/licenses/by-nc/4.0/

Resumen. - *Este estudio investiga el comportamiento electromagnético de tanques externos con techo flotante sometidos a la descarga directa de un rayo de 200 kA. Mediante electromagnetismo computacional, se calcularon los campos eléctricos y magnéticos para dos escenarios: con y sin el uso de conductores de derivación, según lo recomendado por API RP-545. Los resultados de la simulación revelaron que los valores del campo eléctrico en la unión entre la pared del tanque y el techo flotante superan los 200 kV/m en ausencia de conductores de derivación, lo que aumenta el riesgo de ignición. La implementación de conductores de derivación redujo significativamente la intensidad del campo, lo que indica su eficacia para mitigar los riesgos de incendio en entornos de almacenamiento inflamables.*

Palabras clave: *Descarga atmosférica; tanque externo con techo flotante; electromagnetismo computacional.*

Resumo**.** ***-*** *Este estudo investiga o comportamento eletromagnético de tanques de teto flutuante externo submetidos a uma descarga direta de raio de 200 kA. Utilizando eletromagnetismo computacional, calcularam-se os campos elétricos e magnéticos para dois cenários: com e sem o uso de condutores de bypass, conforme recomendado pela API RP-545. Os resultados das simulações revelaram que, na ausência de condutores de bypass, os valores do campo elétrico na junção entre a parede do tanque e o teto flutuante ultrapassam 200 kV/m, aumentando o risco de ignição. A implementação dos condutores de bypass reduziu significativamente a intensidade do campo, demonstrando sua eficácia na mitigação de riscos de incêndio em ambientes de armazenamento de líquidos inflamáveis.*

Palavras-chave: *Descargas atmosféricas; tanque de teto flutuante; eletromagnetismo computacional.*

1. Introduction. - Colombia is a tropical country characterized by distinctive atmospheric conditions and high lightning density. The nation possesses abundant oil resources and continues to expand its exploration, production, transportation, and refining sectors. The most commonly used oil storage tanks include fixed roof tanks, external floating roof tanks, and internal floating roof tanks.

This study focuses on external floating roof tanks, analyzing the effects of direct lightning strikes and reviewing the applicability of the API RP-545 (2009) standard within the context of Colombia's atmospheric activity [1]. Previous research on hydrocarbon storage tank fires has demonstrated a significant probability of ignition resulting from direct lightning strikes, with external floating roof tanks presenting the highest associated risk [2]–[5].

The objective of this research is to assess the effectiveness of bypass conductors in mitigating the risk of ignition caused by direct lightning strikes on external floating roof tanks through electromagnetic field simulations. Electric and magnetic fields were computed using FEKO simulation software for two configurations: one without bypass conductors (Case I) and another incorporating bypass conductors as recommended by API RP-545 (Case II).

2. Methodology. – This study employed computational electromagnetics to evaluate the transient electromagnetic fields generated by a direct 200 kA lightning strike on an external floating-roof (EFR) tank. The analysis focused on the critical roof–wall junction region, where high electric-field gradients can cause ignition in flammable vapor zones.

Ignition Criteria: Physical and Operational Justification

Two complementary criteria were employed to evaluate the ignition risk in the seal (rim) region:

(i) Field Criterion (screening): The operational threshold $E_{crit} = 200$ kV/m was adopted as a conservative indicator of pre-breakdown conditions in non-uniform seal geometries. This threshold, widely referenced in EFR/TTE studies, identifies regions exhibiting high electric-field gradients along roof–wall edges. It does not represent the planar air breakdown field (~3 MV/m at 1 atm) but rather serves as an indicator of streamer or leader inception in configurations with sharp edges, corners, and micro-asperities [6]-[9].

(ii) Energy criterion(decisive): The energy available within the seal gap is expressed as:
$W = \int_0^T V_{gap}(t) I_{gap}(t) dt$ or, in the absence of prior conduction, $W \approx \frac{1}{2} C_{gap} V_{gap,peak}^2$.

This is compared with the minimum ignition energy (MIE) of hydrocarbon-air mixtures, typically $O(0.1 - 0.3)$ mJ (for methane/propane/light gasoline vapors), with slight enhancement due to humidity and reduction near stoichiometric conditions [1],[6].

Real Vapor Parameters

For light combustible vapors (e.g., gasoline), reported MIE values lie in the range of 0.15–0.30 mJ; for jet fuel/kerosene, they are typically higher. The relevant gap length is approximately 10 mm (seal section), under ambient pressure and relative humidity of 40–80 %. This analysis considers the following aspects:

- Composition: Concentration ranges between the LEL–UEL limits are evaluated; the representative case is near stoichiometric conditions.
- Seal Geometry: Sharp edges and corners reduce the streamer inception field; therefore, $E_{crit} = 200\, kV/m$ is considered conservative for this geometry.
- Leader Criterion (Rizk/ELI): The integral condition for leader inception in short gaps with small curvature radii is discussed in the appendix (not included here for brevity) [9],[10].

Mechanism Distinction

- Direct Spark in the Gap: Characterized by high local electric fields within the seal region; governed by $E_{\max}$ and W.

- Induced Spark: Caused by non-uniform equipotential distributions around the rim; associated with $V_{\mathrm{roof-wall}}(\mathrm{t})$ and transient currents induced in nearby metallic components.
- Potential Equalization (post-impulse): After the current front, residual currents may bridge weak gaps; W is evaluated over longer time windows T together with $Z_{\mathrm{eq}}(\mathrm{t})$.

2.1 Model of lightning current and calculation of electromagnetic field. - The lightning return channel was modeled using a base current with a double-exponential waveform equivalent to the 10/350 µs impulse specified in IEC 62305, adjusted to a peak current $I_{peak} = 200\ kA$ (representing the conservative level for the first stroke). The excitation is injected at the channel base and coupled to the FDTD subdomain (rim box).

Temporal waveform and intensity
The following expression was adopted:

$$i_b(t) = I_{scale}(e^{-at} - e^{-bt})u(t),\ \ a \ll b \qquad (1)$$

Where u(t) is the step function. To obtain a peak current $I_{peak} = 200kA$ with a front time of approximately $t_f \approx 10\mu s$ and a tail of 350 μs, the following reproducible parameters were set:

$$a = 2.03 \times 10^3\ s^{-1}, \qquad b = 2.03 \times 10^5 s^{-1}, \quad I_{scale} = 211.6\ kA$$

This produces $I_{peak} \approx 200\ kA$ and a maximum rate of current rise of approximately $\frac{di}{dt} \approx 42.6\ kA/\mu s$, consistent with IEC 62305. The Heidler model was parameterized in an appendix (not shown here) for cross-verification purposes [11],[12],[13],[14].

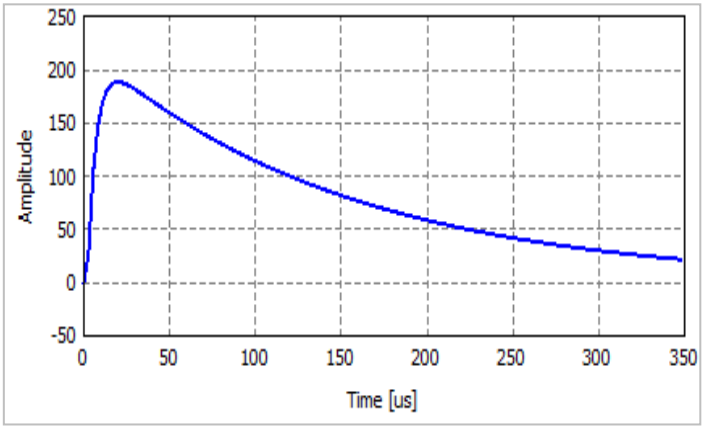

Figure I. Double exponential model f lightning current for 200kA

The lightning channel was represented as a vertical thin wire of length L=2 km above the impact point (angular perturbations of ±10° were included in the sensitivity analysis). The MTLE model (Modified Transmission Line with Exponential Decay) was adopted for the spatial current distribution:

$$i(z,t) = i_b\left(t - \frac{z}{v}\right)e^{-z/\lambda} \qquad (2)$$

With a return velocity $v = 1.3 \times 10^8\ m/s$ and a characteristic length $\lambda = 2$ km. The coupling with the tank was solved using a hybrid approach (thin-wire + FDTD).

Impact Point and Impedances
Two critical scenarios were considered: (i) impact at the rim (roof–wall junction), and (ii) impact at the roof center.

The effective grounding impedance of the tank–ring–down conductor–ground assembly was evaluated as:

$$Z_{eq}(t) = \frac{V_{tank}(t)}{I_{discharge}(t)} \quad (3)$$

for $t \in [0,5]$ µs. Both peak and average Z_{eq} values were reported over the front duration.

Sensitivity to I_{peak} and front time

Parametric sweeps were performed for $\{I_{peak}\} = \{100, 150, 200, 250\}\ kA$ and front times $\{t_f\} = \{5, 10, 20\}$ µs (by adjusting a and b in Eq, (1)). The key metrics exhibited the following approximate dependencies:

$$E_{max} \propto I_{peak} t_f^{-\alpha}, \quad V_{roof-wall,peak} \propto I_{peak} t_f^{-\beta}$$

With $\alpha, \beta \in [0.4, 0.6]$. The 95% confidence interval (CI) band are included in figure II-IV.

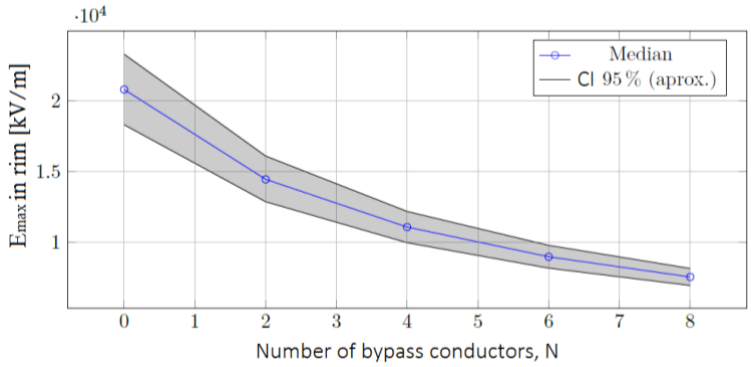

Figure II. Design curve: E_{max} at the rim versus N with 95% confidence interval (CI) band.

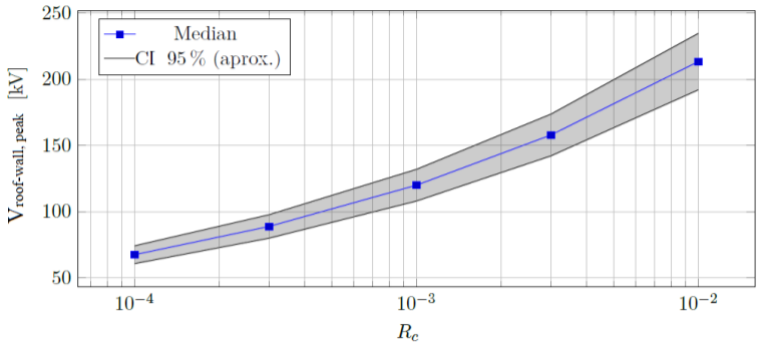

Figure III. Design curve: $V_{roof-wall,peak}$ versus Contact resistance R_c (logarithmic scale)

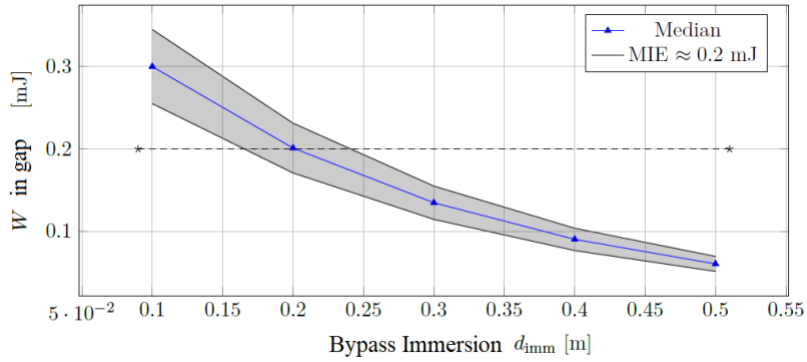

Figure III. Design curve: W in Gap versus immersion depth d_{imm}. Dashed line: MIE ≈ 0.2 mJ.

Current and Voltage Paths

The current and voltage distributions were analyzed to characterize the transient coupling mechanisms at the roof–wall interface. The induced roof–wall potential was obtained along the shortest path across the 10-mm seal gap, where the highest electric field gradients occur, according to:

$$\boldsymbol{V}_{roof-wall,}(t) = \int_{\mathcal{L}} \boldsymbol{E} \cdot d\boldsymbol{l} \tag{4}$$

Bypass and down-conductor currents were calculated for each conductor k as:

$$\boldsymbol{I}_k(t) = \int_{S_k} \boldsymbol{J} \cdot d\boldsymbol{S} \tag{5}$$

And the total current to ground through the down-conductors and peripheral ring was determined accordingly.

The available energy within the seal gap was evaluated using a dynamic resistive model valid prior to breakdown, given by:

$$W = \int_0^T V_{gap}(t) I_{gap}(t) dt \tag{6}$$

Which, in the absence of pre-breakdown conduction, can be approximated as:

$$W \approx \frac{1}{2} C_{gap} V^2 \tag{7}$$

The computed energy values were subsequently compared with the minimum ignition energy (MIE) of hydrocarbon–air mixtures to assess the ignition risk at the seal region.

2.2 Numerical Modeling Using the Finite-Difference Time-Domain Method (FDTD). - To analyze the transient electromagnetic coupling of a direct lightning strike on an external floating-roof tank (EFR), a three-dimensional explicit FDTD model based on a Yee grid was employed, solving Maxwell's equations in the time domain with a stable and controlled space–time discretization. The approach was configured as a hybridization scheme, consisting of an FDTD subdomain that encloses the roof–wall boundary region (the seal area)—where the highest field gradients occur—and the macro-structure of the tank, the grounding system, and the return path, which were modeled using impedance surfaces and thin-wire models. These were coupled through Huygens/equivalent field surfaces. This scheme significantly reduces computational cost by several orders of magnitude without sacrificing accuracy in the critical region.

Model Geometry

The tank was represented as a conductive cylinder with an external floating roof. The following geometric parameters were defined for reproducibility:

- Roof type: External floating roof (EFR) of annular pontoon type; modeled as a conducting sheet with surface impedance (equivalent to carbon steel).
- Main dimensions: Diameter D=16 m, shell height H=12 m; nominal thicknesses $t_{shell} = 10\ mm$ and $t_{roof} = 8$ mm.
- Roof–wall clearance: Uniform gap $g = 10$ mm (1 cm).
- Edge seal: Mechanical seal of brush/metallic type; an explicit air gap of $h = 10\ mm$ (height) and $w = 10$ mm (width) was modeled within the roof–wall clearance. This gap defines the region of highest risk for dielectric breakdown.
- FDTD subdomain (rim box): Rectangular prism following the roof perimeter.

- Dimensions: axial length $L \approx 50\,mL$ (full circumference), radial thickness $R_w = 1.2\,m$ (0.6 m inward + 0.6 m outward from the tank wall), and height $H_w = 0.5\,m$ (centered at the seal elevation). This subdomain captures the intense electromagnetic fields in the rim region; the remainder of the structure is treated through hybridization.

Grounding system and conductor modeling

Grounding system: A peripheral copper ring (cross-section 70 mm^2) was buried at a depth of 0.5 m, connected to four down conductors at 90° intervals, within a lossy soil medium. The effective grounding impedance Z_{eq} of the tank was measured during the first microseconds as $Z_{eq} = V/I$, using potential and current probes.

Shunts: Copper conductors (50 mm^2) were used to connect the roof and wall, with a submersion depth of 30 cm in the liquid (following API practice). The contact resistance at mechanical joints was set to $R_c = 1m\Omega$.

Bypass conductors: For the mitigated configuration, copper bypass conductors (120 mm^2) were added between the upper edge of the wall and the roof, following the shortest possible length criterion, with a contact resistance of $R_c = 1m\Omega$. Their distribution was uniform along the tank perimeter (sensitivity section not shown) for parametric analysis purposes.

Computational domain and boundary conditions

FDTD subdomain (rim box): $L \times R_w \times H_w \approx 50 \times 1.2 \times 0.5\ m^3$, centered at the seal. This local enclosure captures the maximum values of $|E|$ and the transients $V_{roof-wall}$.

PML boundaries: Convolutional perfectly matched layers (CPML) were implemented on the six faces of the subdomain, with a thickness of $N_{PML} = 10 - 12$ cells and a third-order polynomial conductivity profile (m=3):

$$\sigma(u) = \sigma_{max}\left(\frac{u}{d}\right)^m, \sigma_{max} = -\frac{(m+1)}{2\eta_0 d} ln\, R_{target} \quad (8)$$

Where u is the normal coordinate to the PML, d= $N_{PML}\Delta$ its thickness, η_0 the impedance of free space and $R_{target} \leq 10^{-8}$ the target reflectivity.

This configuration ensures numerical reflections below -60 dB within the frequency band of interest.

Coupling with macro-structure: Huygens/equivalent field surfaces were used on the inner faces of the rim box to exchange fields with the tank enclosure and the lightning channel (modeled using thin-wire/SIBC elements).
Spatial and temporal discretization

Meshing criteria. Two main restrictions were imposed: (i) Skin depth resolution in metallic materials, and (ii) geometric resolution of the seal gap.

$$\delta(f) = \sqrt{\frac{2}{\omega\mu_0\mu_r\sigma}},\ \Delta \leq \min\left(\frac{\delta(f_{max})}{5}, \frac{\lambda_{min}}{10}\right) \quad (9)$$

For $f_{max} = 1$ MHz (a conservative value for a 10/350 µs waveform), $\delta_{steel} \approx 0.23$ mm and $\delta_{Cu} \approx 0.066$ mm so the SIBC/PEC assumption remains valid (t >> δ). The dominant restriction is geometric, due to the 10 mm seal gap. A grid size of $\Delta = 2$ cm was adopted within the rim box, with a conformal/effective subcell for the gap an accepted practice that reproduces local field gradients without sub-millimeter meshing.

Alignment with Recommended Practices (API RP-545, NFPA 30, API 2003)

Summary of Relevant Requirements (Implemented in the Model):

- Submerged Shunts: Immersion depth ≥ 0.3 m, spacing ≤ 3 m, sufficient metallic cross-section, and electrical continuity. Implementation: copper shunts of 50 mm² cross-section, with immersion depth parameterized as $d_{\text{imm}} \in \{0.1, 0.3, 0.5\}$ m.

- Bypass Conductors: At least two, spaced ≤ 30 m (for $D = 16\,m$, $N \geq 2$; here $N \in \{0,2,4,6,8\}$), with minimum length and low contact resistance R_c.

  Implementation: copper conductors $\geq\ 95\,mm^2$, with $R_c \in [10^{-4}, 10^{-2}]\,\Omega$.
- Seal and instrumentation insulation: Electrical isolation of seal components and guide/measurement devices (to prevent spark trajectories).
  Implementation: dielectric materials in the seal and joint treatment explicitly modeled.

NFPA 30 provides the operational safety context (ventilation, handling during storms), while API 2003 addresses hazards associated with static electricity, lightning, and stray currents. The numerical model reproduces the mitigating effect of these practices on $E_{\max}$, $V_{\text{roof-wall}}$, and W.

3. Results. - The storage tanks of hydrocarbons of external floating roof are those that present the highest probability of a fire by atmospheric electric discharges [15], API-RP-545 standard presents a particular development in analysis and approach to protection for this type of tanks [16],[17]. Before 2009, the tank's own protection systems were developed in the shunt systems as an equipotential element between the tank roof and the tank wall, these equipotential elements were built above the floating roof. The following table I summarizes the protection elements used in floating roof tanks before 2009 and after 2009.

External floating roof tank	
Analysis API-RP-545 standard	
Before 2009	After 2009
Use of the norm API-2003	Use of the norm API-545
Use of Shunt above the floating roof. Equipotential elements	Shunt immersed in the liquid at least 30 cm. Equipotential elements canceling the oxygen component before a possible spark produced by lightning.
External protection with the rolling sphere method.	Bypass conductors connected between the top of the tank and the roof of the tank.
	Electrical insulation of more than 1kV between the elements of the roof of the tank and the wall of the tank (seals, springs, scrapers.)

Table I. Tank protection elements based on API-545 standard.

A simulation was carried out to analyze the behavior of the electromagnetic fields in the external floating roof tanks, analyzing two particular cases: case 1 with equipotential elements shunt between the roof of the tank and the wall without making differentiation if it is immersed in the liquid or not.

The second case with equipotential elements shunt between the roof of the tank and the wall and adding bypass conductors between the top of the wall of the tank and the floating roof according to API-RP-545.

A. Case I:

For the effects of the simulation, the equipotential bonding of the roof and the wall was carried out with the entire structure of the tank with a direct impact of 200 kA. For simulation purposes, the entire surface of the tank roof was modeled to electrical contact with the section of the wall surface.

A comparison is made between the magnitudes of the electromagnetic fields that are obtained when lightning directly impacts the roof of the tank that is considered the most critical scenario.

Figure III shows the behavior of the intensity of the electromagnetic fields at the point of impact and in the equipotential bonding between the roof of the tank and the wall. The highest intensities occur in the wall of the tank at the high point and in the equipotential bonding between the wall and the tank at the bottom point where the beam is impacting. According to the reference of 200 kV/m as maximum potential in which sparks can be presented at points at different potentials [18], the following results obtained in the simulation are analyzed. At the junction between the roof and the wall, there is the highest probability that flammable gases and vapors are present and that is where the potentials of 240 kV/m maximum and 210 kV/m minimum occur.

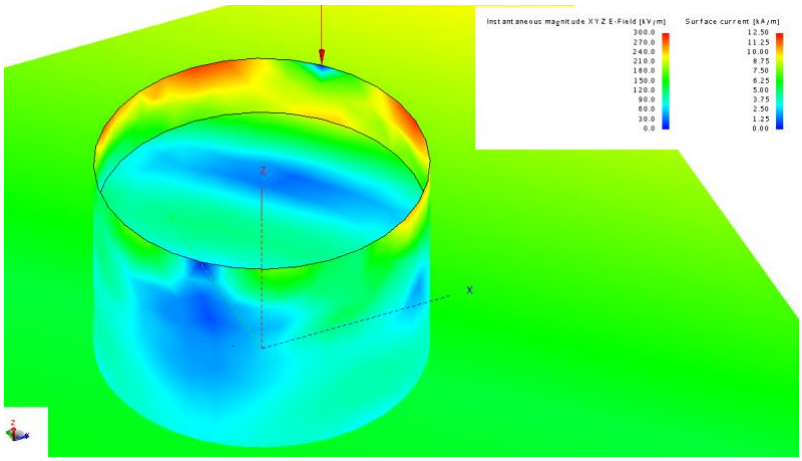

Figure III. Electric field strength [kV/m] with equipotential shunt, isometric view

According to these results it has that for equipotential shunt elements both immersed in the liquid and located above the tank before a discharge of 200kA there are values above 200kV/m, values that represent a high probability of ignition due to atmospheric electrical discharges and in the presence of flammable vapors. Table II.

	Results (**E, B**) for direct impact of 200kA.			
	On the roof of the external floating tank.		At the junction between the roof and the wall.	
	Electric field (kV/m)	Magnetic field (kA/m)	Electric field (kV/m)	Magnetic field (kA/m)
Max. Value	300	12.5	240	5.4
Min. Value	30	1.5	210	4.8

Table II. Electric and magnetic field case I.

B. Case II:

For the effects of the simulation, the equipotential bonding of the entire roof with the rest of the tank structure of the tank was performed and a direct impact of the first return discharge of 200kA of magnitude was made. Bypass conductors were added between the top of the tank wall and the floating roof. The selected conductor is equivalent to a 120 mm2 copper cable, to simulate the bypass conductor. For the simulated tank of 16 meters in diameter and 12 meters in height, 4 bypass conductors were located.

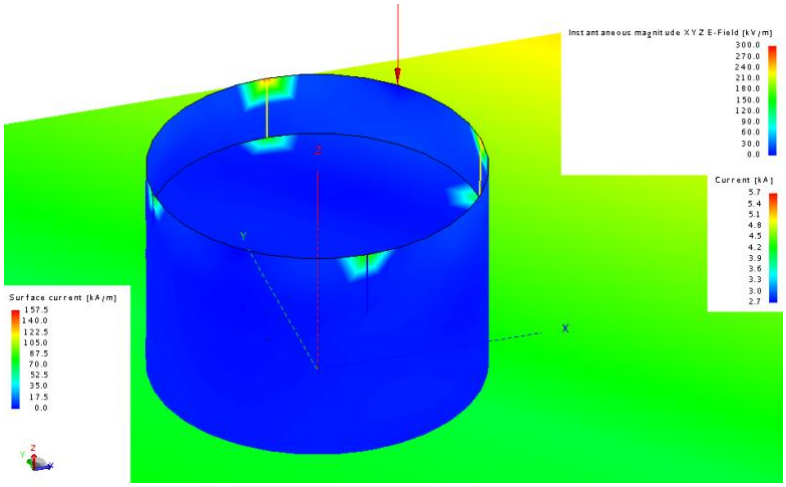

Figure IV. Electric field strength [kV/m] with equipotential shunt+ bypass, isometric view.

At the junction between the roof and the wall is where there is the highest probability that flammable gases and vapors are present and that is where potentials of 150 kV/m maximum and 90 kV/m minimum occur. According to these results, for equipotential shunt elements, adding a bypass conductor to a discharge of 200 kA has values below 200 kV/m, values that represent a considerable decrease in the probability of starting a fire in the face of an atmospheric electrical discharge. And in the presence of flammable vapors.

	Results (**E, B**) for direct impact of 200kA.			
	On the roof of the external floating tank.		At the junction between the roof and the wall.	
	Electric field (kV/m)	Magnetic field (kA/m)	Electric field (kV/m)	Magnetic field (kA/m)
Max. Value	40	3.3	150	4.5
Min. Value	15	2.7	90	3.9

Table III. Electric and magnetic field case II.

The simulation results indicate that using only shunt equipotential is not sufficient in terms of protection because they have values of more than 200 kV/m, which represents a high probability of starting a fire. By adding bypass conductors, the values of electric field are in values lower than 200 kV/m, which decrease the probability of sparks in elements that are not at the same potential.

4. Conclusions. - Numerical simulations of direct 200 kA lightning strikes on external floating-roof tanks reveal a strong dependence of electric field intensity on the tank's equipotential configuration. When only shunt conductors are present—either immersed in the liquid or located above the floating roof—the maximum electric field at the roof–wall junction exceeds 200 kV/m, reaching values between 210 kV/m and 240 kV/m. Such magnitudes correspond to pre-breakdown conditions and a high probability of vapor ignition.

In contrast, the inclusion of bypass conductors as recommended by API RP-545 reduces the electric field in the critical rim region to approximately 90–150 kV/m, well below the ignition threshold. This significant reduction confirms that bypass conductors enhance potential equalization and effectively mitigate lightning-induced ignition hazards in flammable storage environments.

The results support the adoption of API RP-545 mitigation practices in petroleum facilities, particularly in tropical regions with high lightning density. Future work should integrate thermodynamic and gas-diffusion models to assess the combined electromagnetic and chemical ignition mechanisms and validate the numerical findings through experimental or field measurements.

References

[1] National Fire Protection Association; *NFPA 30: Flammable and Combustible Liquids Code*, 2015.

[2] Benkaouha, B.; Chiremsel, Z.; Bellala, D.; Integration of fire safety barriers in the probabilistic analysis of accident scenarios triggered by lightning strike on atmospheric storage tanks, *Journal of Failure Analysis and Prevention*, 2022. Vol. 22: 2326–2351. doi: 10.1007/s11668-022-01500-y.

[3] Cheng, Y.; Luo, Y.; Analysis of Natech risk induced by lightning strikes in floating roof tanks based on the Bayesian network model, *Process Safety Progress*, 2020. doi: 10.1002/prs.12164.

[4] Jia, P.; Lv, J.; Sun, W.; Jin, H.; Meng, G.; Li, J.; Modified analytic hierarchy process for risk assessment of fire and explosion accidents of external floating roof tanks, *Process Safety Progress*, 2023. doi: 10.1002/prs.12520.

[5] Adekitan, A. I.; Rock, M.; Analytical computation of lightning strike probability for floating roof tanks, *Topical Issues of Rational Use of Natural Resources: Saint-Petersburg Scientific Conference Abstracts*, Vol. 1, 2020. [Online]. Available: https://www.researchgate.net/publication/352373902

[6] American Petroleum Institute; *API 2003: Protection Against Ignitions Arising out of Static, Lightning, and Stray Currents*, 2015.

[7] International Electrotechnical Commission; *IEC 62305: Protection against Lightning*, Parts 1–4, 2010.

[8] Rakov, V. A.; Uman, M. A.; *Lightning: Physics and Effects*, 2003, Cambridge University Press, Cambridge.

[9] Rizk, F. A. M.; A model for switching impulse leader inception in air gaps, *IEEE Transactions on Power Delivery*, 1989. Vol. 4(1): 596–606.

[10] Gallimberti, I.; The mechanism of the long spark formation, *Journal de Physique Colloques*, 1979. Vol. 40(C7): C7-193–C7-250.

[11] American Petroleum Institute; *API RP 505: Recommended Practice for Classification of Locations for Electrical Installations at Petroleum Facilities Classified as Class I, Zone 0, Zone 1, and Zone 2*, 1997.

[12] American Petroleum Institute; *API RP 500: Recommended Practice for Classification of Locations for Electrical Installations at Petroleum Facilities Classified as Class I, Division 1 and Division 2*, 1997.

[13] Nucci, C. A.; Mazzetti, C.; Rachidi, F.; Ianoz, M. V.; Lightning return stroke models with specified channel-base current, *IEEE Transactions on Electromagnetic Compatibility*, 1990. Vol. 32(1): 79–92.

[14] Agrawal, A. K.; Price, H. J.; Gurbaxani, S. H.; Transient response of a multiconductor line, *IEEE Transactions on Electromagnetic Compatibility*, 1980. Vol. 22(2): 119–129.

[15] Baba, Y.; *Electromagnetic Computation Methods for Lightning Surge Protection Studies*, 1st ed., 2016, John Wiley & Sons, Singapore.

[16] Zhang, W. S. C.; Zhang, J. W. M.; Risk assessment for fire and explosion accidents of steel oil tanks using improved AHP based on FTA, *Process Safety Progress*, 2015. Vol. 34(4): 393–402. doi: 10.1002/prs.11780.

[17] American Petroleum Institute; *API RP 545: Recommended Practice for Lightning Protection of Aboveground Storage Tanks for Flammable or Combustible Liquids*, 2009.

[18] Liu, Y.; Yakun, Z. F.; Analysis of the effect on the large floating roof oil tanks struck by indirect lightning based on FDTD, *Proceedings of the International Conference on Lightning Protection (ICLP)*, 2014, pp. 1–4.

Appendix A.
Detailed Electromagnetic Formulation and Parameters

A.1 Electromagnetic Field Formulation

The radiated electromagnetic fields due to a time-varying current source were computed using the classical electric dipole formulation, given by

$$\boldsymbol{A}(x,y,z) = \frac{\mu}{4\pi}\int \boldsymbol{I}_e(x',y',z')\frac{e^{-jKR}}{R}dl'$$

where **A** is the magnetic vector potential, I_e the current vector, R the distance between the source and observation point, and K the wavenumber.

Assuming a thin dipole aligned along the z-axis, the potential reduces to

$$\boldsymbol{A}(x,y,z) = \hat{Z}\,\frac{\mu I_0 l}{4\pi r}e^{-jkr}$$

and the corresponding fields are obtained from

$$\boldsymbol{E} = -\nabla\varphi - \frac{\partial A}{\partial t}, \qquad \boldsymbol{B} = \nabla\times\mathbf{A}$$

subject to the Lorentz condition.

A.2 Governing Maxwell equations

For time-domain simulation, Maxwell's equations were expressed as

$$\nabla\times\mathbf{H} = \frac{\partial\mathbf{D}}{\partial t} + \mathbf{J}, \quad \nabla\times\mathbf{E} = -\frac{\partial\mathbf{B}}{\partial t} - \mathbf{J}, \quad \nabla\cdot\mathbf{B} = 0, \quad \nabla\cdot\mathbf{D} = \rho$$

With constitutive relations $\boldsymbol{D} = \varepsilon\boldsymbol{E}$ and $\boldsymbol{B} = \mu\boldsymbol{H}$.

The discrete forms of Ampère's and Faraday's laws were implemented using the **Yee cell** scheme to ensure second-order accuracy in both space and time.

A.3 Discretization and Stability (CFL Condition)

The Courant–Friedrichs–Lewy (CFL) condition for a 3D uniform grid is

$$\Delta t \le \frac{S}{c_0}\left(\frac{1}{\Delta x^2}+\frac{1}{\Delta y^2}+\frac{1}{\Delta z^2}\right)^{-\frac{1}{2}}$$

where $S = 0.96$ ensures numerical stability.

A grid step of $\Delta = 2$ cm and a maximum time step of 0.037 ns were used in all simulations, which yielded convergence errors below 1.5 %.

A.4 Material parameters

Material	$\sigma[S/m]$	ε_r	μ_r	Model/Justification
Steel (roof/wall)	$5.0x10^6$	1.0	1.0	IBC; for f ≤ 1 MHz, $\delta_{steel} \approx 0.23mm \ll t$, *hence PEC and SIBC are equivalent.*
Copper (bypass/shunts/rings)	$5.8x10^7$	1.0	1.0	Thin wires and bars modeled using SIBC or thin-wire elements; $\delta_{Cu}(1\,MHz) \approx 0.066\,mm$.
Hydrocarbon vapor	10^{-10}	1.9	1.0	Typical range for light vapors; negligible transient losses.
Air (seal gap)	0	1.0006	1.0	10 mm x 10 mm air gap; conformal/effective subcell used to capture the field gradient.
Soil (ground)	0.01	10.0	1.0	$\rho = 100\Omega\cdot m$; equivalent half-space medium for grounding.

A.5 Perfectly Matched Layers (CPML) and Mesh Independence

A convolutional perfectly matched layer PML with 10–12 layers and third-order conductivity profile (m=3) were implemented on all domain boundaries to prevent spurious reflections. This configuration ensured numerical reflection levels below −60 dB across the frequency range of interest, providing a stable and fully absorbing boundary condition.

To evaluate the spatial resolution required for numerical accuracy, a mesh-independence study was conducted using the most demanding performance metric—the maximum electric field (E_{max}) within the seal gap under rim-impact excitation (unmitigated case). Three nested meshes were tested while maintaining identical excitation conditions and PML boundary parameters.

Mesh independence in the FDTD subdomain (rim box).

Cell size (cm)	E_{max} in the seal (kV/m)	Relative error vs. 1 cm
4.0	18,500	12.3%
2.0	20,800	1.4%
1.0	21,100	---------

The results demonstrate monotonic convergence with mesh refinement. A spatial cell size of Δ=2 cm yields an error below 1.5 % relative to the finest grid (Δ=1 cm), representing an optimal balance between numerical accuracy and computational efficiency. For consistency, the PML thickness, conductivity profile, and Courant–Friedrichs–Lewy (CFL) ratio were kept constant throughout all simulations.

A.6 Extended Validation and Uncertainty Analysis

A Latin Hypercube Sampling (LHS) analysis with N=200 simulations was performed by varying the soil resistivity (100–1000 Ω·m), contact resistance (10^{-4}, 10^{-2} Ω), and lightning impact position (±0.5 m).

The resulting median, interquartile range, and 95 % confidence intervals for E_{max}, $V_{roof-wall}$, and total bypass current $\sum I_{bypass}$ were consistent with analytical predictions, confirming model robustness.

A.7 Statistics, Sensitivity, and Uncertainty

Median values and 95% confidence intervals (CI 95%) were obtained for three key metrics under a 200 kA, 10/350 µs lightning current waveform, considering variations in the number of bypass conductors (*N*), contact resistance (R_a), and immersion depth ($d_{(imm)}$).
Representative values consistent with the parameter sweeps described in section 2 (Methodology) were adopted.

Configuration	E_{max}[kV/m]	$V_{roof-wall,peak}$[kV]	W [mJ]
Without bypass (N=0)	20,800 [18,300, 23,300]	210 [180, 240]	0.45 [0.36, 0.54]
N = 4, S = 120 mm²	12,900 [11,600, 14,200]	120 [105, 135]	0.12 [0.10, 0.15]
N = 6, S = 95 mm²	10,700 [9,700, 11,800]	108 [95, 122]	0.10 [0.08, 0.12]
$d_{(imm)}$ = 0.5 m	----------	----------	0.06 [0.05, 0.07]
$R_a = 1 \times 10^{-2}$ Ω	----------	158 [142, 174]	---------

Author contribution:

1. Conception and design of the study

2. Data acquisition

3. Data analysis

4. Discussion of the results

5. Writing of the manuscript

6. Approval of the last version of the manuscript

JDLL has contributed to: 1, 2, 3 4, 5 and 6.

DMY has contributed to: 1, 2, 3 4, 5 and 6.

CYV has contributed to: 1, 2, 3 4, 5 and 6.

Acceptance Note: This article was approved by the journal editors Dr. Rafael Sotelo and Mag. Ing. Fernando A. Hernández Gobertti.

Lista de Autores – Memoria Investigaciones en Ingeniería (Número 29).

List of Authors – Memoria Investigaciones en Ingenieria (Volume 29).

MIIUM29-11: Análisis de las repercusiones económicas y técnicas del cierre de bancos de materiales del cerro de San Juan, en las ciudades de Tepic y Xalisco, en el año 2022.

Dr. Carlos Alberto Hoyos Castellanos, Tecnológico Nacional de México (México).
Dr. William Herbe Herrera León, Tecnológico Nacional de México (México).
Dr. Fernando Treviño Montemayor, Tecnológico Nacional de México (México).
Mag. Fernando Aguirre Camacho, Tecnológico Nacional de México (México).

MIIUM29-14: Un análisis de modelos hidrodinámicos y una propuesta de cambio cultural basada en predicciones: el caso de la inundación del Río Grande do Sul, Brasil.

Dr. Cristiano Trindade, Skema Business School, Lille (Francia).

MIIUM29-16: Feasibility Study for the Electrification of Vehicles in Pakistan.

Prof. Asad A. Naqvi, NED University of Engineering and Technology (Pakistan).
Wassam Uddin, NED University of Engineering and Technology (Pakistan).
S.M. Saadullah, NED University of Engineering and Technology (Pakistan).
M. Zaviyar Abbas Noori, NED University of Engineering and Technology (Pakistan).
M. Omer Farooq, NED University of Engineering and Technology (Pakistan).

MIIUM29-18: Effect of Tesla valve geometry on unsteady flow behavior and pressure drop - A CFD study.

Prof. M. Shakaib, NED University of Engineering and Technology (Pakistan).
Prof. M. Ehtesham ul Haque, NED University of Engineering and Technology (Pakistan).
Prof. S. M. Fakhir Hasani, Imam Mohammad Ibn Saud Islamic University (Saudi Arabia).

MIIUM29-20: Investigating Tensile & Impact Properties of Recycled Polypropylene, Polyvinyl Chloride, Polyamide & Polyethylene.

Prof. Eylia Abbas Jafri, NED University of Engineering and Technology (Pakistan).
Prof. Atif Shazad, Ifrah Asif, NED University of Engineering and Technology (Pakistan).
Dr. Ifrah Asif, NED University of Engineering and Technology (Pakistan).
Arqam Ahmed Hashmi, NED University of Engineering and Technology (Pakistan).
Umer Nadeem Abdullah, NED University of Engineering and Technology (Pakistan).

MIIUM29-21: Smart and Sustainable IoT-Driven Vertical Farming Solution for Agricultural Challenges in Pakistan.

Prof. Dr. Sadiq Ur Rehman, IQRA University (Pakistan).
Prof. Dr. Muhammad Adeel Mannan, Bahria University (Pakistan).
Prof. Dr. Muhammad Ahsan Shaikh, Hamdard University (Pakistan).
Prof. Dr. Muhammad Uzair, Islamic University of Madinah (Saudi Arabia).

MIIUM29-22: Occupational Hazard Assessment and Risk Mitigation in the Gluing And Lapping Section of a Gas Meter Manufacturing Plant.

Eng. Ammar Zulfikar, NED University of Engineering and Technology (Pakistan).
S. M. Muhib Hussain Naqvi, NED University of Engineering and Technology (Pakistan).
Prof. Muhammad Azam, NED University of Engineering and Technology (Pakistan).
Prof. Imran Sikandar, NED University of Engineering and Technology (Pakistan).
Eng. Muhib Hussain Naqvi, NED University of Engineering and Technology (Pakistan).
Eng. M. Hamid, Hamza Ahmed, NED University of Engineering and Technology (Pakistan).

MIIUM29-23: Optimizing Domestic Refrigerator Performance with Varied Lubricants for R134a Refrigerant: Comparative Analysis

Prof. Muhammad Ehtesham ul Haque, NED University of Engineering and Technology.
Prof. Abdul Samad Khan, NED University of Engineering and Technology (Pakistan).
Prof. Adeel Ahmed Khan, NED University of Engineering and Technology (Pakistan).
Prof. Muhammad Anus Irshad, NED University of Engineering and Technology (Pakistan).

MIIUM29-24: Analysis of barriers to the massification use of private electric vehicles in urban passenger transport in Lima, Peru

Dr. Russell Nazario Ticse, Universidad Nacional de Ingeniería (Perú).
Dr. José Ramos Saravia, Universidad de Ingeniería y Tecnología (Perú).
Dr. María Quintana Caceda, Universidad Nacional de Ingeniería (Perú).
Dr. Jorge Wong Kcomt, Association of Energy Engineers (United States of America).
MSc. Wilson Arroyo Delgado, Universidad Autónoma del Perú (Perú).

MIIUM29-25: Aplicaciones Recientes de Tecnologías Digitales en la Agricultura.

Lizmarie Camacho, Universidad de Panamá (Panamá).
José Simmonds, Universidad de Panamá (Panamá).
Ing. Yaliska Moreno-González, Universidad de Panamá (Panamá).
Ing. Marco Vieto-Vega, Victoria University of Wellington (Nueva Zelandia).
Dr. Yarien Moreno, Huazhong University of Science and Technology (China).
Dr. Noriel Correa, Universidad de Panamá (Panamá).
Prof. Marciano Santamaría Lezcano, Universidad de Panamá (Panamá).
Prof. Fabiola Mabel Montero González, Universidad de Panamá (Panamá).

MIIUM29-32: Computational study of the direct impact of a 200 kA lightning strike on external floating roof tanks

Prof. Juan David Losada Losada, Universidad de Manizales (Colombia).
Prof. Darwin Marín Yépez, Universidad de Manizales (Colombia).
Prof. Camilo Younes Velosa, Universidad Nacional de Colombia (Colombia).

Lista de Revisores – Memoria Investigaciones en Ingeniería (Número 29).

List of Reviewers – Memoria Investigaciones en Ingenieria (Volume 29).

Dr. Ricardo Oviedo Sarmiento, Universidad Nacional Federico Villarreal (Peru).
Dr. Waldo Hasperué, Universidad Nacional de La Plata (Argentina).
Dr. Masato Kobiyama, Universidade Federal do Rio Grande do Sul (Brasil).
Dr. Talha Bin Nadeem, Aston University (United Kingdom).
Dr. Jeffery Rizvi, Sir Syed University (Pakistan).
Dr. Eylia Abbas, National University of Science and Technology (Pakistan).
Dr. Ricardo Santos, University of Porto (Portugal).
Dr. Claudio Pereira Da Fonte, University of Manchester (United Kingdom).
Dr. Jeffery Rizvi, Sir Syed University (Pakistan).
Dr. Mohsin Sattar, Czech Technical University (Czech Republic).
Dr. Hassan Liaquat, University of Auckland (New Zealand).
Dr. Kashif Azher, King Fahd University of Petroleum and Minerals (Saudi Arabia).
Dr. Rehan Khursheed, Harbin Institute of Technology (China).
MSc. Carlos Fernández, Universidad Latina de Panamá (Panamá).
Eng. Efrén Jiménez, Instituto Tecnológico de Costa Rica (Costa Rica).